

# **Understanding the rhizosphere as a greenhouse gas hotspot in cultivated peatlands**

**Aidan De Sena**

Department of Bioresource Engineering

Faculty of Agricultural and Environmental Sciences

Macdonald Campus of McGill University

November 2024

A thesis submitted to McGill University in partial fulfillment of the requirements  
for the degree of Doctor of Philosophy (Ph.D.)

© Aidan De Sena 2024

## TABLE OF CONTENTS

<b>TABLE OF CONTENTS .....</b>	<b>ii</b>
<b>ABSTRACT.....</b>	<b>vii</b>
<b>RÉSUMÉ .....</b>	<b>ix</b>
<b>ACKNOWLEDGEMENTS .....</b>	<b>xii</b>
<b>CONTRIBUTIONS TO KNOWLEDGE.....</b>	<b>xvi</b>
<b>CONTRIBUTIONS OF AUTHORS .....</b>	<b>xvii</b>
<b>LIST OF FIGURES .....</b>	<b>xviii</b>
<b>LIST OF TABLES .....</b>	<b>xxii</b>
<b>LIST OF ABBREVIATIONS, SYMBOLS AND TERMS.....</b>	<b>xxiii</b>
<b>CHAPTER 1.....</b>	<b>1</b>
<b>1. General introduction .....</b>	<b>1</b>
1.1 Background.....	1
1.2 Research objectives.....	3
1.3 Synopsis of the research methods and significance of the study .....	5
1.4 Thesis structure .....	6
1.5 References.....	7
<b>FORWARD TO CHAPTER 2 .....</b>	<b>8</b>
<b>CHAPTER 2 .....</b>	<b>9</b>
<b>2. The role of the rhizosphere as a hotspot of microbial CO<sub>2</sub> and N<sub>2</sub>O production in cultivated peatlands: A review.....</b>	<b>9</b>
2.1 Greenhouse gas emissions from cultivated peatlands.....	9
2.1.1 Soil factors affecting greenhouse gas emissions from cultivated peatlands .....	11
2.1.1.1 Physical factors .....	11
2.1.1.2 Chemical factors .....	12
2.1.1.3 The effect of peat soil factors on microbial greenhouse gas production .....	13
2.2 The rhizosphere as a greenhouse gas hotspot .....	14
2.2.1 Rhizosphere properties relevant to soil greenhouse gas emissions .....	14
2.2.1.1 Physical properties .....	14
2.2.1.2 Chemical properties .....	15
2.2.1.3 The effect of the rhizosphere on microbial greenhouse gas production .....	18
2.3 Microbial greenhouse gas production.....	19

2.3.1	Aerobic respiration.....	20
2.3.1.1	Microbial actors of aerobic respiration .....	21
2.3.1.2	Soil factors affecting CO <sub>2</sub> production by aerobic respiration.....	22
2.3.2	Nitrification.....	25
2.3.2.1	Microbial actors of nitrification .....	28
2.3.2.2	Soil factors affecting N <sub>2</sub> O production by nitrification.....	32
2.3.3	Denitrification .....	35
2.3.3.1	Microbial actors of denitrification .....	38
2.3.3.2	Soil factors affecting CO <sub>2</sub> and N <sub>2</sub> O production by denitrification .....	41
2.3.4	Nitrifier-denitrification .....	44
2.3.4.1	Microbial actors of nitrifier-denitrification.....	45
2.3.4.2	Soil factors affecting CO <sub>2</sub> and N <sub>2</sub> O production by nitrifier-denitrification .....	45
2.4	Methods for analysis of greenhouse gas hotspots.....	48
2.4.1	Isotopic signature analysis of CO <sub>2</sub> and N <sub>2</sub> O at natural abundance.....	49
2.4.2	Isotope tracing with <sup>13</sup> C, <sup>15</sup> N and <sup>18</sup> O .....	60
2.4.3	<sup>13</sup> C, <sup>15</sup> N and <sup>13</sup> C <sup>15</sup> N-stable isotope probing (SIP).....	62
2.5	Future research directions .....	64
2.6	References.....	67
<b>FORWARD TO CHAPTER 3 .....</b>		<b>103</b>
<b>CHAPTER 3.....</b>		<b>104</b>
<b>3.</b>	<b>Nitrogen transfer from root exudates to the rhizobiome: A <sup>15</sup>N stem feeding method</b>	<b>104</b>
3.1	Abstract.....	104
3.2	Introduction.....	104
3.3	Materials and methods .....	106
3.4	Results and discussion .....	108
3.5	References.....	114
3.6	Appendix: Supplementary materials.....	118
3.6.1	Supplemental text S1 .....	118
3.6.1.1	Assembly of labeling apparatus for stem and leaf feeding .....	118
3.6.1.2	Sample preparation and analysis of <sup>15</sup> N.....	118
3.6.1.3	Calculations.....	119
3.6.2	References.....	127

<b>FORWARD TO CHAPTER 4</b> .....	<b>128</b>
<b>CHAPTER 4</b> .....	<b>129</b>
<b>4. Root exudates are a nitrogen source for nitrous oxide production in the rhizosphere</b> <b>129</b>	
4.1 Abstract.....	129
4.2 Introduction.....	130
4.3 Materials and methods.....	133
4.3.1 Experimental materials.....	133
4.3.2 Experimental design.....	133
4.3.3 Introduction of <sup>15</sup> N-substrates.....	135
4.3.4 Gas, ryegrass biomass and soil sample collection.....	136
4.3.5 Gas analysis.....	137
4.3.6 Ryegrass biomass and rhizosphere soil analysis.....	141
4.3.7 Statistical analyses.....	143
4.4 Results.....	145
4.4.1 N <sub>2</sub> O emissions.....	145
4.4.2 Dynamics of substrate-derived N in the rhizosphere.....	150
4.5 Discussion.....	150
4.5.1 Root exudates are a N source for N <sub>2</sub> O production in the rhizosphere.....	150
4.5.2 N <sub>2</sub> O from the rhizosphere likely produced by bacterial denitrification, nitrifier-denitrification or a combination of the two pathways.....	156
4.5.3 Fate of root exudate-N in the rhizosphere.....	158
4.6 Conclusion.....	159
4.7 References.....	161
4.8 Appendix: Supplementary materials.....	172
<b>FORWARD TO CHAPTER 5</b> .....	<b>181</b>
<b>CHAPTER 5</b> .....	<b>182</b>
<b>5. Peat is a negligible source of carbon dioxide from the rhizosphere of a nitrogen-fertilized peat soil</b> .....	<b>182</b>
5.1 Abstract.....	182
5.2 Introduction.....	183
5.3 Materials and methods.....	186
5.3.1 Experimental materials and design.....	186

5.3.2	Introduction of $^{13}\text{C}$ -substrates .....	187
5.3.3	Gas, ryegrass biomass and soil sample collection .....	189
5.3.4	Gas analysis .....	189
5.3.5	Ryegrass biomass and rhizosphere soil analysis.....	192
5.3.6	Statistical analysis.....	194
5.4	Results.....	195
5.4.1	CO <sub>2</sub> emissions.....	195
5.4.2	Dynamics of substrate-derived C in the rhizosphere .....	200
5.5	Discussion.....	200
5.5.1	Peat is a negligible source of CO <sub>2</sub> from the rhizosphere .....	200
5.5.2	Fate of C derived from rhizodeposits and urea in the rhizosphere .....	205
5.6	Conclusion .....	207
5.7	References.....	209
5.8	Appendix: Supplementary materials.....	219
<b>CHAPTER 6.....</b>		<b>226</b>
<b>6.</b>	<b>General discussion .....</b>	<b>226</b>
6.1	Contributions to knowledge.....	228
6.1.1	Stem feeding is the most effective method for the quantification of root exudate-N transfer from ryegrass roots to the rhizobiome .....	228
6.1.1.1	Explanation .....	228
6.1.1.2	Recommendations and future directions.....	230
6.1.2	The rhizobiome assimilates N derived from root exudates even after N fertilization.....	231
6.1.2.1	Explanation .....	231
6.1.2.2	Recommendations and future directions.....	232
6.1.3	Root exudates are a N source for N <sub>2</sub> O production from the rhizosphere .....	233
6.1.3.1	Explanation .....	233
6.1.3.2	Recommendations and future directions.....	234
6.1.4	The rhizobiome likely produces N <sub>2</sub> O from the rhizosphere of cultivated peatlands via bacterial denitrification, nitrifier-denitrification or a combination of the two pathways 235	
6.1.4.1	Explanation .....	235
6.1.4.2	Recommendations and future directions.....	237

6.1.5	Peat is a negligible source of CO <sub>2</sub> emissions from the rhizosphere of cultivated peatlands	238
6.1.5.1	Explanation .....	238
6.1.5.2	Recommendations and future directions.....	240
6.2	Understanding the rhizosphere as a greenhouse gas hotspot in cultivated peatlands .	242
<b>CHAPTER 7</b>	.....	<b>244</b>
<b>7. General Conclusions</b>	.....	<b>244</b>
<b>8. References</b>	.....	<b>246</b>

## ABSTRACT

Cultivated peatlands are a substantial source of nitrous oxide (N<sub>2</sub>O) and carbon dioxide (CO<sub>2</sub>). However, the emissions from these soils express high spatial heterogeneity, known as greenhouse gas hotspots. Such hotspots could be concentrated in the rhizosphere, where the abundance of root exudates from rhizodeposition and application of nitrogenous fertilizers create a microenvironment of high substrate availability. As a result, these nitrogen (N) and carbon (C) substrates should fuel greenhouse gas production by the rhizosphere microbial community, known as the rhizobiome. With my Ph.D. research, I aimed to explore the capacity of the rhizosphere to function as a hotspot of microbial N<sub>2</sub>O and CO<sub>2</sub> production in cultivated peatlands. The specific objectives of my thesis were to: (i) identify the most sensitive method for quantifying the microbial assimilation of root exudate-derived N by comparing the ability of different plant-labeling methods to enrich the rhizobiome with <sup>15</sup>N; (ii) assess the potential role of root exudates as a substrate for microbial N<sub>2</sub>O production by confirming the assimilation of root exudate-N by the rhizobiome in N-fertilized soil from a cultivated peatland; (iii) determine if root exudates are a source of N<sub>2</sub>O from the rhizosphere through <sup>15</sup>N-tracing; (iv) estimate the dominant pathway of microbial N<sub>2</sub>O production in the rhizosphere of soil from a cultivated peatland through site preference analysis; and (v) partition the contributions of rhizodeposits, urea and peat to CO<sub>2</sub> emissions from the plant-rhizosphere soil system under N fertilization through <sup>13</sup>C-tracing. To achieve the first and second objectives, I conducted a greenhouse experiment with annual ryegrass (*Lolium multiflorum*) plants where I assessed the efficacy of stem and leaf feeding with either <sup>15</sup>N-urea or <sup>15</sup>N-ammonium nitrate at three different concentrations (64.5, 129 or 193 mmol <sup>15</sup>N L<sup>-1</sup>) to evaluate root exudate-derived N transfer to the rhizobiome in N-rich peat soil. Indeed, I found that stem feeding with either <sup>15</sup>N-tracer at the

highest concentration was the most effective method to quantify microbial root exudate-N assimilation, and I confirmed that despite the availability of N in fertilized peat soil, root exudates still supplied the rhizobiome with  $0.07 \pm 0.01\%$  of their absolute biomass-N. To realize the final three objectives, I conducted a second greenhouse experiment on soil collected from a cultivated peatland to understand the rhizosphere cycling of root exudate-derived N and rhizodeposit-derived C using  $^{15}\text{N}$ - and  $^{13}\text{C}$ -tracing, respectively. I found that root exudates contribute roughly one-fifth of  $\text{N}_2\text{O}$  emissions, which was comparable to the  $\text{N}_2\text{O}$  derived from urea applied within 48 h. Additionally, between 67 and 99% of this rhizosphere-emitted  $\text{N}_2\text{O}$  was likely produced by bacterial denitrification, nitrifier-denitrification or a combination of the two, according to site preference analysis. Lastly, I demonstrated that peat was a negligible source of  $\text{CO}_2$ , contributing much less to the total  $\text{CO}_2$  emissions from the plant-rhizosphere soil system, compared to rhizodeposits ( $14 \pm 1.2\%$ ). As a result, my research makes the following contributions to knowledge: (i) stem feeding is the most sensitive method for the quantification of root exudate-N transfer to the rhizobiome; (ii) root exudates are a N source to the rhizobiome in peat soil fertilized with N; (iii) root exudates contribute to the  $\text{N}_2\text{O}$  emissions from the rhizosphere; (iv)  $\text{N}_2\text{O}$  production from the rhizosphere likely occurs through bacterial denitrification, nitrifier-denitrification, or a combination of the two pathways; and (v) peat itself is a negligible source of  $\text{CO}_2$  from the N-fertilized rhizosphere. Altogether, my findings establish the substantial impact of root exudates and rhizodeposits on greenhouse gas production and signify the role of the rhizosphere as a hotspot of greenhouse gas production in cultivated peatlands.

## RÉSUMÉ

Les tourbières cultivées sont une source importante de protoxyde d'azote ( $N_2O$ ) et de dioxyde de carbone ( $CO_2$ ). Cependant, les émissions de ces sols présentent une grande hétérogénéité spatiale, connue sous le nom de points chauds de gaz à effet de serre. Ces points chauds pourraient être concentrés dans la rhizosphère, où l'abondance des exsudats racinaires issus de la rhizodéposition et l'application d'engrais azotés créent un microenvironnement à forte disponibilité de substrats. Par conséquent, ces substrats azotés (N) et carbonés (C) devraient alimenter la production de gaz à effet de serre par la communauté microbienne de la rhizosphère, connue sous le nom de rhizobiome. Dans le cadre de ma recherche doctorale, j'ai cherché à explorer la capacité de la rhizosphère à fonctionner comme un point chaud de production microbienne de  $N_2O$  et de  $CO_2$  dans les tourbières cultivées. Les objectifs spécifiques de ma thèse étaient de : (i) identifier la méthode la plus sensible pour quantifier l'assimilation microbienne du N issu des exsudats racinaires en comparant la capacité de différentes méthodes de marquage des plantes à enrichir le rhizobiome en  $^{15}N$  ; (ii) évaluer le rôle potentiel des exsudats racinaires en tant que substrat pour la production microbienne de  $N_2O$  en confirmant l'assimilation du N des exsudats racinaires par le rhizobiome dans un sol fertilisé en N issu d'une tourbière cultivée ; (iii) déterminer si les exsudats racinaires sont une source de  $N_2O$  dans la rhizosphère par le biais de la traçabilité  $^{15}N$  ; (iv) estimer la voie dominante de production microbienne de  $N_2O$  dans la rhizosphère de sol provenant d'une tourbière cultivée par analyse de la préférence de site ; et (v) partitionner les contributions des rhizodépôts, de l'urée et de la tourbe aux émissions de  $CO_2$  du système sol-rhizosphère des plantes sous fertilisation azotée grâce à la traçabilité  $^{13}C$ . Pour atteindre les premier et deuxième objectifs, j'ai mené une expérience en serre avec des plants de ray-grass annuel (*Lolium multiflorum*) où j'ai évalué

l'efficacité de l'alimentation par la tige et les feuilles avec soit du  $^{15}\text{N}$ -urée, soit du  $^{15}\text{N}$ -nitrate d'ammonium à trois concentrations différentes (64,5, 129 ou 193 mmol  $^{15}\text{N L}^{-1}$ ) afin d'évaluer le transfert du N issu des exsudats racinaires vers le rhizobiome dans un sol tourbeux riche en N. En effet, j'ai constaté que l'alimentation par la tige avec l'un ou l'autre des traceurs  $^{15}\text{N}$  à la concentration la plus élevée était la méthode la plus efficace pour quantifier l'assimilation microbienne du N des exsudats racinaires, et j'ai confirmé que malgré la disponibilité du N dans le sol tourbeux fertilisé, les exsudats racinaires fournissaient encore  $0,07 \pm 0,01$  % de leur biomasse totale en N au rhizobiome. Pour réaliser les trois derniers objectifs, j'ai mené une deuxième expérience en serre sur un sol prélevé dans une tourbière cultivée afin de comprendre le cycle de N issu des exsudats racinaires et de C issu des rhizodépôts dans la rhizosphère, en utilisant respectivement le traçage  $^{15}\text{N}$  et  $^{13}\text{C}$ . J'ai découvert que les exsudats racinaires contribuent à environ un cinquième des émissions de  $\text{N}_2\text{O}$ , ce qui est comparable à la quantité de  $\text{N}_2\text{O}$  provenant de l'urée appliquée dans les 48 heures. De plus, entre 67 et 99 % de ce  $\text{N}_2\text{O}$  émis par la rhizosphère a probablement été produit par la dénitrification bactérienne, la dénitrification des nitrifiants ou une combinaison des deux, selon l'analyse de la préférence de site. Enfin, j'ai démontré que la tourbe était une source négligeable de  $\text{CO}_2$ , contribuant beaucoup moins aux émissions totales de  $\text{CO}_2$  du système sol-rhizosphère des plantes, par rapport aux rhizodépôts ( $14 \pm 1,2$  %). En conséquence, ma recherche apporte les contributions suivantes à la connaissance : (i) l'alimentation par la tige est la méthode la plus sensible pour quantifier le transfert de N des exsudats racinaires vers le rhizobiome ; (ii) les exsudats racinaires sont une source de N pour le rhizobiome dans un sol tourbeux fertilisé en N ; (iii) les exsudats racinaires contribuent aux émissions de  $\text{N}_2\text{O}$  de la rhizosphère ; (iv) la production de  $\text{N}_2\text{O}$  dans la rhizosphère se produit probablement par la dénitrification bactérienne, la dénitrification des nitrifiants, ou une

combinaison des deux voies ; et (v) la tourbe elle-même est une source négligeable de CO<sub>2</sub> dans la rhizosphère. Dans l'ensemble, mes résultats établissent l'impact substantiel des exsudats racinaires et des rhizodépôts sur la production de gaz à effet de serre et signifient le rôle de la rhizosphère comme un point chaud de production de gaz à effet de serre dans les tourbières cultivées.

## ACKNOWLEDGEMENTS

I am forever grateful to all who have been part of helping me through my Ph.D. journey:

Thank you to Chandra Madramootoo for welcoming me into his lab long ago and his steadfast support of me and my endeavors. I am so thankful to have you as a mentor and appreciate all that you have taught me throughout the years. Thank you also to Joann Whalen for providing her expertise during the course of my studies.

I am grateful to the other committee members during my comprehensive and defense for providing constructive feedback on my proposal and thesis: Cynthia Kallenbach, Richard Farrell, Grant Clark, Vijaya Raghavan and Abdolhamid Akbarzadeh Shafaroudi.

I appreciate all the organizations and programs that made my research possible, including the Natural Sciences and Engineering Research Council of Canada (NSERC), the Agricultural Greenhouse Gases Program (AGGP) of Agriculture and Agri-Food Canada (AAFC) and the Fonds de recherche du Québec – Nature et technologies (FRQNT).

Thank you to the team at University of Saskatchewan, especially Richard Farrell, Mark Cooke, Darin Richman and Frank Krijen for making my isotopic analysis dreams possible despite the initial difficulties!

Thank you also to the Insitut de recherche en biologie végétale at the Montréal Botanical Gardens for housing me while I was labless! I appreciate everyone who welcomed me, especially Joan Laur, Martin Lefrançois, Vanessa Grenier, Eszter Sas, Ahmed Jerbi, Éricka Convery, Simon Joly and Mohamed Hijri.

I appreciate Viacheslav Adamchuk, Jan Adamowski, Mohammed Antar, Catherine Bossé, Hicham Benslim, Jean-Benoît Charron, Richard Doucett, Brian Driscoll, Kate Ewert,

Jarek Holoszkiewicz, Cinthya Horvath, Susan Gregus, H el ene Lalande, Kathy Maclean, Joy Matthews, Shirley Mongeau, Khosro Mousavi, Val erie Orsat, Wendy Ouellette, Sarah-Ann Persechino, Ian Ritchie, Emily Schick, Haifeng Song, Christiane Trudeau, and Jo-Ann Zdaniak for their administrative and technical support. I am grateful to Farhan Ahmad, Noura Alsarawi, Naresh Arumugagounder Thangaraju, Zineb Bazza, Calista Brown, Samantha Darling, Sushree Dash, Fang Ding, Rachel Harman-Denhoed, Caitlyn Horsch, Lijun Hou, Chih-Yu Hung, Yutong Jiang, Meaghan Kilmartin, Natasha Lyons, Morgan McMillan, Krisztina Mosdossy, Jessica Nicksy, Sarah Pyton, Lucy Ross-Blevis, Michael Ruppert, Eugene Roy Antony Samy, Elizabeth Shimotakahara, Harsimar Sidana, Emal Sobat and Miranda Xiao for their assistance in the greenhouse and laboratory. I also appreciate the feedback on my research from Naeem Abbasi, Farhan Ahmad, Noura Alsarawi, Elias Andraos, Naresh Arumugagounder Thangaraju, Calista Brown, Sushree Dash, Kosoluchukwu Ekwunife, Mfon Essien, Naresh Gaj, Genevi eve Grenon, Shamim Gul, Lijun Hou, Samuel Ihuoma, Anshika Jain, Yutong Jiang, Cynthia Kallenbach, Meaghan Kilmartin, Emily Lafond, Hannah Lieberman, Guia Mortel, Krisztina Mosdossy, Lucy Ross-Blevis, Elizabeth Shimotakahara, Bhesram Singh, Binjie Sun, Tian Tian, Christian Virgil, Deniz Dutton, Melanie Burnett, Juliette Lebold, Nadia Moukanni, Aaron Price, Daniel Dikio, Joel Harms, Deepak Mishra, Jheuel Carter-Guy, Chih-Yu Hung, Yanyan Zhang and Cassie Miller.

Thank you to Montr al and Qu ebec for housing me for so long. I promise to become fluent in French!

Thank you to the coffee shops and bars in Montr al that have housed me for so long as I write and analyze my data, including La Bo te Gourmande, Fl neur, Br ul erie Saint-Denis on Laurier Est, Byblos, Starbucks by Beaudry and Caf  Sfouf.

I am grateful to my muses: Lana del Rey, Aimee Mann, Fiona Apple, Lisa Hannigan, Charli XCX, Damien Rice, Jens Lekman, Joni Mitchell, Hannah Diamond, Regina Spektor, Japanese Breakfast, Austra, Alvvays, Tori Amos, Renée Elise Goldsberry, Chappell Roan, Kate Bush, Kim Petras, Bonobo, Patti LuPone, Grimes, Chet Baker, Judy Garland, Karen O, Chelsea Wolfe, Sophie, Diane Tell, Safia Nolin, Gabriel Yacoub, Marina Diamond, Florence Welch, Philip Glass, Zbigniew Preisner, Sky Ferreira, Morrissey, Olivia Rodrigo and Weyes Blood.

Thank you to those who inspire me and make me laugh: Ina Garten, Michelle Obama, Tina Fey, Julia Louise-Dreyfuss, Amy Poehler, Seth Meyers, Sarah Jessica Parker, Eileen Davidson, Larry David, Rosalind Russell, Fran Drescher, Molly Shannon, Maya Rudolph, Padma Lakshmi, Rachel Dratch and Kirsten Dunst.

I am thankful for those who kept me company in the lab: Patrick Regan, Catherine Cohen, Bowen Yang, Matt Rogers, George Civeris, Sam Taggart, Brian Joseph McCook, Brian Michael Firkus, Jon Ingle, Carey O'Donnell, Lara Marie Schoenhals, Andy Cohen, Kid Fury, Crissle West, Michelle Collins, Colin Drucker, Johnny Also, Lulu Miller, Latif Nasser, Ira Glass, Ira Flatow, Ben Mandelker and Ronnie Karam.

Thank you to all the friendly faces and angels in my life: Mohammed Leila, Wayne St. Amand, Ekta Amarnani, Sam Darling, Jeff, Line Dietrich, Brighita Lungu, Emma, Hannah Lieberman, Holly Phipps, Bryant Silva, Michael Sullivan, Tori Rulle, Tiffany Eder, Laura Glenn, Max, Roxane Jaff, Ryan Ginter, Laura Gilbert, Julien Valet, James, Adam Salvait, Ian Ignatius Rautenbach, Laurie Malenfant, Kristina Mullahoo, Krisztina Mosdossy, Aniket Choudhuri, Elsa Voytas, Nate Alston, Jordon Vandyke, Katie Kaugars, Kourtenay Plummer, Katie Boretsky, Joe Cross, Marc Hedin, Alicia Blackburn, Kaya Patel, Tanya Nair, Jason Taylor

Jaaved Singh, Klara Winkler, Jeffrey Wu, Serge Bouffard, Sebastien and Lisa Laporte, Eric Poliquin and Dana, and Anne Cat Leduc. I am so grateful to have your friendship in my life.

I would never have made it to this point without the unwavering support of my parents, Laura Hennessey De Sena and Fred De Sena. They have always fostered my interests and encouraged me to pursue my passions. Thank you to my rock, my sister, Bronwen De Sena. She has always been there for me and is a pillar in all aspects of my life. Thank you to Eleanor Hennessey for being a constant and guiding presence in my life. I am so grateful for the love from my family: Erin, Joe and Joseph Firreno; Pat, Tony and Therese Gadaleta; Stella De Sena and Lance Johnson; Fedele and Marie De Sena; Howie and Ruby Bass; Robbie Gendler; Catherine Saint-Hilaire and Joel Gonnevillle; Patrick, Anne and Charles Saint-Hilaire; Claudine Saint-Hilaire; and Michelle and René Saint-Hilaire.

Benoit Saint-Hilaire, my partner, you have been on the frontlines with me during this whole process and have loved me at my best and at my worst. Thank you for the sacrifices you have made while I pursued my doctorate. I am so lucky to have you on my team. Je t'aime, je t'aime, je t'aime toujours.

This thesis is dedicated to my nephew, Elijah Augustine De Sena. I love you, and I am so excited to see you follow your own passions one day.

God bless.

## CONTRIBUTIONS TO KNOWLEDGE

The research I present in this thesis has made the following contributions to knowledge:

- i. **Stem feeding is the most effective method for the quantification of root exudate-N transfer from ryegrass roots to the rhizobiome.**
- ii. **The rhizobiome assimilates N derived from root exudates even after N fertilization.**
- iii. **Root exudates are a source of N<sub>2</sub>O from the rhizosphere.**
- iv. **The rhizobiome likely produces N<sub>2</sub>O from the rhizosphere of cultivated peatlands via bacterial denitrification, nitrifier-denitrification or a combination of the two pathways.**
- v. **Peat is a negligible source of CO<sub>2</sub> emissions from the N-fertilized rhizosphere of peat soil.**

The impact of these contributions to knowledge is discussed in full in Chapter 6.

## CONTRIBUTIONS OF AUTHORS

This work is a manuscript-based thesis. As such, chapters in this thesis written as manuscripts (Chapters 2, 3, 4 and 5) have been published or will be submitted for publication with Aidan De Sena, the Ph.D. candidate, as first author. In these chapters, Aidan De Sena reviewed the current literature, performed the experiments, completed the technical work (i.e., data collection, sample preparation and analysis, data processing and interpretation), wrote the first draft of the manuscripts, and revised them based on the feedback from co-authors and reviewers. Chandra A. Madramootoo and Joann K. Whalen, the co-authors of each manuscript, provided guidance and supervision for this project, approved the experimental design, reviewed the manuscripts and funded the research. Chandra A. Madramootoo read and approved the final version of each manuscript.

### **Thesis chapters that have been or will be submitted for publication**

- Chapter 2: **De Sena A**, Madramootoo CA, Whalen JK. The role of the rhizosphere as a hotspot of microbial CO<sub>2</sub> and N<sub>2</sub>O production in cultivated peatlands: A review. To be submitted.
- Chapter 3: **De Sena A**, Madramootoo CA, Whalen JK (2023). Nitrogen transfer from root exudates to the rhizobiome: A <sup>15</sup>N stem feeding method. *Soil Biology and Biochemistry* 186: 109159. <https://doi.org/10.1016/j.soilbio.2023.109159>
- Chapter 4: **De Sena A**, Madramootoo CA, Whalen JK. Root exudates are a nitrogen source for nitrous oxide production in the rhizosphere. To be submitted.
- Chapter 5: **De Sena A**, Madramootoo CA, Whalen JK. Peat is a negligible source of carbon dioxide from the rhizosphere of a nitrogen-fertilized peat soil. To be submitted.

## LIST OF FIGURES

<b>Figure 1.1</b> Conceptual diagram of the research conducted to address the objectives of my thesis. Numbers represent the objectives addressed. ....	4
<b>Figure 2.1</b> Latitudinal plot and map demonstrating the contribution of cultivated peatlands circa 2000 to total greenhouse gas (GHG) emissions ( $\text{Mg CO}_2\text{e yr}^{-1}$ ) in comparison to N fertilizer and methane from rice cultivation, the top GHG sources from global croplands (Carlson et al. 2017). ....	11
<b>Figure 2.2</b> Conceptual model demonstrating the effect of soil moisture – in terms of volumetric soil moisture ( $\theta$ ), matric potential ( $\psi$ ) and cell osmotic potential ( $\pi$ ) – on some of the biophysicochemical processes (i.e., gas transport, solute transport, metabolic costs, predation) that affect aerobic heterotrophic respiration (Moyano et al. 2013). ....	23
<b>Figure 2.3</b> Conceptual model of the N cycle occurring in soils, composed of nitrification, denitrification and nitrifier-denitrification. AMO, $\text{NH}_3$ monooxygenase; HAO, $\text{NH}_2\text{OH}$ oxidoreductase; NOO, NO oxidoreductase; NXR, $\text{NO}_2^-$ oxidoreductase; Nar/Nap, $\text{NO}_3^-$ reductase; NirK/NirS, $\text{NO}_2^-$ reductase; Nor, NO reductase; NosZ, $\text{N}_2\text{O}$ reductase (Adapted from Lancaster et al. 2018). ....	26
<b>Figure 2.4</b> A conceptual diagram of a potential nitrification aggregate where $\text{NH}_3$ oxidizers and $\text{NO}_2^-$ oxidizers coexist in a mutualistic relationship, shuttling substrates back and forth to complete nitrification. EPS, extracellular polymeric substances; Fe-Siderophores, iron-siderophore complexes; QS, quorum sensing (Daims et al. 2016). ....	31
<b>Figure 2.5</b> Examples of plants known to (solid red lines) and suspected to (dotted red lines) exude different C compounds that inhibit nitrifying enzymes, like $\text{NH}_3$ monooxygenase (AMO) and $\text{NH}_2\text{OH}$ oxidoreductase (HAO). Currently, there are no known root exudates that inhibit $\text{NO}_2^-$ oxidoreductase (NXR; Coskun et al. 2017). ....	34
<b>Figure 3.1</b> The $^{15}\text{N}$ enrichment ( $\text{atm}\%$ excess) of shoots, roots and rhizosphere soil (inset) at each labeling solution concentration ( $\text{mmol } ^{15}\text{N L}^{-1}$ ) for stem and leaf feeding after a 24-h $^{15}\text{N}$ enrichment period of annual ryegrass ( <i>L. multiflorum</i> ) plants grown in a greenhouse for 107 d. Ryegrass plants were exposed to twelve $^{15}\text{N}$ -labeling methods at 106 d that varied according to the technique of introducing the tracer (stem or leaf feeding), $^{15}\text{N}$ -tracer solution (urea or $\text{NH}_4\text{NO}_3$ ), and concentration (64.5, 129 or 193 $\text{mmol } ^{15}\text{N L}^{-1}$ ) to enrich root exudates with $^{15}\text{N}$ . Points represent the mean for their respective introduction technique at that concentration with standard deviation bars. The best-fit line of association is shown for a technique if significant ( $p < 0.05$ ). Data were pooled for $^{15}\text{N}$ -tracers within the stem feeding group or the leaf feeding group because plant and soil enrichment was not affected by the type of $^{15}\text{N}$ -tracer (Figure 3.6.S2, Table 3.6.S2). Regressions were produced using statsmodels.api and pandas packages on Spyder 5.2.2 (Spyder Project Contributors 2020). ....	110
<b>Figure 4.1</b> The partitioning of the recovered N (%) from root exudates and urea among the rhizosphere pools of annual ryegrass ( <i>L. multiflorum</i> ) plants measured 24 h and 48 h after introducing $^{15}\text{N}$ -root exudates or $^{15}\text{N}$ -urea fertilizer into the rhizosphere: a) the separate pools of daily $\text{N}_2\text{O}$ emissions, rhizosphere soil, microbial biomass; and b) a magnified inset to show the size of recovered N in the daily $\text{N}_2\text{O}$ emissions with the combined pools of rhizosphere soil and microbial biomass (note the difference in the y-axis scales). Each bar in the stacked bar	

represents the mean value of  $^{15}\text{N}$  recovered in a specific pool for a respective  $^{15}\text{N}$ -substrate treatment pooled together for both time-points. Error bars indicate the standard error of the mean values. The stacked bar for the  $^{15}\text{N}$ -root exudate treatment had a sample size of  $n = 6$ , while  $^{15}\text{N}$ -urea fertilizer had a sample size of  $n = 5$  due to negative values. In Figure 4.1b, different lowercase letters indicate a significant difference in the recovered  $^{15}\text{N}$  between the pools for a respective  $^{15}\text{N}$ -substrate treatment. All differences were assessed for significance ( $p < 0.05$ ) using generalized linear model analysis with a gamma probability distribution followed by pairwise comparisons of the estimated marginal means with Tukey post hoc analysis. .... 147

**Figure 4.2** The proportion of soil-emitted  $\text{N}_2\text{O-N}$  (%) derived from root exudates and urea fertilizer in the rhizosphere of annual ryegrass (*L. multiflorum*) plants. “Other Sources” represents the remainder of  $\text{N}_2\text{O-N}$  not derived from either  $^{15}\text{N}$ -substrate. Each boxplot shows the distribution of the pooled results measured 24 h and 48 h after the introduction of  $^{15}\text{N}$ -root exudates or  $^{15}\text{N}$ -urea fertilizer into the rhizosphere. The bottom and top of the boxplot signify the 25% and 75% quartiles, respectively, with the center line representing the median and the whiskers showing the range. The boxplot for the  $^{15}\text{N}$ -root exudate treatment had a sample size of  $n = 7$ , while the  $^{15}\text{N}$ -urea fertilizer treatment and other sources have a sample size of  $n = 5$  due to negative values. .... 148

**Figure 4.3** The proportion of soil-emitted  $\text{N}_2\text{O-N}$  (%) derived from bacterial denitrification or nitrifier-denitrification based on the concentration-weighted site preference values of  $\text{N}_2\text{O-N}$  fluxes from natural abundance controls. The boxplot shows the distribution of the pooled results measured 24 h and 48 h after the introduction of root exudates (i.e., stem feeding) or urea fertilizer at natural abundance into the rhizosphere. The bottom and top of the boxplot signify the 25% and 75% quartiles, respectively, with the center line representing the median and the whiskers showing the range ( $n = 6$  due to sample destruction by the instrument). .... 149

**Figure 4.4** The partitioning of the recovered N (%) from root exudates and urea among the soil and microbial biomass pools in the rhizosphere of annual ryegrass (*L. multiflorum*) plants measured 3, 9, 24 and 48 h after introducing  $^{15}\text{N}$ -root exudates or  $^{15}\text{N}$ -urea fertilizer into the rhizosphere. Each bar in the stacked bar represents the mean value of  $^{15}\text{N}$  recovered in a specific pool for a respective  $^{15}\text{N}$ -substrate treatment at a specific time-point. Error bars indicate the standard error of the mean values. All mean  $^{15}\text{N}$  values had a sample size of  $n = 4$  except for those stacked bars with an asterisk (\*), denoting  $n = 3$  due to negative values. Different uppercase letters on the right of a bar indicate a significant difference in the partitioning of the recovered  $^{15}\text{N}$  among the pools between time-points for a specific  $^{15}\text{N}$ -substrate treatment. The presence of an apostrophe (') on the right of a bar indicates a significant difference in the partitioning of the recovered  $^{15}\text{N}$  among pools between  $^{15}\text{N}$ -substrate treatments at a specific time-point. All differences were assessed for significance ( $p < 0.05$ ) using generalized linear model analysis with a gamma probability distribution followed by pairwise comparisons of the estimated marginal means with Tukey post hoc analysis. .... 152

**Figure 4.5** The proportion of N (%) derived from root exudates and urea in the rhizosphere pools of annual ryegrass (*L. multiflorum*) plants measured 3, 9, 24 and 48 h after introducing  $^{15}\text{N}$ -root exudates or  $^{15}\text{N}$ -urea fertilizer into the rhizosphere: a) rhizosphere soil; and b) microbial biomass. Markers indicate the mean substrate-derived N value in a respective pool at a specific time-point, with error bars representing the standard error of the mean. All mean values had a sample size of

n = 4 except for those markers with an asterisk (\*), denoting n = 3 due to negative values. Differences in the proportion of substrate-derived N for a pool are shown if significant ( $p < 0.05$ ) regarding substrate, time or their interaction. All differences were assessed for significance using generalized linear model analysis with a gamma probability distribution followed by pairwise comparisons of the estimated marginal means with Tukey post hoc analysis..... 153

**Figure 5.1** Distribution of the total  $^{13}\text{C}$  (%) from the rhizodeposits and urea treatments recovered among the rhizosphere pools ( $\text{CO}_2$  emissions, microbial biomass of the rhizobiome, rhizosphere soil) of annual ryegrass (*L. multiflorum*) plants measured 21 h and 45 h after the start of the final  $^{13}\text{C}$ -labeling period. Each bar in the stacked bar shows the mean value with standard error bars for the  $^{13}\text{C}$  recovered in a respective pool after exposure to a specific  $^{13}\text{C}$ -substrate treatment, composited together for both time-points. The stacked bar for  $^{13}\text{C}$ -urea fertilizer had a sample size of n = 8, while the  $^{13}\text{C}$ -rhizodeposit treatment had a sample size of n = 7 due to a negative value for microbial biomass. Significant differences in recovered  $^{13}\text{C}$  between pools for a specific  $^{13}\text{C}$ -substrate treatment are represented with different lowercase letters. Significant differences in recovered  $^{13}\text{C}$  between  $^{13}\text{C}$ -substrate treatments for a specific pool are represented by an apostrophe ('). Differences were considered significant when  $p < 0.05$  according to the generalized linear model analysis with the inverse Gaussian distribution followed by pairwise comparisons of the estimated marginal means with Tukey post hoc analysis..... 198

**Figure 5.2** The proportion of  $\text{CO}_2\text{-C}$  (%) derived from ryegrass (*L. multiflorum*) plant respiration and different C substrates in the rhizosphere soil: a) contributions from plant-assimilated C (shoot and root respiration, rhizodeposits), urea and peat; and b) magnified inset to visualize the differences in the  $\text{CO}_2\text{-C}$  contributions from the different C substrates in the rhizosphere soil. We assumed that any remaining  $\text{CO}_2\text{-C}$  not derived from plant respiration, rhizodeposits or urea was derived from peat. Boxplots represent the composited results from the  $\text{CO}_2\text{-C}$  measurements taken 21 h and 45 h after the start of the final  $^{13}\text{C}$ -labeling period. The 25% and 75% quartiles of the results are shown with the bottom and top of the boxplot, respectively, while the median is represented by the center line and the range shown with the whiskers. The boxplot for urea had a sample size of n = 8, while the rest of the boxplots had a sample size of n = 7 due to an outlier in the measurements of  $\text{CO}_2\text{-C}$  derived from plant-assimilated C. No statistical comparison was conducted due to the dependent relationship of the variables. .... 199

**Figure 5.3** Distribution of recovered  $^{13}\text{C}$  (%) from rhizodeposits and urea among the microbial biomass and soil pools of the rhizosphere for annual ryegrass (*L. multiflorum*) plants measured 0, 6, 21 and 45 h after the start of the final  $^{13}\text{C}$ -labeling period. Each bar in the stacked bar shows the mean value with standard error bars for the  $^{13}\text{C}$  recovered in each pool after exposure to a specific  $^{13}\text{C}$ -substrate treatment at a respective time-point. Each stacked bar had a sample size of n = 4 except for those marked with an asterisk (\*; n = 3 due to negative microbial biomass values). .... 201

**Figure 5.4** The proportion of C (%) derived from rhizodeposits and urea in the rhizosphere pools of annual ryegrass (*L. multiflorum*) plants measured 0, 6, 21 and 45 h after the start of the final  $^{13}\text{C}$ -labeling period: a) rhizosphere soil; b) magnified inset to visualize the proportion of C in the rhizosphere soil derived from urea; and c) microbial biomass of the rhizobiome. The mean values of substrate-derived C are represented by markers with standard error bars. The sample

size for each marker was  $n = 4$  besides those denoted with an asterisk (\*;  $n = 3$  due to negative values). Significant differences in the proportion of substrate-derived C between different time-points for a specific  $^{13}\text{C}$ -substrate treatment are represented by different lowercase letters. Differences were considered significant when  $p < 0.05$  according to the two-way analysis variance (ANOVA) followed by pairwise comparisons with Tukey post hoc analysis. .... 202

## LIST OF TABLES

<b>Table 2.1</b> Summary of methods for the analysis of greenhouse gas hotspots including their advantages, limitations and examples.....	50
<b>Table 2.2</b> Natural abundance ranges for site preference, the $^{15}\text{N}$ -isotopic signature of $\text{N}_2\text{O}$ ( $\delta^{15}\text{N}\text{-N}_2\text{O}$ ) and the $^{18}\text{O}$ -isotopic signature of $\text{N}_2\text{O}$ ( $\delta^{18}\text{O}\text{-N}_2\text{O}$ ) for microbial $\text{N}_2\text{O}$ -producing pathways as measured from pure microbial cultures (Adapted from Zaman et al. 2021). .....	60
<b>Table 3.1</b> Microbial biomass N and microbial biomass enriched with $^{15}\text{N}$ in the rhizosphere soil of annual ryegrass ( <i>L. multiflorum</i> ) plants grown in a greenhouse for 107 d. Ryegrass plants were exposed to twelve $^{15}\text{N}$ -labeling methods at 106 d that varied according to the technique of introducing the tracer (stem or leaf feeding), $^{15}\text{N}$ -tracer solution (urea or $\text{NH}_4\text{NO}_3$ ), and concentration (64.5, 129 or 193 mmol $^{15}\text{N L}^{-1}$ ) to enrich root exudates with $^{15}\text{N}$ during a 24-h period. Values are the mean $\pm$ standard error ( $n = 4$ , while those with an asterisk (*) were $n = 3$ due to negative values).....	109
<b>Table 4.1</b> Range and mean of total and substrate-derived daily $\text{N}_2\text{O}$ emissions from the rhizosphere of annual ryegrass ( <i>L. multiflorum</i> ) plants measured 24 h and 48 h after introducing $^{15}\text{N}$ -root exudates or $^{15}\text{N}$ -urea fertilizer into the rhizosphere. The mean values for the substrate-derived $\text{N}_2\text{O}$ emissions are the pooled results for both time-points ( $n = 7$ for $^{15}\text{N}$ -root exudates due to a negative value; $n = 5$ for $^{15}\text{N}$ -urea due to negative values).....	145
<b>Table 4.2</b> The total and substrate-derived N in the soil and microbial biomass pools of the rhizosphere of annual ryegrass ( <i>L. multiflorum</i> ) plants measured 3, 9, 24 and 48 h after introducing $^{15}\text{N}$ -root exudates or $^{15}\text{N}$ -urea fertilizer into the rhizosphere. Each value is the mean $\pm$ standard error ( $n = 4$ , while those with an asterisk (*) were $n = 3$ due to negative values). ...	151
<b>Table 5.1</b> Range and mean of total and substrate-derived daily $\text{CO}_2$ emissions from the rhizosphere of annual ryegrass ( <i>L. multiflorum</i> ) plants measured 21 h and 45 h after the start of the final $^{13}\text{C}$ -labeling period. Mean values are mean $\pm$ standard error ( $n = 8$ ) except for those with an asterisk (*; $n = 7$ due to outliers).....	197
<b>Table 5.2</b> The total and substrate-derived C in the soil and microbial biomass pools of the rhizosphere of annual ryegrass ( <i>L. multiflorum</i> ) plants measured 0, 6, 21 and 45 h after the start of the final $^{13}\text{C}$ -labeling period. Rhizosphere soil ( $^{13}\text{C}$ ) is the difference between total ( $^{13}\text{C}$ ) found in the rhizosphere soil and ( $^{13}\text{C}$ ) in the microbial biomass. All values are the mean $\pm$ standard error ( $n = 4$ ) except for those with an asterisk (*; $n = 3$ due to negative values). .....	197

## LIST OF ABBREVIATIONS, SYMBOLS AND TERMS

$^{13}\text{C}$	carbon-13 isotope
$^{13}\text{C}$ -	$^{13}\text{C}$ -labeled
$^{13}\text{C}^{15}\text{N}$ -	$^{13}\text{C}^{15}\text{N}$ -labeled
$^{15}\text{N}$	nitrogen-15 isotope
$^{15}\text{N}$ -	$^{15}\text{N}$ -labeled
$^{15}\text{N}_\alpha$	the nitrogen atom in the inner (alpha) position of the nitrous oxide molecule; its $\delta^{15}\text{N}$ signature at natural abundance is necessary for site preference analysis
$^{15}\text{N}_\beta$	the nitrogen atom in the outer (beta) position of the nitrous oxide molecule; its $\delta^{15}\text{N}$ signature at natural abundance is necessary for site preference analysis
<b>16S rRNA</b>	a highly conserved gene for the rRNA component of the 30S ribosomal subunit in prokaryotes that the DNA or rRNA of which can be sequenced for taxonomic identification of archaea and bacteria
$^{18}\text{O}$	oxygen-18 isotope
$^{18}\text{O}$ -	$^{18}\text{O}$ -labeled
<b>18S rRNA</b>	a highly conserved gene for the rRNA component of the 40S ribosomal subunit found in eukaryotes that the DNA or rRNA of which can be sequenced for taxonomic identification of fungi, protists and animals
<b>ABC</b>	ATP-Binding Cassette protein transporter family
<b>absolute atm% excess</b>	percent of atoms enriched with isotope in excess of the control without accounting for the enrichment of the tracer
<b>AMO, Amo</b>	ammonia monooxygenase
<b>Amt</b>	Amt-type ammonia transporter protein
<b>ANOVA</b>	analysis of variance
<b>atm%, atom%</b>	percent of atoms enriched with isotope
<b>atm% excess</b>	percent of atoms enriched with isotope in excess of the control
<b>ATP</b>	adenosine triphosphate
<b>C</b>	carbon
<b>Chip-SIP</b>	stable isotope probing technique where the DNA or RNA of a microbial community exposed to a $^{13}\text{C}$ - and/or $^{15}\text{N}$ -labeled substrate is hybridized to predetermined probes on a microarray, or chip, to identify the microbes involved in a metabolic pathway and determine the degree of their involvement
<b>cNor</b>	cytochrome c-dependent nitric oxide reductase
<b>CO<sub>2</sub></b>	carbon dioxide
<b>CO<sub>2</sub>-C</b>	carbon dioxide in terms of carbon
<b>CO<sub>2</sub>e</b>	carbon dioxide equivalent

<b>CoA</b>	coenzyme A
<b>CsCl</b>	cesium chloride
<b>CsTFA</b>	cesium trifluoroacetate
<b>Cu</b>	copper
<b>CuANor</b>	copper-containing quinol-dependent nitric oxide reductase
<b>Cu-Hao</b>	copper-containing hydroxylamine oxidoreductase
<b>cyt c554</b>	cytochrome c554 enzyme
<b>cyt P460</b>	cytochrome P460 enzyme
<b><math>D_{0, O_2}</math></b>	diffusion of oxygen in air
<b><math>D_{S, O_2}</math></b>	diffusion of oxygen in soil
<b>dfr</b>	derived from root exudation or rhizodeposition
<b>diam</b>	diameter
<b>DNA</b>	deoxyribonucleic acid(s)
<b>e-</b>	electron(s)
<b>EPS</b>	extracellular polymeric substances
<b>FAO</b>	Food and Agriculture Organization of the United Nations
<b>Fe-Siderophores</b>	iron-siderophore complexes
<b>fum</b>	fumigated
<b>GHG</b>	greenhouse gas
<b>H<sup>+</sup></b>	proton(s)
<b>H<sub>2</sub>O</b>	water
<b>H<sub>2</sub>SO<sub>4</sub></b>	sulfuric acid
<b>HAO, Hao</b>	hydroxylamine oxidoreductase
<b>HCl</b>	hydrochloric acid
<b>IFA</b>	International Fertilizer Association
<b>IPCC</b>	Intergovernmental Panel on Climate Change
<b>ITS rRNA</b>	highly conserved spacer genes that the DNA or rRNA of which can be sequenced for taxonomic identification of fungi
<b>K, K<sub>2</sub>O</b>	potassium
<b>K<sub>2</sub>SO<sub>4</sub></b>	potassium sulfate
<b>KCl</b>	potassium chloride
<b><math>k_{EC}</math></b>	extraction coefficient for microbial biomass carbon
<b><math>k_{EN}</math></b>	extraction coefficient for microbial biomass nitrogen
<b><i>L.</i></b>	genus <i>Lolium</i>
<b>L., Lam.</b>	Lamarck
<b>MFS</b>	Major Facilitator Superfamily protein transporter family
<b>Mmo</b>	methane monooxygenase
<b>mRNA</b>	messenger ribonucleic acid(s)
<b>N</b>	nitrogen
<b>N<sub>2</sub></b>	dinitrogen

<b>N<sub>2</sub>O</b>	nitrous oxide
<b>N<sub>2</sub>O-N</b>	nitrous oxide in terms of nitrogen
<b>NADH</b>	nicotinamide adenine dinucleotide hydrogen
<b>NAP, Nap</b>	periplasmic nitrate reductase
<b>NAR, Nar</b>	cytoplasmic nitrate reductase
<b>NarG</b>	one monomer of the dimer active site of Nar
<b>NarH</b>	one monomer of the dimer active site of Nar
<b>NarK</b>	nitrite/nitrate protein porter
<b>NarO</b>	nitrate protein transporter
<b>NarT</b>	nitrate protein transporter
<b>NH<sub>2</sub>OH</b>	hydroxylamine
<b>NH<sub>3</sub></b>	ammonia
<b>NH<sub>4</sub><sup>+</sup></b>	ammonium
<b>NH<sub>4</sub>NO<sub>3</sub></b>	ammonium nitrate
<b>NirK,Cu-NirK</b>	copper-containing/dependent nitrite reductase
<b>NirS</b>	cytochrome cd1-type/iron-dependent nitrite reductase
<b>NO</b>	nitric oxide
<b>NO<sup>2-</sup></b>	nitrite
<b>NO<sup>3-</sup></b>	nitrate
<b>NOO, Noo</b>	nitric oxide oxidoreductase
<b>Nor, NorB, NorBC</b>	nitric oxide reductase
<b>NosZ</b>	nitrous oxide reductase
<b>NXR, Nxr</b>	nitrite oxidoreductase
<b>O, O<sub>2</sub></b>	oxygen
<b>P, P<sub>2</sub>O<sub>5</sub></b>	phosphorus
<b>P<sub>450</sub>-Nor</b>	cytochrome P450-type nitric oxide reductase
<b>pH</b>	power/potential of hydrogen; measure of acidity/basicity
<b>qNor</b>	quinol-dependent nitric oxide reductase
<b>qPCR</b>	quantitative polymerase chain reaction
<b>QS</b>	quorum sensing
<b>qSIP</b>	quantitative stable isotope probing; stable isotope probing technique using models that assume the normal distribution of taxa across buoyant density fractions and quantify the degree of enrichment of individual microbial taxa as a metric for metabolic rate
<b>R</b>	isotopic ratio
<b>Rh</b>	Rh-type ammonia transporter protein
<b>RNA</b>	ribonucleic acid(s)
<b>rRNA</b>	ribosomal ribonucleic acid(s)
<b>RT-qPCR</b>	reverse transcription quantitative polymerase chain reaction

<b>SIP</b>	stable isotope probing
<b>SMB</b>	soil microbial biomass
<b>SP</b>	site preference
<b>TCA</b>	tricarboxylic acid
<b>TNM</b>	total nitrogen module
<b>TOC</b>	total organic carbon
<b>TRAP</b>	Tripartite ATP-independent Periplasmic protein transporter family
<b>UHPLC-MS/MS</b>	ultra-high-performance liquid chromatography-tandem mass spectrometry
<b>unfum</b>	unfumigated
<b>USA</b>	United States of America
<b>USDA</b>	United States Department of Agriculture
<b>δ</b>	delta; isotopic signature
<b>θ</b>	theta; soil moisture
<b>π</b>	pi; cell osmotic potential
<b>ψ</b>	psi; matric potential

## CHAPTER 1

### 1. General introduction

#### 1.1 Background

Soils are the foundation of terrestrial ecosystems and are integral to global ecological processes. Yet, soil itself is a complex ecosystem and arguably the most diverse and populous on Earth. Although flora and macrofauna contribute to the bioabundance and biodiversity found in soils, microorganisms are vastly dominant in this environment, both in terms of biomass ( $>0.1$  kg carbon (C)  $m^{-2}$ ; Fierer 2017) and diversity (at least 1 trillion species in soil globally; Locey and Lennon 2016). Their immense phylogenetic diversity includes archaea, bacteria, fungi, protists, and viruses, altogether representing the soil microbiome.

Microorganisms drive the ecological processes in soil (e.g., decomposition, nutrient cycling, energy flow) via the oxidation of dissolved organic matter or reactive nitrogen (N) species and the reduction of final electron acceptors. However, these natural microbial functions result in the unavoidable respiration of potent greenhouse gases, like nitrous oxide ( $N_2O$ ) and carbon dioxide ( $CO_2$ ). These greenhouse gas-producing metabolic processes include (i) nitrification releasing  $N_2O$ , (ii) denitrification releasing  $N_2O$  and  $CO_2$ , (iii) nitrifier-denitrification releasing  $N_2O$  and  $CO_2$ , and (iv) aerobic respiration releasing  $CO_2$ .

Greenhouse gases produced by microorganisms can be consumed in soil by other microbial metabolic processes. However, if the rate of greenhouse gas production exceeds consumption,  $N_2O$  and  $CO_2$  will diffuse from the soil into the atmosphere. The emission of these greenhouse gases from soil is influenced by many soil factors that affect gas diffusion, such as temperature, pressure, humidity, moisture and porosity. Yet, fundamentally, microbial production of greenhouse gases is a substrate-driven process. The availability of reactive N (e.g.,

Avrahami et al. 2002, Kang et al. 2022) and C substrates (e.g., Rui et al. 2016) to microorganisms largely controls the magnitude of greenhouse gases released from soil. Sites rich in these substrates are conducive for microbial activity and considered greenhouse gas hotspots. These hotspots are especially common in cultivated soils because crop production creates a favorable soil environment for microorganisms around plant roots, known as the rhizosphere. Here, plants release substrates from their roots, known as root exudates and rhizodeposits, supplying this environment with assimilable N- and C-containing compounds. Additionally, the application of fertilizer infuses the rhizosphere with reactive N forms. Thus, this interface between root and soil contains the essential energy-rich substrates and nutrients for greenhouse gas production by the microbial community residing in the rhizosphere, known as the rhizobiome.

The rhizosphere of cultivated peatlands should be fertile ground for the genesis of greenhouse gas hotspots. When peatlands are first drained and tilled, the soil mixing disperses the peaty matrix, making it more porous and allowing gas and water diffusion, which encourages microbial processes that emit greenhouse gases. After crops are sown or transplanted, their root system releases N- and C-containing root exudates and rhizodeposits into the soil that fuel microbial growth. Agricultural activities such as fertilizer application and irrigation are also expected to stimulate microbial processes in cultivated peatlands. Furthermore, the ephemeral fine roots that are shed during the growing season, along with root and shoot residuals left after harvest, are processed by saprophytic bacteria, all of which respire CO<sub>2</sub> and release other gaseous byproducts during normal metabolism. At the same time, in contrast to mineral soils, the elevated organic matter content of cultivated peatlands (i.e., >200 g organic matter kg<sup>-1</sup>; Grenon et al. 2021) enriches the rhizosphere with a surplus of N and C substrates that may further fuel

microbial metabolism. If these conditions promote greenhouse gas hotspots in the rhizosphere, then we must understand their dynamics to reduce N<sub>2</sub>O and CO<sub>2</sub> emissions from cultivated peatlands. Yet, we lack detailed knowledge of the mechanisms behind hotspots. This issue stems from the complexity in quantifying microbial processes at the microscale, when the smallest functional unit that we can readily measure is at the milliscale, a difference of three orders of magnitude. Effectively, this means that we are generalizing discrete microbial processes and often neglecting to accurately represent the spatial heterogeneity of their microenvironments. Recent advancements in isotope technology hold promise to elucidate the mechanisms driving greenhouse gas production from hotspots. Thus, equipped with such knowledge, we may be able to better manage greenhouse gas hotspots of the rhizosphere to control microbially-mediated N<sub>2</sub>O and CO<sub>2</sub> emissions from cultivated peatlands.

## **1.2 Research objectives**

The purpose of my Ph.D. research is to investigate the status of the rhizosphere as a hotspot of N<sub>2</sub>O and CO<sub>2</sub> production in a temperate cultivated peatland (Figure 1.1). The five specific objectives of my research are:

1. Identify the most sensitive method for quantifying the assimilation of N derived from root exudates by the rhizobiome via comparing the capacity of different plant labeling methods to enrich the rhizobiome of the ryegrass (*Lolium multiflorum*) rhizosphere with <sup>15</sup>N.
2. Assess the potential of root exudates as a substrate used for microbial N<sub>2</sub>O production by confirming the assimilation of nitrogenous root exudates from ryegrass (*Lolium multiflorum*) by the rhizobiome in N-fertilized soil from a cultivated peatland.

3. Determine the role of root exudates as N source for microbial N<sub>2</sub>O production in the rhizosphere through <sup>15</sup>N-tracing.
4. Estimate the dominant pathway(s) of microbial N<sub>2</sub>O production in the ryegrass (*L. multiflorum*) rhizosphere of soil from a cultivated peatland through site preference analysis.
5. Partition the contributions of ryegrass (*L. multiflorum*) rhizodeposits, urea and peat to the CO<sub>2</sub> emissions from the plant-rhizosphere soil system under N fertilization through <sup>13</sup>C-tracing.

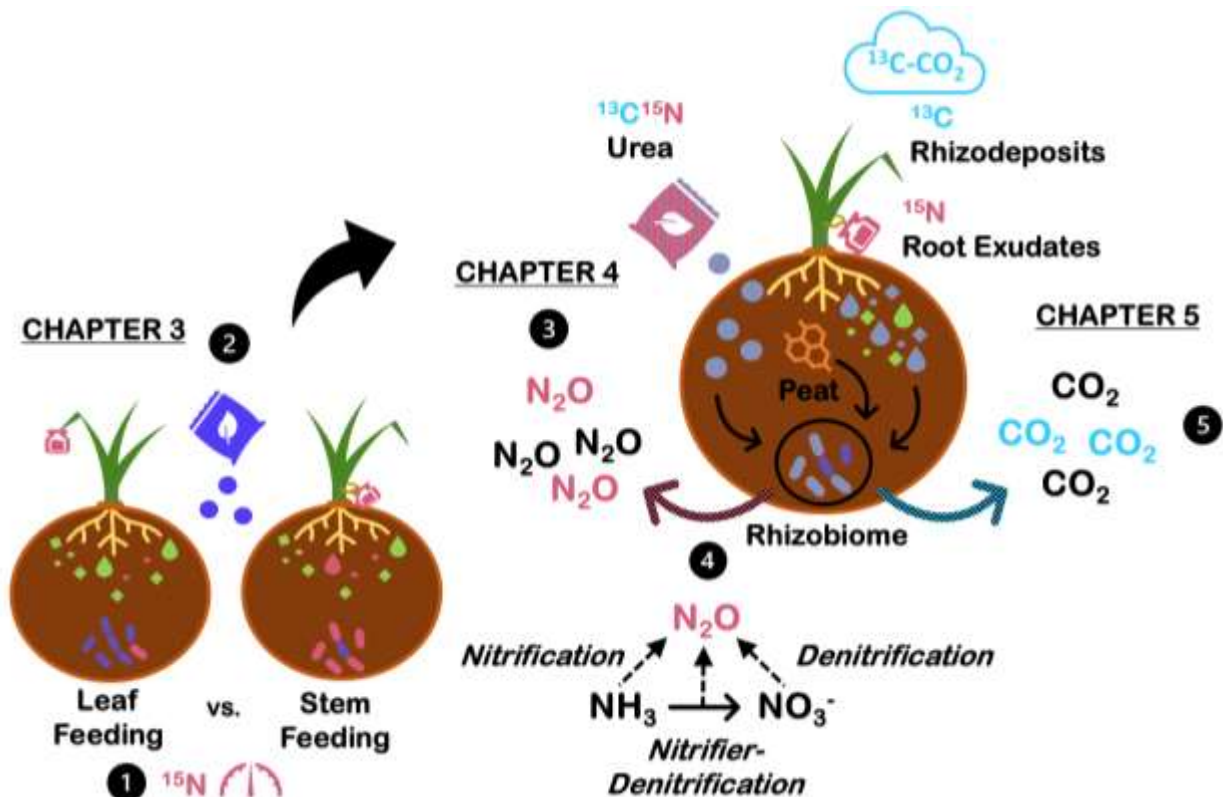


**Figure 1.1** Conceptual diagram of the research conducted to address the objectives of my thesis.

Numbers represent the objectives addressed.

### 1.3 Synopsis of the research methods and significance of the study

Hotspots of intense microbial greenhouse gas production in cultivated peatlands are expected to occur at sites with high availability of easily assimilable N and C substrates, like the rhizosphere. Such an assessment of the rhizosphere is possible by following the N and C cycles occurring in this environment through isotope tracing with relevant substrates, such as root exudates, rhizodeposits and fertilizers (e.g., urea).

This research employed isotope tracing with  $^{15}\text{N}$  and  $^{13}\text{C}$  using  $^{15}\text{N}$ -root exudates,  $^{13}\text{C}$ -rhizodeposits and  $^{13}\text{C}^{15}\text{N}$ -urea during greenhouse experiments with annual ryegrass (*L. multiflorum*) plants to track the fate of N and C in the rhizosphere of soil from cultivated peatlands. For these experiments,  $^{13}\text{C}^{15}\text{N}$ -urea is easily purchased from chemical suppliers, but root exudates and rhizodeposits are more difficult to label. Their generation requires isotopically labeling plants with both  $^{15}\text{N}$  and  $^{13}\text{C}$ , which subsequently enriches their root exudates and rhizodeposits with these tracers. Incorporating  $^{13}\text{C}$  into rhizodeposits is simpler as plants will fix  $^{13}\text{C}$  naturally via photosynthesis when exposed to  $^{13}\text{C}$ - $\text{CO}_2$  and transfer this  $^{13}\text{C}$  to their roots. In contrast, introducing  $^{15}\text{N}$  into plants for  $^{15}\text{N}$ -root exudate generation is more difficult since  $^{15}\text{N}$  cannot be added to soil, the natural route for plant N uptake. Clever methods have been developed to generate root exudates enriched in  $^{15}\text{N}$ , such as by exposing the plant to  $^{15}\text{N}$ -compounds (e.g., urea, ammonium nitrate ( $\text{NH}_4\text{NO}_3$ )) via plant stem feeding, leaf tip feeding or foliar application. However, studies using such methods have yet to confirm (i) the metabolism of the generated  $^{15}\text{N}$ -root exudates by the microbiome in cultivated soils where reactive N is abundant or (ii) the transformation of nitrogenous root exudates into  $\text{N}_2\text{O}$  through  $^{15}\text{N}$  enrichment analysis. To do so, the  $^{15}\text{N}$ -labeling method must generate sufficient  $^{15}\text{N}$ -enriched root exudates so that the  $^{15}\text{N}$ -tracer can be detected in the microbial biomass and emitted  $\text{N}_2\text{O}$ .

Altogether, this research contributes to a more comprehensive understanding of the mechanisms at the core of greenhouse gas production from the rhizosphere in cultivated peatlands. The findings from this work can be used to improve our ability to accurately measure greenhouse gases from cultivated peatlands and predict the magnitude of N<sub>2</sub>O and CO<sub>2</sub> emissions from the rhizosphere as a greenhouse gas hotspot. These contributions to knowledge can also be used to improve biogeochemical models and national inventories on greenhouse gases based on finer-scale (Tier II and Tier III) methodologies. Thus, with my research, we can better reflect the reality of hotspot emissions from cultivated peatlands and include their management in the climate-smart future of agriculture.

#### **1.4 Thesis structure**

This work is a manuscript-based thesis. Chapter 2 summarizes the current literature relevant to this thesis. Chapters 3 addresses objectives 1 and 2, Chapter 4 addresses objectives 3 and 4, and Chapter 5 addresses objective 5. These chapters are written as manuscripts in the acceptable format for publication in peer-reviewed journals. Chapter 6 is a general discussion on the contributions to knowledge from my research. Chapter 7 is a final conclusion.

## 1.5 References

- Avrahami, S., Conrad, R., Braker, G., 2002. Effect of soil ammonium concentration on N<sub>2</sub>O release and on the community structure of ammonia oxidizers and denitrifiers. *Applied and Environmental Microbiology* 68, 5685–5692. <https://doi.org/10.1128/AEM.68.11.5685-5692.2002>.
- Fierer, N., 2017. Embracing the unknown: disentangling the complexities of the soil microbiome. *Nature Reviews Microbiology* 15, 579–590. <https://doi.org/10.1038/nrmicro.2017.87>.
- Grenon, G., Singh, B., De Sena, A., et al., 2021. Phosphorus fate, transport and management on subsurface drained agricultural organic soils: A review. *Environmental Research Letters* 16, 013004. <https://doi.org/10.1088/1748-9326/abce81>.
- Kang, H., Lee, J., Zhou, X., et al., 2022. The effects of N enrichment on microbial cycling of non-CO<sub>2</sub> greenhouse gases in soils – A review and a meta-analysis. *Microbial Ecology* 84, 945–957. <https://doi.org/10.1007/s00248-021-01911-8>.
- Locey, K.J., Lennon, J.T., 2016. Scaling laws predict global microbial diversity. *Proceedings of the National Academy of Sciences* 113, 597–5975. <https://doi.org/10.1073/pnas.1521291113>.
- Rui, Y., Murphy, D.V., Wang, X., et al., 2016. Microbial respiration, but not biomass, responded linearly to increasing light fraction organic matter input: Consequences for carbon sequestration. *Scientific Reports* 6, 35496. <https://doi.org/10.1038/srep35496>.

## **FORWARD TO CHAPTER 2**

The objective of Chapter 2 is to critically review our current knowledge on microbially mediated greenhouse gas production in the rhizosphere hotspots of cultivated peatlands. First, I consider the significance of the CO<sub>2</sub> and N<sub>2</sub>O emissions generated from cultivated peatlands. Then, I describe the rhizosphere as a source of greenhouse gases in soils under crop production. I discuss the soil properties of the rhizosphere that make this soil zone ideal for microbial activity, including those unique to cultivated peatlands, and thus, the development of greenhouse gas hotspots. Subsequently, I examine the different greenhouse gas-producing pathways that can occur in hotspots of the rhizosphere and the microorganisms that mediate them. Finally, I review the most promising methodological techniques for the assessment of microbial CO<sub>2</sub> and N<sub>2</sub>O production in greenhouse gas hotspots of the rhizosphere.

## CHAPTER 2

### **2. The role of the rhizosphere as a hotspot of microbial CO<sub>2</sub> and N<sub>2</sub>O production in cultivated peatlands: A review**

#### **2.1 Greenhouse gas emissions from cultivated peatlands**

Peatlands are either natural wetlands (e.g., fens, bogs, pocosins, swamps) or derived from them. Despite only occupying 2–5% of the global land area (2.6–4.4 million km<sup>2</sup>; Carlson et al. 2017, Berglund et al. 2019), peatlands represent one third of soil carbon (C) storage in the world (~445.7 Pg C; Berglund et al. 2019, Lahtinen et al. 2022). This vast C stock originates from the arrested breakdown of organic matter (i.e., plant residues) in saturated peat environments (Kasimir-Klemedtsson et al. 1997), most of which have existed since the last glaciation period in the early Holocene (Maljanen et al. 2010, Yu et al. 2010). The resulting peat is rich in C and nitrogen (N), but these chemical elements will remain in the organic matter if anoxic conditions persist. Consequently, peatlands can either be a sink or source of C and N, depending on their saturation and oxygen (O<sub>2</sub>) concentration since these factors control microbial metabolism.

Beginning in the 1800s (Glenn et al. 1993), the urgent need for land during the industrialization of agriculture resulted in the drainage of many peatlands (~250,000 km<sup>2</sup>; Lahtinen et al. 2022). Expansion of agricultural activities was especially prevalent in the Northern Hemisphere, where boreal and temperate peatlands were drained in Scandinavia (2–40%; Kløve et al. 2017), Central Europe (70–85%; Berglund et al. 2019) and southern Ontario and Québec (20–50%; Glenn et al. 1993). Draining these peatlands created productive soils that continue to support high-value crops like cereals (oats, barley, spring wheat), vegetables (carrots, celery, onions, potatoes, parsnips) and grasses for grazing (Rochette et al. 2010, Norberg et al. 2016a, b, Kløve et al. 2017, Lloyd et al. 2019). However, cultivation alters the C and N dynamics

of the peatlands. Draining peatlands creates oxic conditions that favor microbial mineralization of peat, releasing carbon dioxide (CO<sub>2</sub>) and reactive N forms (i.e., ammonium (NH<sub>4</sub><sup>+</sup>), nitrite (NO<sub>2</sub><sup>-</sup>), nitrate (NO<sub>3</sub><sup>-</sup>)), the precursors of nitrous oxide (N<sub>2</sub>O) emissions (Kløve et al. 2017). Tillage aerates these soils and exposes fresh peat to further mineralization (Elder and Lal 2008). Additionally, cultivated peatlands absorb solar radiation due to their dark color (Elder and Lal 2008), increasing soil temperature and promoting microbial activity. Lastly, amending these soils with N fertilizers supplies reactive N as a substrate for N<sub>2</sub>O-producing microbes (Norberg et al. 2016a, Kløve et al. 2017). Thus, cultivation transforms peatlands from C and N sinks to sources of CO<sub>2</sub> and N<sub>2</sub>O.

Globally, cultivated peatlands are responsible for ~32% of greenhouse gas emissions from croplands, 89% of which is CO<sub>2</sub> and 11% of which is N<sub>2</sub>O (Figure 2.1; Carlson et al. 2017). In temperate and boreal climates, annual emissions from cultivated peatlands are 350–3000 g CO<sub>2</sub>-C m<sup>-2</sup> y<sup>-1</sup> and 30–9600 mg N<sub>2</sub>O-N m<sup>-2</sup> y<sup>-1</sup>, with mean fluxes reaching maximums of 1200 mg CO<sub>2</sub>-C m<sup>-2</sup> h<sup>-1</sup> and 6250 µg N<sub>2</sub>O-N m<sup>-2</sup> h<sup>-1</sup> (Elder and Lal 2008, Maljanen et al. 2010, Rochette et al. 2010, Petersen et al. 2012, Norberg et al. 2016a, b, Lloyd et al. 2019). Despite occupying a minor portion of Earth's surface, cultivated peatlands are represented disproportionately in greenhouse gas inventories compared to other land uses. For example, emissions from drained peatlands represent 6–8% of the domestic greenhouse gas budget of Sweden, even though this land use only occupies 2% of its land area (Kløve et al. 2017, Norberg et al. 2021). As such, cultivated peatlands pose a substantial climate risk due to their capacity to produce greenhouse gases.

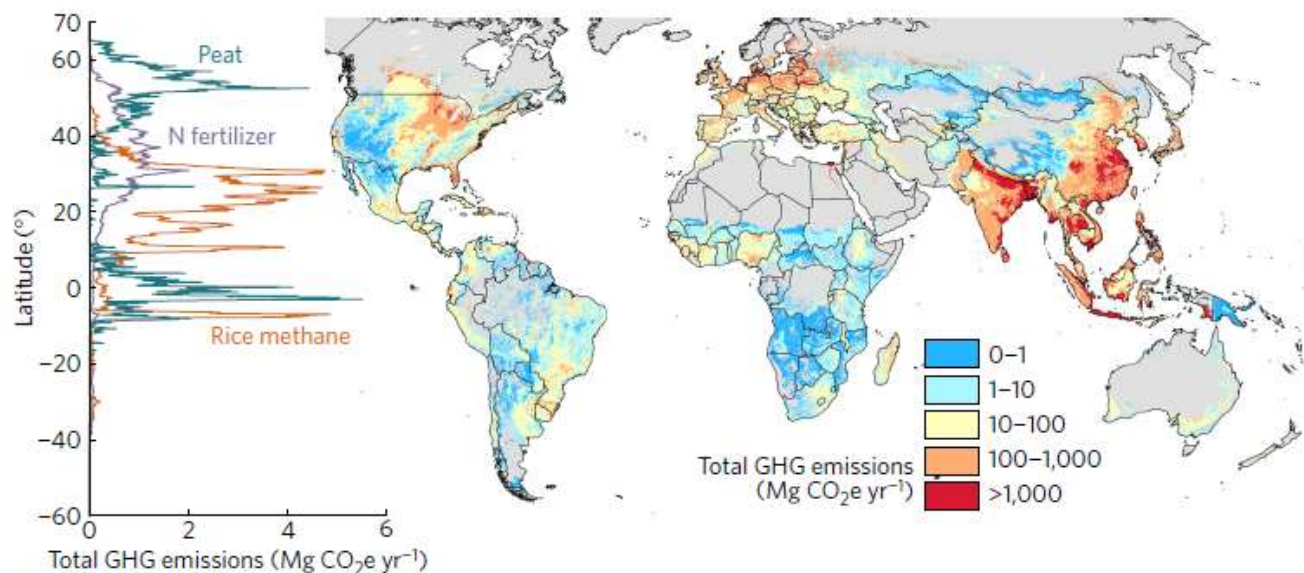


**Figure 2.1** Latitudinal plot and map demonstrating the contribution of cultivated peatlands circa 2000 to total greenhouse gas (GHG) emissions ( $\text{Mg CO}_2\text{e yr}^{-1}$ ) in comparison to N fertilizer and methane from rice cultivation, the top GHG sources from global croplands (Carlson et al. 2017).

### 2.1.1 Soil factors affecting greenhouse gas emissions from cultivated peatlands

Studies on greenhouse gas emissions from cultivated peatlands have identified several important soil factors that control microbially generated  $\text{CO}_2$  and  $\text{N}_2\text{O}$ .

#### 2.1.1.1 Physical factors

Physical properties of peatland soils, primarily soil structure and moisture, are crucial factors to understand soil emissions. The diffusivity of greenhouse gases is governed by soil structure, a dynamic characteristic in peatlands. These soils have a high degree of porosity (0.68–0.81; Elder and Lal 2008, Lloyd et al. 2019) due to their low bulk density ( $0.21\text{--}0.39 \text{ g cm}^{-3}$ ; Lloyd et al. 2019, De Sena et al. 2022a). Yet, as peat decomposes during microbial oxidation, the soil compacts and reduces gas diffusivity (Kasimir-Klemedtsson et al. 1997). Similarly, the soil structure in cultivated peatlands will change with moisture. Peat expands when it absorbs water,

limiting gas diffusivity. Upon drying, peat soils contract and soil pores collapse (Kasimir-Klemedtsson et al. 1997) but newly-formed cracks and fissures create new pathways for gas diffusion.

Soil moisture also has consequences for biological activity, which influences greenhouse gas production. Upon wetting, peat can retain soil moisture for extended periods through its absorbent properties (Rezanezhad et al. 2016). However, drying will expose the hydrophobic moieties of peat. This dual nature means that peat can either attract or repel water (Michel and Kerloch 2017), which helps determine whether aerobic or anaerobic processes dominate microbially mediated greenhouse gas production in peatland soils. At the macroscale, the groundwater level of cultivated peatlands impacts greenhouse gas production. The depth of the water table determines the extent of O<sub>2</sub> penetration in the soil profile, meaning that more mineralization occurs in a larger volume of soil when water table depth is low. For example, CO<sub>2</sub> emissions increased by as much as four-fold due to the microbial mineralization of peat when soil moisture was reduced to levels emulating a water table of 20–60 cm below the soil surface (Säurich et al. 2019). Pulses of N<sub>2</sub>O flux are observed during wetting-drying events (i.e., irrigation, water table management, precipitation), suggesting that water table fluctuations generate N<sub>2</sub>O (Norberg et al. 2021). Consequently, structural dynamics and changes in soil moisture are associated with the variation in CO<sub>2</sub> and N<sub>2</sub>O released from cultivated peatlands.

#### *2.1.1.2 Chemical factors*

Peatland chemical characteristics relevant to greenhouse gas emissions include soil organic C, total N, and nutrient availability. While CO<sub>2</sub> emissions are not consistently related to total soil organic C stocks in cultivated peatlands, the proportion of soil organic C located above the water table corresponds to CO<sub>2</sub> production. For example, more than 87% of the variation in CO<sub>2</sub>

emissions was explained by organic C stocks and groundwater level in three cultivated soils, including two peatlands (Pohl et al. 2015). Available C substrates (e.g., glucose) can also trigger N<sub>2</sub>O emissions, suggesting that despite the rich soil organic C stocks in peatlands, N<sub>2</sub>O-producing microbes in these soils are C-limited (Amha and Bohne 2011, Miller et al. 2012). Like soil organic C, soil N stocks above the water table are also predictive of CO<sub>2</sub> emissions (Pohl et al. 2015). Although C and N are important determinants of CO<sub>2</sub> and N<sub>2</sub>O production, other nutrients required for microbial activity can affect their overall metabolism and production of greenhouse gases in cultivated peatlands. Peak CO<sub>2</sub> fluxes from peat columns were strongly linked to soil available phosphorus ( $r = 0.85$ ) and potassium ( $r = 0.86$ ; Säurich et al. 2019). Similarly, phosphorus availability explained 46–75% of N<sub>2</sub>O fluxes from Scandinavian peatlands – 73% of which were either under active cultivation or cultivated previously (Liimatainen et al. 2018) – while copper explained nearly all (~98%) of the N<sub>2</sub>O production occurring from peat microcosms (Liimatainen et al. 2018). Thus, the production of CO<sub>2</sub> and N<sub>2</sub>O in cultivated peatlands is influenced by soil chemical characteristics.

### *2.1.1.3 The effect of peat soil factors on microbial greenhouse gas production*

Despite the evidence for edaphic control of microbial greenhouse gas emissions from cultivated peatlands, we are still unsure of the dominant microbial pathway that produce CO<sub>2</sub> and N<sub>2</sub>O from these soils. The porous nature of cultivated peat appears to permit sufficient aeration, which is necessary for CO<sub>2</sub> generation by aerobic respiration and N<sub>2</sub>O generation by nitrification.

Alternatively, anaerobic conditions may dominate cultivated peatlands due to water retention by peat and fluctuating water table levels in peatlands, which trigger CO<sub>2</sub> and N<sub>2</sub>O production via denitrification. Moreover, if cultivated peatlands frequently oscillate between aerobic and anaerobic conditions, nitrifier-denitrification would likely be the dominant process that produces

CO<sub>2</sub> and N<sub>2</sub>O. However, these scenarios remain to be investigated with appropriate analytical techniques. Isotopic analysis is a robust procedure to decipher the dominant pathways of greenhouse gas production in cultivated peatlands, as will be discussed below (See Section 2.4).

## **2.2 The rhizosphere as a greenhouse gas hotspot**

Crop roots create conditions in the rhizosphere that differ from the bulk soil with regards to physical and chemical properties. These rhizosphere effects are spatially heterogeneous, depending on macroscale field conditions – like soil structure, the crop grown, and agronomic practices (i.e., tillage) – and characteristics of the root-specific microenvironment – like moisture and root type (e.g., root hair, tap root).

### ***2.2.1 Rhizosphere properties relevant to soil greenhouse gas emissions***

#### ***2.2.1.1 Physical properties***

Plant roots manipulate the porosity of the soil by compacting soil particles via root growth, stabilizing pore structures via root networks, and generating biopores following turnover of dead roots (Bodner et al. 2014, Kuzyakov and Blagodatskaya 2015, Koebernick et al. 2017, Helliwell et al. 2019, Lucas et al. 2019). Such modifications to porosity are important to greenhouse gas production since pores are a conduit for water, O<sub>2</sub> and greenhouse gases. The characteristics of the rhizosphere pore network (e.g., pore water distribution, surface area, air flow status) also create unique microhabitats for microorganisms to colonize and subsequently affect their abundance, diversity and activity. Decreased pore connectivity and pore size tend to increase microbial abundance (9–10-fold) and diversity (48–52%), suggesting that isolated, small pores create specialized niches in the soil environment (Carson et al. 2010, Hartmann and Six 2023). For example, large pores (>30 µm) containing plant residue with high connectivity hosted copiotrophs from phyla Bacteroidetes, Actinobacteria and Firmicutes, whereas smaller pores

with reduced connectivity hosted these copiotrophs but also oligotrophs from Acidobacteriae (Negassa et al. 2015). Additionally, fungi reside on microaggregate surfaces and in large pores ( $>10\ \mu\text{m}$ ; Chenu et al. 2001, Gupta and Germida 2015, Hartmann and Six 2023). This separation implies niche specialization based on porosity.

Likewise, roots regulate the moisture content in the rhizosphere via their rapid and constant uptake of soil pore water. This regulation is important because moisture can control the soil redox conditions and thereby affects the electron acceptors and donors available to microorganisms for  $\text{CO}_2$  and  $\text{N}_2\text{O}$  production. The wicking effect associated with roots increases the aggregation of soil particles relative to the surrounding bulk soil (Moradi et al. 2011), leaving more voids that increase porosity, hydraulic conductivity and contribute to the greater water holding capacity of the rhizosphere. Water uptake by roots also drives soil water flux in the rhizosphere, which is necessary for microbial movement and the diffusion of essential substrates for the metabolism of rhizosphere microbes. However, under dry conditions, mucilage secreted by roots may prevent excessive moisture loss (Carminati et al. 2010, Moradi et al. 2011). This retention of water in the rhizosphere buffers microbial life from water stress. As such, the porosity and moisture of the rhizosphere are properties modulated by crop roots, which will affect microbial greenhouse gas production.

#### *2.2.1.2 Chemical properties*

The rhizosphere also provides ample soluble C substrates for the microbial metabolic processes that drive  $\text{CO}_2$  and  $\text{N}_2\text{O}$  production. Dissolved monomeric and oligomeric C substrates are essential for greenhouse gas production as their metabolism by microorganisms leads to the release of  $\text{CO}_2$  and  $\text{N}_2\text{O}$ . Such organic substrates are abundant in the crop rhizosphere as plants release C-rich substances from their roots, in a process called rhizodeposition. Rhizodeposits

consist of complex carbonaceous materials like ephemeral roots, but also simple low- and high-molecular-weight organic compounds exuded via passive and active processes, known as root exudates. These root exudates can represent a considerable amount of the total C fixed by plants via photosynthesis (5–21%) and include compounds like amino acids, simple sugars, organic acids, fatty acids, sterols, plant growth factors, vitamins, enzymes and proteins, phenolics, terpenes and terpenoids (De Sena et al. 2022b). The metamorphosis of photosynthates in a plant to root exudates in the rhizosphere is swift, often occurring in a matter of hours for grasses and crops (Bardgett and van der Putten 2014) and ensures a dependable energy source for microbes. The residence time of low-molecular-weight C compounds like root exudates can span from seconds to days due to their rapid microbial consumption, compared to the relatively long turnover periods associated with particulate organic matter (days to years), aggregate C (years to decades) and mineral associated organic matter (decades to centuries; Abramoff et al. 2018). As much as 50% of these organic substrates are metabolized in a few hours by the root-associated microbiome once exuded into the rhizosphere (Bardgett and van der Putten 2014), deriving up to 80% of their C from root exudates (Hütsch et al. 2002). These C substrates act as a selecting force for microbial activity and community composition. Root exudates can stimulate denitrifier activity by a factor of five under anaerobic conditions (90% water-filled pore space; Langarica-Fuentes et al. 2018). In terms of microbial composition, root exudates attract both copiotrophs (microbes with ~8% greater rRNA operon count in the rhizosphere; Ling et al. 2022) and oligotrophs (microbes with generation time ~2 times longer on average in rhizosphere; Zhalnina et al. 2018). This effect may indicate that root exudation provides simple C substrates, which favor copiotrophic lifestyles, while also providing a reliable supply of energy that permits the slow-growth patterns associated with oligotrophic microbes. Regardless of microbial life history,

the perpetual release of rhizodeposits during a plant's lifespan sustains the metabolism of the rhizosphere microbiome, and therefore, their respiration of greenhouse gases.

Rhizodeposits also alter the mineralization of organic matter in the rhizosphere through the rhizosphere priming effect (Huo et al. 2017). If these C substrates satisfy the nutrient requirements of rhizosphere microorganisms, rhizodeposition will depress the microbial mineralization of organic matter (Dijkstra et al. 2013). If not, rhizodeposits will induce a stoichiometric imbalance in microbes, resulting in the microbial release of extracellular enzymes capable of depolymerizing soil organic matter, like peat. The enzymes will break down the organic matter into assimilable organic substrates that microbes can metabolize and scavenge for N and other nutrients. These processes – known as negative and positive rhizosphere priming, respectively – have been observed in the field. Nonetheless, positive rhizosphere priming is more likely to occur, with organic matter decomposition increasing by 59%, on average (Huo et al. 2017), and stimulating the microbial production of CO<sub>2</sub> (Cheng et al. 2003, Kuzyakov 2006) and N<sub>2</sub>O (Ai et al. 2020). Thus, rhizodeposition is a fundamental controller of organic matter mineralization by microbes, which has direct consequences on greenhouse gas production from the rhizosphere.

In addition to being C substrates, some rhizodeposits also contain N – like root exudates including amino acids, proteins and some organic acids – and can represent up to 15% of the total N acquired by plants during the growing season (Sasse et al. 2018). Microbes can transform organic N into reactive N either through the production of extracellular enzymes that mineralize N (e.g., aminization, urea hydrolysis) or the assimilation of organic N forms that are mineralized internally (e.g., ammonification). Despite our thorough understanding of the microbial metabolism of rhizodeposit-derived C, the amount of N that microorganisms derive from root

exudates in cultivated soils and the resulting N<sub>2</sub>O emissions remain to be investigated via isotope tracing with <sup>15</sup>N-labeled root exudates.

In the rhizosphere of cultivated soils, most of the reactive N comes from nitrogenous fertilizers (e.g., anhydrous urea, NH<sub>4</sub>NO<sub>3</sub>, manure). Farmers apply fertilizer to ensure the peak performance of crops, often in bands next to the growing root system. This placement ensures efficient diffusion of the fertilizer to the crop root system. As application rates can be as high as 150 kg N ha<sup>-1</sup> depending on the crop, the rhizosphere is inundated with reactive N. Although some of the N is taken up by the plant, crop N use efficiency is typically low (25–50%; Javed et al. 2022). Incomplete absorption of fertilizer N leaves a substantial amount of reactive N in the rhizosphere that can be metabolized by the microbial community. For example, total bacterial abundance rose by ~22%, on average, with a 5-fold increase in urea-N application rate (Zhu et al. 2016). Further investigation is required to determine whether this change was in direct response to the urea, the associated change in rhizodeposition (~130% increase), or a combination of both. Reactive N forms also function as key reagents in microbial metabolism. NO<sub>3</sub><sup>-</sup> and subsequent intermediates serve as electron acceptors during the denitrification reactions, whereas ammonium (NH<sub>4</sub><sup>+</sup>) is the initial substrate oxidized during nitrification and nitrifier-denitrification. Accordingly, N fertilization increases the abundance of genes associated with both nitrification (500%) and denitrification (74–78%) in the rhizosphere (Zhu et al. 2016, Ouyang et al. 2018). Thus, rhizodeposition and fertilization introduce reactive N forms into the rhizosphere that can serve as metabolic substrates for greenhouse gas production.

### *2.2.1.3 The effect of the rhizosphere on microbial greenhouse gas production*

Farmers prepare a hospitable environment for crops through soil modification (e.g., fertilization) that encourages the development of a robust root network. The subsequent crop root system

makes further modifications to the soil by adjusting soil structure and moisture and releasing assimilable C and N substrates that encourage the growth and activity of root-associated microorganisms. As such, the rhizosphere is the nexus of the soil factors that control microbial respiration and thus is a greenhouse gas hotspot. That being said, the crop rhizosphere suppresses nitrification compared to the bulk soil (~35% decrease in gene abundance; Ling et al. 2022), suggesting that fluctuating oxic conditions created by the O<sub>2</sub> consumption of roots and oxidizing microbes promote microaerophilic and anaerobic processes (Lecomte et al. 2018). It may be that nitrification is less important than denitrification as a N<sub>2</sub>O-producing process in the rhizosphere. However, whether these conditions hold in the rhizosphere of cultivated peatlands remains to be seen. For example, the dry conditions from root water uptake and associated peat shrinkage would preserve pore connectivity and favor aeration of the rhizosphere. We are also unsure of how certain triggers contribute to the total greenhouse gas emissions from the rhizosphere of cultivated peatlands, like rhizodeposition and nitrogenous fertilizers. Thus, deducing the mechanisms driving emissions from the greenhouse gas hotspots of the rhizosphere requires research using <sup>13</sup>C<sup>15</sup>N-isotope tracing.

### **2.3 Microbial greenhouse gas production**

This section focuses on the major microbial pathways of CO<sub>2</sub> and N<sub>2</sub>O production in cultivated soils. Other microbial pathways can produce CO<sub>2</sub> (e.g., fermentation) and N<sub>2</sub>O (e.g., anaerobic ammonia (NH<sub>3</sub>) oxidation) in soils, but these processes are likely a minor source of greenhouse gases because cultivated peatlands are drained and mechanically cultivated to generate aerobic soil conditions for crop growth. Abiotic soil processes can also produce greenhouse gases (e.g., N<sub>2</sub>O derived from chemodenitrification; Chalk and Smith 2020). However, microbial pathways are likely more important to CO<sub>2</sub> and N<sub>2</sub>O production occurring in the rhizosphere of cultivated

peatlands than abiotic sources due to their environmental conditions being conducive for biological activity, as discussed above. While soils can also produce methane (CH<sub>4</sub>), studies on peatlands under intensive cultivation have demonstrated these soils are typically CH<sub>4</sub> sinks (Lloyd et al. 2019). Thus, the following sections describe the metabolic pathways, enzymes, microbial actors and triggers of aerobic respiration, nitrification, denitrification, and nitrifier-denitrification.

### ***2.3.1 Aerobic respiration***

Aerobic respiration is the fundamental catabolic pathway for non-photosynthetic microorganisms – known as organoheterotrophs – and releases CO<sub>2</sub> as a byproduct. The pervasiveness of this metabolic process across phylogenetic groups is a direct result of its efficiency. By using O<sub>2</sub> as the final electron acceptor, microbes can achieve maximal energy production, producing up to five moles of the energy molecule, adenosine triphosphate (ATP), per mole of assimilated C (Fenchel et al. 2012). While assimilated C is used to build microbial biomass, microorganisms will dedicate a portion of their C intake for aerobic respiration to profit from its immense energetic capacity. For example, soil bacteria allocate an estimated  $38 \pm 17\%$  of assimilated C to respiration (Saifuddin et al. 2019). Yet, with this portion, the soil microbiome produces approximately  $3.60 \times 10^{-6}$  Watts g biomass C<sup>-1</sup> (Hoehler et al. 2023). To harvest this energy by aerobic respiration, microbes must convert assimilated C substrates into acetyl-coenzyme A (CoA), oxidize this newly formed acetyl-CoA by the tricarboxylic acid (TCA) cycle, and perform oxidative phosphorylation, which releases CO<sub>2</sub>.

Microorganisms catabolize a wide range of assimilated C substrates via aerobic respiration, such as sugars, amino acids and lipids. However, these substrates must first be transformed into acetyl CoA, the molecule required for entry into the TCA cycle. Some of the

biochemical pathways that generate acetyl-CoA produce CO<sub>2</sub>. For example, glucose undergoes glycolysis into pyruvate, which is then catabolized into acetyl-CoA by pyruvate dehydrogenase, releasing CO<sub>2</sub> (Wessner et al. 2013). In contrast, assimilated lipids are dismantled into separate fatty acid chains by lipases before undergoing beta-oxidation into acetyl-CoA, all occurring without the emission of CO<sub>2</sub>. Thus, converting some, but not all, substrates into acetyl-CoA can release CO<sub>2</sub>.

With the assimilated substrate converted into acetyl-CoA, aerobic respiration can continue via the TCA cycle (i.e., Krebs cycle, citric acid cycle) and oxidative phosphorylation. The TCA cycle will transform the newly-created acetyl-CoA into various metabolites. The main purpose of this cycle is to produce electron carriers (i.e., nicotinamide adenine dinucleotide hydrogen (NADH)) for oxidative phosphorylation, releasing two moles of CO<sub>2</sub> with each rotation (Wessner et al. 2013). These generated NADH will undergo oxidative phosphorylation and transfer their electrons to the electron transport chain for ATP synthesis. However, this final process of aerobic respiration does not emit CO<sub>2</sub>. Consequently, microbes can only release CO<sub>2</sub> during the conversion of the assimilated C into acetyl-CoA and the TCA cycle.

#### *2.3.1.1 Microbial actors of aerobic respiration*

Aerobic respiration-derived CO<sub>2</sub> is emitted from a phylogenetically diverse assemblage of microbes with various life strategies. As a result, there is considerable diversity in this pathway. For example, while the entire pathway of archaeal and bacterial respiration occurs in the cytosol of their cells, fungi perform the final step of oxidative phosphorylation on the membranes of their eukaryotic cell organ, the mitochondrion. Certain microbial groups alter steps in aerobic respiration processes, like glycolysis and the TCA cycle (Wessner et al. 2013). Although some microbes depend on aerobic respiration as their sole catabolic process, most are facultative

aerobes, capable of performing both aerobic respiration and anaerobic catabolic processes. This diversity is reflected directly in the variety of genes (e.g., cytochrome oxidases) controlling aerobic respiration across domains (Eggleston et al. 2015). Since aerobic respiration appears to have evolved multiple times in microbes, it is a universal metabolic process for most microorganisms, regardless of their phylogeny.

#### *2.3.1.2 Soil factors affecting CO<sub>2</sub> production by aerobic respiration*

Aerobic respiration – and its corresponding CO<sub>2</sub> emissions – depend on the physical characteristics of soil, including porosity and moisture. These two soil properties are important because they control the availability of O<sub>2</sub>, the terminal electron acceptor required for aerobic respiration to proceed. Increased soil porosity and pore connectivity ensure the circulation of air, bringing in fresh O<sub>2</sub> from the atmosphere and cycling out respired greenhouse gases from the pore space. In general, soil must have a relative O<sub>2</sub> diffusivity ( $D_{S, O_2}/D_{0, O_2}$ ) of  $\geq 0.005$ – $0.025$  for aerobic microbial activities (e.g., nitrification), depending on soil texture (Schjønning et al. 2003). However, this variable was not specifically measured for aerobic respiration, and the current literature does not describe the optimal diffusivity in soil for other parameters related to aerobic respiration (i.e., microbial metabolic quotient, heterotrophic respiration). Such information is necessary to ensure proper representation of soil porosity and its effect on aerobic respiration in models of soil C stocks.

Likewise, soil moisture affects the capacity for microbes to perform aerobic respiration and emit CO<sub>2</sub> (Figure 2.2). Water present in the soil pore is necessary for aerobic respiration as it permits the diffusion of metabolizable C substrates (Davidson et al. 2012). Yet, as soil moisture reduces the amount of pore volume available to O<sub>2</sub>, excess moisture can limit aerobic respiration. Therefore, aerobic respiration reaches a maximum at a water-filled pore space of 51–78% (Linn

and Doran 1984, Franzluebbers 1999, Yan et al. 2016) or matric potential of -3 to -33 kPa (Franzluebbers 1999, Castellano et al. 2010, Moyano et al. 2013) and then decreases beyond this threshold due to the  $O_2$  limitation.

The chemical properties of soil also impact aerobic respiration rates, like pH and the availability of C and N. Soil pH strongly dictates microbial life, with peak bacterial abundance and diversity centered at a near-neutral pH (Lauber et al. 2009, Fierer 2017, Bahram et al. 2018), while fungi prefer more acidic conditions (Rousk et al. 2010). Since bacteria are the most abundant of the microbial domains in cultivated soils, aerobic respiration from croplands closely mirrors their soil pH window, with a maximum microbial metabolic quotient occurring at a pH  $\sim 6.3$  (Xu et al. 2017).

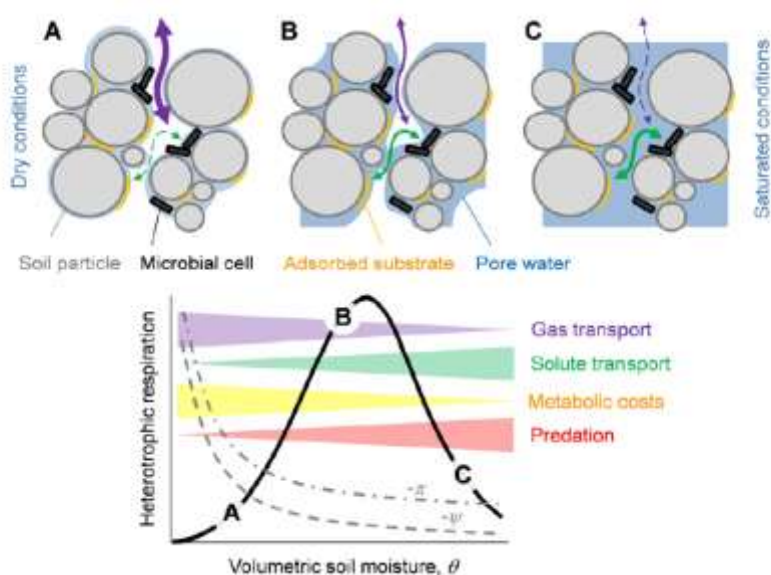


**Figure 2.2** Conceptual model demonstrating the effect of soil moisture – in terms of volumetric soil moisture ( $\theta$ ), matric potential ( $\psi$ ) and cell osmotic potential ( $\pi$ ) – on some of the biophysicochemical processes (i.e., gas transport, solute transport, metabolic costs, predation) that affect aerobic heterotrophic respiration (Moyano et al. 2013).

As the electron donors for this metabolic pathway, C substrates are necessary for aerobic respiration to occur. Subsequently, increasing the supply of available C will promote microbial metabolism and their respiration of CO<sub>2</sub> (Rui et al. 2016). While a greater amount of C substrates will drive aerobic respiration, quality of the C substrates is just as important. Dissolved C substrates (<600 Da) – like many root exudates (e.g., amino acids, organic acids, sugars) – are easily assimilated and rapidly metabolized by microbes, respiring CO<sub>2</sub> (Lehmann and Kleber 2015). In contrast, complex organic matter, like crop residues, requires degradation followed by depolymerization via extracellular enzymes before organic compounds are available to microbes. Furthermore, the stabilization of C substrates in the soil matrix (e.g., aggregation, mineral association) impedes the ability of microorganisms to assimilate and metabolize organic compounds. For example, iron mineral fixation reduced the respiration of simple organic compounds in soils by 65%, on average (Adhikari et al. 2019). Thus, the effect of C substrates on aerobic respiration depends on their amount, quality, and interaction with the soil matrix.

Aerobic respiration has a varied response to N availability, depending on other management and edaphic factors. Soil incubations demonstrate that mineral N fertilization has either no effect (Chen et al. 2014) or reduces microbial respiration (Ramirez et al. 2010). However, when combined with a C substrate, NH<sub>4</sub><sup>+</sup> (150 kg N ha<sup>-1</sup>) increases aerobic respiration-derived CO<sub>2</sub> (17–67%) compared to the substrate alone, through either the stimulation of native soil organic matter priming (sucrose) or metabolism of the substrate (maize straw; Chen et al. 2014). When the plant root system is included, the addition of N seems to elicit an alternative effect, contingent on the reactive N form. NH<sub>4</sub><sup>+</sup> additions (240 mg N kg<sup>-1</sup>) not only produced 17–20% less CO<sub>2</sub> than NO<sub>3</sub><sup>-</sup> but also suppressed rhizosphere priming (Wang and Tang 2018). The authors attributed these differences to the acidification of the rhizosphere (pH ~4.2)

by  $\text{NH}_4^+$  compared to  $\text{NO}_3^-$  (pH  $\sim$ 5.2) and its effect on the microbial biomass and activity. Consequently, the impact of reactive N on aerobic respiration depends on soil management.

Aerobic respiration should be the dominant source of  $\text{CO}_2$  from cultivated peatlands under aerobic conditions. The pH of cultivated peatlands (pH 5.4–6.6; Lloyd et al. 2019, De Sena et al. 2022a) is typically within the pH range where the microbial metabolic quotient is at its maximum. Additionally, these soils are rich in organic matter, the decomposition of which should release C substrates. Because of the low mineral content in peatlands, these organic compounds likely avoid fixation to the soil matrix and therefore remain available for microbial metabolism. Also, cultivated peatlands have an elevated level of reactive N from fertilization and organic matter decomposition. One must consider that this reactive N will modulate aerobic respiration, depending on the form. As ammoniacal fertilizers (e.g., anhydrous  $\text{NH}_3$ , urea) are the most commonly applied mineral N fertilizer to cultivated soils (Cao et al. 2018) and are less prone to loss via leaching than  $\text{NO}_3^-$ , we should expect that the rate of aerobic respiration will be slightly decreased overall. Nevertheless, cultivated peatlands should be a prime source of aerobic respiration-derived  $\text{CO}_2$ .

### **2.3.2 Nitrification**

Within the N cycle (Figure 2.3), nitrification is responsible for the transformation of reactive N species (e.g.,  $\text{NH}_3/\text{NH}_4^+$ ,  $\text{NO}_2^-$ ) in aerobic soil (micro)sites, releasing  $\text{N}_2\text{O}$ . In contrast to aerobic respiration, nitrification is a chemolithoautotrophic reaction, which harvests energy from inorganic N forms rather than organic compounds. A series of oxidative steps, nitrification involves four reactions: the oxidation of  $\text{NH}_3$ , hydroxylamine ( $\text{NH}_2\text{OH}$ ), nitric oxide ( $\text{NO}$ ) and  $\text{NO}_2^-$ .

Like all catabolic reactions,  $\text{NH}_3$  oxidation commences with the assimilation of the substrate of interest,  $\text{NH}_3$  or  $\text{NH}_4^+$ . Although  $\text{NH}_3$  can either diffuse through the microbial membrane itself (Jung et al. 2022) or cross the membrane via protein transporters (e.g., Amt, Rh), the absorption of  $\text{NH}_4^+$  requires a protein transporter to enter the periplasm (van Kessel et al. 2015, Xu et al. 2020). However,  $\text{NH}_3$  is the only known metabolic substrate for the  $\text{NH}_3$  oxidation reaction (Lehtovirta-Morley et al. 2016, Xu et al. 2020). Therefore, any assimilated  $\text{NH}_4^+$  requires deprotonation to  $\text{NH}_3$  for  $\text{NH}_3$  oxidation to occur.

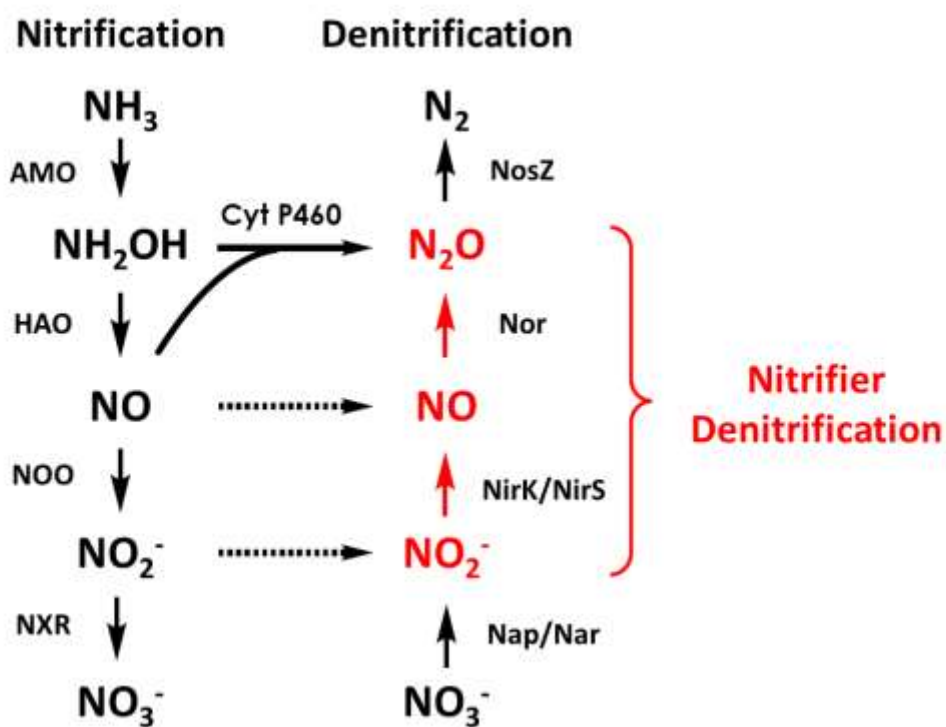


**Figure 2.3** Conceptual model of the N cycle occurring in soils, composed of nitrification, denitrification and nitrifier-denitrification. AMO,  $\text{NH}_3$  monooxygenase; HAO,  $\text{NH}_2\text{OH}$  oxidoreductase; NOO,  $\text{NO}$  oxidoreductase; NXR,  $\text{NO}_2^-$  oxidoreductase; Nar/Nap,  $\text{NO}_3^-$  reductase; NirK/NirS,  $\text{NO}_2^-$  reductase; Nor,  $\text{NO}$  reductase; NosZ,  $\text{N}_2\text{O}$  reductase (Adapted from Lancaster et al. 2018).

Once in the proper form, this NH<sub>3</sub> is oxidized by NH<sub>3</sub>-oxidizing microorganisms, or “NH<sub>3</sub> oxidizers”. These microbes transform NH<sub>3</sub> with NH<sub>3</sub> monooxygenase (Amo), typically a cytoplasmic membrane-bound enzyme (Jung et al. 2022) though a cytoplasm-soluble Amo has been found in *Nitrosomonas europaea* (Gilch et al. 2009). This O<sub>2</sub>-dependent reaction occurs under aerobic conditions with electrons (e<sup>-</sup>) and protons (H<sup>+</sup>), producing ATP, the energy molecule, along with NH<sub>2</sub>OH and water (H<sub>2</sub>O; Caranto and Lancaster 2017):



As NH<sub>3</sub> oxidation is an endergonic reaction, NH<sub>3</sub> oxidizers conserve energy via the exergonic oxidation of NH<sub>2</sub>OH (Kuypers et al. 2018). Originally, the dogma was that oxidizing NH<sub>2</sub>OH by the periplasm-soluble enzyme, NH<sub>2</sub>OH oxidoreductase (Hao), formed NO<sub>2</sub><sup>-</sup> with N<sub>2</sub>O as a byproduct (Cedervall et al. 2013). However, recent evidence suggests that NH<sub>2</sub>OH oxidation forms NO instead, in addition to e<sup>-</sup> and H<sup>+</sup> by the following reaction (Caranto and Lancaster 2017):



Surprisingly, the oxidation of NH<sub>2</sub>OH occurs with or without O<sub>2</sub>. The revised pathway suggests that (i) O<sub>2</sub> is not a direct requirement of NH<sub>2</sub>OH oxidation; (ii) NO<sub>2</sub><sup>-</sup> results from an unknown enzymatic mechanism that oxidizes NO (e.g., reverse catalysis of copper-containing-NO<sub>2</sub><sup>-</sup> reductase (Cu-NirK); Lancaster et al. 2018); and (iii) any N<sub>2</sub>O emitted from nitrification originates from the oxidation of NH<sub>2</sub>OH by cyt P460 rather than the Hao enzyme. Other possibilities are that N<sub>2</sub>O is generated from NO reduction by NO reductase (NorBC), cyt P460, cyt *c*<sub>554</sub>, or NO oxidoreductase (Noo; Caranto et al. 2016, Caranto and Lancaster 2017, Lancaster et al. 2018). Consequently, this recent evidence suggests that there is a necessity to re-examine the NH<sub>2</sub>OH and NO oxidation steps of nitrification.

$\text{NO}_2^-$  oxidation is the final step of nitrification. If not performed by the  $\text{NH}_3$  oxidizer,  $\text{NO}_2^-$ -oxidizing microbes – “nitrifiers” – must take up the  $\text{NO}_2^-$  from the soil environment. The next step requires  $\text{NO}_2^-$  oxidoreductase (Nxr), a membrane-bound protein that can either be periplasmic or cytoplasmic facing (Daims et al. 2016, Lu et al. 2020). The orientation of the membrane-bound protein determines the cellular machinery required for this reaction. If periplasmic, then  $\text{NO}_2^-$  diffuses into the periplasm where the active site of Nxr will catalyze its oxidation. However, when the active site of Nxr is in the cytoplasm, the microorganism requires a  $\text{NO}_2^-$  transporter protein to shuttle the  $\text{NO}_2^-$  across the plasma membrane before  $\text{NO}_2^-$  oxidation. Cytoplasmic orientation of the Nxr may impede the rate of  $\text{NO}_2^-$  oxidation and could explain the slow growth rate of some nitrifiers.

Once the substrate reaches the nitrifier enzyme,  $\text{NO}_2^-$  is oxidized by Nxr, producing ATP,  $\text{NO}_3^-$ ,  $\text{H}^+$  and  $\text{e}^-$  (Kuypers et al. 2018):



This oxidative reaction does not produce  $\text{N}_2\text{O}$ , but if the soil transitions to anoxia, the  $\text{NO}_3^-$  product can be used as an electron donor during denitrification, which releases  $\text{N}_2\text{O}$  and  $\text{CO}_2$  (See Section 2.3.3 Denitrification). Therefore, these two pathways can be coupled in soils.

### 2.3.2.1 Microbial actors of nitrification

Chemolithoautotrophic archaea and bacteria can catalyse nitrification reactions. The  $\text{NH}_3$  oxidation step is performed by genera of archaea (e.g., from the phyla Thaumarchaeota and Nitrososphaerota) and bacteria (e.g., *Nitrosomonas*, *Nitrosocystis*, *Nitrospira* and *Nitrosolobus*; Fenchel et al. 2012). Members of the archaea and bacteria domains rely on the same reactions to complete  $\text{NH}_3$  oxidation. However, their amino acid sequences for Amo share only 40% similarity, suggesting that archaeal and bacterial Amo evolved from different proteins

(Lancaster et al. 2018). Interestingly, bacterial Amo is more similar (~70%) to methane monooxygenase (Mmo) than archaeal Amo, which suggests that the bacterial Amo and Mmo proteins share a common ancestral gene; this also explains why methane-oxidizing bacteria are able to partially oxidize  $\text{NH}_3$  (Martikainen 2022). Thus,  $\text{NH}_3$  oxidation by archaea and bacteria seems to have arisen through convergent evolution.

The  $\text{NH}_2\text{OH}$  oxidation step of nitrification is performed by  $\text{NH}_3$ -oxidizing bacteria, yet there is no evidence that  $\text{NH}_3$ -oxidizing archaea can catalyze this reaction. However, if  $\text{NH}_3$ -oxidizing archaea emit  $\text{N}_2\text{O}$  and the current nitrification model identifies  $\text{NH}_2\text{OH}$  and/or  $\text{NO}$  oxidation as the  $\text{N}_2\text{O}$  emitting steps, then archaea that oxidize  $\text{NH}_2\text{OH}$  may exist. Consequently, there is an open question on whether  $\text{NH}_3$ -oxidizing archaea are also capable of  $\text{NH}_2\text{OH}$  oxidation, and if so, what enzyme they use to catalyze this reaction (e.g., Cu-Hao; Kozłowski et al. 2016).

Autotrophic bacteria are the dominant microorganisms that oxidize  $\text{NO}_2^-$ . Well-known nitrifying bacteria include members of the phyla Alphaproteobacteria (the most famous being *Nitrobacter*), Betaproteobacteria, Gammaproteobacteria, Chloroflexi, Nitrospinae and Nitrospirae (Kuypers et al. 2018). Up to 30% of their total protein content can be  $\text{N}_x\text{r}$ , but nitrifying bacteria likely oxidize  $\text{NO}_2^-$  in addition to other substrates to meet their energy requirements due to the meager energy return from  $\text{NO}_2^-$  oxidation alone ( $-74 \text{ kJ mol}^{-1}$ ; Lancaster et al. 2018). Many nitrifiers have diverse metabolisms and are capable of dihydrogen oxidation, as well as the aerobic and anaerobic oxidation of formate (Koch et al. 2015, Daims et al. 2016). Some of these bacterial genera can also hydrolyze urea (Koch et al. 2015, Lancaster et al. 2018) and cyanate (Palatinszky et al. 2015, Lancaster et al. 2018) into  $\text{NH}_4^+$ , adding more functions to their eclectic metabolic profile. Thus, the namesake of this guild may not completely

describe the full range of metabolic pathways that nitrifiers rely on to meet their energy requirements.

Some  $\text{NH}_3$  oxidizers and nitrifiers are heterotrophic bacteria and fungi. In contrast to autotrophic archaea and bacteria, these microbes do not depend on the oxidation of N to supply energy, since they can derive energy from oxidizing organic substances that are co-metabolized with  $\text{NH}_3/\text{NH}_4^+$  and  $\text{NO}_2^-$  (Ward 2013). Heterotrophic  $\text{NH}_3$  oxidizers and nitrifiers are thus able to ‘nitrify’ organic N compounds. Furthermore, some heterotrophs can simultaneously nitrify and denitrify (Zhu et al. 2020, Martikainen 2022; See Section 2.3.3 Denitrification). While some heterotrophic  $\text{NH}_3$  oxidizers possess Amo and Hao, many demonstrate the capacity for nitrification reactions without a known enzyme for doing so (Martikainen 2022). However, the relevance of heterotrophic nitrification in cultivated soils and the contribution of this group to  $\text{N}_2\text{O}$  emissions remain unknown due to limited research on this topic. The barrier to understanding heterotrophic nitrification is that the putative mechanisms and reaction pathways are not discovered yet. Consequently, there is scope for further study of heterotrophic nitrification to quantify the contribution of this group to the soil N cycle.

The full sequence of nitrification reactions is rarely achieved by a single organism and the microbial guilds (e.g.,  $\text{NH}_3$  oxidizers and nitrifiers) responsible for the separate phases of the pathway are often found in proximity to one another. As confirmed in biofilms (Pelissari et al. 2018) and volcanic soils (Daebeler et al. 2014), these microbial guilds likely exist in a tightly knit community, known as a nitrification aggregate, in cultivated soils (Figure 2.4; Daims et al. 2016). Here,  $\text{NH}_3$  oxidizers and nitrifiers engage in a mutualistic interaction and shuttle substrates back and forth to complete nitrification. This may explain the fate of N fertilizer that is deliberately added to soil. For example, the application of ammoniacal fertilizers releases  $\text{NH}_3$

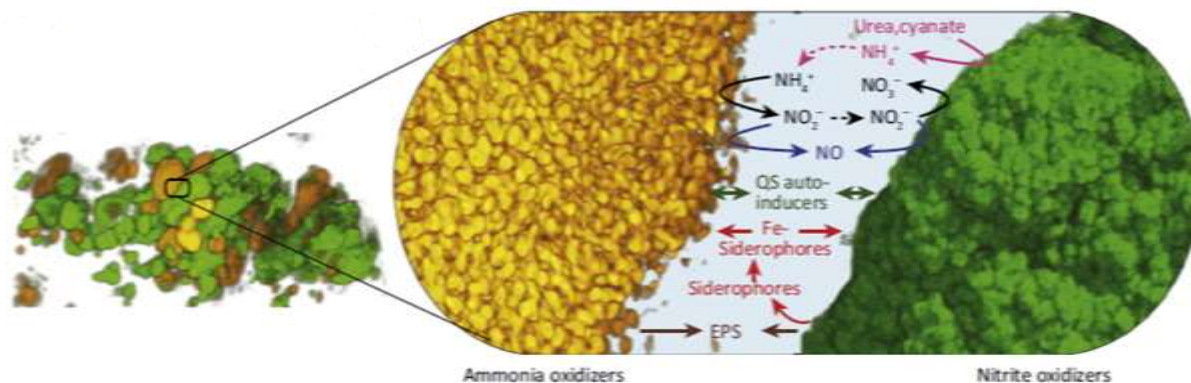


**Figure 2.4** A conceptual diagram of a potential nitrification aggregate where  $\text{NH}_3$  oxidizers and  $\text{NO}_2^-$  oxidizers coexist in a mutualistic relationship, shuttling substrates back and forth to complete nitrification. EPS, extracellular polymeric substances; Fe-Siderophores, iron-siderophore complexes; QS, quorum sensing (Daims et al. 2016).

into soil solution, where it is oxidized by  $\text{NH}_3$ -oxidizing bacteria into  $\text{NO}_2^-$  (Daims et al. 2016). As  $\text{NO}_2^-$  is a toxic compound, its oxidation by neighboring nitrifiers into  $\text{NO}_3^-$  protects the community within the nitrification aggregate. Alternatively, soils fertilized with urea might stimulate nitrifiers to transform urea into  $\text{NH}_4^+$ , generating substrates for nitrification (Daims et al. 2016). The assembly mechanisms that allow for cooperative metabolic processes in the nitrification aggregate are not yet understood but likely involve quorum sensing (i.e., the capacity of microorganisms to coordinate their behavior based on cell-to-cell communication via signal molecules; Pappenfort and Bassler 2016). Thus, there is a need for future mechanistic studies to confirm the presence of nitrification aggregates in cultivated soils and determine how the community-level interactions are initiated and sustained at relevant spatio-temporal scales.

While it is uncommon, some bacteria can oxidize  $\text{NH}_3$  fully into  $\text{NO}_3^-$  in a process known as complete  $\text{NH}_3$  oxidation (comammox). As of now, the only bacteria known to perform comammox are species of *Nitrospira* (Daims et al. 2015, van Kessel et al. 2015), a bacterial

genus that is found in various environments, including cultivated soils (Xu et al. 2020). Yet, comammox remains enigmatic, especially the microbial actors that may be capable of this pathway besides the slow-growing chemotroph *Nitrospira*. It has proven challenging to study the metabolism of *Nitrospira* in controlled environments (Lancaster et al. 2018), and their behavior in realistic soil environments remains poorly documented. Consequently, further research is needed to determine the impact of the comammox microbial community on the N cycle in cultivated soils.

#### 2.3.2.2 Soil factors affecting $N_2O$ production by nitrification

Since  $NH_3$  oxidation requires  $O_2$  to commence, soil porosity and moisture are the critical physical factors affecting nitrification. As aerobic microbial activity needs a relative  $O_2$  diffusivity of  $\geq 0.005$ – $0.025$ , soil porosity that permits such levels of aeration will achieve peak rates of nitrification (Schjønning et al. 2003). If not,  $NH_3$  oxidizers can become  $O_2$ -limited, decreasing nitrification rates substantially. For example, nitrification-derived  $N_2O$  decreases  $\sim 7$ – $16$ -fold when transitioning from aerobic (21% v/v  $O_2$ ) to microaerophilic conditions (0.5% v/v  $O_2$ ; Zhu et al. 2013). Although Hao and Nxr can function under both aerobic and anaerobic conditions, their activity is still suboptimal in anaerobic environments (Lancaster et al. 2018). Thus, nitrification should be considered as a microbial metabolic pathway that is optimal in soil under aerobic conditions.

Regarding soil moisture, nitrification occurs when the water-filled pore space is within the range of 35–83% (Schjønning et al. 2003, Bateman and Baggs 2005, Friedl et al. 2017, 2018) or the soil has a matric potential between -14 and -43 kPa (Schjønning et al. 2003, Bello et al. 2019). While this metabolic pathway requires aerobic conditions, nitrification will not occur under excessively dry conditions (approximately -51 to -80 kPa). This effect is partially due to

impeded substrate diffusion under low soil moisture conditions, but also the osmotic stress on  $\text{NH}_3$  oxidizers, with  $\text{NH}_3$ -oxidizing archaea most affected by water stress compared to their bacterial counterparts (Bello et al. 2019). As such, low water availability can limit substrate diffusion and desiccate the microbial communities involved in nitrification.

Additionally, nitrification depends on the chemical edaphic factors of soil pH, C substrates and reactive N forms. Generally, greater nitrification is observed in neutral and alkaline soils (pH 7–8), though  $\text{NH}_3$ -oxidizing activity can be comparable under acidic conditions (pH  $\leq 6.0$ ) when certain archaeal species (e.g., *Candidatus Nitrosotalea devanaterrea*; Lehtovirta-Morley et al. 2016) and bacterial strains (TAO100 of the Gammaproteobacteria; Hayatsu et al. 2017) are present. As such,  $\text{N}_2\text{O}$  emissions from nitrification are greatest in neutral and basic soils, but substantial nitrification can still occur in acidic soils, depending on the presence of acidophilic  $\text{NH}_3$  oxidizers.

Since most  $\text{NH}_3$  oxidizers and nitrifiers are autotrophs that rely on  $\text{CO}_2$  as their C source, C substrates are not necessary for nitrification to proceed. However, particular C compounds can impede nitrification, including alkynes that inhibit archaeal Amo (Wright et al. 2020) and root exudates that inhibit both  $\text{NH}_3$  and  $\text{NH}_2\text{OH}$  oxidation (e.g., methyl 3-(3-hydroxyphenyl) propionate, sorgoleone, brachialactone; Figure 2.5; Haichar et al. 2014, Coskun et al. 2017, Subbarao et al. 2021). Consequently, while organic compounds are not a substrate of nitrification, certain forms can hinder this metabolic pathway and should not be ignored.

Reactive N forms control nitrification because these N compounds function as the electron donors in this metabolic pathway.  $\text{NH}_4^+$  is specifically a trigger as its deprotonation produces  $\text{NH}_3$ , the substrate that initiates the first reaction of nitrification. While most  $\text{NH}_3$ -oxidizing bacteria thrive in  $\text{NH}_4^+$ -rich environments like cultivated soils (Cui et al. 2016, Song et

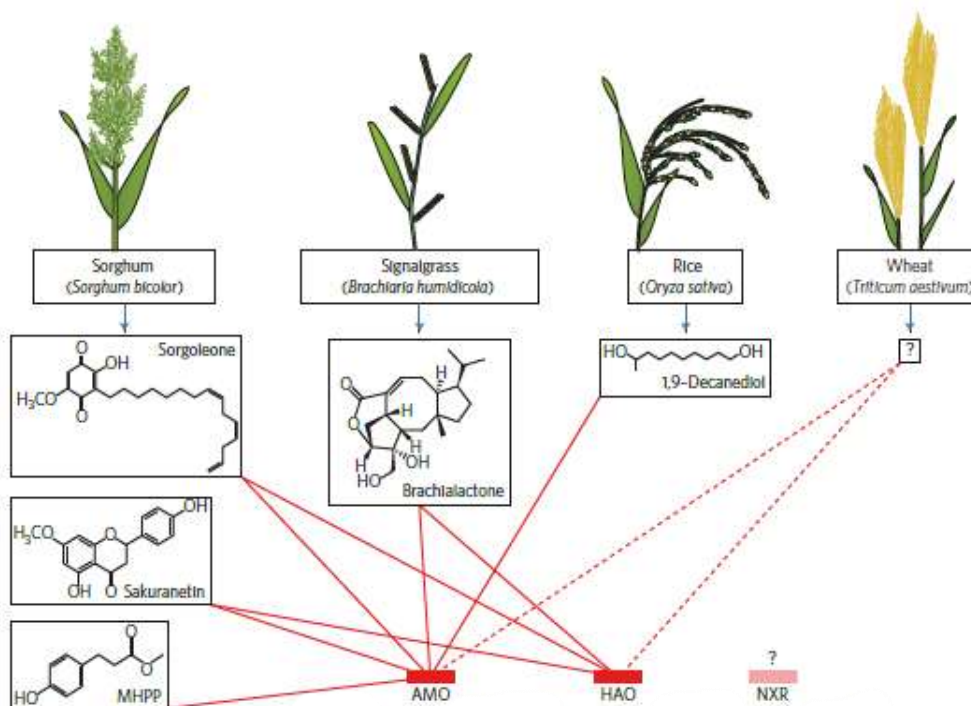


**Figure 2.5** Examples of plants known to (solid red lines) and suspected to (dotted red lines) exude different C compounds that inhibit nitrifying enzymes, like  $\text{NH}_3$  monooxygenase (AMO) and  $\text{NH}_2\text{OH}$  oxidoreductase (HAO). Currently, there are no known root exudates that inhibit  $\text{NO}_2^-$  oxidoreductase (NXR; Coskun et al. 2017).

al. 2018), the comammox bacteria and  $\text{NH}_3$ -oxidizing archaea are dominant in unfertilized, oligotrophic soils, preferring  $\text{NH}_3$  derived from native organic N forms (Kits et al. 2017, Lu et al. 2020). This is an important distinction because bacterial  $\text{NH}_3$  oxidizers produce more  $\text{N}_2\text{O}$  than their archaeal and comammox counterparts (Hink et al. 2017, Kits et al. 2019). Similarly, heterotrophic nitrifiers prefer environments where organic N substrates, like amino acids, are the main source of  $\text{NH}_3$  and  $\text{NH}_4^+$  for  $\text{NH}_3$  oxidation (Martikainen 2022). The contribution of these heterotrophic nitrifiers to soil  $\text{N}_2\text{O}$  emissions remains uncharacterized but are expected to be minor. Consequently, soils amended with ammoniacal fertilizers should emit substantial amounts of  $\text{N}_2\text{O}$  derived from nitrification if under appropriate edaphic conditions due to the  $\text{NH}_3$ -

oxidizing bacteria communities adapted to metabolize the surplus of  $\text{NH}_3$  into  $\text{NO}_2^-$  and  $\text{NO}_3^-$  products.

Considering the assumed  $\text{NH}_4^+$  availability of well-fertilized peatlands under cultivation, nitrification could be prevalent in well-aerated microsites. However, the overall acidic pH of these soils may limit the  $\text{N}_2\text{O}$  emissions from nitrification. Therefore, other sources of  $\text{N}_2\text{O}$  could dominate in cultivated peatlands.

### **2.3.3 Denitrification**

Denitrification is a series of reactions that reduces N species ( $\text{NO}_3^-$ ,  $\text{NO}_2^-$ ,  $\text{NO}$ ,  $\text{N}_2\text{O}$ ) during the microbial oxidation of a substrate, typically organic matter (Figure 2.3). At any point, the intermediate N ions and gases can leave the microbial cell and enter the environment. This is why denitrification is a source of  $\text{N}_2\text{O}$  along with  $\text{CO}_2$  released from the oxidation of organic matter. As the heterotrophic microbes performing this pathway – known as denitrifiers – use N forms as electron acceptors instead of  $\text{O}_2$ ,  $\text{O}_2$ -depleted soil (micro)sites are conducive for their metabolism. Therefore, heterotrophic anaerobic microorganisms are considered denitrifiers when they can catalyze any one of the four sequential reactions of denitrification: the reduction of  $\text{NO}_3^-$ ,  $\text{NO}_2^-$ ,  $\text{NO}$  and  $\text{N}_2\text{O}$ .

Heterotrophs must assimilate an oxidizable C substrate as an electron donor and C source before they reduce N species through the denitrification process. Denitrifiers take up a variety of organic monomers – amino acids, organic acids and sugars – using many different protein transporters such as the Major Facilitator Superfamily (MFS), Tripartite ATP-independent Periplasmic (TRAP) and ATP-Binding Cassette (ABC) transporter families (Zhalnina et al. 2018). Once within the cell, the organic compound is catabolized and releases  $\text{CO}_2$  in the same manner as aerobic respiration (e.g., glycolysis, TCA cycle), except that (i) at least one

denitrifying enzyme exists in the electron transport chain, transferring an electron to a N species, and (ii) this process conveys less  $H^+$  across the membrane, generating a weaker  $H^+$  motive force. Due to the energy balance, denitrifiers obtain less ATP (~16-fold decrease; Wessner et al. 2013) from denitrification reactions than through aerobic respiration.

Once the C substrate enters the microbial cell, denitrification starts with the reduction of  $NO_3^-$  into  $NO_2^-$ .  $NO_3^-$  reduction occurs via the periplasmic  $NO_3^-$  reductase (Nap) or the cytoplasmic  $NO_3^-$  reductase (Nar) via the following reaction (Kuypers et al. 2018):



Both Nap and Nar are dissimilatory membrane-bound enzymes, but their active sites have a different orientation (Sparacino-Watkins et al. 2014). If reduced by Nap, the  $NO_3^-$  present in the periplasm – either from cellular metabolism (e.g.,  $NO_2^-$  oxidation) or that transported from the extracellular environment through the cell wall via porins (Nikaido 2003, Fowler and Hanson 2015, Kamennaya et al. 2020) – can simply diffuse through the periplasmic space before encountering the active site of Nap. For Nar catalysis,  $NO_3^-$  must also cross the inner cell membrane through a protein transporter, like NarK, NarO or NarT (Fukuda et al. 2015, Alvarez et al. 2019), to enter the cytoplasm. Here, the active site of Nar – the dimer NarG and NarH – can reduce  $NO_3^-$  to  $NO_2^-$  (Kuypers et al. 2018). The periplasmic orientation of Nap prevents its participation in the electron transport chain, thus resulting in lower rates of ATP synthesis for the denitrifier (Kuypers et al. 2018). Although the involvement of Nar in the electron transport chain produces ATP, its cytoplasmic reduction of  $NO_3^-$  generates toxic  $NO_2^-$  within the cell. Thus, the microbe must have the cellular machinery to shuttle  $NO_2^-$  from the cytoplasm to the periplasm, such as by a  $NO_2^-/NO_3^-$  porter (e.g., NarK; Fukuda et al. 2015), to avoid cell toxicity.

In either case,  $\text{NO}_2^-$  must reach the periplasm for the second denitrification reaction to occur:  $\text{NO}_2^-$  reduction. If the denitrifier is not capable of the previous denitrification step –  $\text{NO}_3^-$  reduction – the  $\text{NO}_2^-$  can be sourced from either other microbial reactions (e.g., nitrification) or the environment. Once in the periplasm, denitrifiers involved in this reaction can reduce  $\text{NO}_2^-$  with  $\text{NO}_2^-$  reductase that is either a cytochrome  $\text{cd}_1$ -type/iron-dependent (NirS) or a copper-dependent (NirK) type by the following reaction (Maia and Moura 2014):



As both Nir forms exist in the periplasmic space, these reactions do not synthesize ATP for the microbe (Kuypers et al. 2018). However, these enzymes likely detoxify  $\text{NO}_2^-$  in the microbial cell. It appears that NirS tethers itself to the cytoplasmic membrane, close to other denitrification enzymes – if they are present in the cell – via electrostatic interactions (Borrero-de Acuña et al. 2016, Terasaka et al. 2017). In this configuration, NirS can reduce  $\text{NO}_2^-$  and transfer NO rapidly to compatible denitrifying enzymes for further reduction. Whether NirK functions in a denitrifying supracomplex remains to be determined. Regardless, the efficient reduction of  $\text{NO}_2^-$  is necessary to protect the microbe from this toxic by-product.

Like  $\text{NO}_2^-$ , the NO product is toxic to cells. As a result, microbes need a pathway to reduce NO into  $\text{N}_2\text{O}$  to protect the cell and for energy recovery. This reaction is catalyzed with NO reductase (Nor):



The Nor enzymes are the most diverse of denitrification enzymes, with structures that include flavoproteins and haem-copper oxidases (Kuypers et al. 2018), suggesting convergent evolution. These Nor enzymes either straddle the inner microbial membrane – like the cytochrome-c-dependent (c), quinol-dependent (q), and copper-containing quinol-dependent ( $\text{Cu}_A$ ) Nor

enzymes – or are present in the cytosol and mitochondria, such as the cytochrome P<sub>450</sub>-type Nor enzyme (P<sub>450</sub>-Nor; Aldossari and Ishii 2021). However, only the membrane-bound Nor contributes to microbial respiration. Nevertheless, whether it is a membrane-bound enzyme or an enzyme present in the cytosol, Nor is of interest for its ability to produce N<sub>2</sub>O, a potent greenhouse gas. Denitrifiers that are not able to reduce the N<sub>2</sub>O into dinitrogen (N<sub>2</sub>) will thus release N<sub>2</sub>O from the cell into the atmosphere.

The final reaction of denitrification uses the periplasmic N<sub>2</sub>O reductase (NosZ), to reduce N<sub>2</sub>O into N<sub>2</sub> (Kuypers et al. 2018):



A metalloprotein with two copper centers (Zhang et al. 2019), NosZ returns enzymes in the electron transport chain (i.e., the cytochrome *c*/cupredoxin pool) into their oxidized state, thus regenerating them and allowing ATP production to continue (Simon and Klotz 2013). While this enzyme does not contribute directly to the H<sup>+</sup> motive force for microbial ATP synthesis (Kuypers et al. 2018), at the ecosystem scale, the activity of NosZ is the only known sink for N<sub>2</sub>O (Jones et al. 2014). Consequently, NosZ is essential in preventing N<sub>2</sub>O fluxes from soil denitrifiers and their release into the atmosphere.

### *2.3.3.1 Microbial actors of denitrification*

Denitrifiers are present in all three domains: bacteria, archaea, and eukarya. Most denitrifiers are classified as facultative anaerobic heterotrophs that initiate denitrification when more efficient terminal electron acceptors, like O<sub>2</sub>, are unavailable for respiration (Gregorich et al. 2015). These denitrifiers may perform one, a few or all reactions of the denitrification pathway, depending on their genetic capacity and their expression of the genes that encode for the enzyme-driven reactions (Hallin et al. 2018). For example, about half of Proteobacteria (e.g., genera of

Betaproteobacteria and Gammaproteobacteria) can perform all steps in the denitrification reaction, while the other half – mostly genera in Alphaproteobacteria – do some of the steps in denitrification (Graf et al. 2014). Hence, denitrification is considered a modular pathway that involves an assemblage of microorganisms with partial or complete denitrifying abilities.

Denitrifiers involved in  $\text{NO}_3^-$  reduction include bacteria (e.g., *Escherichia coli*, *Bradyrhizobium japonicum*), archaea (e.g., *Candidatus Methanoperedens* spp.), and fungi (e.g., *Stagonosporopsis tanacetii*; Simon and Klotz 2013, Higgins et al. 2018, Kuypers et al. 2018). Many bacteria – especially Proteobacteria – possess both Nar and Nap, like *Paracoccus denitrificans* (Simon and Klotz 2013). Archaea appear to reduce  $\text{NO}_3^-$  with Nar only (Simon and Klotz 2013). However, fungi involved in  $\text{NO}_3^-$  reduction are more likely to use Nap than Nar for catalysis, based on the observation that fungal genomes containing Nap outnumbered Nar by one order of magnitude (712 genomes; Higgins et al. 2018, Aldossari and Ishii 2021). Thus, the reduction process largely depends on the genetic capacity of each microbial domain.

The  $\text{NO}_2^-$  reduction step also involves diverse microorganisms, including Proteobacteria, anaerobic  $\text{NH}_3$ -oxidizing bacteria, and Bacteroidetes (Kuypers et al. 2018). While there are exceptions (e.g., *Pseudomonas stutzeri*), most  $\text{NO}_2^-$ -reducing microorganisms (98.5%) have either NirK or NirS, the enzymes responsible for this reaction, but not both (Graf et al. 2014). There are some phylogenetic trends based on the  $\text{NO}_2^-$  reductase inherited, like the exclusive possession of NirS by archaeal phylum Crenarchaeota, as well as NirK by fungi and archaeal phyla Euryarchaeota and Thaumarchaeota (Graf et al. 2014, Li et al. 2022). However, bacteria may inherit either form; for example, more than one third of  $\text{NO}_2^-$  reducers in Proteobacteria possess NirS. Whether a bacteria has NirS or NirK affects the type of other denitrification enzymes present in the cell. For example,  $\text{NO}_2^-$  reducers with NirS typically also inherit Nor

(96.4%) and NosZ (80%), whereas NirK  $\text{NO}_2^-$  reducers are 1.5 times less likely to reduce NO and ~3 times less likely to reduce  $\text{N}_2\text{O}$  (Graf et al. 2014). The ratio of NirS to NirK is thought to be an indication of complete versus incomplete denitrification pathways within bacteria (Jones et al. 2014) but this interpretation should be made with caution when the analysis is based on gene copies rather than direct mechanistic analysis (Frosteegård et al. 2022).

NO reducers include archaea (e.g., genera within Euryarchaeota and Crenarchaeota), bacteria (e.g., species within *Pseudomonas*) and fungi (genera within Ascomycota; Graf et al. 2014, Kuypers et al. 2018, Aldossari and Ishii 2021). Prokaryotes capable of NO reduction have qNor, cNor and  $\text{Cu}_A\text{Nor}$  enzymes that function in the plasma membrane, whereas NO reduction with the fungal  $\text{P}_{450}\text{-Nor}$  occurs in the cytosol and on the mitochondrial membrane (Aldossari and Ishii 2021). Although fungal and bacterial NO reducers are typically found in cultivated soils, archaeal NO reducers tend to be extremophiles in hypersaline, hyperthermal and highly acidic environments (Torregrosa-Crespo et al. 2017, Zou et al. 2020). As such, archaeal denitrifiers are not expected to be a source of  $\text{N}_2\text{O}$  in cultivated soils, especially temperate peatlands under crop production.

The archaea and bacteria responsible for the final denitrification reaction have garnered substantial interest resulting from their capacity to mitigate soil  $\text{N}_2\text{O}$  emissions. This interest fueled intensive soil gene sequencing and “-omic” research that revealed the existence of two main microbial clades possessing NosZ, known as Clade I (e.g., genera of Euryarchaeota, Alphaproteobacteria, Betaproteobacteria, Gammaproteobacteria) and Clade II (e.g., genera of Bacteroidetes, Gemmatimonadetes and Deltaproteobacteria; Hallin et al. 2018). The main distinction between the two clades is that these microbial groups employ different mechanisms to export the  $\text{N}_2\text{O}$  reductase enzyme from the cytoplasm into the periplasm (Hallin et al. 2018). In

soil, the abundance of Clade II is often greater than or equal to Clade I (Jones et al. 2013), which has important implications as members of Clade II are often incomplete denitrifiers that do not possess other denitrifying enzymes (e.g., *Anaeromyxobacter dehalogenans*; Graf et al. 2014, Kuypers et al. 2018). As such, Clade II is considered less prone to emitting N<sub>2</sub>O while also abating the risk of this greenhouse gas through its reduction of N<sub>2</sub>O (Domeignoz-Horta et al. 2016), and thus, may determine the capacity of a soil to function as a N<sub>2</sub>O sink.

Like nitrification, denitrification is typically performed by a patchwork of denitrifying microbes rather than a sole microorganism. As a result, one would expect that these microbes would exist in denitrifying communities, woven together through the exchange of the terminal electron acceptors involved in denitrification. Many denitrifiers (e.g., *Pseudomonas aeruginosa*, *Paracoccus denitrificans*) possess the capacity for quorum sensing through signal molecules like N-acyl-homoserine lactones (Wang et al. 2021a), a potential mechanism that could unite denitrifiers and initiate this communal denitrification. However, no such evidence exists of “denitrification aggregates” in cultivated soils, likely due to the difficulty in studying quorum sensing in soils (Wang et al. 2021a). Therefore, opportunities exist for future research into the genesis and maintenance of microbial communities that complete denitrification in soils under cultivation.

#### 2.3.3.2 Soil factors affecting CO<sub>2</sub> and N<sub>2</sub>O production by denitrification

Denitrification is a function of soil porosity and moisture as these soil physical characteristics influence O<sub>2</sub> availability. The absence of O<sub>2</sub> promotes denitrification because O<sub>2</sub> inhibits the enzymes involved in denitrification (e.g., NirS, Nor, NosZ; Graf et al. 2014). As a result, soils with weak pore connectivity (low relative O<sub>2</sub> diffusivity:  $\leq 0.005$ – $0.025$ ; Balaine et al. 2013, 2016) will prevent O<sub>2</sub> from impeding the function of denitrifying enzymes, allowing

denitrification to be the dominant N<sub>2</sub>O-producing process in soils (100% N<sub>2</sub>O emissions derived from denitrification; Zhu et al. 2013). Smaller pores can also limit O<sub>2</sub> availability and subsequently, incur denitrifying conditions faster. However, such pores (<10 μm) may promote the full reduction of NO<sub>3</sub><sup>-</sup> into N<sub>2</sub> compared to larger pores (>35 μm) that are able to vent N<sub>2</sub>O before its final reduction step (Kravchenko et al. 2017). Consequently, N<sub>2</sub>O emissions from denitrification are contingent on sufficient pore connectivity that permit their flux into the atmosphere.

Soil moisture is a trigger of denitrification, with denitrification-derived N<sub>2</sub>O fluxes often observed after precipitation or irrigation events (Wagner-Riddle et al. 2020). Sufficient soil moisture permits the diffusion of the substrates necessary for denitrification. Moisture also limits O<sub>2</sub>, creating conducive conditions for this anaerobic reaction to occur. As a result, reducing environments with high moisture are considered ideal for denitrification, with a water-filled pore space >67% (Zhu et al. 2013, Balaine et al. 2013, Baral et al. 2016) and matric potential between -1.5 and -6.0 kPa (Balaine et al. 2013). Yet, drier soils (30–45% water-filled pore space) can still host denitrification microsites, generated by organic residues absorbing moisture (Kravchenko et al. 2017) or by depletion of O<sub>2</sub> during catabolism. Thus, while a soil environment may be considered aerobic as a whole based on its moisture content, organic matter can create hotspots of denitrification through their moisture sorption and catabolism by microbes.

Denitrification is also modified by the chemical characteristics of a soil, like pH, and C and N availability. While there is no optimum pH for denitrification, the rate of this reaction tends to increase with a rising pH, possibly due to its effects on mineral availability (Li et al. 2022). Soils with a pH ≥6.8 are also more likely to permit full denitrification (i.e., the complete reduction into N<sub>2</sub>), possibly resulting from the functionality of NosZ under more alkaline

conditions (Hénault et al. 2019, Frostegård et al. 2022). The different microbial clades that make up denitrifiers can have different responses to pH, as well. For example, microbes of NosZ Clade II are influenced more by pH than those of NosZ Clade I (Jones et al. 2014, Tsiknia et al. 2015). Whether this difference exists for other denitrifiers (i.e., Nap/Nar  $\text{NO}_3^-$  reducers, NirS/NirK  $\text{NO}_2^-$  reducers) remains to be investigated. Nevertheless, the influence of pH alone on NosZ functionality and abundance of Clade II – often incapable of performing the other denitrifying steps – could determine the magnitude of  $\text{N}_2\text{O}$  emissions from a soil.

Quality of organic C may even determine the denitrifiers present, with more genera of NosZ Clade II found in the rhizosphere than NosZ Clade I (Graf et al. 2016), possibly suggesting their preference for assimilable organic rhizodeposits, such as root exudates. Furthermore, if the C substrate is stabilized to the soil matrix via mineral interactions, it is unavailable for microbial metabolism (Lehmann and Kleber 2015). Organic substrates not only function as electron donors for denitrification but also stimulate anoxia from the initial metabolism of organic compounds by aerobic respiration. This effect can start and sustain anaerobic conditions, creating sites of denitrification (e.g., rhizosphere, detritosphere) in otherwise well-aerated soils (Kravchenko et al. 2017, Ling et al. 2022). Therefore, C is an important determinant of denitrification and its resulting greenhouse gas emissions.

The availability of reactive N forms, especially  $\text{NO}_3^-$ , is a determining factor of denitrification as they function as the terminal electron acceptors of this metabolic pathway. Soil environments rich in  $\text{NO}_3^-$  are ideal for denitrifiers, with denitrification rate showing a strong positive relationship with  $\text{NO}_3^-$  ( $R^2 = 0.58$ ,  $n = 2493$ ,  $p < 0.001$ ; Li et al. 2022). This effect of  $\text{NO}_3^-$  is expected, as this reactive N form is the initial electron acceptor in the denitrification pathway. The application of  $\text{NO}_3^-$  with a C substrate can increase the denitrification rate of soils

by as much as two-fold (Li et al. 2022). The rate of denitrification also shows a strong relationship with soil total N ( $R^2 = 0.59$ ,  $n = 2640$ ,  $p < 0.001$ ; Li et al. 2022). Although a portion of this total N is made up of reactive N forms (e.g.,  $\text{NO}_3^-$ ), organic N forms can also become a source of  $\text{NO}_3^-$  through mineralization. Hence, denitrification will not initiate without a  $\text{NO}_3^-$  supply.

Denitrification should be a major source of  $\text{CO}_2$  and  $\text{N}_2\text{O}$  from cultivated peatlands. As the pH of these soils are typically  $< 6.8$ , the full reduction of  $\text{NO}_3^-$  into  $\text{N}_2$  will most likely not occur, resulting in  $\text{N}_2\text{O}$  emissions instead. Cultivated peatlands also have a supply of electron donors for denitrification, with both the assimilable C compounds exuded from crop roots and organic substrates released from the decomposition of their elevated organic matter. Although these organic forms may initially be metabolized via aerobic respiration, this metabolic pathway's rapid depletion of  $\text{O}_2$  should create anaerobic zones in the soil, prompting facultative anaerobes to shift into denitrification. The presence of  $\text{NO}_3^-$  for denitrification depends on the N fertilizer applied. However, even if ammoniacal fertilizers are applied, the resulting  $\text{NH}_4^+$  can be transformed into  $\text{NO}_3^-$  via nitrification (See Section 2.3.2) or nitrifier-denitrification (See Section 2.3.4). Consequently, denitrification is likely a dominant metabolic pathway in cultivated peatlands, emitting  $\text{CO}_2$  and  $\text{N}_2\text{O}$  from these soils.

### ***2.3.4 Nitrifier-denitrification***

Microbes capable of performing nitrifier-denitrification fuse the nitrification and denitrification pathways by performing denitrification with intermediates from the nitrification reaction under shifting redox conditions (Figure 2.3). This amalgam pathway begins with the nitrification steps of  $\text{NH}_3$  oxidation,  $\text{NH}_2\text{OH}$  oxidation and  $\text{NO}$  oxidation. If the soil approaches hypoxic conditions (e.g.,  $\text{O}_2$  level 0.5–3.0% v/v  $\text{O}_2$  concentration; Zhu et al. 2013) the nitrifier will shift

to denitrification. As such, the NO and NO<sub>2</sub><sup>-</sup> generated by nitrification are repurposed as the terminal electron acceptors during the oxidation of electron donors. As in denitrification, the reduction of the NO intermediate by NO reductase (Nor) during nitrifier-denitrification will produce N<sub>2</sub>O along with CO<sub>2</sub> as a C substrate is oxidized in tandem.

#### *2.3.4.1 Microbial actors of nitrifier-denitrification*

Nitrifier-denitrification occurs when microorganisms possess enzymes for both nitrification and denitrification. This differs from simultaneous nitrification denitrification, which happens when nitrogenous substrates are shuttled from separate, neighboring NH<sub>3</sub> oxidizer/nitrifier and denitrifier communities under fluctuating oxic conditions. As NH<sub>3</sub>-oxidizing bacteria – like the genera *Nitrosomonas* and *Nitrospira* – possess both nitrifying and denitrifying enzymes, these microbes are currently the only known microbes capable of performing nitrifier-denitrification (Stein 2019). For example, *Nitrosomonas europaea* contain genes encoding the nitrifying enzymes, Amo and Hao, as well as those that encode denitrifying enzymes, NirK and NorB (Yoon et al. 2019). There is evidence that NH<sub>3</sub>-oxidizing archaea are also nitrifier-denitrifiers, based on controlled incubation studies (Jung et al. 2014, Stieglmeier et al. 2014, Wrage-Mönnig et al. 2018). However, none have demonstrated mechanistically that NH<sub>3</sub>-oxidizing archaea possess denitrifying enzymes. Consequently, the current literature suggests that most nitrifier-denitrification activity leading to soil N<sub>2</sub>O emissions is performed by NH<sub>3</sub>-oxidizing bacteria.

#### *2.3.4.2 Soil factors affecting CO<sub>2</sub> and N<sub>2</sub>O production by nitrifier-denitrification*

Since nitrifier-denitrification can only occur when appropriate O<sub>2</sub> concentrations exist in soil, porosity and moisture should be important determinants of this microbial pathway and its greenhouse gas emissions. Some research exists on the optimal moisture conditions for nitrifier-denitrification. For example, nitrifier-denitrification occurring in a sandy soil contributed to only

3.9–7.9% of total N<sub>2</sub>O emissions at a 90% water-filled pore space, whereas this metabolic pathway contributed 37–57% and 24–50% at a water-filled pore space of 50% and 70%, respectively (Kool et al. 2011). Otherwise, there is a general paucity of research on the soil porosity and moisture conducive for nitrifier-denitrification (Wrage-Mönnig et al. 2018). One could assume that the porosity and moisture conditions favorable for nitrifier-denitrification would be similar to those supporting NH<sub>3</sub> oxidation as NH<sub>3</sub>-oxidizing bacteria are the microbes responsible for this metabolic pathway. However, such an assumption requires robust analytical study for confirmation. Consequently, it is evident that further research is needed to better understand the conditions of the physical soil environment that manifest nitrifier-denitrification.

It is well established that nitrifier-denitrification requires a hypoxic soil environment to commence. Indeed, N<sub>2</sub>O derived from nitrifier-denitrification increased by one to two orders of magnitude in a N-fertilized clay soil under hypoxia (0.5–3% O<sub>2</sub> v/v) compared to the same soil when oxygenated (21% O<sub>2</sub> v/v; Zhu et al. 2013, Wrage-Mönnig et al. 2018). Soils incur such hypoxic conditions from fluctuating water tables due to irrigation, drainage and freeze-thaw/wet-dry cycles, thus being prime environments for nitrifier-denitrification (Wagner-Riddle et al. 2020). Yet, N<sub>2</sub>O emissions from nitrifier-denitrification may be curbed by the number of repeated cycles, as supported by the 2-fold reduction in N<sub>2</sub>O from *Nitrosomonas europaea* after 13 anaerobic/aerobic cycles (18 h/6 h) in a bioreactor (Yu et al. 2018). It remains to be determined (i) whether these findings hold in less-controlled environments, and (ii) if the same effect is observed with CO<sub>2</sub>. Nevertheless, this effect does demonstrate the capacity for nitrifier-denitrifiers to adapt to fluctuating environments and reduce N<sub>2</sub>O emissions, a potential mechanism in soils.

As with the other greenhouse gas-producing pathways, the chemical characteristics of soil are thought to be important for nitrifier-denitrification, including pH and the availability of C and N. Originally, this metabolic pathway was assumed to occur under more acidic conditions through theoretical speculation based on thermodynamics (Wrage et al. 2001). However, studies have not provided robust evidence of any relationship between nitrifier-denitrification and soil pH due to insufficient methodology (Wrage-Mönnig et al. 2018). Thus, while one could assume that soils with a near-neutral pH would support nitrifier-denitrification based on the preferences of  $\text{NH}_3$ -oxidizing bacteria, mechanistic research is needed to improve our understanding of nitrifier-denitrification under acidic and basic soil conditions.

The availability of C is thought to impact nitrifier-denitrification, but the direction and magnitude are debated. Research has assumed that a surplus of N (i.e., C limitation) would lower microbial N use efficiency and promote gaseous N losses – including through nitrifier-denitrification (Mooshammer et al. 2014). However, as this metabolic pathway also requires C substrates to proceed into its denitrification component, this theory is incomplete. Additionally, a study by Köster et al. (2011) found that nitrifier-denitrification was a significant source of  $\text{N}_2\text{O}$  after application of food waste residue, an amendment rich in C substrates (Wrage-Mönnig et al. 2018). Therefore, the current perception of nitrifier-denitrification is severely limited without insight into the effects of C abundance, quality and stabilization.

For  $\text{NH}_3$ -oxidizing bacteria to perform nitrifier-denitrification, they require reactive N forms, especially the protonated form of the initiating electron donor:  $\text{NH}_4^+$ . Indeed,  $\text{N}_2\text{O}$  emissions from nitrifier-denitrification doubled with each order of magnitude increase in  $\text{NH}_4^+$  from an artificial urine experiment (Wrage et al. 2004). In environments rich with ammoniacal substrates, microbes with the appropriate genes have two choices: nitrification or nitrifier-

denitrification. Researchers propose that microbes capable of performing either will shift into nitrifier-denitrification, when possible (i.e., hypoxia), as this reaction spends more inorganic N than nitrification. As such, this strategy not only functions to reduce excess inorganic N in the environment but is also thought to serve as a redox balancing tactic, venting excess electron donors present that could injure the cell (Lancaster et al. 2018, Wrage-Mönnig et al. 2018). Consequently, the chemical characteristics of soils will determine the occurrence of nitrifier-denitrification.

Evidently, the current literature does not describe the soil factors that promote nitrifier-denitrification beyond hypoxia and the requirement of  $\text{NH}_4^+$ . As a result, it is difficult to predict the occurrence of this metabolic pathway in cultivated peatlands other than the fact that fluctuating water tables are common in such soils and ammoniacal compounds are a conventional fertilizer. Such soil moisture changes and availability of  $\text{NH}_4^+$  could generate the hypoxic conditions and provide sufficient reactive N necessary for nitrifier-denitrification. Still, how the interaction of other edaphic factors modulates the  $\text{N}_2\text{O}$  output from nitrifier-denitrification requires extensive study, along with the impact of the soil environment on  $\text{CO}_2$  derived from nitrifier-denitrification. Thus, only then, will we truly understand the capacity of cultivated peatlands to generate  $\text{CO}_2$  and  $\text{N}_2\text{O}$  from nitrifier-denitrification.

## **2.4 Methods for analysis of greenhouse gas hotspots**

Most investigations of greenhouse gas emissions from cultivated peatlands rely on field-scale measurements that, while essential for global greenhouse gas inventories, are too coarse in resolution to understand the dynamics of microbial greenhouse gas production. This limitation makes it challenging to understand the underlying microscale mechanisms occurring within greenhouse gas hotspots such as the rhizosphere. However, innovation in isotopic methods have

made it possible to achieve this analytical precision. Such technology has been successfully applied in soil environments, including (i) isotopic signature analysis of CO<sub>2</sub> and N<sub>2</sub>O at natural abundance to understand the sources of emissions, (ii) isotopic enrichment experiments to trace the fate of C and N from different substrates in soil pools and their eventual contribution to total greenhouse gas emissions, and (iii) <sup>13</sup>C-/<sup>15</sup>N-/<sup>13</sup>C<sup>15</sup>N-stable isotope probing (SIP) of deoxyribonucleic acids (DNA) or ribonucleic acids (RNA) to determine the identity and activity of the microbes responsible for metabolizing different substrates and producing greenhouse gases (Table 2.1).

#### ***2.4.1 Isotopic signature analysis of CO<sub>2</sub> and N<sub>2</sub>O at natural abundance***

Compounds in soil possess a distinct ratio of heavy and light isotopes, known as their isotopic signature. Smaller isotopic signatures (i.e., greater number of light isotopes) are typical of biological pools. This effect arises from both (i) the slower physical diffusion of the compound with the heavier isotope in the environment and therefore less opportunity for heavy compounds to be assimilated by biological organisms, and (ii) the thermodynamic discrimination by enzymes against compounds with heavier isotopes (Werth and Kuzyakov 2010, Lennon and Houlton 2017). As a result, researchers attempted to use this distinction to partition greenhouse gas sources in the soil environment, but this approach is complicated by the fact that detecting isotope fractions depends on the number of biological reactions involved and detection limits of the analysis used (Whalen et al. 2022). Nevertheless, the isotopic signatures of C-CO<sub>2</sub> ( $\delta^{13}\text{C}$ ), N-N<sub>2</sub>O ( $\delta^{15}\text{N}$ ) and O-N<sub>2</sub>O ( $\delta^{18}\text{O}$ ) can indicate the origin of greenhouse gases, to some degree.

Based on the available literature, CO<sub>2</sub> derived from root respiration has a smaller  $\delta^{13}\text{C}$  ( $-2.1 \pm 2.2\text{‰}$  for C<sub>3</sub> plants and  $-1.3 \pm 2.4\text{‰}$  for C<sub>4</sub> plants) than that of CO<sub>2</sub> derived from microbial

**Table 2.1** Summary of methods for the analysis of greenhouse gas hotspots including their advantages, limitations and examples.

<b>Methods</b>	<b>Advantages</b>	<b>Limitations</b>	<b>Examples</b>
Isotopic Signature Analysis ( <sup>13</sup> C, <sup>15</sup> N and/or <sup>18</sup> O Natural Abundance)	<ul style="list-style-type: none"> <li>- More affordable than isotope tracing experiments since expensive labeled substrates are not required and fees associated with enriched sample analysis are not incurred</li> <li>- <sup>15</sup>N natural abundance experiments permit site preference analysis to determine the metabolic pathways responsible for microbial N<sub>2</sub>O production (Zaman et al. 2021)</li> </ul>	<ul style="list-style-type: none"> <li>- High instrumental accuracy and precision required to detect small differences in isotopic signatures at natural abundance (Werth and Kuzyakov 2010)</li> <li>- Differences between signatures at natural abundance can be too small or overlap, preventing source partitioning (Werth and Kuzyakov 2010, Hu et al. 2015, Chalk et al. 2019)</li> <li>- Unclear if <sup>13</sup>C signatures of microbially respired CO<sub>2</sub> at natural abundance mirror the <sup>13</sup>C signature of specific pools (e.g., light vs. heavy soil density fractions; Philben et al. 2022)</li> </ul>	<ul style="list-style-type: none"> <li>Kravchenko et al. (2017)</li> <li>Volk et al. (2018)</li> <li>Xu et al. (2019)</li> <li>Daly and Hernandez-Ramirez (2020)</li> <li>Philben et al. (2022)</li> <li>Cui et al. (2023)</li> </ul>
Isotope Tracing ( <sup>13</sup> C, <sup>15</sup> N and/or <sup>18</sup> O Enrichment)	<ul style="list-style-type: none"> <li>- Can partition the contribution of different sources to CO<sub>2</sub> and N<sub>2</sub>O production by labeling substrates with <sup>13</sup>C and/or <sup>15</sup>N</li> <li>- Analysis of <sup>18</sup>O enrichment in N<sub>2</sub>O after introducing <sup>18</sup>O-H<sub>2</sub>O can help determine the role of ammonia oxidation and nitrifier-denitrification in microbial N<sub>2</sub>O production (Wrage-Mönnig et al. 2018)</li> </ul>	<ul style="list-style-type: none"> <li>- Enrichment and concentration of labeled substrates must be carefully tailored for the experiment so that they are relevant to the environmental setting, as well as high enough for eventual detection as a greenhouse gas but not too elevated that they saturate the detectors of analytical instruments</li> </ul>	<ul style="list-style-type: none"> <li>Müller et al. (2014)</li> <li>Whitman and Lehmann (2015)</li> <li>Jansen-Willems et al. (2016)</li> <li>Weng et al. (2017)</li> <li>Wang et al. (2021b)</li> <li>Liu et al. (2023)</li> </ul>

	<ul style="list-style-type: none"> <li>- In experiments where the isotopic signatures of three substrates are known at natural abundance, the inclusion of a treatment with one of the substrates in an enriched form can determine the contribution of all three sources to greenhouse gases (Whitman and Lehmann 2015)</li> </ul>	<ul style="list-style-type: none"> <li>- Cannot perform site preference analysis to determine microbial pathways of N<sub>2</sub>O production when applying <sup>15</sup>N-labeled substrates</li> <li>- Analysis of microbial N<sub>2</sub>O production with <sup>18</sup>O may be unsuccessful due to the exchange of O between H<sub>2</sub>O and nitrogen oxides (Wrage-Mönnig et al. 2018)</li> </ul>	
DNA Stable Isotope Probing with <sup>13</sup> C and/or <sup>15</sup> N ( <sup>13</sup> C-, <sup>15</sup> N-, or <sup>13</sup> C <sup>15</sup> N-DNA-SIP)	<ul style="list-style-type: none"> <li>- Can identify the microorganisms responsible for metabolizing substrates in hotspots and therefore potentially producing greenhouse gases</li> <li>- Does not rely on culturing techniques, which are limited in their capacity to capture the scope of the hotspot microbiome (Wawrick 2014)</li> <li>- If used in tandem with quantitative SIP (qSIP), can determine the amount of label incorporated into the DNA of individual microorganisms as a metric for metabolic rate (Hungate et al. 2015)</li> </ul>	<p><i>General</i></p> <ul style="list-style-type: none"> <li>- Can be cost prohibitive due to the expense of isotopes, sequencing, and number of samples to run for the appropriate representation of the hotspot microbiome (Wang and Yao 2021)</li> <li>- The content of guanine and cytosine in DNA affects its density due to the hydration of these nucleotides, which could result in the misidentification of microbes as labeled (Lueders et al. 2016, Angel 2019a)</li> <li>- Cross-feeding can mischaracterize the microbes involved in hotspot metabolic pathways (Angel 2019a)</li> </ul>	<p>Haichar et al. (2012) Hou et al. (2018) Starr et al. (2018) Maarastawi et al. (2018) Dong et al. (2022) Chen et al. (2023)</p>

---

- Metabolism of a labeled substrate does not imply the definite incorporation of the label into nucleic acids, thus all microorganisms involved in the metabolic pathway are not necessarily identified or their activity characterized (Dumont et al. 2011)

- For taxonomic identification with the ITS, 16S or 18S rRNA gene, sequencing that targets variable regions of the gene can only safely achieve genus-level classification (Johnson et al. 2019)

- If performing DNA-SIP with internal transcribed spacer (ITS), 16S or 18S rRNA gene sequencing, can only identify microbes without understanding their greenhouse gas-producing activity

- If performing DNA-SIP with metagenomics or quantitative polymerase chain reaction (qPCR) analysis of specific functional genes, can only infer potential greenhouse gas-producing activity from genes of the labeled microorganisms

---

- If performing DNA-SIP with ITS, 16S or 18S rRNA gene sequencing, shorter genes will have a greater chance of being amplified, creating an artefact

- If performing DNA-SIP with metagenomics, DNA from the most abundant microbes is more likely to be sequenced, creating an artefact (Wawrick 2014)

*<sup>13</sup>C-DNA-SIP*

- At least 20–30% of C in DNA must be labeled for isolation, which could be unfeasible for the conditions to be replicated (Wawrick 2014, Lueders et al. 2016, Angel 2019a, Wang and Yao 2021)\*

*<sup>15</sup>N-DNA-SIP*

- At least 25–30% of N in DNA must be labeled for isolation, which could be unfeasible for the conditions to be replicated (Wawrick 2014, Angel 2019a)\*

- The adenosine and thymine content of DNA can mischaracterize microbes as unlabeled due to their lower N content (Angel 2019a)

---

		<p>- Separation of labeled and unlabeled DNA is more difficult due to the low N content of nucleotides, preventing the analysis of enriched microorganisms (Angel 2019a)</p> <p>- As greenhouse gas-producing pathways involving N are dissimilatory, <math>^{15}\text{N}</math>-labeled substrates will not result in enrichment and therefore provide limited information on the microorganisms involved in these pathways unless anabolism of the nitrogen species occurs concurrently with the energy-extracting reactions (Angel 2019a, b)</p>	
<p>RNA Stable Isotope Probing with <math>^{13}\text{C}</math> and/or <math>^{15}\text{N}</math> (<math>^{13}\text{C}</math>-, <math>^{15}\text{N}</math>-, or <math>^{13}\text{C}^{15}\text{N}</math>-RNA-SIP)</p>	<p>- Ribosomal (r)RNA-SIP permits taxonomic identification of microbes in hotspots, while messenger (m)RNA-SIP with metatranscriptomics or reverse transcription quantitative polymerase chain reaction (RT-qPCR) analysis of functional transcripts permits the analysis of microbial activity in hotspots including greenhouse gas production (Lueders et al. 2016)</p>	<p><i>General</i></p> <p>- Can be cost prohibitive due to the expense of isotopes, sequencing, and number of samples to run for the appropriate representation of the hotspot microbiome (Wang and Yao 2021)</p> <p>- RNA is very delicate and requires careful extraction and handling protocols that are time-consuming (Lueders et al. 2016, Wang and Yao 2021)</p>	<p>Drigo et al. (2010) Pratscher et al. (2011) Haichar et al. (2012) Mayali et al. (2012) Hernández et al. (2015) Nuccio et al. (2021)</p>

---

- 
- Does not rely on culturing techniques, which are limited in their capacity to capture the scope of the hotspot microbiome (Wawrick 2014)
  - More sensitive than DNA-SIP because the label is incorporated faster into RNA due to its turnover (Lueders et al. 2016, Angel 2019a, Wang and Yao 2021)
  - Unlike DNA-SIP, biosynthesis and cell division are not prerequisites for successful RNA-SIP analysis, permitting a more accurate representation of the hotspot microbiome (Pratscher et al. 2011, Lueders et al. 2016)
  - Can detect the immediate response of the hotspot microbiome to changes in environmental conditions (Lueders et al. 2016)
  - If used in tandem with qSIP, can determine the amount of label incorporated into the RNA of individual microorganisms as a metric for metabolic rate (Zemb et al. 2012)
  - Metabolism of a labeled substrate does not imply the definite incorporation of the label into nucleic acids, thus all microorganisms involved in the metabolic pathway are not necessarily identified or their activity characterized (Dumont et al. 2011)
  - Taxonomic identification with rRNA-SIP can be biased by the number of ribosomes and growth rate of a microorganism compared to ITS, 16S or 18S rRNA gene sequencing (Dumont et al. 2011, Nuccio et al. 2021)
  - mRNA is less abundant than rRNA (<5% of total RNA), often requiring pre-amplification and - enrichment (Lueders et al. 2016, Angel 2019a, Wang and Yao 2021)
  - While labeled mRNA indicates that the related gene is being expressed, it does not necessarily imply that the transcript will be successfully translated into a functioning protein

- 
- More RNA than DNA in microbial cells (Ghori et al. 2019)
  - Cross-feeding can mischaracterize the microbes involved in hotspot metabolic pathways (Angel 2019a)
  - The cesium trifluoroacetate (CsTFA) used for the separation of labeled RNA is more difficult to find than the cesium chloride (CsCl) used for DNA-SIP
  - For taxonomic identification with ITS, 16S or 18S rRNA, sequencing that targets variable regions of the transcript can only safely achieve genus-level classification (Johnson et al. 2019)
  - If performing RNA-SIP with ITS, 16S or 18S rRNA sequencing, shorter transcripts will have a greater chance of being amplified, creating an artefact
  - If performing RNA-SIP with metatranscriptomics, RNA from the most abundant microbes is more likely to be sequenced, creating an artefact (Wawrick 2014)

---

- Difficult to extract high quality RNA at a high enough quantity for sequencing

*<sup>13</sup>C-RNA-SIP*

- At least 10–30% of C in RNA must be labeled for isolation, which could be unfeasible for the conditions to be replicated (Wawrick 2014, Angel 2019a, Ghori et al. 2019)\*

*<sup>15</sup>N-RNA-SIP*

- At least 25–30% of N in RNA must be labeled for isolation, which could be unfeasible for the conditions to be replicated (Wawrick 2014, Angel 2019a, Ghori et al. 2019)\*

- Separation of labeled and unlabeled RNA is more difficult due to the low N content of nucleotides, preventing the analysis of enriched microorganisms (Angel 2019a)

- The adenosine and uracil content of RNA can mischaracterize microbes as unlabeled due to their lower N content (Angel 2019a)

---

- As greenhouse gas-producing pathways involving N are dissimilatory, <sup>15</sup>N-labeled substrates will not result in enrichment and therefore provide limited information on the microorganisms involved in these pathways unless anabolism of the nitrogen species occurs concurrently with the energy-extracting reactions (Angel 2019a, b)

---

\*qSIP, Chip-SIP or ultra-high-performance liquid chromatography-tandem mass spectrometry (UHPLC-MS/MS) can reduce the necessary enrichment of nucleic acids to a few atm% (Mayali et al. 2012, Hungate et al. 2015, Lueders et al. 2016, Angel 2019a)

---

aerobic respiration ( $0.7 \pm 2.8\%$ ; Werth and Kuzyakov 2010). Experimental manipulations where  $C_3$  or  $C_4$  plants are grown on the contrasting soil (soil organic matter derived from  $C_3$  or  $C_4$  plants) can differentiate the contribution of roots and rhizodeposition to the  $CO_2$  budget, compared to the  $CO_2$  derived from soil organic matter metabolism (Chalk et al. 2021). Additionally, some studies suggest that the  $\delta^{13}C$  of microbially respired  $CO_2$  resembles that of the derived C pool (Volk et al. 2018). However, other studies determined that the  $CO_2$  can be depleted or enriched in  $^{13}C$  compared to the soil organic matter (Philben et al. 2022). Therefore, partitioning sources based on the  $\delta^{13}C$  is complicated but deserves further research investment to better understand the C dynamics of soil.

Possessing two N atoms,  $N_2O$  can exist as either  $^{15}N^{14}NO$ ,  $^{14}N^{15}NO$ , or  $^{15}N^{15}NO$ . As a result, measuring the  $\delta^{15}N$  at the inner ( $\alpha$ ) and outer ( $\beta$ ) positions of  $N_2O$  can determine the site preference, or the difference of  $\delta^{15}N_\alpha$  and  $\delta^{15}N_\beta$  (Hu et al. 2015, Chalk et al. 2019). Additionally, one can measure the overall signature of  $N_2O$  for N ( $\delta^{15}N$ ) and O ( $\delta^{18}O$ ). Altogether, these parameters can assist in partially differentiating biological pathways (Table 2.2). However, the considerable overlap of different microbial pathways often obscures the sources of  $N_2O$ . The most appropriate use of isotopic signatures of  $N_2O$  at natural abundance levels is to isolate the  $N_2O$  produced from nitrifier denitrification compared to other pathways. More work is needed to create accurate isotope mixing models for the nitrification and denitrification reactions.

Due to their slight differences,  $^{15}N$ - $N_2O$  isotopomers at natural abundance cannot be resolved with standard mass spectrometry. Isotopic signatures at natural abundance can be determined using isotope ratio mass spectrometry, a method that is able to separate isotopomers of  $CO_2$  and  $N_2O$ , often with magnetic fields (Zaman et al. 2021). Spectroscopic methods are also used, relying on the different energy holding capacities of isotopomers. These methods include

cavity ring down spectroscopy (Oertel et al. 2016) and quantum cascade laser absorption spectroscopy (Hu et al. 2015, Chalk et al. 2019). These techniques are especially promising due to their capacity for continuous measurements but can be cost prohibitive. Thus, progress in our understanding of the microbial pathways that produce greenhouse gases in soil hotspots is limited by analytical constraints at this time.

**Table 2.2** Natural abundance ranges for site preference, the  $^{15}\text{N}$ -isotopic signature of  $\text{N}_2\text{O}$  ( $\delta^{15}\text{N}-\text{N}_2\text{O}$ ) and the  $^{18}\text{O}$ -isotopic signature of  $\text{N}_2\text{O}$  ( $\delta^{18}\text{O}-\text{N}_2\text{O}$ ) for microbial  $\text{N}_2\text{O}$ -producing pathways as measured from pure microbial cultures (Adapted from Zaman et al. 2021).

Microbial $\text{N}_2\text{O}$ -producing pathway	Site preference	$\delta^{15}\text{N}-\text{N}_2\text{O}$ ‰	$\delta^{18}\text{O}-\text{N}_2\text{O}^*$
Nitrification	32.0 to 38.7	-64 to -47	$23.5 \pm 3$
Nitrifier denitrification	-13.6 to 1.9	-61 to -53	12.4 to 19.4
Denitrification by fungi	27.2 to 39.9	-46 to -31	31.2 to 45.7
Denitrification by bacteria	-7.5 to 3.7	-37 to -10	7.3 to 46.5

#### 2.4.2 Isotope tracing with $^{13}\text{C}$ , $^{15}\text{N}$ and $^{18}\text{O}$

Whereas isotopic signature analysis alone relies on the difference in the natural abundance of isotopes in  $\text{CO}_2$  and  $\text{N}_2\text{O}$  for source partitioning, isotope tracing introduces substrates artificially enriched in isotopes to follow their path from cradle (i.e., introduction) to grave (i.e.,  $\text{CO}_2$  and  $\text{N}_2\text{O}$ ). Depending on their chemical makeup, substrates can be enriched in  $^{13}\text{C}$ ,  $^{15}\text{N}$  or the combination of the two. Once the isotope is introduced, isotopic enrichment analysis of emitted greenhouse gases can determine the contribution of the substrate to greenhouse gas production. Additionally, studies assessing soil  $\text{N}_2\text{O}$  emissions can also introduce  $^{18}\text{O}$ -enriched  $\text{H}_2\text{O}$  to isolate certain microbial  $\text{N}_2\text{O}$  production pathways (i.e., ammonia oxidation, nitrifier-denitrification). Moreover, destructive sampling of soil at relevant timepoints permits isotopic enrichment analysis of different soil pools to track the path of the isotope prior to its potential

evolution as a greenhouse gas. This greater resolution provides insight into the soil mechanisms that control greenhouse gas production.

The potential origins of CO<sub>2</sub> can be assessed by introducing a variety of different <sup>13</sup>C-enriched organic substrates to soil. These C forms can include simple assimilable organic compounds – like glucose (Geyer et al. 2019, Mehnaz et al. 2019) and rhizodeposits (Pang et al. 2021) – or complex organic matter – like crop residues (Chen et al. 2022). The application of such organic substrates to soil environments not only allows researchers to quantify their contribution to CO<sub>2</sub> production via isotopic enrichment analysis, but also to determine how different factors can influence their contribution to CO<sub>2</sub> emissions like environmental factors (e.g., elevated CO<sub>2</sub> on rhizodeposition) and management practices (e.g., tillage). As such, substrates enriched with <sup>13</sup>C can provide a deeper understanding of CO<sub>2</sub> production in cultivated soils.

Similarly, triggers of N<sub>2</sub>O production in soils can be studied by using relevant nitrogenous substrates enriched with <sup>15</sup>N. These compounds can include reactive N compounds – such as NH<sub>4</sub><sup>+</sup>, NO<sub>2</sub><sup>-</sup> and NO<sub>3</sub><sup>-</sup> (Baggs and Blum 2004, Shaw et al. 2006, Kool et al. 2010, Müller et al. 2014) – or organic N forms – such as amino acids (Jansen-Willems et al. 2016) and residues (Liu et al. 2023). The introduction of these enriched nitrogenous forms allows the determination of their fate in soil and contribution to N<sub>2</sub>O evolution via isotopic enrichment analysis. Additionally, the inclusion of <sup>18</sup>O-labeled H<sub>2</sub>O with enriched nitrogenous substrates can help determine the contribution of NH<sub>3</sub> oxidation and nitrifier-denitrification to N<sub>2</sub>O emissions (Hu et al. 2015, Wrage-Mönnig et al. 2018). This partitioning is thought to be possible because these metabolic pathways should incorporate the <sup>18</sup>O from enriched H<sub>2</sub>O at different rates into the N<sub>2</sub>O molecule (Wrage-Mönnig et al. 2018). However, the sole use of <sup>15</sup>N-labeled substrates

and  $^{18}\text{O}$ -labeled  $\text{H}_2\text{O}$  poses experimental limitations and difficulties. Unlike natural abundance experiments, site preference analysis is not possible with  $^{15}\text{N}$ -tracing. Additionally, measuring  $^{18}\text{O}$  incorporation is difficult in practice due to the potential exchange of O between  $\text{H}_2\text{O}$  and pathway intermediates (Wrage-Mönnig et al. 2018). Nevertheless,  $^{15}\text{N}$ -tracing is a powerful tool in partitioning the contribution of substrates to  $\text{N}_2\text{O}$  emissions, while enrichment experiments with  $^{18}\text{O}$  can isolate the role of nitrification and nitrifier-denitrification in  $\text{N}_2\text{O}$  production. As such, these methods should be used in conjunction with  $^{15}\text{N}$ -natural abundance methods.

Isotopic enrichment analysis of  $\text{CO}_2$  and  $\text{N}_2\text{O}$  can be detected with the same spectrometric and spectroscopic methods as are used for isotopic signature analysis at natural abundance. However, due to their elevated isotopic concentration, the resulting greenhouse gases from enrichment experiments must be analyzed with the appropriate standards to accommodate their elevated enrichment. Additionally, the substrates added to soil in enrichment experiments must be labeled with the isotope to a sufficient level and applied at a high enough concentration for the eventual detection of the isotope in greenhouse gas emissions. Yet, the application rate of these substrates must simulate the soil's typical exposure to avoid unrealistic experimental conditions. Thus, it is often necessary to perform trial experiments to calibrate the appropriate enrichment and concentration of the substrate for successful application of isotopic tracing and enrichment analysis of  $\text{CO}_2$  and  $\text{N}_2\text{O}$ .

#### **2.4.3 $^{13}\text{C}$ , $^{15}\text{N}$ and $^{13}\text{C}^{15}\text{N}$ -stable isotope probing (SIP)**

Isotopic analysis of gases is an essential tool in identifying the dominant metabolic pathways occurring in greenhouse gas hotspots and the triggers that generate them. However, this method alone excludes an essential actor in greenhouse gas production: the soil microbiome. The microorganisms metabolizing C and N substrates are the catalyst of greenhouse gas production,

generating and sustaining greenhouse gas hotspots in soil. Consequently, before we can control the emissions from greenhouse hotspots in the crop rhizosphere, we must identify the key microbes that metabolize the precursors to these greenhouse gases, an endeavor made possible with the isotopic method of SIP.

At the moment, most SIP research on cultivated soils uses DNA to identify the microorganisms metabolizing various agriculturally-derived substrates. This method involves adding substrates labeled with isotopes (e.g.,  $^{13}\text{C}$ ,  $^{15}\text{N}$ ) and determining the microorganisms responsible for their metabolism by isolating the labeled DNA from the soil (Neufeld et al. 2007). For example, Maarastawi et al. (2018) demonstrated that a small portion of soil bacteria and fungi is responsible for rice straw degradation in both the rhizosphere and bulk soil using  $^{13}\text{C}$ -DNA-SIP. Likewise, España et al. (2011) employed DNA-SIP with crop residues (maize and soybean), but those isotopically labeled with  $^{15}\text{N}$ , to determine those microorganisms that assimilate the N present in crop residues. However, DNA-SIP only determines the soil microorganisms that have metabolized substrates linked to greenhouse gas production. Therefore, other methods are required to determine microorganisms that both actively metabolize agriculturally relevant substrates and produce greenhouse gases.

In contrast to DNA-SIP, RNA-SIP can provide information on both the identity and activity of the microorganisms that metabolize agriculturally relevant substrates. RNA-SIP also requires the addition of isotopically labeled substrates for uptake by microorganisms but isolates their labeled RNA rather than DNA (Whiteley et al. 2007). As a result, this method bridges both identity – via ribosomal (r)RNA – and activity – via messenger (m)RNA – of the hotspot microbiome. Application of this method is uncommon in soils, but there are exceptions. Pratscher et al. (2011) revealed the coupling of  $\text{CO}_2$  fixation and  $\text{NH}_3$  oxidation by archaea and

bacteria in agricultural soils using RNA-SIP with  $^{13}\text{C}$ - $\text{CO}_2$ . However, as this study used  $^{13}\text{C}$ - $\text{CO}_2$  and primers for  $\text{NH}_3$  monooxygenase transcripts, the results concentrated on only  $\text{NH}_3$  oxidation rather than the other metabolic pathways occurring in soils. Consequently, while providing valuable knowledge on  $\text{NH}_3$  oxidation, questions remain about the microorganisms performing other greenhouse gas-producing pathways.

Alternatively, RNA-SIP can be combined with metatranscriptomics to identify the microorganisms involved in greenhouse gas production via a diverse array of metabolic pathways. While this method has not been applied in agricultural soils, the integration of RNA-SIP and metatranscriptomics has been successfully implemented in other settings. Dumont et al. (2013) used RNA-SIP with  $^{13}\text{C}$ -methane to obtain a targeted metatranscriptome of methanotrophs in sediments, revealing the full methane consumption pathway and C assimilation mechanism. Similarly, Fortunato and Huber (2016) employed RNA-SIP with  $^{13}\text{C}$ -bicarbonate near deep-sea hydrothermal vents and found that chemolithoautotrophs were active methanogens and  $\text{NO}_3^-$  reducers. Evidently, RNA-SIP in conjunction with metatranscriptomics is an effective tool in unlocking the microorganisms performing metabolic pathways, including those producing greenhouse gases, in various environmental settings.

## **2.5 Future research directions**

During the past decades, the power of isotope technology has transformed our understanding of the greenhouse gas-producing pathways occurring in soils (e.g., Zhu et al. 2013) and at the same time, revolutionized our knowledge of the soil microbiome by pinpointing their active members, which drive C and N cycling in the rhizosphere (e.g., Starr et al. 2021). However, despite the evident link between the two fields of research, few studies attempt their synthesis, especially in cultivated peatlands. Those that do typically correlate the abundance of greenhouse gas-

producing genes in soil and emissions without providing the mechanistic link. Hence, isotopic methods – a technology already used to study the two fields separately – should be employed to bridge greenhouse gas-producing pathways and the microbes that mediate them, the core components of greenhouse gas hotspots.

Another exciting research opportunity made possible with isotope technology is the study of the CO<sub>2</sub> and N<sub>2</sub>O emissions derived from a specific substrate. Some studies attempt such analysis by measuring total CO<sub>2</sub> and N<sub>2</sub>O emissions from fields after the introduction of a particular substrate (e.g., residue application, fertilization). Yet, the coarse resolution of such an experimental design is unable to parse out the actual mechanisms and link the emissions to a specific greenhouse gas hotspot. Isotope tracing permits such analytical power but is often performed with only one tracer – <sup>13</sup>C or <sup>15</sup>N – despite the fact that most relevant agricultural substrates possess both C and N (e.g., rhizodeposits, urea). This approach narrows the determination of substrate-derived greenhouse gases to only CO<sub>2</sub> or N<sub>2</sub>O. As such, a dual isotope strategy should be favored for the simultaneous analysis of these greenhouse gases and a holistic comprehension of the substrate-driven genesis of greenhouse gas hotspots.

Of particular interest is the future application of dual isotope tracing to determine whether the spatial heterogeneity in greenhouse gas emissions – or hotspots – observed in cultivated soils is a function of rhizodeposition in the rhizosphere. The rhizosphere is already recognized as a microbial hotspot due to rhizodeposition (Kuzyakov and Blagodatskaya 2015). However, despite our understanding of the activity in the rhizosphere and that the microbiome mediates a vast majority of the greenhouse gas-producing mechanisms, the direct contribution of rhizodeposition to both CO<sub>2</sub> and N<sub>2</sub>O is rarely studied. Consequently, the rhizosphere and its

potential role as a hotspot must be considered as we endeavor to address the unexplained spatial variability in greenhouse gas emissions from cultivated soils.

Such an assessment of the rhizosphere is possible by isotopically labeling plants with both  $^{13}\text{C}$  and  $^{15}\text{N}$ , which subsequently enriches their rhizodeposits with these tracers. Incorporating  $^{13}\text{C}$  into rhizodeposits is relatively simple as plants will fix  $^{13}\text{C}$  via photosynthesis when exposed to  $^{13}\text{C}\text{-CO}_2$  and transfer this  $^{13}\text{C}$  to rhizodeposits. In contrast, introducing  $^{15}\text{N}$  into plants is more difficult since  $^{15}\text{N}$  cannot be added to soil, the natural route for plant N uptake. The way to generate rhizodeposits enriched in  $^{15}\text{N}$  is to expose the plant to  $^{15}\text{N}$ -labeled compounds (e.g., urea,  $\text{NH}_4\text{NO}_3$ ) via plant stem infiltration, leaf tip feeding or foliar application (Hertenberger and Wanek 2004). However, studies using such methods have yet to establish how simple N compounds are transformed into  $^{15}\text{N}$ -rhizodeposits, how much is released from the root and is incorporated into the root microbiome of cultivated soils, and what proportion is released as  $^{15}\text{N}\text{-N}_2\text{O}$ . To do so, the  $^{15}\text{N}$ -labeling method must generate sufficiently enriched  $^{15}\text{N}$ -rhizodeposits so that the  $^{15}\text{N}$ -tracer can be detected in the microbial biomass and emitted  $\text{N}_2\text{O}$ . Consequently, the role of the rhizosphere as a greenhouse gas hotspot cannot be confirmed until we fully trace the transformation of the  $^{15}\text{N}$ -labeled substrate into  $^{15}\text{N}$ -rhizodeposits that are assimilated by the microbiome and used for respiration, generating  $\text{CO}_2$  and  $\text{N}_2\text{O}$  as the final products.

## 2.6 References

- Abramoff, R., Xu, X., Hartman, M., et al., 2018. The Millennial Model: In search of measurable pools and transformations for modeling soil carbon in the new century. *Biogeochemistry* 137, 51–71. <https://doi.org/10.1007/s10533-017-0409-7>.
- Adhikari, D., Dunham-Cheatham, S.M., Wordofa, D.N., et al., 2019. Aerobic respiration of mineral-bound organic carbon in a soil. *Science of the Total Environment* 651, 1253–1260. <https://doi.org/10.1016/j.scitotenv.2018.09.271>.
- Ai, C., Zhang, M., Sun, Y., et al., 2020. Wheat rhizodeposition stimulates soil nitrous oxide emission and denitrifiers harboring the *nosZ* clade I gene. *Soil Biology and Biochemistry* 143, 107738. <https://doi.org/10.1016/j.soilbio.2020.107738>.
- Aldossari, N., Ishii, S., 2021. Fungal denitrification revisited – Recent advancements and future opportunities. *Soil Biology and Biochemistry* 157, 108250. <https://doi.org/10.1016/j.soilbio.2021.108250>.
- Alvarez, L., Sanchez-Hevia, D., Sánchez, M., et al., 2019. A new family of nitrate/nitrite transporters involved in denitrification. *International Microbiology* 22, 19–28. <https://doi.org/10.1007/s10123-018-0023-0>.
- Amha, Y., Bohne, H., 2011. Denitrification from the horticultural peats: effects of pH, nitrogen, carbon, and moisture contents. *Biology and Fertility of Soils* 47, 293–302. <https://doi.org/10.1007/s00374-010-0536-y>.

- Angel, R., 2019a. Experimental Setup and Data Analysis Considerations for DNA- and RNA-SIP Experiments in the Omics Era. In: Dumont, M., Hernández García, M. (Eds.), Stable Isotope Probing. Methods in Molecular Biology, Volume 2046. Humana, New York, New York, pp. 1–15. [https://doi.org/10.1007/978-1-4939-9721-3\\_1](https://doi.org/10.1007/978-1-4939-9721-3_1).
- Angel, R., 2019b. Stable Isotope Probing Techniques and Methodological Considerations Using  $^{15}\text{N}$ . In: Dumont, M., Hernández García, M. (Eds.), Stable Isotope Probing. Methods in Molecular Biology, Volume 2046. Humana, New York, New York, pp. 175–187. [https://doi.org/10.1007/978-1-4939-9721-3\\_14](https://doi.org/10.1007/978-1-4939-9721-3_14).
- Baggs, E.M., Blum, H., 2004.  $\text{CH}_4$  oxidation and emissions of  $\text{CH}_4$  and  $\text{N}_2\text{O}$  from *Lolium perenne* swards under elevated atmospheric  $\text{CO}_2$ . Soil Biology and Biochemistry 36, 713–723. <https://doi.org/10.1016/j.soilbio.2004.01.008>.
- Bahram, M., Hildebrand, F., Forslund, S.K., et al., 2018. Structure and function of the global topsoil microbiome. Nature 560, 233–237. <https://doi.org/10.1038/s41586-018-0386-6>.
- Balaine, N., Clough, T.J., Beare, M.H., et al., 2013. Changes in relative gas diffusivity explain soil nitrous oxide flux dynamics. Soil Science Society of America Journal 77, 1496–1505. <https://doi.org/10.2136/sssaj2013.04.0141>.
- Balaine, N., Clough, T.J., Beare, M.H., et al., 2016. Soil gas diffusivity controls  $\text{N}_2\text{O}$  and  $\text{N}_2$  emissions and their ratio. Soil Science Society of America Journal 80, 529–540. <https://doi.org/10.2136/sssaj2015.09.0350>.

- Baral, K.R., Arthur, E., Olesen, J., et al., 2016. Predicting nitrous oxide emissions from manure properties and soil moisture: An incubation experiment. *Soil Biology and Biochemistry* 97, 112–120. <https://doi.org/10.1016/j.soilbio.2016.03.005>.
- Bardgett, R.D., van der Putten, W.H., 2014. Belowground biodiversity and ecosystem functioning. *Nature* 515, 505–511. <https://doi.org/10.1038/nature13855>.
- Bateman, E.J., Baggs, E.M., 2005. Contributions of nitrification and denitrification to N<sub>2</sub>O emissions from soils at different water-filled pore space. *Biology and Fertility of Soils* 41, 379–388. <https://doi.org/10.1007/s00374-005-0858-3>.
- Bello, M.O., Thion, C., Gubry-Rangin, C., et al., 2019. Differential sensitivity of ammonia oxidising archaea and bacteria to matrix and osmotic potential. *Soil Biology and Biochemistry* 129, 184–190. <https://doi.org/10.1016/j.soilbio.2018.11.017>.
- Berglund, Ö., Berglund, K., Jordan, S., et al., 2019. Carbon capture efficiency, yield, nutrient uptake and trafficability of different grass species on a cultivated peat soil. *Catena* 173, 175–182. <https://doi.org/10.1016/j.catena.2018.10.007>.
- Bodner, G., Leitner, D., Kaul, H.-P., 2014. Coarse and fine root plants affect pore size distributions differently. *Plant and Soil* 380, 133–151. <https://doi.org/10.1007/s11104-014-2079-8>.
- Borrero-de Acuña, J., Rohde, M., Wissing, J., et al., 2016. Protein network of the *Pseudomonas aeruginosa* denitrification apparatus. *Journal of Bacteriology* 198, 1401–1413. <https://doi.org/10.1128/jb.00055-16>.

- Cao, P., Lu, C., Yu, Z., 2018. Historical nitrogen fertilizer use in agricultural ecosystems of the contiguous United States during 1850–2015: Application rate, timing, and fertilizer types. *Earth System Science Data* 10, 969–984. <https://doi.org/10.5194/essd-10-969-2018>.
- Caranto, J.D., Lancaster, K.M., 2017. Nitric oxide is an obligate bacterial nitrification intermediate produced by hydroxylamine oxidoreductase. *Proceedings of the National Academy of Sciences of the United States of America* 114, 8217-8222. <https://doi.org/10.1073/pnas.1704504114>.
- Caranto, J.D., Vilbert, A.C., Lancaster, K.M., 2016. *Nitrosomonas europaea* cytochrome P460 is a direct link between nitrification and nitrous oxide emission. *Proceedings of the National Academy of Sciences of the United States of America* 113, 14704–14709. <https://doi.org/10.1073/pnas.1611051113>.
- Carlson, K.M., Gerber J.S., Mueller, ND., et al., 2017. Greenhouse gas emissions intensity of global croplands. *Nature Climate Change* 7, 63–68. <https://doi.org/10.1038/nclimate3158>.
- Carminati, A., Moradi, A.B., Vetterlein, D., et al., 2010. Dynamics of soil water in the rhizosphere. *Plant and Soil* 332: 163–176. <https://doi.org/10.1007/s11104-010-0283-8>.
- Carson, J.K., Gonzalez-Quiñones, V., Murphy, D.V., et al., 2010. Low pore connectivity increases bacterial diversity in soil. *Applied Environmental and Microbiology* 76, 3936–3942. <https://doi.org/10.1128/AEM.03085-09>.

Castellano, M.J., Schmidt, J.P., Kaye, J.P., et al., 2010. Hydrological and biogeochemical controls on the timing and magnitude of nitrous oxide flux across an agricultural landscape. *Global Change Biology* 16, 2711–2720. <https://doi.org/10.1111/j.1365-2486.2009.02116.x>.

Cedervall, P., Hooper, A.B., Wilmot, C.M., 2013. Structural studies of hydroxylamine oxidoreductase reveal a unique heme cofactor and a previously unidentified interaction partner. *Biochemistry* 52, 6211–6218. <https://doi.org/10.1021/bi400960w>.

Chalk, P.M., Inácio, C.T., Chen, D., 2019. An overview of contemporary advances in the usage of  $^{15}\text{N}$  natural abundance ( $\delta^{15}\text{N}$ ) as a tracer of agro-ecosystem N cycle processes that impact the environment. *Agriculture, Ecosystems and Environment* 283, 106570. <https://doi.org/10.1016/j.agee.2019.106570>.

Chalk, P.M., Smith, C.J., 2020. The role of agroecosystems in chemical pathways of  $\text{N}_2\text{O}$  production. *Agriculture, Ecosystems and Environment* 290, 106783. <https://doi.org/10.1016/j.agee.2019.106783>.

Chalk, P.M., Balieiro, F.C., Chen, D., 2021. Quantitative estimation of carbon dynamics in terrestrial ecosystems using natural variations in the  $\delta^{13}\text{C}$  abundance of soils and biota. *Advances in Agronomy* 167, 63–104. <https://doi.org/10.1016/bs.agron.2020.12.002>.

- Chen, M., Xu, J., Li, Z., et al., 2023. Combined pot experiments and subsequent DNA-SIP incubations reveal a core microbiota involved in modulating crop nitrogen uptake derived from soil. *Applied Soil Ecology* 192, 105098.  
<https://doi.org/10.1016/j.apsoil.2023.105098>.
- Chen, R., Senbayram, M., Blagodatsky, S., et al., 2014. Soil C and N availability determine the priming effect: Microbial N mining and stoichiometric decomposition theories. *Global Change Biology* 20, 2356–2367. <https://doi.org/10.1111/gcb.12475>.
- Chen, Z., Kumar, A., Brookes, P.C., et al., 2022. Three source-partitioning of CO<sub>2</sub> fluxes based on a dual-isotope approach to investigate interactions between soil organic carbon, glucose and straw. *Science of The Total Environment* 811, 152163.  
<https://doi.org/10.1016/j.scitotenv.2021.152163>.
- Cheng, W., Johnson, D.W., Fu, S., 2003. Rhizosphere effects on decomposition: Controls of plant species, phenology, and fertilization. *Soil Science Society of America Journal* 67, 1418–1427. <https://doi.org/10.2136/sssaj2003.1418>.
- Chenu, C., Hassink, J., Bloem, J., 2001. Short-term changes in the spatial distribution of microorganisms in soil aggregates as affected by glucose addition. *Biology and Fertility of Soils* 34, 349–356. <https://doi.org/10.1007/s003740100419>.
- Coskun, D., Britto, D.T., Shi, W., et al., 2017. Nitrogen transformations in modern agriculture and the role of biological nitrification inhibition. *Nature Plants* 3, 17074.  
<https://doi.org/10.1038/nplants.2017.74>.

- Cui, H., Mo, C., Chen, P., et al., 2023. Impact of rhizosphere priming on soil organic carbon dynamics: Insights from the perspective of carbon fractions. *Applied Soil Ecology* 189, 104982. <https://doi.org/10.1016/j.apsoil.2023.104982>.
- Cui, P., Fan, F., Yin, C., et al., 2016. Long-term organic and inorganic fertilization alters temperature sensitivity of potential N<sub>2</sub>O emissions and associated microbes. *Soil Biology and Biochemistry* 93, 131–141. <https://doi.org/10.1016/j.soilbio.2015.11.005>.
- Daebeler, A., Bodelier, P.L.E., Yan, Z., et al., 2014. Interactions between Thaumarchaea, *Nitrospira* and methanotrophs modulate autotrophic nitrification in volcanic grassland soil. *The International Society for Microbial Ecology Journal* 8, 2397–2410. <https://doi.org/10.1038/ismej.2014.81>.
- Daims, H., Lebedeva, E.V., Pjevac, P., et al., 2015. Complete nitrification by *Nitrospira* bacteria. *Nature* 528, 504–509. <https://doi.org/10.1038/nature16461>.
- Daims, H., Lückner, S., Wagner, M., 2016. A new perspective on microbes formerly known as nitrite-oxidizing bacteria. *Trends in Microbiology* 24, 699–712. <https://doi.org/10.1016/j.tim.2016.05.004>.
- Daly, E.J., Hernandez-Ramirez, G., 2020. Sources and priming of soil N<sub>2</sub>O and CO<sub>2</sub> production: Nitrogen and simulated exudate additions. *Soil Biology and Biochemistry* 149, 107942. <https://doi.org/10.1016/j.soilbio.2020.107942>.

- Davidson, E.A., Samantha, S., Caramori, S.S., et al., 2012. The Dual Arrhenius and Michaelis-Menten kinetics model for decomposition of soil organic matter at hourly to seasonal time scales. *Global Change Biology* 18, 371–384.  
<https://doi.org/10.1111/j.1365-2486.2011.02546.x>.
- De Sena, A., Madramootoo, C.A., Whalen, J.K. et al., 2022a. Nucleic acids are a major pool of hydrolyzable organic phosphorus in arable organic soils of Southern Ontario, Canada. *Biology and Fertility of Soils* 58, 7–16. <https://doi.org/10.1007/s00374-021-01603-y>.
- De Sena, A., Mosdossy, K., Whalen, J.K., et al., 2022b. Root exudates and microorganisms. In: Goss, M., Oliver, M. (Eds.), *Encyclopedia of Soils in the Environment*, 2nd ed. Elsevier, Cambridge, Massachusetts, pp. 343–356. <https://doi.org/10.1016/B978-0-12-822974-3.00125-7>.
- Dijkstra, F.A., Carrillo, Y., Pendall, E., et al., 2013. Rhizosphere priming: A nutrient perspective. *Frontiers in Microbiology* 4, 216. <https://doi.org/10.3389/fmicb.2013.00216>.
- Domeignoz-Horta, L.A., Putz, M., Spor, A., et al., 2016. Non-denitrifying nitrous oxide-reducing bacteria - An effective N<sub>2</sub>O sink in soil. *Soil Biology and Biochemistry* 103, 376–379.  
<https://doi.org/10.1016/j.soilbio.2016.09.010>.
- Dong, W., Yang, Q., George, T.S., et al., 2022. Investigating bacterial coupled assimilation of fertilizer-nitrogen and crop residue-carbon in upland soils by DNA-qSIP. *Science of the Environment* 845, 157279. <https://doi.org/10.1016/j.scitotenv.2022.157279>.

- Drigo, B., Pijl, A.S., Duyts, H., et al., 2010. Shifting carbon flow from roots into associated microbial communities in response to elevated atmospheric CO<sub>2</sub>. *Proceedings of the National Academy of Sciences of the United States of America* 107, 10938–10942. <https://doi.org/10.1073/pnas.0912421107>.
- Dumont, M.G., Pommerenke, B., Casper, P., 2013. Using stable isotope probing to obtain a targeted metatranscriptome of aerobic methanotrophs in lake sediment. *Environmental Microbiology Reports* 5, 757–764. <https://doi.org/10.1111/1758-2229.12078>.
- Dumont, M.G., Pommerenke, B., Casper, P., et al., 2011. DNA-, rRNA- and mRNA-based stable isotope probing of aerobic methanotrophs in lake sediment. *Environmental Microbiology* 13, 1153–1167. <https://doi.org/10.1111/j.1462-2920.2010.02415.x>.
- Eggleston, E.M., Lee, D.Y., Owens, M.S., et al., 2015. Key respiratory genes elucidate bacterial community respiration in a seasonally anoxic estuary. *Environmental Microbiology* 17, 2306–2318. <https://doi.org/10.1111/1462-2920.12690>.
- Elder, J.W., Lal, R., 2008. Tillage effects on gaseous emissions from an intensively farmed organic soil in North Central Ohio. *Soil and Tillage Research* 98, 45–55. <https://doi.org/10.1016/j.still.2007.10.003>.
- España, M., Rasche, F., Kandeler, E., et al., 2011. Identification of active bacteria involved in decomposition of complex maize and soybean residues in a tropical Vertisol using <sup>15</sup>N-DNA stable isotope probing. *Pediobiologia – International Journal of Soil Biology* 54, 187–193. <https://doi.org/10.1016/j.pedobi.2011.03.001>.

- Fenchel, T., King, G.M., Blackburn, T.H., 2012. Bacterial metabolism. In: Fenchel, T., King, G.M., Blackburn, T.H. (Eds.), *Bacterial Biogeochemistry*, 3rd edn. Academic Press, Elsevier, Massachusetts, pp. 1–34. <https://doi.org/10.1016/B978-0-12-415836-8.00001-3>.
- Fierer, N., 2017. Embracing the unknown: disentangling the complexities of the soil microbiome. *Nature Reviews Microbiology* 15, 579–590. <https://doi.org/10.1038/nrmicro.2017.87>.
- Fortunato, C.S., Huber, J.A., 2016. Coupled RNA-SIP and metatranscriptomics of active chemolithoautotrophic communities at a deep-sea hydrothermal vent. *The International Society for Microbial Ecology Journal* 10, 1925–1938. <https://doi.org/10.1038/ismej.2015.258>.
- Fowler, R.C., Hanson, N.D., 2015. The OpdQ porin of *Pseudomonas aeruginosa* is regulated by environmental signals associated with cystic fibrosis including nitrate-induced regulation involving the NarXL two-component system. *MicrobiologyOpen* 4, 967–982. <https://doi.org/10.1002/mbo3.305>.
- Franzluebbers, A.J., 1999. Microbial activity in response to water-filled pore space of variably eroded southern Piedmont soils. *Applied Soil Ecology* 11, 91–101. [https://doi.org/10.1016/S0929-1393\(98\)00128-0](https://doi.org/10.1016/S0929-1393(98)00128-0).

- Friedl, J., De Rosa, D., Rowlings, D.W., et al., 2018. Dissimilatory nitrate reduction to ammonium (DNRA), not denitrification dominates nitrate reduction in subtropical pasture soils upon rewetting. *Soil Biology and Biochemistry* 125, 340–349.  
<https://doi.org/10.1016/j.soilbio.2018.07.024>.
- Friedl, J., Scheer, C., Rowlings, D.W., et al., 2017. The nitrification inhibitor DMPP (3,4-dimethylpyrazole phosphate) reduces N<sub>2</sub> emissions from intensively managed pastures in subtropical Australia. *Soil Biology and Biochemistry* 108, 55–64.  
<https://doi.org/10.1016/j.soilbio.2017.01.016>.
- Frostegård, Å., Vick, S.H.W., Lim, N.Y.N., et al., 2022. Linking meta-omics to the kinetics of denitrification intermediates reveals pH-dependent causes of N<sub>2</sub>O emissions and nitrite accumulation in soil. *The International Society for Microbial Ecology Journal* 16, 26–37. <https://doi.org/10.1038/s41396-021-01045-2>.
- Fukuda, M., Takeda, H., Kato, H., et al., 2015. Structural basis for dynamic mechanism of nitrate/nitrite antiport by NarK. *Nature Communications* 6, 7097.  
<https://doi.org/10.1038/ncomms8097>.
- Geyer, K.M., Dijkstra, P., Sinsabaugh, R., et al., 2019. Clarifying the interpretation of carbon use efficiency in soil through methods comparison. *Soil Biology and Biochemistry* 128, 79–88. <https://doi.org/10.1016/j.soilbio.2018.09.036>.

- Ghori, N.-U.-H., Moreira-Grez, B., Vuong, P., et al., 2019. RNA Stable Isotope Probing (RNA-SIP). In: Dumont, M., Hernández García, M. (Eds.), Stable Isotope Probing. Methods in Molecular Biology, Volume 2046. Humana, New York, New York, pp. 31–44.  
[https://doi.org/10.1007/978-1-4939-9721-3\\_3](https://doi.org/10.1007/978-1-4939-9721-3_3).
- Gilch, S., Vogel, M., Lorenz, M.W., et al., 2009. Interaction of the mechanism-based inactivator acetylene with ammonia monooxygenase of *Nitrosomonas europaea*. *Microbiology* 155, 279–284. <https://doi.org/10.1099/mic.0.023721-0>.
- Glenn, S., Hayes, A., Moore, T., 1993. Carbon dioxide and methane fluxes from drained peat soils, southern Quebec. *Global Biogeochemical Cycles* 7, 247–257.  
<https://doi.org/10.1029/93GB00469>.
- Graf, D.R., Jones, C.M., Hallin, S., 2014. Intergenomic comparisons highlight modularity of the denitrification pathway and underpin the importance of community structure for N<sub>2</sub>O emissions. *PLoS One* 9, e114118. <https://doi.org/10.1371/journal.pone.0114118>.
- Graf, D.R.H., Zhao, M., Jones, C.M., et al., 2016. Soil type overrides plant effect on genetic and enzymatic N<sub>2</sub>O production potential in arable soils. *Soil Biology and Biochemistry* 100, 125–128. <https://doi.org/10.1016/j.soilbio.2016.06.006>.
- Gregorich, E., Janzen, H.H., Helgason, B., et al., 2015. Chapter Two - Nitrogenous gas emissions from soils and greenhouse gas effects. *Advances in Agronomy* 132, 39–74.  
<https://doi.org/10.1016/bs.agron.2015.02.004>.

- Gupta, V.V.S.R., Germida, J.J., 2015. Soil aggregation: Influence on microbial biomass and implications for biological processes. *Soil Biology and Biochemistry* 80, A3–A9. <https://doi.org/10.1016/j.soilbio.2014.09.002>.
- Haichar, F.e.Z., Roncato, M.-A., Achouak, W., 2012. Stable isotope probing of bacterial community structure and gene expression in the rhizosphere of *Arabidopsis thaliana*. *Federation of European Microbiological Societies Microbiology Ecology* 81, 291–302. <https://doi.org/10.1111/j.1574-6941.2012.01345.x>.
- Haichar, F.e.Z., Santaella, C., Heulin, T., et al., 2014. Root exudates mediated interactions belowground. *Soil Biology and Biochemistry* 77, 69–80. <https://doi.org/10.1016/j.soilbio.2014.06.017>.
- Hallin, S., Philippot, L., Löffler, F.E., et al., 2018. Genomics and ecology of novel N<sub>2</sub>O-reducing microorganisms. *Trends in Microbiology* 26, 43–55. <https://doi.org/10.1016/j.tim.2017.07.003>.
- Hartmann, M., Six, J., 2023. Soil structure and microbiome functions in agroecosystems. *Nature Reviews Earth & Environment* 4, 4–18. <https://doi.org/10.1038/s43017-022-00366-w>.
- Hayatsu, M., Tago, K., Uchiyama, I., et al., 2017. An acid-tolerant ammonia-oxidizing  $\gamma$ -proteobacterium from soil. *The International Society for Microbial Ecology Journal* 11, 1130–1141. <https://doi.org/10.1038/ismej.2016.191>.

- Helliwell, J.R., Sturrock, C.J., Miller, A.J., et al., 2019. The role of plant species and soil condition in the structural development of the rhizosphere. *Plant, Cell & Environment* 42, 1974–1986. <https://doi.org/10.1111/pce.13529>.
- Hénault, C., Bourennane, H., Ayzac, A., et al., 2019. Management of soil pH promotes nitrous oxide reduction and thus mitigates soil emissions of this greenhouse gas. *Scientific Reports* 9, 20182. <https://doi.org/10.1038/s41598-019-56694-3>.
- Hernández, M., Dumont, M.G., Yuan, Q., et al., 2015. Different bacterial populations associated with the roots and rhizosphere of rice incorporate plant-derived carbon. *Applied and Environmental Microbiology* 81, 2244–2253. <https://doi.org/10.1128/AEM.03209-14>.
- Hertenberger, G., Wanek, W., 2004. Evaluation of methods to measure differential <sup>15</sup>N labeling of soil and root N pools for studies of root exudation. *Rapid Communications in Mass Spectrometry* 18, 2415–2425. <https://doi.org/10.1002/rcm.1615>.
- Higgins, S.A., Schadt, C.W., Matheny, P.B., et al., 2018. Phylogenomics reveal the dynamic evolution of fungal nitric oxide reductases and their relationship to secondary metabolism. *Genome Biology and Evolution* 10, 2474–2489. <https://doi.org/10.1093/gbe/evy187>.
- Hink, L., Nicol, G.W., Prosser, J.I., 2017. Archaea produce lower yields of N<sub>2</sub>O than bacteria during aerobic ammonia oxidation in soil. *Environmental Microbiology* 19, 4829–4837. <https://doi.org/10.1111/1462-2920.13282>.

- Hoehler, T.M., Mankel, D.J., Girguis, P.R., et al., 2023. The metabolic rate of the biosphere and its components. *Proceedings of the National Academy of Sciences of the United States of America* 120, e2303764120. <https://doi.org/10.1073/pnas.2303764120>.
- Hou, S., Ai, C., Zhou, W., et al., 2018. Structure and assembly cues for rhizospheric *nirK*- and *nirS*-type denitrifier communities in long-term fertilized soils. *Soil Biology and Biochemistry* 119, 32–40. <https://doi.org/10.1016/j.soilbio.2018.01.007>.
- Hu, H.-W., Chen, D., He, J.-Z., 2015. Microbial regulation of terrestrial nitrous oxide formation: understanding the biological pathways for prediction of emission rates. *Federation of European Microbiological Societies Microbiology Reviews*, 39, 729–749. <https://doi.org/10.1093/femsre/fuv021>.
- Hungate, B.A., Mau, R.L., Schwartz, E., et al., 2015. Quantitative microbial ecology through stable isotope probing. *Applied and Environmental Microbiology* 81, 7570–7581. <https://doi.org/10.1128/AEM.02280-15>.
- Huo, C., Luo, Y., Cheng, W., 2017. Rhizosphere priming effect: A meta-analysis. *Soil Biology and Biochemistry* 111, 78–84. <https://doi.org/10.1016/j.soilbio.2017.04.003>.
- Hütsch, B.W., Augustin, J., Merbach, W., 2002. Plant rhizodeposition – An important source for carbon turnover in soils. *Journal of Plant Nutrition and Soil Science* 165, 397–407. [https://doi.org/10.1002/1522-2624\(200208\)165:4<397::AID-JPLN397>3.0.CO;2-C](https://doi.org/10.1002/1522-2624(200208)165:4<397::AID-JPLN397>3.0.CO;2-C).

- Jansen-Willems, A.B., Lanigan, G.J., Clough, T.J., et al., 2016. Long-term elevation of temperature affects organic N turnover and associated N<sub>2</sub>O emissions in a permanent grassland soil. *SOIL* 2, 601–614. <https://doi.org/10.5194/soil-2-601-2016>.
- Javed, T., Indu, I., Singhal, R.K., et al., 2022. Recent advances in agronomic and physiological approaches for improving nitrogen use efficiency in crop plants. *Frontiers in Plant Science* 13, 877544. <https://doi.org/10.3389/fpls.2022.877544>.
- Johnson, J.S., Spakowicz, D.J., Hong, B.-Y., et al., 2019. Evaluation of 16S rRNA gene sequencing for species and strain-level microbiome analysis. *Nature Communications* 10, 5029. <https://doi.org/10.1038/s41467-019-13036-1>.
- Jones, C.M., Graf, D.R.H., Bru, D., et al., 2013. The unaccounted yet abundant nitrous oxide-reducing microbial community: a potential nitrous oxide sink. *The International Society for Microbial Ecology Journal* 7, 417–426. <https://doi.org/10.1038/ismej.2012.125>.
- Jones, C.M., Spor, A., Brennan, F.P., et al., 2014. Recently identified microbial guild mediates soil N<sub>2</sub>O sink capacity. *Nature Climate Change* 4, 801–805. <https://doi.org/10.1038/nclimate2301>.
- Jung, M.-Y., Well, R., Min, D., et al., 2014. Isotopic signatures of N<sub>2</sub>O produced by ammonia-oxidizing archaea from soils. *The International Society for Microbial Ecology Journal* 8, 1115–1125. <https://doi.org/10.1038/ismej.2013.205>.

Jung, M.-Y., Sedlacek, C.J., Kits, K.D., et al., 2022. Ammonia-oxidizing archaea possess a wide range of cellular ammonia affinities. *The International Society for Microbial Ecology Journal* 16, 272–283. <https://doi.org/10.1038/s41396-021-01064-z>.

Kamennaya, N.A., Geraki, K., Scanlan, D.J., et al., 2020. Accumulation of ambient phosphate into the periplasm of marine bacteria is proton motive force dependent. *Nature Communications* 11, 2642. <https://doi.org/10.1038/s41467-020-16428-w>.

Kasimir-Klmedtsson, Å., Klmedtsson, L., Berglund, K., et al., 1997. Greenhouse gas emissions from farmed organic soils: A review. *Soil Use and Management* 13, 245–250. <https://doi.org/10.1111/j.1475-2743.1997.tb00595.x>.

Kits, K.D., Jung, M.Y., Vierheilig, J., et al., 2019. Low yield and abiotic origin of N<sub>2</sub>O formed by the complete nitrifier *Nitrospira inopinata*. *Nature Communications* 10, 1836. <https://doi.org/10.1038/s41467-019-09790-x>.

Kits, K.D., Sedlacek, C.J., Lebedeva, E.V., Han, P., et al., 2017. Kinetic analysis of a complete nitrifier reveals an oligotrophic lifestyle. *Nature* 549, 269–272. <https://doi.org/10.1038/nature23679>.

Kløve, B., Berglund, K., Berglund, Ö., et al., 2017. Future options for cultivated Nordic peat soils: Can land management and rewetting control greenhouse gas emissions? *Environmental Science & Policy* 69, 85–93. <https://doi.org/10.1016/j.envsci.2016.12.017>.

- Koch, H., Lücker, S., Albertsen, M., et al., 2015. Expanded metabolic versatility of ubiquitous nitrite-oxidizing bacteria from the genus *Nitrospira*. *Proceedings of the National Academy of Sciences of the United States of America* 112, 11371–11376.  
<https://doi.org/10.1073/pnas.1506533112>.
- Koebnick, N., Daly, K.R., Keyes, S.D., et al., 2017. High-resolution synchrotron imaging shows that root hairs influence rhizosphere soil structure formation. *New Phytologist* 216, 124–135. <https://doi.org/10.1111/nph.14705>.
- Kool, D.M, Wrage, N., Zechmeister-Boltenstern, S., et al., 2010. Nitrifier denitrification can be a source of N<sub>2</sub>O from soil: a revised approach to the dual-isotope labelling method. *European Journal of Soil Science* 61, 759–772. <https://doi.org/10.1111/j.1365-2389.2010.01270.x>.
- Kool, D.M., Dolfing, J., Wrage, N., et al., 2011. Nitrifier denitrification as a distinct and significant source of nitrous oxide from soil. *Soil Biology and Biochemistry* 43, 174–178.  
<https://doi.org/10.1016/j.soilbio.2010.09.030>.
- Köster, J.R., Cárdenas, L., Senbayram, M., et al., 2011. Rapid shift from denitrification to nitrification in soil after biogas residue application as indicated by nitrous oxide isotopomers. *Soil Biology and Biochemistry* 43, 1671–1677.  
<https://doi.org/10.1016/j.soilbio.2011.04.004>.

- Kozłowski, J.A., Stieglmeier, M., Schleper, C., et al., 2016. Pathways and key intermediates required for obligate aerobic ammonia-dependent chemolithotrophy in bacteria and Thaumarchaeota. *The International Society for Microbial Ecology Journal* 10, 1836–1845. <https://doi.org/10.1038/ismej.2016.2>.
- Kravchenko, A.N., Toosi, E.R., Guber, A.K., et al., 2017. Hotspots of soil N<sub>2</sub>O emission enhanced through water absorption by plant residue. *Nature Geoscience* 10, 496–500. <https://doi.org/10.1038/ngeo2963>.
- Kuypers, M.M.M., Marchant, H.K., Kartal, B., 2018. The microbial nitrogen-cycling network. *Nature Reviews Microbiology* 16, 263–276. <https://doi.org/10.1038/nrmicro.2018.9>.
- Kuzyakov, Y., 2006. Sources of CO<sub>2</sub> efflux from soil and review of partitioning methods. *Soil Biology and Biochemistry* 38, 425–448. <https://doi.org/10.1016/j.soilbio.2005.08.020>.
- Kuzyakov, Y., Blagodatskaya, E., 2015. Microbial hotspots and hot moments in soil: Concept & review. *Soil Biology and Biochemistry* 83, 184–199. <https://doi.org/10.1016/j.soilbio.2015.01.025>.
- Lahtinen, L., Mattila, T., Myllyviita, T., et al., 2022. Effects of paludiculture products on reducing greenhouse gas emissions from agricultural peatlands. *Ecological Engineering* 175, 106502. <https://doi.org/10.1016/j.ecoleng.2021.106502>.
- Lancaster, K.M., Caranto, J.D., Majer, S.H., et al., 2018. Alternative bioenergy: Updates to and challenges in nitrification metalloenzymology. *Joule* 2, 421–441. <https://doi.org/10.1016/j.joule.2018.01.018>.

- Langarica-Fuentes, A., Manrubia, M., Giles, M.E., et al., 2018. Effect of model root exudate on denitrifier community dynamics and activity at different water-filled pore space levels in a fertilised soil. *Soil Biology and Biochemistry* 120, 70–79.  
<https://doi.org/10.1016/j.soilbio.2018.01.034>.
- Lauber, C.L., Hamady, M., Knight, R., et al., 2009. Pyrosequencing-based assessment of soil pH as a predictor of soil bacterial community structure at the continental scale. *Applied and Environmental Microbiology* 75, 5111–5120. <https://doi.org/10.1128/AEM.00335-09>.
- Lecomte, S.M., Achouak, W., Abrouk, D., et al., 2018. Diversifying anaerobic respiration strategies to compete in the rhizosphere. *Frontiers in Environmental Science* 6, 139.  
<https://doi.org/10.3389/fenvs.2018.00139>.
- Lehmann, J., Kleber, M., 2015. The contentious nature of soil organic matter. *Nature* 528, 60–68.  
<https://doi.org/10.1038/nature16069>.
- Lehtovirta-Morley, L.E., Sayavedra-Soto, L.A., Gallois, N., et al., 2016. Identifying potential mechanisms enabling acidophily in the ammonia-oxidizing archaeon “*Candidatus Nitrosotalea devanattera*”. *Applied and Environmental Microbiology* 82, 2608–2619.  
<https://doi.org/10.1128/AEM.04031-15>.
- Lennon, E.F.E., Houlton, B.Z., 2017. Coupled molecular and isotopic evidence for denitrifier controls over terrestrial nitrogen availability. *The International Society for Microbial Ecology Journal* 11, 727–740. <https://doi.org/10.1038/ismej.2016.147>.

- Li, Z., Tang, Z., Song, Z., et al., 2022. Variations and controlling factors of soil denitrification rate. *Global Change Biology* 28, 2133–2145. <https://doi.org/10.1111/gcb.16066>.
- Liimatainen, M., Voigt, C., Martikainen, P.J., et al., 2018. Factors controlling nitrous oxide emissions from managed northern peat soils with low carbon to nitrogen ratio. *Soil Biology and Biochemistry* 122, 186–195. <https://doi.org/10.1016/j.soilbio.2018.04.006>.
- Ling, N., Wang, T., Kuzyakov, Y., 2022. Rhizosphere bacteriome structure and functions. *Nature Communications* 13, 836. <https://doi.org/10.1038/s41467-022-28448-9>.
- Linn, D.M., Doran, J.W., 1984. Effect of water-filled pore space on carbon dioxide and nitrous oxide production in tilled and nontilled soils. *Soil Science Society of America Journal* 48, 1267–1272. <https://doi.org/10.2136/sssaj1984.03615995004800060013x>.
- Liu, X., Li, Q., Liu, M., et al., 2023. Responses of N<sub>2</sub>O emissions to straw addition under different tillage soils: A <sup>15</sup>N labelling study. *Applied Soil Ecology* 183, 104744. <https://doi.org/10.1016/j.apsoil.2022.104744>.
- Lloyd, K., Madramootoo, C.A., Edwards, K.P., et al., 2019. Greenhouse gas emissions from selected horticultural production systems in a cold temperate climate. *Geoderma* 349, 45–55. <https://doi.org/10.1016/j.geoderma.2019.04.030>.
- Lu, X., Taylor, A.E., Myrold, D.D., et al., 2020. Expanding perspectives of soil nitrification to include ammonia-oxidizing archaea and comammox bacteria. *Soil Science Society of America Journal* 84, 287–302. <https://doi.org/10.1002/saj2.20029>.

- Lucas, M., Schlüter, S., Vogel, H.-J., et al., 2019. Roots compact the surrounding soil depending on the structures they encounter. *Scientific Reports* 9, 16236. <https://doi.org/10.1038/s41598-019-52665-w>.
- Lueders, T., Dumont, M.G., Bradford, L., et al., 2016. RNA-stable isotope probing: From carbon flow within key microbiota to targeted transcriptomes. *Current Opinion in Biotechnology* 41, 83–89. <https://doi.org/10.1016/j.copbio.2016.05.001>.
- Maarastawi, S.A., Frindte, K., Geer, R., et al., 2018. Temporal dynamics and compartment specific rice straw degradation in bulk soil and the rhizosphere of maize. *Soil Biology and Biochemistry* 127, 200–212. <https://doi.org/10.1016/j.soilbio.2018.09.028>.
- Maia, L.B., Moura, J.J.G., 2014. How biology handles nitrite. *Chemical Reviews* 114, 5273–5357. <https://doi.org/10.1021/cr400518y>.
- Maljanen, M., Sigurdsson, B.D., Gudmundsson, J., et al., 2010. Greenhouse gas balances of managed peatlands in the Nordic countries – present knowledge and gaps. *Biogeosciences* 7, 2711–2738. <https://doi.org/10.5194/bg-7-2711-2010>.
- Martikainen, P.J., 2022. Heterotrophic nitrification – An eternal mystery in the nitrogen cycle. *Soil Biology and Biochemistry* 168, 108611. <https://doi.org/10.1016/j.soilbio.2022.108611>.
- Mayali, X., Weber, P.K., Brodie, E.L., et al., 2012. High-throughput isotopic analysis of RNA microarrays to quantify microbial resource use. *The International Society for Microbial Ecology Journal* 6, 1210–1221. <https://doi.org/10.1038/ismej.2011.175>.

- Mehnaz, K.R., Corneo, P.E., Keitel, C., et al., 2019. Carbon and phosphorus addition effects on microbial carbon use efficiency, soil organic matter priming, gross nitrogen mineralization and nitrous oxide emission from soil. *Soil Biology and Biochemistry* 134, 175–186. <https://doi.org/10.1016/j.soilbio.2019.04.003>.
- Michel, J.-C., Kerloch, E., 2017. Evolution of hydraulic properties and wettability of organic growing media during cultivation according to irrigation strategies. *Scientia Horticulturae* 217, 28–35. <https://doi.org/10.1016/j.scienta.2017.01.023>.
- Miller, J.O., Hunt, P.G., Ducey, T.F., et al., 2012. Denitrification and gas emissions from organic soils under different water table and flooding management. *Transactions of the American Society of Agricultural and Biological Engineers* 55, 1793–1800. <https://doi.org/10.13031/2013.42371>.
- Mooshammer, M., Wanek, W., Hämmerle, I., et al., 2014. Adjustment of microbial nitrogen use efficiency to carbon:nitrogen imbalances regulates soil nitrogen cycling. *Nature Communications* 5, 3694. <https://doi.org/10.1038/ncomms4694>.
- Moradi, A.B., Carminati, A., Vetterlein, D., et al., 2011. Three-dimensional visualization and quantification of water content in the rhizosphere. *New Phytologist* 192, 653–663. <https://doi.org/10.1111/j.1469-8137.2011.03826.x>.
- Moyano, F.E., Manzoni, S., Chenu, C., 2013. Responses of soil heterotrophic respiration to moisture availability: An exploration of processes and models. *Soil Biology and Biochemistry* 59, 72–85. <https://doi.org/10.1016/j.soilbio.2013.01.002>.

Müller, C., Laughlin, R.J., Spott, O., et al., 2014. Quantification of N<sub>2</sub>O emission pathways via a <sup>15</sup>N tracing model. *Soil Biology and Biochemistry* 72, 44–54.

<https://doi.org/10.1016/j.soilbio.2014.01.013>.

Negassa, W.C., Guber, A.K., Kravchenko, A.N., et al., 2015. Properties of soil pore space regulate pathways of plant residue decomposition and community structure of associated bacteria. *PLoS ONE* 10, e0123999. <https://doi.org/10.1371/journal.pone.0123999>.

Neufeld, J.D., Vohra, J., Dumont, M.G., et al., 2007. DNA stable-isotope probing. *Nature Protocols* 2, 860–866. <https://doi.org/10.1038/nprot.2007.109>.

Nikaido, H., 2003. Molecular basis of bacterial outer membrane permeability revisited.

*Microbiology and Molecular Biology Reviews* 67, 593–656.

<https://doi.org/10.1128/membr.67.4.593-656.2003>.

Norberg, L., Berglund, Ö., Berglund, K., 2016a. Nitrous oxide and methane fluxes during the growing season from cultivated peat soils, peaty marl and gyttja clay under different cropping systems. *Acta Agriculturae Scandinavica, Section B – Soil & Plant Science* 66, 602–612. <https://doi.org/10.1080/09064710.2016.1205126>.

Norberg, L., Berglund, Ö., Berglund, K., 2016b. Seasonal CO<sub>2</sub> emission under different cropping systems on Histosols in southern Sweden. *Geoderma Regional* 7, 338–345.

<https://doi.org/10.1016/j.geodrs.2016.06.005>.

- Norberg, L., Hellman, M., Berglund, K., et al., 2021. Methane and nitrous oxide production from agricultural peat soils in relation to drainage level and abiotic and biotic factors. *Frontiers in Environmental Science* 9, 631112. <https://doi.org/10.3389/fenvs.2021.631112>.
- Nuccio, E.E., Nguyen, N.H., Nunes da Rocha, U., et al., 2021. Community RNA-Seq: Multi-kingdom responses to living versus decaying roots in soil. *International Society for Microbial Ecology Communications* 1, 72. <https://doi.org/10.1038/s43705-021-00059-3>.
- Oertel, C., Matschullat, J., Zurba, K., et al., 2016. Greenhouse gas emissions from soils—A review. *Chemie der Erde* 76, 327–352. <https://doi.org/10.1016/j.chemer.2016.04.002>.
- Ouyang, Y., Evans, S.E., Friesen, M.L., et al., 2018. Effect of nitrogen fertilization on the abundance of nitrogen cycling genes in agricultural soils: A meta-analysis of field studies. *Soil Biology and Biochemistry* 127, 71–78. <https://doi.org/10.1016/j.soilbio.2018.08.024>.
- Palatinszky, M., Herbold, C., Jehmlich, N., et al., 2015. Cyanate as an energy source for nitrifiers. *Nature* 524, 105–108. <https://doi.org/10.1038/nature14856>.
- Pang, R., Xu, X., Tian, Y., et al., 2021. *In-situ*  $^{13}\text{CO}_2$  labeling to trace carbon fluxes in plant-soil-microorganism systems: Review and methodological guideline. *Rhizosphere* 20, 100441. <https://doi.org/10.1016/j.rhisph.2021.100441>.

Papenfort, K., Bassler, B., 2016. Quorum sensing signal-response systems in Gram-negative bacteria. *Nature Reviews Microbiology* 14, 576-588.

<https://doi.org/10.1038/nrmicro.2016.89>

Pelissari, C., Guivernau, M., Viñas, M., et al., 2018. Effects of partially saturated conditions on the metabolically active microbiome and on nitrogen removal in vertical subsurface flow constructed wetlands. *Water Research* 141, 185–195.

<https://doi.org/10.1016/j.watres.2018.05.002>.

Petersen, S.O., Hoffmann, C.C., Schäfer, C.-M., et al., 2012. Annual emissions of CH<sub>4</sub> and N<sub>2</sub>O, and ecosystem respiration, from eight organic soils in Western Denmark managed by agriculture. *Biogeosciences* 9, 403–422. <https://doi.org/10.5194/bg-9-403-2012>.

Philben, M., Bowering, K., Podrebarac, F.A., et al., 2022. Enrichment of <sup>13</sup>C with depth in soil organic horizons is not explained by CO<sub>2</sub> or DOC losses during decomposition.

*Geoderma* 424, 116004. <https://doi.org/10.1016/j.geoderma.2022.116004>.

Pohl, M., Hoffman, M., Hagemann, U., et al., 2015. Dynamic C and N stocks – key factors controlling the C gas exchange of maize in heterogenous peatland. *Biogeosciences* 12, 2737–2752. <https://doi.org/10.5194/bg-12-2737-2015>.

Pratscher, J., Dumont, M.G., Conrad, R., 2011. Ammonia oxidation coupled to CO<sub>2</sub> fixation by archaea and bacteria in an agricultural soil. *Proceedings of the National Academy of Sciences of the United States of America* 108, 4170–4175.

<https://doi.org/10.1073/pnas.1010981108>.

- Ramirez, K.S., Craine, J.M., Fierer, N., 2010. Nitrogen fertilization inhibits soil microbial respiration regardless of the form of nitrogen applied. *Soil Biology and Biochemistry* 42, 2336–2338. <https://doi.org/10.1016/j.soilbio.2010.08.032>.
- Rezanezhad, F., Price, J.S., Quinton, W.L., et al., 2016. Structure of peat soils and implications for water storage, flow and solute transport: A review update for geochemists. *Chemical Geology* 429, 75–84. <https://doi.org/10.1016/j.chemgeo.2016.03.010>.
- Rochette, P., Tremblay, N., Fallon, E., et al., 2010. N<sub>2</sub>O emissions from an irrigated and non-irrigated organic soil in eastern Canada as influenced by N fertilizer addition. *European Journal of Soil Science* 61, 186–196. <https://doi.org/10.1111/j.1365-2389.2009.01222.x>.
- Rousk, J., Brookes, P.C., Bååth, E., 2010. Investigating the mechanisms for the opposing pH relationships of fungal and bacterial growth in soil. *Soil Biology and Biochemistry* 42, 926–934. <https://doi.org/10.1016/j.soilbio.2010.02.009>.
- Rui, Y., Murphy, D.V., Wang, X., et al., 2016. Microbial respiration, but not biomass, responded linearly to increasing light fraction organic matter input: Consequences for carbon sequestration. *Scientific Reports* 6, 35496. <https://doi.org/10.1038/srep35496>.
- Saifuddin, M., Bhatnagar, J.M., Segrè, D., et al., 2019. Microbial carbon use efficiency predicted from genome-scale metabolic models. *Nature Communications* 10, 3568. <https://doi.org/10.1038/s41467-019-11488-z>.

- Sasse, J., Martinoia, E., Northen, T., 2018. Feed your friends: Do plant exudates shape the root microbiome? *Trends in Plant Science* 23, 25–41.  
<https://doi.org/10.1016/j.tplants.2017.09.003>.
- Säurich, A, Tiemeyer, B., Dettmann, U., et al., 2019. How do sand addition, soil moisture and nutrient status influence greenhouse gas fluxes from drained organic soils? *Soil Biology and Biochemistry* 135 71–84. <https://doi.org/10.1016/j.soilbio.2019.04.013>.
- Schjønning, P., Thomsen, I.K., Moldrup, P., et al., 2003. Linking soil microbial activity to water- and air-phase contents and diffusivities. *Soil Science Society of America Journal* 67, 156–165. <https://doi.org/10.2136/sssaj2003.1560>.
- Shaw, L.J., Nicol, G.W., Smith, Z., et al., 2006. *Nitrosospira* spp. can produce nitrous oxide via a nitrifier denitrification pathway. *Environmental Microbiology* 8, 214–222.  
<https://doi.org/10.1111/j.1462-2920.2005.00882.x>.
- Simon, J., Klotz, M.G., 2013. Diversity and evolution of bioenergetic systems involved in microbial nitrogen compound transformations. *Biochimica et Biophysica Acta* 1827, 114–135. <https://doi.org/10.1016/j.bbabi.2012.07.005>.
- Song, A., Liang, Y., Zeng, X., et al., 2018. Substrate-driven microbial response: A novel mechanism contributes significantly to temperature sensitivity of N<sub>2</sub>O emissions in upland arable soil. *Soil Biology and Biochemistry* 118, 18–26.  
<https://doi.org/10.1016/j.soilbio.2017.11.021>.

Sparacino-Watkins, C., Stolz, J.F., Basu, P., 2014. Nitrate and periplasmic nitrate reductases.

Chemical Society Reviews 43, 676–706. <https://doi.org/10.1039/C3CS60249D>.

Starr, E.P., Shi, S., Blazewicz, S.J., et al., 2018. Stable isotope informed genome-resolved metagenomics reveals that Saccharibacteria utilize microbially-processed plant-derived carbon. Microbiome 6, 122. <https://doi.org/10.1186/s40168-018-0499-z>.

Starr, E.P., Shi, S., Blazewicz, S.J., et al., 2021. Stable-isotope-informed, genome-resolved metagenomics uncovers potential cross-kingdom interactions in rhizosphere. mSphere 6, e00085-21. <https://doi.org/10.1128/mSphere.00085-21>.

Stein, L.Y., 2019. Insights into the physiology of ammonia-oxidizing microorganisms. Current Opinion in Chemical Biology 49, 9–15. <https://doi.org/10.1016/j.cbpa.2018.09.003>.

Stieglmeier, M., Mooshammer, M., Kitzler, B., et al., 2014. Aerobic nitrous oxide production through N-nitrosating hybrid formation in ammonia-oxidizing archaea. The International Society for Microbial Ecology Journal 8, 1135–1146. <https://doi.org/10.1038/ismej.2013.220>.

Subbarao, G.V., Kishii, M., Bozal-Leorri, A., et al., 2021. Enlisting wild grass genes to combat nitrification in wheat farming: A nature-based solution. Proceedings of the National Academy of Sciences of the United States of America 118, e2106595118. <https://doi.org/10.1073/pnas.2106595118>.

- Terasaka, E., Yamada, K., Wang, P.-H., et al., 2017. Dynamics of nitric oxide controlled by protein complex in bacterial system. *Proceedings of the National Academy of Sciences of the United States of America* 114, 9888–9893. <https://doi.org/10.1073/pnas.1621301114>.
- Torregrosa-Crespo, J., González-Torres, P., Bautista, V., et al., 2017. Analysis of multiple haloarchaeal genomes suggests that the quinone-dependent respiratory nitric oxide reductase is an important source of nitrous oxide in hypersaline environments. *Environmental Microbiology Reports* 9, 788–796. <https://doi.org/10.1111/1758-2229.12596>.
- Tsiknia, M., Paranychianakis, N.V., Varouchakis, E.A., et al., 2015. Environmental drivers of the distribution of nitrogen functional genes at a watershed scale. *Federation of European Microbiological Societies Microbiology Ecology* 91, fiv052. <https://doi.org/10.1093/femsec/fiv052>.
- van Kessel, M.A.H.J., Speth, D.R., Albertsen, M., et al., 2015. Complete nitrification by a single microorganism. *Nature* 528, 555–559. <https://doi.org/10.1038/nature16459>.
- Volk, M., Bassin, S., Lehmann, M.F., et al., 2018. <sup>13</sup>C isotopic signature and C concentration of soil density fractions illustrate reduced C allocation to subalpine grassland soil under high atmospheric N deposition. *Soil Biology and Biochemistry* 125, 178–184. <https://doi.org/10.1016/j.soilbio.2018.07.014>.

- Wagner-Riddle, C., Baggs, E.M., Clough, T.J., et al., 2020. Mitigation of nitrous oxide emissions in the context of nitrogen loss reduction from agroecosystems: managing hot spots and hot moments. *Current Opinion in Environmental Sustainability* 47, 46–53.  
<https://doi.org/10.1016/j.cosust.2020.08.002>.
- Wang, J., Yao, H., 2021. Applications of DNA/RNA-Stable Isotope Probing (SIP) in *Environmental Microbiology*. *Methods in Microbiology* 48, 227–267.  
<https://doi.org/10.1016/bs.mim.2020.11.004>.
- Wang, N., Gao, J., Liu, Y., et al., 2021a. Realizing the role of N-acyl-homoserine lactone-mediated quorum sensing in nitrification and denitrification: A review. *Chemosphere* 274, 129970. <https://doi.org/10.1016/j.chemosphere.2021.129970>.
- Wang, R., Bicharanloo, B., Shirvan, M.B., et al., 2021b. A novel  $^{13}\text{C}$  pulse-labelling method to quantify the contribution of rhizodeposits to soil respiration in a grassland exposed to drought and nitrogen addition. *New Phytologist* 230, 857–866.  
<https://doi.org/10.1111/nph.17118>.
- Wang, X., Tang, C., 2018. The role of rhizosphere pH in regulating the rhizosphere priming effect and implications for the availability of soil-derived nitrogen to plants. *Annals of Botany* 121, 143–151. <https://doi.org/10.1093/aob/mcx138>.
- Ward, B.B., 2013. Nitrification. In: Fath, B. (Ed.), *Encyclopedia of Ecology*, 2nd edn. Elsevier, Oxford, United Kingdom, pp. 351–358. <https://doi.org/10.1016/B978-0-12-409548-9.00697-7>.

- Wawrick, B., 2014. Stable Isotope Probing the Nitrogen Cycle: Current Applications and Future Directions. In: Marco, D. (Ed.), *Metagenomics of the Microbial Nitrogen Cycle: Theory, Methods and Applications*, 1st edn. Caister Academic Press, Norfolk, United Kingdom, pp. 87–110.
- Weng, Z.(H.), Van Zwieten, L., Singh, B.P., et al., 2017. Biochar built soil carbon over a decade by stabilizing rhizodeposits. *Nature Climate Change* 7, 371–376.  
<https://doi.org/10.1038/nclimate3276>.
- Werth, M., Kuzyakov, Y., 2010.  $^{13}\text{C}$  fractionation at the root–microorganisms–soil interface: A review and outlook for partitioning studies. *Soil Biology and Biochemistry* 42, 1372–1384. <https://doi.org/10.1016/j.soilbio.2010.04.009>.
- Wessner, D., Dupont, C., Charles, T., 2013. *Microbiology*, 1st edn. Wiley, Hoboken, New Jersey.
- Whalen, E.D., Grandy, A.S., Sokol, N.W., et al., 2022. Clarifying the evidence for microbial- and plant-derived soil organic matter, and the path toward a more quantitative understanding. *Global Change Biology* 28, 7167–7185.  
<https://doi.org/10.1111/gcb.16413>.
- Whiteley, A.S., Thomson, B., Lueders, T., et al., 2007. RNA stable-isotope probing. *Nature Protocols* 2, 838–844. <https://doi.org/10.1038/nprot.2007.115>.

- Whitman, T., Lehmann, J., 2015. A dual-isotope approach to allow conclusive partitioning between three sources. *Nature Communications* 6, 8708.  
<https://doi.org/10.1038/ncomms9708>.
- Wrage, N., Velthof, G.L., van Beusichem, M.L., et al., 2001. Role of nitrifier denitrification in the production of nitrous oxide. *Soil Biology and Biochemistry* 33, 1723–1732.  
[https://doi.org/10.1016/S0038-0717\(01\)00096-7](https://doi.org/10.1016/S0038-0717(01)00096-7).
- Wrage, N., Velthof, G.L., Laanbroek, H.J., et al., 2004. Nitrous oxide production in grassland soils: assessing the contribution of nitrifier denitrification. *Soil Biology and Biochemistry* 36, 229–236. <https://doi.org/10.1016/j.soilbio.2003.09.009>.
- Wrage-Mönnig, N., Horn, M.A., Well, R., et al., 2018. The role of nitrifier denitrification in the production of nitrous oxide revisited. *Soil Biology and Biochemistry* 123, A3–A16.  
<https://doi.org/10.1016/j.soilbio.2018.03.020>.
- Wright, C.L., Schatteman, A., Crombie, A.T., et al., 2020. Inhibition of ammonia monooxygenase from ammonia-oxidizing archaea by linear and aromatic alkynes. *Applied and Environmental Microbiology* 86, e02388-19.  
<https://doi.org/10.1128/AEM.02388-19>.
- Xu, Q., Wang, X., Tang, C., 2019. Rhizosphere priming of two near-isogenic wheat lines varying in citrate efflux under different levels of phosphorus supply. *Annals of Botany* 124, 1033–1042. <https://doi.org/10.1093/aob/mcz082>.

- Xu, S., Wang, B., Li, Y., et al., 2020. Ubiquity, diversity, and activity of comammox *Nitrospira* in agricultural soils. *Science of The Total Environment* 706, 135684.  
<https://doi.org/10.1016/j.scitotenv.2019.135684>.
- Xu, X., Schimel, J.P., Janssens, I.A., et al., 2017. Global pattern and controls of soil microbial metabolic quotient. *Ecological Monographs* 87, 429–441.  
<https://doi.org/10.1002/ecm.1258>.
- Yan, Z., Liu, C., Todd-Brown, K.E., et al., 2016. Pore-scale investigation on the response of heterotrophic respiration to moisture conditions in heterogeneous soils. *Biogeochemistry* 131, 121–134. <https://doi.org/10.1007/s10533-016-0270-0>.
- Yoon, S., Song, B., Phillips, R.L., et al., 2019. Ecological and physiological implications of nitrogen oxide reduction pathways on greenhouse gas emissions in agroecosystems. *Federation of European Microbiological Societies Microbiology Ecology* 95, fiz066.  
<https://doi.org/10.1093/femsec/fiz066>.
- Yu, R., Perez-Garcia, O., Lu, H., et al., 2018. *Nitrosomonas europaea* adaptation to anoxic-oxic cycling: Insights from transcription analysis, proteomics and metabolic network modeling. *Science of the Total Environment* 615, 1566–1573.  
<https://doi.org/10.1016/j.scitotenv.2017.09.142>.
- Yu, Z., Loisel, J., Brosseau, D.P., et al., 2010. Global peatland dynamics since the Last Glacial Maximum. *Geophysical Research Letters* 37, 1–5.  
<https://doi.org/10.1029/2010GL043584>.

- Zaman, M., Heng, L., Müller, C., 2021. Measuring Emission of Agricultural Greenhouse Gases and Developing Mitigation Options using Nuclear and Related Techniques: Applications of Nuclear Techniques for GHGs. Springer, International Atomic Energy Agency, Austria, Vienna. <https://doi.org/10.1007/978-3-030-55396-8>.
- Zemb, O., Lee, M., Gutierrez-Zamora, M.L., et al., 2012. Improvement of RNA-SIP by pyrosequencing to identify putative 4-n-nonylphenol degraders in activated sludge. *Water Research* 46, 601–610. <https://doi.org/10.1016/j.watres.2011.10.047>.
- Zhalnina, K., Louie, K.B., Hao, Z., et al., 2018. Dynamic root exudate chemistry and microbial preferences drive patterns in rhizosphere microbial community assembly *Nature Microbiology* 3, 470–480. <https://doi.org/10.1038/s41564-018-0129-3>.
- Zhang, L., Wüst, A., Prasser, B., et al., 2019. Functional assembly of nitrous oxide reductase provides insights into copper site maturation. *Proceedings of the National Academy of Sciences of the United States of America* 116,12822–12827. <https://doi.org/10.1073/pnas.1903819116>.
- Zhu, S., Vivanco, J.M., Manter, D.K., 2016. Nitrogen fertilizer rate affects root exudation, the rhizosphere microbiome and nitrogen-use-efficiency of maize. *Applied Soil Ecology* 107, 324–333. <https://doi.org/10.1016/j.apsoil.2016.07.009>.

- Zhu, X., Burger, M., Doane, T.A., et al., 2013. Ammonia oxidation pathways and nitrifier denitrification are significant sources of N<sub>2</sub>O and NO under low oxygen availability. *Proceedings of the National Academy of Sciences of the United States of America* 110, 6328–6333. <https://doi.org/10.1073/pnas.1219993110>.
- Zhu, Z., Yang, Y., Fang, A., et al., 2020. Quorum sensing systems regulate heterotrophic nitrification-aerobic denitrification by changing the activity of nitrogen-cycling enzymes. *Environmental Science and Ecotechnology* 2, 100026. <https://doi.org/10.1016/j.esec.2020.100026>.
- Zou, Y., Ning, D., Huang, Y., et al., 2020. Functional structures of soil microbial community relate to contrasting N<sub>2</sub>O emission patterns from a highly acidified forest. *Science of the Total Environment* 725, 138504. <https://doi.org/10.1016/j.scitotenv.2020.138504>.

### FORWARD TO CHAPTER 3

The objective of Chapter 2 was to critically review our current knowledge on microbially-mediated greenhouse gas production in the rhizosphere hotspots of cultivated peatlands. As can be seen, recent developments in isotope technology have the potential to unlock our understanding of the mechanisms occurring in the rhizosphere that create greenhouse gas hotspots, such as rhizodeposition and root exudation. However, while there are established techniques for measuring the contribution of rhizodeposition to microbial CO<sub>2</sub> production, none exist for the contribution of root exudation to N<sub>2</sub>O. Such an endeavor would require (i) the development of a <sup>15</sup>N-labeling method for plants that efficiently quantifies the transfer of <sup>15</sup>N-labeled root exudates to the rhizobiome, and (ii) the confirmation of their transfer to the rhizobiome in fertilized soils. In Chapter 3, I compare the capacity of different methods to produce sufficient <sup>15</sup>N-root exudates and confirm their metabolism by the rhizosphere microbiome in a N-rich soil from a cultivated peatland using two different <sup>15</sup>N-labeling techniques for plants (leaf tip feeding or stem feeding), two different nitrogen compounds (<sup>15</sup>N-urea or <sup>15</sup>N-NH<sub>4</sub>NO<sub>3</sub>) and three different concentrations (64.5, 129 or 193 mmol <sup>15</sup>N L<sup>-1</sup>).

The following manuscript has been published in *Soil Biology and Biochemistry*:

**De Sena, A.,** Madramootoo, C.A., Whalen, J.K. (2023). Nitrogen transfer from root exudates to the rhizobiome: A <sup>15</sup>N stem feeding method. *Soil Biology and Biochemistry* 186: 109159.

<https://doi.org/10.1016/j.soilbio.2023.109159>

## CHAPTER 3

### 3. Nitrogen transfer from root exudates to the rhizobiome: A $^{15}\text{N}$ stem feeding method

Aidan De Sena, Chandra A. Madramootoo, Joann K. Whalen

#### 3.1 Abstract

Plant roots exude nitrogen (N)-containing compounds, which are assimilated by the rhizobiome to maintain stoichiometric homeostasis. Various  $^{15}\text{N}$ -tracing methods exist to estimate the rhizobiome-N derived from root exudation but have never been validated with a full factorial experiment. We exposed ryegrass (*Lolium multiflorum*) to  $^{15}\text{N}$  solutions through different plant organs (stem or leaf feeding), with different  $^{15}\text{N}$ -tracers (urea or  $\text{NH}_4\text{NO}_3$ ) and concentrations (64.5, 129 or 193 mmol  $^{15}\text{N L}^{-1}$ ). Stem feeding with either  $^{15}\text{N}$ -source at the highest concentration was the only effective way to quantify root exudate-N assimilation by the rhizobiome, and we recommend this  $^{15}\text{N}$ -labeling method for the reliable assessment of microbiome-N dynamics in the rhizosphere.

#### 3.2 Introduction

Plant root exudates supply nitrogen (N) to the microbial community living in the rhizosphere, or rhizobiome (Sasse et al. 2018). The transfer of nitrogenous root exudates to the rhizobiome is quantified by  $^{15}\text{N}$ -labeling the root exudates via the exposure of a  $^{15}\text{N}$ -tracer, typically  $^{15}\text{N}$ -urea, to plant organs like roots (Schenck zu Schweinsberg-Mickan et al. 2010), stems (Mayer et al. 2003, Wichern et al. 2010) or leaves (Kušlienė et al. 2014). However, elevated urea concentrations (>0.24% N) elicit toxicity in plants (Hertenberger and Wanek 2004) due to the excessive ammonia ( $\text{NH}_3$ ) and ammonium ( $\text{NH}_4^+$ ) concentrations that accumulate in plant tissues

after urea hydrolysis by urease. These negative physiological effects include elevated root respiration (Britto et al. 2001), the depression of essential cations in tissues and reduced net photosynthesis (Britto and Kronzucker 2002). Thus, the toxicity risk of this method may be eliminated by the use of another  $^{15}\text{N}$ -tracer, like doubly  $^{15}\text{N}$ -labeled ammonium nitrate ( $\text{NH}_4\text{NO}_3$ ), which only produces one molecule of  $\text{NH}_4^+$  – versus two from urea – and the application of which has a synergistic growth response from plants (Britto and Kronzucker 2002, Hachiya and Sakakibara 2017).

Additionally, root labeling with  $^{15}\text{N}$  is technically demanding, requiring either hydroponic compartments or complex rhizoboxes. Such growth conditions disturb root systems and create artificial root environments. In contrast, stem and leaf feeding preserve normal growth conditions for roots and may be a more effective  $^{15}\text{N}$ -labeling strategy. A standardized method that effectively labels root exudates without triggering a toxic physiological response in plants or disturbing their root system would resolve the uncertainty around the rhizobiome-N derived from root exudates, which is estimated at 0.004–11% (Wichern et al. 2008, Schenck zu Schweinsberg-Mickan et al. 2010, 2012, Kušlienė et al. 2014).

Our objective was to validate the capacity of different plant  $^{15}\text{N}$ -labeling methods to enrich the rhizobiome with  $^{15}\text{N}$  to quantify their assimilation of nitrogenous root exudates after 24 h. We hypothesized that stem feeding with  $^{15}\text{N}$ - $\text{NH}_4\text{NO}_3$  will allow tracing of the  $^{15}\text{N}$ -root exudates assimilated by the rhizobiome because (i) the stem contains more phloem vessels, which are directly connected to the root system, and (ii) there is a synergistic growth response observed in plants to  $\text{NH}_4^+$  and  $\text{NO}_3^-$  in tandem, permitting their rapid transfer to root exudates.

### 3.3 Materials and methods

The experiment had three factors: introduction technique (stem or leaf feeding),  $^{15}\text{N}$ -tracer ( $^{15}\text{N}$ - $\text{NH}_4\text{NO}_3$  or  $^{15}\text{N}$ -urea), and labeling solution concentration (64.5, 129 or 193  $\text{mmol } ^{15}\text{N L}^{-1}$ ). We prepared four replicates for each factorial combination plus four controls for each factor, in total 56 experimental pots. Each pot ( $236 \text{ cm}^3$ ) was filled with air-dried peat soil (165 g oven-dry mass) and planted with annual ryegrass (six seeds, Semican Atlantic Inc. (Plessisville, Québec, Canada)). Peat soil (Terric Humisol) came from the top 10 cm of a cultivated peatland in Sherrington, Québec, Canada ( $45^\circ 07' 44'' \text{ N}$ ,  $73^\circ 31' 09'' \text{ W}$ ) in November 2019. It was sieved ( $\leq 3 \text{ mm}$ ) and stored at  $4^\circ \text{C}$  until pot preparation. Soil physico-chemical characteristics are compiled in Table 3.6.S1.

Pots were placed in a greenhouse (randomized complete block design, average temperature:  $22^\circ \text{C}$ , daylength: 10 h) and maintained at 65% water-filled pore space. We thinned pots to one seedling – equivalent to  $\sim 170 \text{ seeds m}^{-2}$  – 21 d after planting. We prepared the stem feeding apparatus (Mahieu et al. 2009) on day 105 and the leaf feeding apparatus (Yasmin et al. 2006) on day 106 (See Section 3.6.1 Supplemental text S1). Each vial of the apparatus contained 2 mL of deionized water until  $^{15}\text{N}$ -labeling commenced.

Also on day 106, we added 1 mL of fertilizer solution ( $8.58 \text{ mol N L}^{-1}$  from urea,  $0.273 \text{ mol phosphorus (P) L}^{-1}$  from triple superphosphate and  $0.353 \text{ mol potassium (K) L}^{-1}$  from potassium chloride (KCl)) for an N- $\text{P}_2\text{O}_5$ - $\text{K}_2\text{O}$  rate of 150-20-20  $\text{kg ha}^{-1}$  and subsequently watered all pots. This delayed application ensured plant N deficiency that promoted their N uptake – including from the  $^{15}\text{N}$ -tracer – while still generating N-rich soil conditions reflective of a cultivated soil. Deionized water was removed from vials  $\sim 22 \text{ h}$  after installing the stem feeding apparatus and  $\sim 3.5 \text{ h}$  after installing the leaf feeding apparatus. Then, vials were filled with

2 mL  $^{15}\text{N-NH}_4\text{NO}_3$  ( $\geq 98$  atm%; Cambridge Isotope Laboratories, Andover, Massachusetts, USA) or  $^{15}\text{N-urea}$  ( $\geq 98$  atm%; Cambridge Isotope Laboratories, Andover, Massachusetts, USA) at 64.5, 129 or 193 mmol  $^{15}\text{N L}^{-1}$ . While there was a difference in the plant acclimation period for the two different introduction techniques as a result of the time required for their preparation, there was no change in the exposure time to  $^{15}\text{N}$ . Controls were handled identically except that vials were filled with 2 mL fresh deionized water. After 24 h from adding the  $^{15}\text{N}$  solutions, the pots were destructively sampled, prepared and analyzed for  $\delta^{15}\text{N}$  of the shoots, roots, rhizosphere soil and microbial biomass (See Section 3.6.1 Supplemental text S1). Rhizosphere soil was carefully removed from the root system to avoid  $^{15}\text{N}$  contamination from fine root fragments in rhizosphere soil and the soil microbial biomass.

The  $^{15}\text{N}$  enrichment of soil microbial biomass was calculated by a modified isotope balance equation (See Section 3.6.1 Supplemental text S1; Voroney et al. 2008). N derived from root exudation (i.e., the percentage of  $^{15}\text{N}$  exuded by the plant to the total  $^{15}\text{N}$  taken up by the plant) was based on modified rhizodeposition mass balance equations (See Section 3.6.1 Supplemental text S1; Hupe et al. 2016). We assumed that (i) any  $^{15}\text{N}$  present in the rhizosphere and rhizobiome after 24 h was derived from root exudates rather than rhizodeposits (e.g., fine root turnover), (ii) this  $^{15}\text{N}$  represents net root exudation and net assimilation by the rhizobiome thus accounting for plant reuptake, and (iii) that this brief  $^{15}\text{N}$  exposure period limited the influence of cross-feeding on  $^{15}\text{N}$ -microbial biomass N. Negative values of replicates were excluded as outliers, indicating unsuccessful  $^{15}\text{N}$  enrichment of the pool for that replicate. When more than one replicate had a negative value, the mean value of the pool for that respective treatment was considered to be zero. Simple linear regression models generated the best-fit relationship between the  $^{15}\text{N}$  concentration of the labeling solution and the  $^{15}\text{N}$  enrichment of

shoots, roots, and rhizosphere soil, as well as the  $^{15}\text{N}$  concentration of the labeling solution and N derived from root exudation, and their significance ( $p < 0.05$ ) using statsmodels.api and pandas packages on Spyder 5.2.2 (Spyder Project Contributors 2020).

### 3.4 Results and discussion

Stem feeding with either  $^{15}\text{N}$ -tracer at the highest concentration ( $193 \text{ mmol } ^{15}\text{N L}^{-1}$ ) was effective at tracking the N assimilation from ryegrass root exudates by the rhizobiome in peat soil (Table 3.1). This finding partially confirmed our hypothesis. Stem feeding was superior to leaf feeding because it transferred more  $^{15}\text{N}$  to the shoots (121–150% greater), roots (144–174% greater) and rhizosphere soil (105–145% greater; Figure 3.1). All plants appeared healthy and maintained similar rates of N exudation (Figure 3.6.S1), regardless of the method, suggesting no visible perturbation of ryegrass physiology. The rhizobiome-N derived from root exudation was a minor portion of their biomass-N (mean:  $0.07 \pm 0.01\%$ ), but this enrichment is comparable to the 0.01–0.02% rhizobiome-N derived from root exudation of perennial ryegrass (*L. perenne*) in a similar study (48-h leaf feeding with urea at  $160 \text{ mmol } ^{15}\text{N L}^{-1}$ ; Kušlienė et al. 2014). We remarked that the rhizobiome accumulated  $^{15}\text{N}$  from root exudates even with the abundance of soil soluble N (rhizobiome-N measured 27 h after adding  $52 \text{ mmol N kg}^{-1}$  soil). Thus, root exudates remained a source of N for the rhizobiome despite the N-rich soil conditions.

Leaf feeding was not as effective at introducing  $^{15}\text{N}$  to ryegrass as stem feeding and did not result in an observable  $^{15}\text{N}$  enrichment of the rhizobiome. Typically, leaf feeding is recommended for grass species due to their delicate stems, as demonstrated by its ~10-fold greater  $^{15}\text{N}$  enrichment of perennial ryegrass roots than stem feeding after a 48-h exposure period to  $^{15}\text{N-NH}_4\text{NO}_3$  ( $20 \text{ mmol } ^{15}\text{N L}^{-1}$ ; Hertenberger and Wanek 2004). These contrasting results may arise from the three times lower  $^{15}\text{N}$ -tracer concentration compared to the lowest

**Table 3.1** Microbial biomass N and microbial biomass enriched with  $^{15}\text{N}$  in the rhizosphere soil of annual ryegrass (*L. multiflorum*) plants grown in a greenhouse for 107 d. Ryegrass plants were exposed to twelve  $^{15}\text{N}$ -labeling methods at 106 d that varied according to the technique of introducing the tracer (stem or leaf feeding),  $^{15}\text{N}$ -tracer solution (urea or  $\text{NH}_4\text{NO}_3$ ), and concentration (64.5, 129 or 193  $\text{mmol } ^{15}\text{N L}^{-1}$ ) to enrich root exudates with  $^{15}\text{N}$  during a 24-h period. Values are the mean  $\pm$  standard error ( $n = 4$ , while those with an asterisk (\*) were  $n = 3$  due to negative values).

Method		Concentration	Microbial Biomass N	$^{15}\text{N}$ -Microbial Biomass N
Technique	Tracer	( $\text{mmol } ^{15}\text{N L}^{-1}$ )	( $\text{mg N kg}^{-1}$ )	( $\mu\text{g } ^{15}\text{N kg}^{-1}$ )
Stem Feeding	$^{15}\text{N-NH}_4\text{NO}_3$	64.5	$64.9 \pm 25.3$	0
		129	$75.1 \pm 24.3$	0
		193	$103 \pm 4$	$60.2 \pm 22.0$
	$^{15}\text{N-Urea}$	64.5	$40.7 \pm 16.4$	0
		129	$50.2 \pm 6.7$	0
		193	$87.5 \pm 18.1$	$71.3 \pm 6.7 *$
Leaf Feeding	$^{15}\text{N-NH}_4\text{NO}_3$	64.5	$28.9 \pm 7.1$	0
		129	$38.3 \pm 7.9$	0
		193	$34.9 \pm 7.5 *$	0
	$^{15}\text{N-Urea}$	64.5	$25.5 \pm 2.0 *$	0
		129	$7.52 \pm 3.64 *$	0
		193	$109 \pm 63$	0

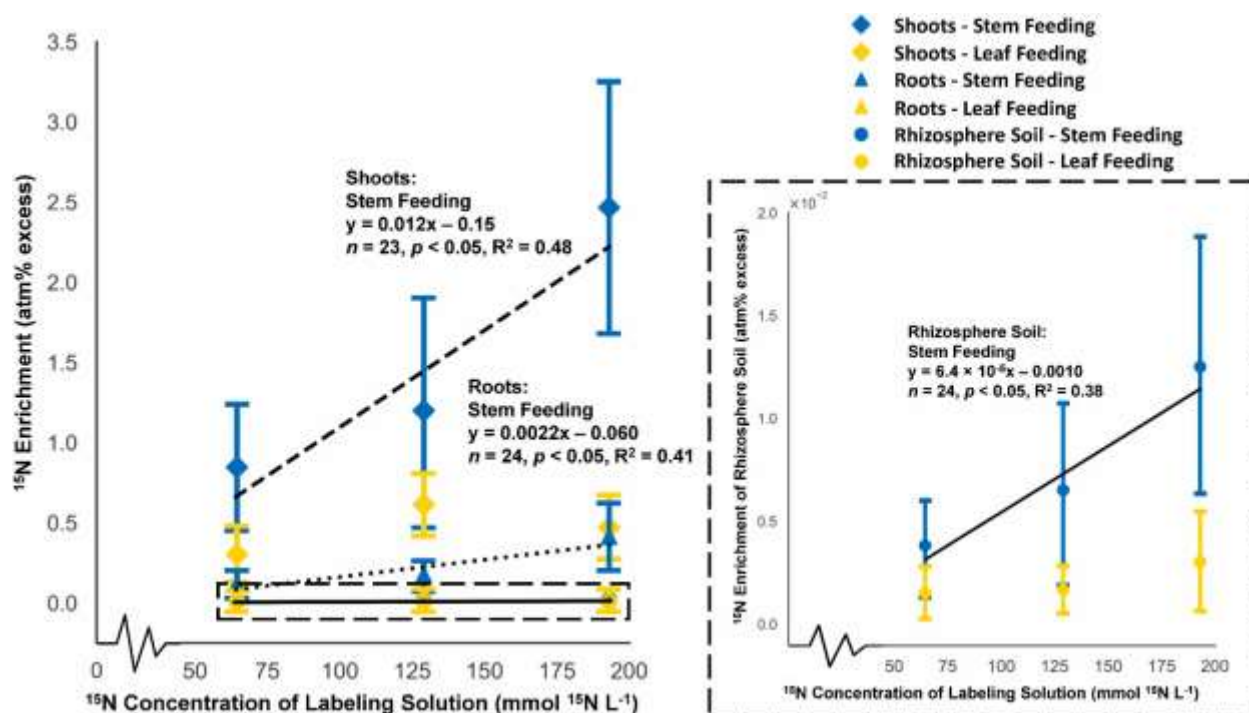


**Figure 3.1** The  $^{15}\text{N}$  enrichment (atm% excess) of shoots, roots and rhizosphere soil (inset) at each labeling solution concentration (mmol  $^{15}\text{N}$  L $^{-1}$ ) for stem and leaf feeding after a 24-h  $^{15}\text{N}$  enrichment period of annual ryegrass (*L. multiflorum*) plants grown in a greenhouse for 107 d. Ryegrass plants were exposed to twelve  $^{15}\text{N}$ -labeling methods at 106 d that varied according to the technique of introducing the tracer (stem or leaf feeding),  $^{15}\text{N}$ -tracer solution (urea or  $\text{NH}_4\text{NO}_3$ ), and concentration (64.5, 129 or 193 mmol  $^{15}\text{N}$  L $^{-1}$ ) to enrich root exudates with  $^{15}\text{N}$ . Points represent the mean for their respective introduction technique at that concentration with standard deviation bars. The best-fit line of association is shown for a technique if significant ( $p < 0.05$ ). Data were pooled for  $^{15}\text{N}$ -tracers within the stem feeding group or the leaf feeding group because plant and soil enrichment was not affected by the type of  $^{15}\text{N}$ -tracer (Figure 3.6.S2, Table 3.6.S2). Regressions were produced using statsmodels.api and pandas packages on Spyder 5.2.2 (Spyder Project Contributors 2020).

concentration used in our study ( $64.5 \text{ mmol } ^{15}\text{N L}^{-1}$ ). Additionally, leaf feeding may require a longer labeling period, based on the doubling of  $^{15}\text{N}$  enrichment in perennial ryegrass roots between 24 and 48 h during leaf feeding (Hertenberger and Wanek 2004), albeit without a comparison to stem feeding. However, a longer  $^{15}\text{N}$  exposure period does not necessarily imply a relationship between  $^{15}\text{N}$ -tracer concentration and  $^{15}\text{N}$  enrichment for this introduction technique, as observed with stem feeding. Since the  $^{15}\text{N}$ -tracer must enter the apoplast with leaf feeding, active transport processes permit selective control of  $^{15}\text{N}$ -tracer uptake regardless of concentration and thus allows plant regulation of  $^{15}\text{N}$  enrichment (Sattelmacher 2001, Fernández and Brown 2013). Nevertheless, more frequent measurements (e.g., hours rather than days) would confirm the efficacy of stem and leaf feeding and their patterns of  $^{15}\text{N}$  transfer to plant organs and the rhizobiome.

The  $^{15}\text{N}$  enrichment of root exudates and their assimilation by the rhizobiome was not affected by  $^{15}\text{N}$ -tracer chemistry. We reject the hypothesis that  $^{15}\text{N-NH}_4\text{NO}_3$  is a more effective tracer than  $^{15}\text{N-urea}$ , based on the similar transfer of the  $^{15}\text{N}$  from these two sources to the rhizobiome with the optimal stem feeding technique and concentration ( $193 \text{ mmol } ^{15}\text{N L}^{-1}$ ). While there was no difference between the two  $^{15}\text{N}$ -tracers, stem feeding as a whole gave a significant best-fit line with the  $^{15}\text{N}$  enrichment in shoots ( $n = 23, p < 0.05, R^2 = 0.48$ ), roots ( $n = 24, p < 0.05, R^2 = 0.41$ ) and rhizosphere soil ( $n = 24, p < 0.05, R^2 = 0.38$ ; Figure 3.1). We explain the similarity in  $^{15}\text{N-urea}$  and  $^{15}\text{N-NH}_4\text{NO}_3$  by noting that urease is a pervasive enzyme in plant tissue (Bobille et al. 2019), capable of converting urea into  $\text{NH}_3$  that is then protonated to  $\text{NH}_4^+$ . However, as this enzyme remains undocumented in the phloem (Rodríguez-Celma et al. 2016), there are two locations where such urease activity could occur. Urease may hydrolyze  $^{15}\text{N-urea}$  in the mesophyll or companion cells of the vascular bundles. Accounting for the

minimal  $\text{NH}_4^+$  concentrations in the phloem under natural conditions (Dinant et al. 2010), it is unlikely that this urea-derived  $\text{NH}_4^+$  would be exported into the phloem, suggesting that the  $^{15}\text{N}$ - $\text{NH}_4^+$  is assimilated as a  $^{15}\text{N}$ -labeled amino acid before export into the phloem. Conversely, the  $^{15}\text{N}$ -urea may enter the phloem directly during stem feeding, facilitating its transport to the root tissue where it may be hydrolyzed and exuded either as  $^{15}\text{N}$ - $\text{NH}_4^+$  or an assimilated  $^{15}\text{N}$ -amino acid. Verification of these proposed pathways requires  $^{15}\text{N}$ -tracing at the appropriate resolution to fully comprehend the  $^{15}\text{N}$ -tracer dynamics in the plant-root exudate compartments.

Like all  $^{15}\text{N}$ -tracing root exudation and rhizodeposition studies, there are aspects of our proposed approach that deserve consideration. First, using the stem to deliver the  $^{15}\text{N}$ -tracer relies upon an artificial uptake route for N and could create biases in the partitioning of the  $^{15}\text{N}$ . Such labeling artefacts were observed with leaf feeding on red clover (*Trifolium pratense*) using  $^{15}\text{N}$ -urea, where 0.5% of the introduced  $^{15}\text{N}$  entered the rhizosphere during the first day after labeling, described as the “leakage effect” (Gasser et al. 2015). Since our study only had a 24-h  $^{15}\text{N}$  exposure period, we cannot assess whether this artefact occurred during stem feeding. Regardless, the  $^{15}\text{N}$ -microbial biomass N determined still represents the N that the rhizobiome assimilated from root exudation, albeit potentially a maximum. Additionally, we analyzed the  $^{15}\text{N}$  enrichment of bulk roots as is standard in this field (e.g., Schenck zu Schweinsberg-Mickan et al. 2010, Kušlienė et al. 2014, Hupe et al. 2016). However, including root-extractable  $^{15}\text{N}$  would provide greater resolution as this pool represents nitrogenous compounds potentially exuded by roots and permits analysis of specific N forms (e.g.,  $^{15}\text{N}$ -amino acids,  $^{15}\text{N}$ - $\text{NH}_4^+$ ; Hertenberger and Wanek 2004, Bobille et al. 2019). This N pool should be measured explicitly in future studies. Moreover, despite the easy removal of peat soil from root systems, fine root fragments could still be present in the rhizosphere soil. As such, their contamination could result

in an overestimation of root exudation. Lastly, although the resulting  $\text{NH}_4^+$  concentrations from either  $^{15}\text{N}$ -tracer did not trigger any visible signs of toxicity (e.g., chlorosis), the resulting concentrations approach the higher end of those observed in the cytosol of *Poaceae* under experimental  $\text{NH}_4^+$  exposure ( $\sim 358 \text{ mmol N-NH}_4^+ \text{ L}^{-1}$ ; Britto et al. 2001) and could trigger toxic symptoms during longer labeling periods. Furthermore, plant species have different capacities to tolerate  $\text{NH}_4^+$  toxicity. Thus, future applications of this method must consider the potential physiological responses of their model organism to  $\text{NH}_4^+$ , especially if the N concentration or duration of N exposure are increased.

From this mechanistic experiment, we validated through a full factorial design that stem feeding with either  $^{15}\text{N}$ -tracer at the highest concentration ( $193 \text{ mmol } ^{15}\text{N L}^{-1}$ ) was the only effective plant  $^{15}\text{N}$ -labeling method in enriching the rhizobiome with  $^{15}\text{N}$ , permitting analysis of root exudate assimilation by the rhizobiome. Indeed, employing stem feeding confirmed that root exudation was a source of N for the rhizobiome despite the N-rich soil environment, a novel finding of our experiment. The broad application of this method could standardize measurements of the rhizobiome-N derived from the root exudates of grass species and address questions regarding N dynamics in the rhizosphere.

### 3.5 References

- Bobille, H., Fustec, J., Robins, R.J., Cukier, C., Limami, A.M., 2019. Effect of water availability on changes in root amino acids and associated rhizosphere on root exudation of amino acids in *Pisum sativum* L. *Phytochemistry* 161, 75–85.  
<https://doi.org/10.1016/j.phytochem.2019.01.015>.
- Britto, D.T., Kronzucker, H.J., 2002.  $\text{NH}_4^+$  toxicity in higher plants: a critical review. *Journal of Plant Physiology* 159, 567–584. <https://doi.org/10.1078/0176-1617-0774>.
- Britto, D.T., Siddiqi, M.Y., Glass, A.D.M., Kronzucker, H.J., 2001. Futile transmembrane  $\text{NH}_4^+$  cycling: A cellular hypothesis to explain ammonium toxicity in plants. *Proceedings of the National Academy of Sciences* 98, 4255–4258. <https://doi.org/10.1073/pnas.061034698>.
- Dinant, S., Bonnemain, J.,-L., Girousse, C., Kehr, J., 2010. Phloem sap intricacy and interplay with aphid feeding. *Comptes Rendus Biologies* 333, 504–515.  
<https://doi.org/10.1016/j.crv.2010.03.008>.
- Fernández, V., Brown, P.H., 2013. From plant surface to plant metabolism: The uncertain fate of foliar-applied nutrients. *Frontiers in Plant Science* 4, 289.  
<https://doi.org/10.3389/fpls.2013.00289>.
- Gasser, M., Hammelehle, A., Oberson, A., Frossard, E., Mayer, J., 2015. Quantitative evidence of overestimated rhizodeposition using  $^{15}\text{N}$  leaf-labelling. *Soil Biology and Biochemistry* 85, 10–20. <https://doi.org/10.1016/j.soilbio.2015.02.002>.
- Hachiya, T., Sakakibara, H., 2017. Interactions between nitrate and ammonium in their uptake, allocation, assimilation, and signaling in plants. *Journal of Experimental Biology* 68, 2501–2512. <https://doi.org/10.1093/jxb/erw449>.

- Hertenberger, G., Wanek, W., 2004. Evaluation of methods to measure differential  $^{15}\text{N}$  labeling of soil and root N pools for studies of root exudation. *Rapid Communications in Mass Spectrometry* 18, 2415–2425. <https://doi.org/10.1002/rcm.1615>.
- Hupe, A., Schulz, H., Bruns, C., Joergensen, R.G., Wichern, F., 2016. Digging in the dirt – Inadequacy of belowground plant biomass quantification. *Soil Biology and Biochemistry* 96, 137–144. <https://doi.org/10.1016/j.soilbio.2016.01.014>.
- Kušlienė, G., Rasmussen, J., Kuzyakov, Y., Eriksen, J., 2014. Medium-term response of microbial community to rhizodeposits of white clover and ryegrass and tracing of active processes induced by  $^{13}\text{C}$  and  $^{15}\text{N}$  labelled exudates. *Soil Biology and Biochemistry* 76, 22–33. <https://doi.org/10.1016/j.soilbio.2014.05.003>.
- Mahieu, S., Fustec, J., Jensen, E.S., Crozat, Y., 2009. Does labelling frequency affect N rhizodeposition assessment using the cotton-wick method? *Soil Biology and Biochemistry* 41, 2236–2243. <https://doi.org/10.1016/j.soilbio.2009.08.008>.
- Mayer, J., Buegger, F., Jensen, E.S., Schloter, M., Heß, J., 2003. Estimating N rhizodeposition of grain legumes using a  $^{15}\text{N}$  in situ stem labelling method. *Soil Biology and Biochemistry* 35, 21–28. [https://doi.org/10.1016/S0038-0717\(02\)00212-2](https://doi.org/10.1016/S0038-0717(02)00212-2).
- Rodríguez-Celma, J., Ceballos-Laita, L., Grusak, M.A., Abadía, J., López-Millán, A.,-F., 2016. Plant fluid proteomics: Delving into the xylem sap, phloem sap and apoplastic fluid proteomes. *Biochimica et Biophysica Acta* 1864, 991–1002. <https://doi.org/10.1016/j.bbapap.2016.03.014>.
- Sasse, J., Martinoia, E., Northen, T., 2018. Feed your friends: Do plant exudates shape the root microbiome? *Trends in Plant Science* 23, 25–41. <https://doi.org/10.1016/j.tplants.2017.09.003>.

- Sattelmacher, B., 2001. The apoplast and its significance for plant mineral nutrition. *New Phytologist* 149, 167–192. <https://doi.org/10.1046/j.1469-8137.2001.00034.x>.
- Schenck zu Schweinsberg-Mickan, M., Joergensen, R.G., Müller, T., 2010. Fate of  $^{13}\text{C}$  and  $^{15}\text{N}$ -labelled rhizodeposition of *Lolium perenne* as function of the distance to the root surface. *Soil Biology and Biochemistry* 42, 910–918. <https://doi.org/10.1016/j.soilbio.2010.02.007>.
- Schenck zu Schweinsberg-Mickan, M., Jörgensen, R.G., Müller, T., 2012. Rhizodeposition: Its contribution to microbial growth and carbon and nitrogen turnover within the rhizosphere. *Journal of Plant Nutrition and Soil Science* 175, 750–760. <https://doi.org/10.1002/jpln.201100300>.
- Spyder Project Contributors, 2020. Spyder: The Scientific Python Development Environment. <https://www.spyder-ide.org/> (accessed 26 April 2023).
- Voroney, R.P., Brookes, P.C., Beyaert, R.P., 2008. Soil microbial biomass C, N, P, and S. In: Carter, M.R., Gregorich, E.G. (Eds.), *Soil Sampling and Methods of Analysis*, 2nd edn. CRC Press, Florida, pp. 637–651.
- Wichern, F., Eberhardt, E., Mayer, J., Joergensen, R.G., Müller, T., 2008. Nitrogen rhizodeposition in agricultural crops: Methods, estimates and future prospects. *Soil Biology and Biochemistry* 40, 30–48. <https://doi.org/10.1016/j.soilbio.2007.08.010>.

Wichern, F., Mayer, J., Joergensen, R., Müller, T., 2010. Evaluation of the wick method for in situ  $^{13}\text{C}$  and  $^{15}\text{N}$  labelling of annual plants using sugar-urea mixtures. *Plant and Soil* 329, 105–115. <https://doi.org/10.1007/s11104-009-0138-3>.

Yasmin, K., Cadisch, G., Baggs, E.M., 2006. Comparing  $^{15}\text{N}$ -labelling techniques for enriching above- and below-ground components of the plant-soil system. *Soil Biology and Biochemistry* 38, 397–400. <https://doi.org/10.1016/j.soilbio.2005.05.011>.

### 3.6 Appendix: Supplementary materials

#### 3.6.1 *Supplemental text S1*

##### 3.6.1.1 *Assembly of labeling apparatus for stem and leaf feeding*

On day 105, we prepared the stem feeding apparatus (Mahieu et al. 2009). In each pot, a cotton wick was threaded through the ryegrass stem with a sterilized needle. On both sides of the stem, the wick was covered with Tygon tubing (diam: 0.75 cm) and inserted through the silicone septum of a 20 mL vial secured to the pot. The wick was then saturated by injecting 2 mL of deionized water into the vial. On day 106, we prepared the leaf feeding apparatus (Yasmin et al. 2006). One fully-formed leaf with a leaf sheath and unfurled blade was selected at random, trimmed with sterilized scissors, inserted into a 4 mL vial taped to the pot, and the leaf was submerged in 2 mL of deionized water.

##### 3.6.1.2 *Sample preparation and analysis of $^{15}\text{N}$*

First, stem and leaf feeding apparatus were removed from the pots. Then, shoots were cut at the base (1 mm above the soil surface) before removing the soil-root mass. We separated roots from the bulk soil manually and shook the roots to remove loosely-adhering soil. From these roots, rhizosphere soil was removed from the root surface manually, with careful attention to not contaminate the rhizosphere soil with fine root fragments. Shoots and roots were rinsed and dried (55 °C for 2 d). Half the rhizosphere soil was also dried (55 °C for 2 d), while the other half was placed into a plastic bag and stored at 4 °C.

Dried ryegrass shoots, roots and rhizosphere soil were finely ground and weighed into tin capsules. Two 20 g subsamples of the rhizosphere soil stored at 4 °C were removed for chloroform-fumigation extraction (Voroney et al. 2008). Fumigated samples and unfumigated controls were then extracted with 0.5 mol  $\text{K}_2\text{SO}_4 \text{ L}^{-1}$  at a 1:4 ratio for 1 h. Total dissolved N was

measured in the 0.5 mol K<sub>2</sub>SO<sub>4</sub> L<sup>-1</sup> extracts from fumigated soil samples and unfumigated controls with the Shimadzu TOC-L total organic C analyzer equipped with a TNM-L total N module (Shimadzu Corporation, Kyoto, Japan). A 10 mL aliquot was removed from each 0.5 mol K<sub>2</sub>SO<sub>4</sub> L<sup>-1</sup> extract and freeze-dried with a Martin Christ Gefriertrocknungsanlagen GmbH Gamma 1–16 LSCplus (Osterode, Lower Saxony, Germany) at 0.85 mbar for 3 d. All freeze-dried samples were weighed into tin capsules.

All tin encapsulated samples were analyzed for  $\delta^{15}\text{N}$  with an Elementar vario MICRO cube elemental analyzer interfaced to a Sercon Europa 20-20 isotope ratio mass spectrometer at the Stable Isotope Facility at the University of California, Davis (Davis, California, USA).

### 3.6.1.3 Calculations

We determined total soil microbial biomass N from the total dissolved N measured in the 0.5 mol K<sub>2</sub>SO<sub>4</sub> L<sup>-1</sup> extracts using the extraction coefficient  $k_{EN} = 0.5$  (Voroney et al. 2008). The <sup>15</sup>N enrichment of soil microbial biomass was calculated according to the modified soil microbial biomass N equation:

$${}^{15}\text{N}_{SMB} = \frac{\left( \left( \frac{{}^{15}\text{Nat}\%_{fum} - {}^{15}\text{Nat}\%_{fumcontrol}}{100} \right) \times N_{fum} - \left( \frac{{}^{15}\text{Nat}\%_{unfum} - {}^{15}\text{Nat}\%_{unfumcontrol}}{100} \right) \times N_{unfum} \right)}{K_{EN}} \quad (3.1)$$

where  ${}^{15}\text{N}_{SMB}$  represents <sup>15</sup>N-soil microbial biomass,  ${}^{15}\text{Nat}\%_{fum}$  and  ${}^{15}\text{Nat}\%_{fumcontrol}$  are the <sup>15</sup>N enrichment of the freeze-dried 0.5 mol K<sub>2</sub>SO<sub>4</sub> L<sup>-1</sup> extracts from fumigated samples and their respective labeling technique controls,  $N_{fum}$  is the total dissolved N measured directly in the 0.5 mol K<sub>2</sub>SO<sub>4</sub> L<sup>-1</sup> extracts of fumigated soil samples,  ${}^{15}\text{Nat}\%_{unfum}$  and  ${}^{15}\text{Nat}\%_{unfumcontrol}$  are the <sup>15</sup>N enrichment of the freeze-dried 0.5 mol K<sub>2</sub>SO<sub>4</sub> L<sup>-1</sup> extracts from unfumigated samples and their respective <sup>15</sup>N-labeling technique controls,  $N_{unfum}$  is the total

dissolved N measured directly in the 0.5 mol K<sub>2</sub>SO<sub>4</sub> L<sup>-1</sup> extracts of unfumigated soil samples, and  $k_{EN}$  is the extraction efficiency coefficient (0.5).

N derived from root exudation (i.e., the percentage of <sup>15</sup>N exuded by the plant compared to the total <sup>15</sup>N taken up by the plant) was determined based on the modified mass balance equations for rhizodeposition (Hupe et al. 2016). First, we found the <sup>15</sup>N mass fraction of the sample in each of the studied pools (i.e., shoots, roots, rhizosphere soil) using the following calculation:

$${}^{15}\text{N mass fraction} = \frac{(\text{atom}\% {}^{15}\text{N} \times \text{atomic weight } {}^{15}\text{N})}{[(100 - \text{atom}\% {}^{15}\text{N}) \times \text{atomic weight } {}^{14}\text{N}] + (\text{atom}\% {}^{15}\text{N} \times \text{atomic weight } {}^{15}\text{N})} \quad (3.2)$$

where  $\text{atom}\% {}^{15}\text{N}$  is the total <sup>15</sup>N enrichment of the sample,  $\text{atomic weight } {}^{15}\text{N}$  is the atomic weight of the <sup>15</sup>N isotope (15.0001 u), and  $\text{atomic weight } {}^{14}\text{N}$  is the atomic weight of the <sup>14</sup>N isotope (14.0031 u). This mass fraction was used to calculate the mass of <sup>15</sup>N (mg) in the sample for each pool:

$${}^{15}\text{N (mg)} = {}^{15}\text{N mass fraction} \times \text{total N (mg)} \quad (3.3)$$

where  ${}^{15}\text{N mass fraction}$  is the mass fraction of <sup>15</sup>N calculated with Equation 3.2 and  $\text{total N (mg)}$  is the mass of total N determined in the sample. Then, we determined the <sup>15</sup>N enrichment in the sample above natural abundance ( $\text{Atom}\% {}^{15}\text{N}_{\text{excess}}$ ) with the following equation:

$$\text{Atom}\% {}^{15}\text{N}_{\text{excess}} = \text{Atom}\% {}^{15}\text{N} - \text{Atom}\% {}^{15}\text{N}_{\text{control}} \quad (3.4)$$

where  $Atom\% \text{ }^{15}\text{N}$  is the total  $^{15}\text{N}$  enrichment of the sample and  $Atom\% \text{ }^{15}\text{N}_{control}$  is the  $^{15}\text{N}$  enrichment of the sample's respective labeling technique control. We could then find the proportion of  $^{15}\text{N}_{tracer}$  (% of  $^{15}\text{N}$ ) through the following equation:

$$^{15}\text{N}_{tracer} (\% \text{ of } ^{15}\text{N}) = \frac{Atom\% \text{ }^{15}\text{N}_{excess}}{Atom\% \text{ }^{15}\text{N}} \quad (3.5)$$

where  $Atom\% \text{ }^{15}\text{N}_{excess}$  is the excess  $^{15}\text{N}$  enrichment in the sample above natural abundance as determined with Equation 3.4, and  $Atom\% \text{ }^{15}\text{N}$  is the total  $^{15}\text{N}$  enrichment of the sample. This proportion was then used to find the mass of the  $^{15}\text{N}_{tracer}$  (mg) in the sample for each pool:

$$^{15}\text{N}_{tracer} (mg) = ^{15}\text{N}_{tracer} (\% \text{ of } ^{15}\text{N}) \times ^{15}\text{N} (mg) \quad (3.6)$$

where  $^{15}\text{N}_{tracer} (\% \text{ of } ^{15}\text{N})$  is the proportion of  $^{15}\text{N}$ -tracer in the sample as calculated with Equation 3.5 and  $^{15}\text{N} (mg)$  is the mass of  $^{15}\text{N}$  in the sample as determined with Equation 3.3. Once these values were calculated for the sample in each pool, we could find the  $^{15}\text{N}$ -tracer in the soil derived from root exudation as a percentage:

$$^{15}\text{N}_{tracer}dfr (\%) = \frac{^{15}\text{N}_{tracer}soil (mg)}{^{15}\text{N}_{tracer}soil (mg) + ^{15}\text{N}_{tracer}roots (mg) + ^{15}\text{N}_{tracer}shoots (mg)} \times 100 \quad (3.7)$$

where  $^{15}\text{N}_{tracer}shoots (mg)$  is the mass of the  $^{15}\text{N}$ -tracer in the shoots as determined with Equation 3.6,  $^{15}\text{N}_{tracer}roots (mg)$  is the mass of the  $^{15}\text{N}$ -tracer in the roots as determined with Equation 3.6 and  $^{15}\text{N}_{tracer}soil (mg)$  is the mass of  $^{15}\text{N}$ -tracer in the rhizosphere soil as determined with Equation 3.6. Since the  $^{15}\text{N}$ -tracer is used to measure root exudation, this percentage is also representative of the ratio of total N exuded by the plant to the plant's total N, or the N derived from root exudation ( $Ndfr (\%)$ ):

$$N_{dfr} (\%) = \frac{^{15}\text{N}_{tracer}}{^{15}\text{N}} dfr (\%) \quad (3.8)$$

**Table 3.6.S1** Physico-chemical characteristics of the organic peat soil used in this experiment.

The soil was collected (top 10 cm) from a cultivated peatland (Terriic Humisol) in Sherrington, Québec, Canada (45° 07' 44" N, 73° 31' 09" W) in November 2019. Soil was sieved ( $\leq 3$  mm) and stored in containers at 4 °C before analysis. Values are presented as mean  $\pm$  standard error.

Soil Properties	Value
Bulk Density ( $\text{g cm}^{-3}$ ) <sup>a</sup>	0.43 $\pm$ 0.02
Organic Matter ( $\text{Mg ha}^{-1}$ ) <sup>b</sup>	175 $\pm$ 1
Cation Exchange Capacity ( $\text{cmol kg}^{-1}$ ) <sup>c</sup>	49.6 $\pm$ 6.9
pH <sup>d</sup>	7.1 $\pm$ 0.4
Total Nitrogen ( $\text{kg ha}^{-1}$ ) <sup>e</sup>	14900 $\pm$ 3700
Phosphorus ( $\text{kg ha}^{-1}$ ) <sup>f</sup>	66 $\pm$ 6
Potassium ( $\text{kg ha}^{-1}$ ) <sup>f</sup>	343 $\pm$ 65
Magnesium ( $\text{kg ha}^{-1}$ ) <sup>f</sup>	2690 $\pm$ 420
Calcium ( $\text{kg ha}^{-1}$ ) <sup>f</sup>	17300 $\pm$ 2300
Aluminum ( $\text{kg ha}^{-1}$ ) <sup>f</sup>	33.5 $\pm$ 6.9
Sodium ( $\text{kg ha}^{-1}$ ) <sup>f</sup>	64.9 $\pm$ 11.6

<sup>a</sup> mass of a soil core (radius: 3 cm, height: 4 cm;  $n = 4$ ) after drying (70 °C for 48 h)

<sup>b</sup> loss on ignition at 360 °C ( $n = 2$ )

<sup>c</sup> calculated from ions measured through inductively coupled plasma-optical emission spectrometry ( $n = 2$ )

<sup>d</sup> 1:1 (soil:deionized water) slurries ( $n = 2$ )

<sup>e</sup> combustion of finely ground dried soil (55 °C for 72 h) encapsulated in tin with a Flash EA

1112 Series CN soil analyzer (Thermo Fisher Scientific, Waltham, Massachusetts, USA;  $n = 6$ )

<sup>f</sup> inductively coupled plasma-optical emission spectrometry ( $n = 2$ )

**Table 3.6.S2** Linear regression of the  $^{15}\text{N}$  concentration in the labeling solution ( $\text{mmol } ^{15}\text{N L}^{-1}$ ) and the  $^{15}\text{N}$  enrichment ( $\text{atm}\%$  excess) in ryegrass shoots, roots and rhizosphere soil. Linear regression is also presented for the  $^{15}\text{N}$  concentration of the labeling solution ( $\text{mmol } ^{15}\text{N L}^{-1}$ ) in relation to the N derived from root exudation (%). Results are from after a 24-h  $^{15}\text{N}$  enrichment period of annual ryegrass (*Lolium multiflorum*) plants grown in a greenhouse for 107 d. Ryegrass plants were exposed to twelve  $^{15}\text{N}$ -labeling methods at 106 d that varied according to the technique of introducing the tracer (stem or leaf feeding),  $^{15}\text{N}$ -tracer solution (urea or  $\text{NH}_4\text{NO}_3$ ), and concentration (64.5, 129 or 193  $\text{mmol } ^{15}\text{N L}^{-1}$ ) to enrich root exudates with  $^{15}\text{N}$ . Regressions were produced using statsmodels.api and pandas packages on Spyder 5.2.2 (Spyder Project Contributors 2020).

Pool	Method		Equation	<i>n</i>	<i>p</i>	$R^2$
	Introduction Technique	$^{15}\text{N}$ -Tracer				
Shoots	Stem Feeding	Urea	$y = 0.016x - 0.65$	11	<0.05	0.68
		$\text{NH}_4\text{NO}_3$	$y = 0.0096x + 0.25$	12	0.053	0.33
	Leaf Feeding	Urea	$y = 0.0013x + 0.18$	12	0.072	0.29
		$\text{NH}_4\text{NO}_3$	$y = 0.0012x + 0.38$	12	0.44	0.060
Roots	Stem Feeding	Urea	$y = 0.0028x - 0.12$	12	<0.05	0.51
		$\text{NH}_4\text{NO}_3$	$y = 0.0016x - 0.0010$	12	0.060	0.31
	Leaf Feeding	Urea	$y = 2.4 \times 10^{-4}x + 0.015$	12	0.10	0.25
		$\text{NH}_4\text{NO}_3$	$y = -2.0 \times 10^{-6}x + 0.041$	12	0.98	0
Rhizosphere Soil	Stem Feeding	Urea	$y = 7.0 \times 10^{-5}x - 0.0021$	12	<0.05	0.55
		$\text{NH}_4\text{NO}_3$	$y = 5.9 \times 10^{-5}x + 7.5 \times 10^{-5}$	12	0.083	0.27
	Leaf Feeding	Urea	$y = 1.4 \times 10^{-5}x + 6.6 \times 10^{-4}$	11	0.27	0.13
		$\text{NH}_4\text{NO}_3$	$y = 8.0 \times 10^{-6}x + 4.0 \times 10^{-4}$	9	0.46	0.080
Root Exudation	Stem Feeding	Urea	$y = -4.1 \times 10^{-4}x + 0.25$	11	0.36	0.095
		$\text{NH}_4\text{NO}_3$	$y = 2.2 \times 10^{-4}x + 0.16$	12	0.63	0.024
	Leaf Feeding	Urea	$y = -1.8 \times 10^{-4}x + 0.29$	11	0.90	0.0020
		$\text{NH}_4\text{NO}_3$	$y = 0.0011x - 0.0042$	9	0.43	0.093

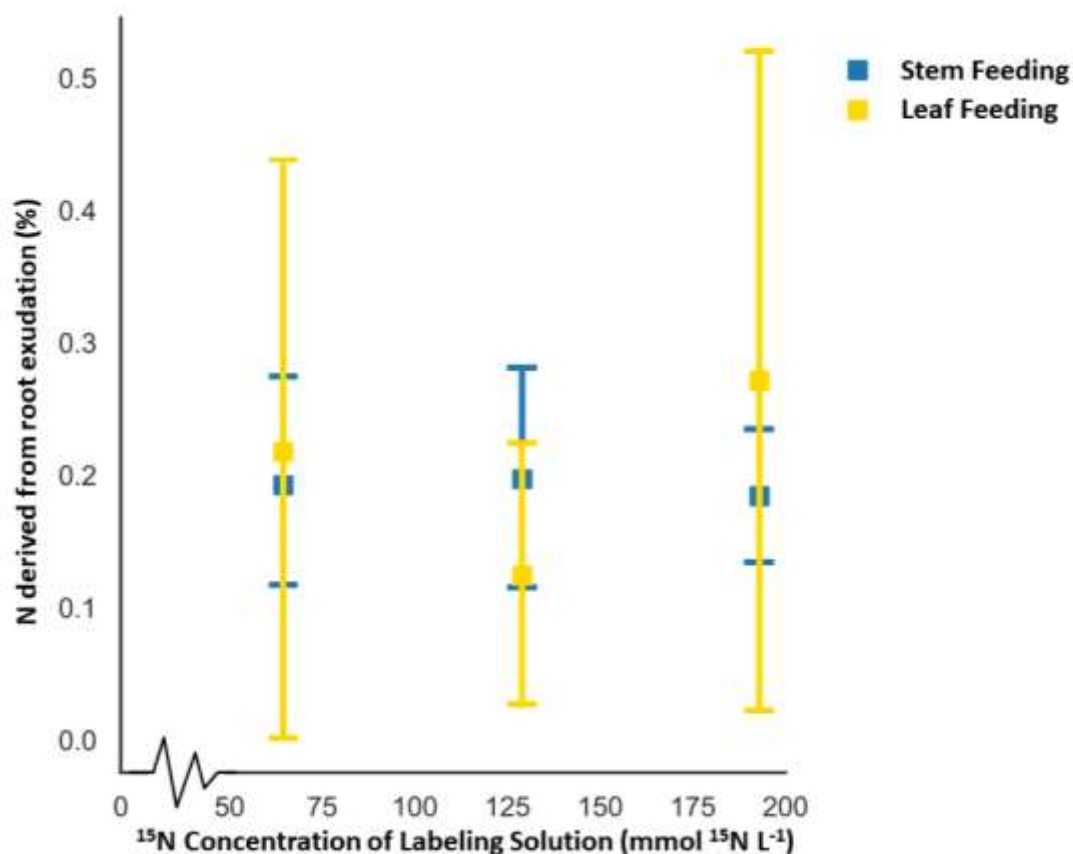


**Figure 3.6.S1** The N derived from root exudation (%) according to the N concentration (mmol  $^{15}\text{N L}^{-1}$ ) of labeling solutions used for stem and leaf feeding. Data were collected after a 24-h  $^{15}\text{N}$  enrichment of annual ryegrass (*Lolium multiflorum*) plants grown in a greenhouse for 107 d. Ryegrass plants were exposed to twelve  $^{15}\text{N}$ -labeling methods at 106 d that varied according to the technique of introducing the tracer (stem or leaf feeding),  $^{15}\text{N}$ -tracer solution (urea or  $\text{NH}_4\text{NO}_3$ ), and concentration (64.5, 129 or 193 mmol  $^{15}\text{N L}^{-1}$ ) to enrich root exudates with  $^{15}\text{N}$ . Points are the mean of each treatment with standard deviation bars. Due to negative values, all points had a sample size of  $n = 8$  besides stem feeding with 64.5 mmol  $^{15}\text{N L}^{-1}$  ( $n = 7$ ), and leaf feeding with 64.5 mmol  $^{15}\text{N L}^{-1}$  ( $n = 6$ ), and 129 and 193 mmol  $^{15}\text{N L}^{-1}$  ( $n = 7$ ). There was no difference in points with an increasing  $^{15}\text{N}$  concentration in the labeling solution ( $p > 0.05$ ).

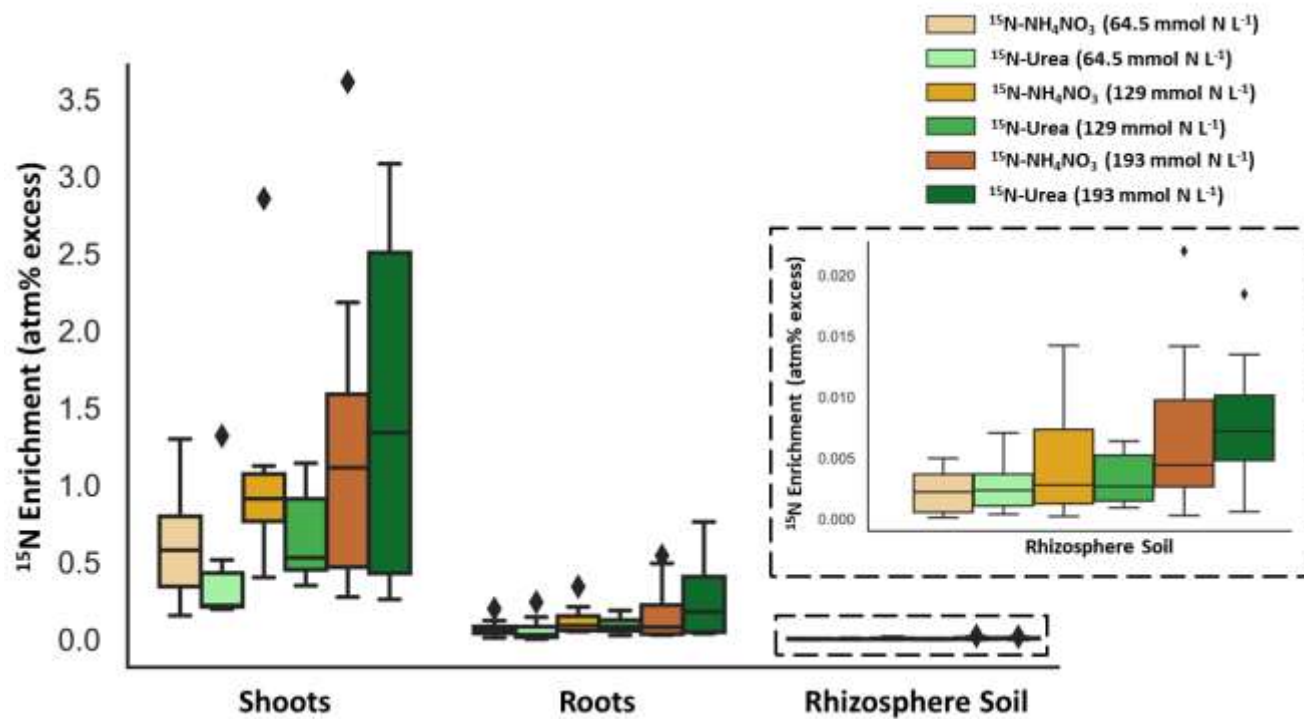


**Figure 3.6.S2** The  $^{15}\text{N}$  enrichment (atm% excess) of shoots, roots and rhizosphere soil (inset) for  $^{15}\text{N}$ -urea and  $^{15}\text{N-NH}_4\text{NO}_3$  at concentrations of 64.5, 129 and 193 mmol  $^{15}\text{N L}^{-1}$  after a 24-h  $^{15}\text{N}$  enrichment period of annual ryegrass (*Lolium multiflorum*) plants grown in a greenhouse for 107 d. Ryegrass plants were exposed to twelve  $^{15}\text{N}$ -labeling methods at 106 d that varied according to the technique of introducing the tracer (stem or leaf feeding),  $^{15}\text{N}$ -tracer solution (urea or  $\text{NH}_4\text{NO}_3$ ), and concentration (64.5, 129 or 193 mmol  $^{15}\text{N L}^{-1}$ ) to enrich root exudates with  $^{15}\text{N}$ . Boxplots show the distribution of the results, where the box represents the 25% and 75% quartiles, the center line shows the median, the whiskers display the minimum and maximum, and points represent outliers. All boxplots had a sample size of  $n = 8$  besides  $^{15}\text{N}$ -urea (64.5 mmol  $^{15}\text{N L}^{-1}$ ) for shoots and rhizosphere soil and  $^{15}\text{N-NH}_4\text{NO}_3$  (64.5, 129 and 193 mmol  $^{15}\text{N L}^{-1}$ ) for rhizosphere soil ( $n = 7$ ) due to negative values. The results from a three-way ANOVA demonstrated that there was no significant difference between  $^{15}\text{N}$ -urea and  $^{15}\text{N-NH}_4\text{NO}_3$  ( $p > 0.05$ ). The ANOVA was produced using statsmodels.api and pandas packages on Spyder 5.2.2 (Spyder Project Contributors 2020).

### 3.6.2 References

- Hupe, A., Schulz, H., Bruns, C., Joergensen, R.G., Wichern, F., 2016. Digging in the dirt – Inadequacy of belowground plant biomass quantification. *Soil Biology and Biochemistry* 96, 137–144. <https://doi.org/10.1016/j.soilbio.2016.01.014>.
- Mahieu, S., Fustec, J., Jensen, E.S., Crozat, Y., 2009. Does labelling frequency affect N rhizodeposition assessment using the cotton-wick method? *Soil Biology and Biochemistry* 41, 2236–2243. <https://doi.org/10.1016/j.soilbio.2009.08.008>.
- Spyder Project Contributors, 2020. Spyder: The Scientific Python Development Environment. <https://www.spyder-ide.org/> (accessed 26 April 2023).
- Voroney, R.P., Brookes, P.C., Beyaert, R.P., 2008. Soil microbial biomass C, N, P, and S. In: Carter, M.R., Gregorich, E.G. (Eds.), *Soil Sampling and Methods of Analysis*, 2nd edn. CRC Press, Florida, pp. 637–651.
- Yasmin, K., Cadisch, G., Baggs, E.M., 2006. Comparing <sup>15</sup>N-labelling techniques for enriching above- and below-ground components of the plant-soil system. *Soil Biology and Biochemistry* 38, 397–400. <https://doi.org/10.1016/j.soilbio.2005.05.011>.

## FORWARD TO CHAPTER 4

In Chapter 3, I determined that stem feeding with either  $^{15}\text{N}$ -urea or  $^{15}\text{N}$ - $\text{NH}_4\text{NO}_3$  at the highest concentration ( $193 \text{ mmol } ^{15}\text{N L}^{-1}$ ) generated root exudates sufficiently enriched in  $^{15}\text{N}$  after 24 h to quantify root exudate-derived N transfer to the rhizobiome. Additionally, I demonstrated that this assimilation took place even under N-rich conditions. Such confirmation was necessary to show their metabolism by the rhizobiome in conditions relevant to the cultivated rhizosphere. Consequently, in Chapter 4, I applied this method to not only demonstrate assimilation of N derived from root exudates by the rhizobiome, but also their dissimilation. This permitted the assessment of the contribution of root exudates to  $\text{N}_2\text{O}$  emissions from the rhizosphere. As a comparison, I used  $^{15}\text{N}$ -urea, a simple substrate similar to root exudates and a relevant nitrogenous fertilizer, to assess its contribution to  $\text{N}_2\text{O}$  production in the rhizosphere of cultivated peatlands. Furthermore, I also included natural abundance controls to assess the microbial dissimilatory pathways potentially responsible for the production of this  $\text{N}_2\text{O}$  from the cultivated peat rhizosphere using site preference analysis.

The following manuscript will be submitted for publication:

**De Sena A, Madramootoo CA, Whalen JK (2023).** Root exudates are a source of nitrous oxide from the rhizosphere of annual ryegrass (*Lolium multiflorum* L.)

## CHAPTER 4

### **4. Root exudates are a nitrogen source for nitrous oxide production in the rhizosphere**

Aidan De Sena, Chandra A. Madramootoo, Joann K. Whalen

#### **4.1 Abstract**

Root exudation releases nitrogen (N) into the rhizosphere, which can be assimilated into the biomass of the rhizosphere microbiome, known as the rhizobiome. However, this root exudate-derived N might also be a source of energy for the rhizobiome via dissimilatory processes – like nitrification, denitrification and nitrifier-denitrification – producing N<sub>2</sub>O as a result. The objective of this study was to assess the role of root exudate-N in the generation of N<sub>2</sub>O from the rhizosphere. To achieve this objective, we conducted a greenhouse experiment with ryegrass (*Lolium multiflorum*) plants, the rhizosphere of which we exposed to either <sup>15</sup>N-root exudates or <sup>15</sup>N-urea fertilizer, as a comparison. We measured N<sub>2</sub>O fluxes emitted from the soil and their enrichment 24 h and 48 h after <sup>15</sup>N-substrate introduction. We also assessed the <sup>15</sup>N enrichment of the rhizosphere soil and rhizobiome 3, 9, 24 and 48 h after <sup>15</sup>N-substrate introduction. We found that even though only  $0.0020 \pm 0.0012\%$  of the total root exudate-N contributed to direct N<sub>2</sub>O emissions, this root exudate-derived N<sub>2</sub>O made up almost one-fifth of total N<sub>2</sub>O emissions, on average. These emissions were comparable to those produced from urea fertilizer in our study ( $5.37 \pm 1.63\%$ ). Site preference analysis of N<sub>2</sub>O from natural abundance controls implies that 67–99% of the N<sub>2</sub>O emissions are produced by bacterial denitrification, nitrifier-denitrification or a combination of the two pathways in the rhizosphere. Consequently, our study establishes the direct contribution of root exudates to N<sub>2</sub>O emissions from the rhizosphere, which must be accounted for to accurately portray N<sub>2</sub>O emissions from soils under cultivation.

## 4.2 Introduction

Plants exude nitrogen (N)-containing compounds from their roots into the rhizosphere. These nitrogenous root exudates can represent up to 15% of plant-acquired N (Sasse et al. 2018) and consist of inorganic species, such as ammonium ( $\text{NH}_4^+$ ) and nitrate ( $\text{NO}_3^-$ ; Hertenberger and Wanek 2004), as well as organic molecules, including amino acids, nucleotides and their respective polymers (De Sena et al. 2022). Their function for the plant is largely microbial in nature, serving as either chemo-attractants for beneficial microorganisms (e.g., amino acids and peptides promote root colonization by *Bacillus* spp.; Allard-Massicotte et al. 2016, Xie et al. 2022), inhibitors of potential pathogens (e.g., canavanine and phytosphingosine are microbial antimetabolites; Cai et al. 2009, Li et al. 2020) or even as defense mechanisms against ongoing pathogenic infections (e.g., small (s)RNAs silence the expression of fungal pathogenic genes; Zhang et al. 2016, Cai et al. 2018). However, as plants release 1 to 44.5 g N m<sup>-2</sup> y<sup>-1</sup> from their roots (equivalent to 10 to 445 kg N ha<sup>-1</sup> y<sup>-1</sup>; Høgh-Jensen and Schjoerring 2001, López-Bellido et al. 2011, Dhamala et al. 2017, Rasmussen et al. 2021), an ancillary effect of these root-derived compounds is their metabolism as a N source by the rhizosphere microbiome, known as the rhizobiome. Thus, while the plant attempts to tailor the rhizobiome to its needs via the exudation of N-containing substances, these exuded compounds also supply N to the rhizobiome, promoting their nutrition.

The rhizobiome uses the N derived from root exudates for anabolism, synthesizing biomolecules, such as proteins and nucleic acids, to create and maintain their biomass. Between 0.004% and 11% of the N in the rhizobiome biomass originates from root exudates (Wichern et al. 2008, Schenck zu Schweinsberg-Mickan et al. 2010, 2012, Kušlienė et al. 2014, De Sena et al. 2023). Although this N source generates biomass for the rhizobiome, the rhizobiome may also

use root exudate-derived N to generate energy, possibly through the dissimilatory processes of nitrification, denitrification and nitrifier-denitrification. Assessing the contribution of root exudates to these processes is important, as all three are pathways for the production of nitrous oxide ( $\text{N}_2\text{O}$ ), a potent greenhouse gas.

For these  $\text{N}_2\text{O}$ -producing pathways to proceed, the rhizobiome requires their initial N reactants. These reactive N forms are  $\text{NH}_4^+$  – for nitrification and nitrifier-denitrification – and  $\text{NO}_3^-$  – for denitrification – both of which root exudates can supply to the rhizobiome. The rhizobiome harvests the reactive N forms from root exudates by either (i) direct uptake of exuded  $\text{NH}_4^+$  and  $\text{NO}_3^-$ , (ii) direct uptake of simple exudates (e.g., amino acids, nucleotides) followed by their intracellular ammonification into  $\text{NH}_4^+$ , or (iii) uptake of  $\text{NH}_4^+$  and ammonifiable substrates produced from the depolymerization of exuded macromolecules, such as proteins and nucleic acids, by extracellular enzymes (e.g., proteases, nucleases; Myrold 2021). Consequently, root exudates should be a N source for  $\text{N}_2\text{O}$  production in the rhizosphere since the initial reactants of nitrification, denitrification and nitrifier-denitrification are either  $\text{NH}_4^+$  or  $\text{NO}_3^-$ , both of which are root exudates and by-products of root exudates.

Along with the availability of  $\text{NH}_4^+$  and  $\text{NO}_3^-$ , additional factors should influence the capacity of the rhizobiome to perform  $\text{N}_2\text{O}$ -producing pathways using root exudate-derived N. The quantity and quality of carbon (C) impact denitrification and nitrifier-denitrification as these processes require assimilable C as electron donors for microbial oxidation (Wrage-Mönnig et al. 2018, Liu et al. 2022). In the rhizosphere, root exudation and shedding release ~7% of plant gross primary productivity (Pausch and Kuzyakov 2018) and should ensure abundant organic C forms for denitrifier and nitrifier-denitrifier metabolism. Besides C availability, oxygen ( $\text{O}_2$ ) also affects these processes, with aerobic conditions promoting nitrification (Zhu et al. 2013,

Lancaster et al. 2018). Despite the efficient water uptake by roots that could foster such an environment for nitrification in the rhizosphere, the abundance of nitrifying genes in the rhizobiome is roughly two-thirds of that found in the bulk soil microbiome (Ling et al. 2022). This observation implies that (i) the rhizosphere restrains nitrifiers, and (ii) roots and facultative anaerobes consume any available  $O_2$  rapidly, likely creating a hypoxic or anoxic environment around the root (Lecomte et al. 2018). Such conditions would suit denitrifiers and nitrifier-denitrifiers, suggesting that their namesake processes could be responsible for  $N_2O$  production from the rhizosphere. Parsing out these specific  $N_2O$ -producing pathways is important, as prescribed mitigation efforts often rely on understanding these pathways to avoid triggering them, thereby reducing  $N_2O$  emissions.

Given these uncertainties regarding root exudates as a N source for  $N_2O$  production, we aimed to trace the fate of N derived from root exudates in and from the rhizosphere of cultivated soil, the largest anthropogenic producer of  $N_2O$  ( $2.3 \text{ Tg N yr}^{-1}$ ; Tian et al. 2020). Specifically, we looked at the partitioning of root exudate-derived N among the rhizosphere-relevant pools, as well as the proportion this N represents of the total N in a pool. As a comparison, we also followed N derived from urea fertilizer, another substrate relevant to cultivated soils and established emitter of  $N_2O$  through its hydrolysis into  $NH_4^+$  by soil urease (Sigurdarson et al. 2018). To achieve this objective, we conducted a  $^{15}N$ -tracing experiment with annual ryegrass (*Lolium multiflorum* L.) plants grown in soil from a temperate cultivated peatland. We hypothesized that root exudates would be a substantial source of  $N_2O$  because plant roots exude large quantities of reactive N forms – or precursors of them – that can serve as reactants for  $N_2O$  production in the rhizosphere. We also hypothesized that denitrification, nitrifier-denitrification or a combination of the two would be the dominant pathways for rhizosphere  $N_2O$  production

due to the surplus of reactive N from both root exudates and urea fertilizer, the availability of assimilable C and the expected microaerophilic conditions surrounding the root.

### 4.3 Materials and methods

#### 4.3.1 *Experimental materials*

We collected the soil (120 kg) for this study from the top 10 cm of a buffer strip on a cultivated peatland in Sherrington, Québec, Canada (45° 07' 44" N, 73° 31' 09" W) during November 2019. This peatland region has been drained since 1952 and intensively cultivated for the production of vegetables like carrots, lettuce and onions (Lloyd 2016). Producers typically apply synthetic N fertilizers at a rate between 90–100 kg N ha<sup>-1</sup> (Lloyd et al 2019). The organic peat soil was classified as a Terric Humisol containing 810 ± 10 g sand kg<sup>-1</sup> and 40 ± 0 g clay kg<sup>-1</sup> with 406 ± 3 g organic matter kg<sup>-1</sup> and a pH of 7.1 ± 0.4 ( $n = 2$ ). Additional soil physico-chemical properties are described in Table 4.S1. We sieved ( $\leq 3$  mm) and air-dried (3 d) the field-moist soil before storing the soil in plastic bins at 4 °C.

We chose annual ryegrass (*Lolium multiflorum*) as our model organism since it is a robust grass species with a fibrous root network, thus increasing the surface area of the rhizosphere. Seeds of annual ryegrass (*L. multiflorum* Lam.) were obtained from Semican Atlantic Inc. (Plessisville, Québec, Canada) and were viable based on a 91 ± 3% germination success of 100 seeds incubated on triplicate petri dishes at 20 °C for five days in the dark.

#### 4.3.2 *Experimental design*

The experimental unit was a plastic pot (810 cm<sup>3</sup>) lined with plastic wrap to prevent N leaching (Mahieu et al. 2009) and packed with 165 g (oven-dry basis) of air-dried soil to a bulk density of 0.43 g cm<sup>-3</sup>. We assigned pots at random to the two treatments of isotopically-labeled substrates – <sup>15</sup>N-root exudates or <sup>15</sup>N-urea – or to the natural abundance controls. The isotopically-labeled

substrates were also labeled with  $^{13}\text{C}$ , the fate of which is the subject of the next chapter (See Chapter 5). Pots were destructively sampled during one of the four sampling time-points (3, 9, 24 or 48 h since  $^{15}\text{N}$ -substrate introduction) to trace the fate of N derived from root exudates and urea in the rhizosphere. Each factorial treatment (substrate or control  $\times$  sampling time combination) was replicated four times for a total of 48 experimental units. The start of the experiment for the treatments was staggered by a day as we only had one  $\text{CO}_2$  labeling chamber, separating pots undergoing pulse labeling with  $^{13}\text{C}$ - $\text{CO}_2$  ( $^{15}\text{N}$ -root exudates pots;  $n = 16$ ) and  $\text{CO}_2$  at natural abundance ( $^{15}\text{N}$ -urea and natural abundance control pots;  $n = 32$ ; See Section 5.3.2 *Introduction of  $^{13}\text{C}$ -substrates*).

The growing period of the study (80 d) began by planting three ryegrass seeds 2 cm deep into the soil of each pot (Figure 4.S1). We adjusted the soil moisture to 70% water-filled pore space with distilled water and recorded the mass, so that the soil moisture content could be maintained by watering the soil to this value every other morning prior to the experimental period. Once prepared, the pots were placed in a randomized complete block design on a bench within a greenhouse (average daily temperature of 27 °C and daylength of 15 h). To account for any potential confounding factors associated with the greenhouse environment, we rotated the pots and shifted them by one row every week during the study. At 21 d after planting, we thinned the ryegrass to one plant per pot.

Pots received fertilizer twice before the introduction of  $^{15}\text{N}$ -substrates due to visible signs of nutrient deficiency. On the 71<sup>st</sup> d after planting, all pots received 3 mL of fertilizer solution before watering, made up of 0.286 mol N L<sup>-1</sup> from urea, 0.0908 mol P L<sup>-1</sup> from triple superphosphate and 0.118 mol K L<sup>-1</sup> from KCl. This fertilizer dose was equivalent to an application rate of 15-20-20 kg ha<sup>-1</sup> of N-P<sub>2</sub>O<sub>5</sub>-K<sub>2</sub>O. Likewise, 89 d after planting, all pots

received 1.5 mL of fertilizer solution before watering, made up of 0.286 mol N L<sup>-1</sup> from urea, 0.0908 mol P L<sup>-1</sup> from triple superphosphate and 0.118 mol K L<sup>-1</sup> from KCl. This fertilizer dose was equivalent to an application rate of 7.5-10-10 kg ha<sup>-1</sup> of N-P<sub>2</sub>O<sub>5</sub>-K<sub>2</sub>O.

#### 4.3.3 Introduction of <sup>15</sup>N-substrates

The experimental period began 81 d after planting (commenced with <sup>13</sup>C-CO<sub>2</sub> pulse labeling; See Section 5.3.2 *Introduction of <sup>13</sup>C-substrates*) and ended 105 d after planting (after the introduction of <sup>15</sup>N-substrates). <sup>15</sup>N enrichment occurred at the end of the experimental period due to the mobility of nitrogen (e.g., volatilization) and to measure exudation of N rather than rhizodeposition. During this experimental period (24 d), we watered the pots to 70% water-filled pore space at 9:00 daily.

To introduce the <sup>15</sup>N-substrates, we first labeled ryegrass root exudates with <sup>15</sup>N by the stem feeding method (De Sena et al. 2023) 105 d after planting. Briefly, 104 d after planting, we prepared the stem feeding labeling apparatus by first inserting a sterilized needle threaded with a cotton wick through the stem of the ryegrass plant, 3 cm above the soil surface. We placed Tygon tubing (diam: 0.75 cm) around the exposed cotton wick to prevent evaporative losses. Then, we inserted the Tygon tubing through a Teflon-coated silicone septum of a 20 mL vial and submerged the exposed thread in 2 mL of distilled water. We used tape to stabilize the Tygon tubing to the plant and secure the vial to the pot. The next morning before watering, we removed any remaining distilled water from the stem feeding vials. Then, we submerged the cotton thread of the vials in 5 mL of <sup>15</sup>N-urea (≥98 atom%; Cambridge Isotope Laboratories, Andover, Massachusetts, USA) at 193 mmol <sup>15</sup>N L<sup>-1</sup>. Those pots not designated for the <sup>15</sup>N-root exudate treatment were still subjected to stem feeding but with urea at natural abundance (203 mmol <sup>14</sup>N L<sup>-1</sup>).

Immediately after  $^{15}\text{N}$ -labeling the root exudates, we also added 3 mL of fertilizer solution containing  $^{15}\text{N}$ -urea ( $\geq 98$  atom%  $^{15}\text{N}$ ; Cambridge Isotope Laboratories, Andover, Massachusetts, USA) at  $2.61 \text{ mol } ^{15}\text{N L}^{-1}$  to the soil of pots designated for the  $^{15}\text{N}$ -urea treatment. This fertilizer dose was added right before watering at 9:00 and equivalent to an application of  $150\text{-}0\text{-}0 \text{ kg ha}^{-1}$  of  $\text{N-P}_2\text{O}_5\text{-K}_2\text{O}$ . Those pots not designated for the  $^{15}\text{N}$ -urea treatment were still subjected to N fertilization but with urea at natural abundance ( $2.86 \text{ mol } ^{14}\text{N L}^{-1}$ ).

#### **4.3.4 Gas, ryegrass biomass and soil sample collection**

The sampling period (2 d) began 105 d after planting, during which the plants were still watered to 70% water-filled pore space at 9:00 daily. We collected samples at 3, 9, 24 or 48 h after introducing the  $^{15}\text{N}$ -substrates, depending on the sampling time-point designated for the pot.

Each sampling event began with gas sampling, which first involved removing the stem feeding apparatus from the plant and then taking five 20 mL headspace gas samples at 0, 20, 40 and 60 min after placing a stationary chamber ( $3534 \text{ cm}^3$ ) on top of the pot. Headspace gas samples were taken with an air-tight syringe from a septum fitted to Tygon tubing connected to the chamber. Each of the five headspace gas samples was transferred into a separate 12 mL Exetainer (Labco, Lampeter, Wales, United Kingdom) for analysis of either  $\delta^{13}\text{C}$  (See Section 5.3.4 *Gas analysis*),  $\delta^{15}\text{N}$  or total  $\text{N}_2\text{O}$  concentration (three replicates). After gas sampling, the pot was transferred into a Ziploc bag and stored at  $4 \text{ }^\circ\text{C}$  until destructive sampling.

Pots were destructively sampled by first removing ryegrass shoots at their base with scissors. We then removed the soil root-mass, which was gently shaken to detach any bulk soil. Then, we removed rhizosphere soil from the surface of the roots manually. Ryegrass shoots and roots were rinsed and dried ( $55 \text{ }^\circ\text{C}$  for 3 d). We dried a portion of the resulting rhizosphere soil

(55 °C for 3 d), while the remainder was placed in a Ziploc plastic bag and stored at 4 °C until soil microbial biomass extraction.

#### 4.3.5 Gas analysis

We analyzed the volumetric concentration of N<sub>2</sub>O with a Bruker 520 Gas Chromatographer System (Bruker, Billerica, Massachusetts, USA) by injecting samples onto a channel equipped with an electron capture detector set at 350 °C with argon (flow rate: 10 mL min<sup>-1</sup>) as a carrier gas. We determined the <sup>15</sup>N enrichment of N<sub>2</sub>O using the N<sub>2</sub>O Gas Isotope Analyzer (Model SSIM2-G5131i, Picarro, Santa Clara, California, USA) at the University of Saskatchewan (Saskatoon, Saskatchewan, Canada), providing us with the isotopic signatures of  $\delta^{15}N_{bulk}$  (average <sup>15</sup>N enrichment of the two N atoms in N<sub>2</sub>O),  $\delta^{15}N_{\alpha}$  (<sup>15</sup>N enrichment of the central N atom in N<sub>2</sub>O) and  $\delta^{15}N_{\beta}$  (<sup>15</sup>N enrichment of the outer N atom in N<sub>2</sub>O; Toyoda and Yoshida 1999). We assumed that (i) any N<sub>2</sub>O emitted from the soil originated from the rhizosphere, as ryegrass roots were permitted to grow in pots (810 cm<sup>3</sup>) for at least 104 d, and (ii) that the <sup>15</sup>N enrichment of N<sub>2</sub>O after <sup>15</sup>N-stem feeding was derived from root exudates as opposed to rhizodeposits (e.g., fine root turnover) because of the brief exposure period of the plant to <sup>15</sup>N-urea. Due to limited funding, we only analyzed the gas samples from the sampling time-points occurring 24 h and 48 h after introducing the <sup>15</sup>N-substrates.

We calculated the gravimetric concentration of N<sub>2</sub>O ( $C_g$  in mg N<sub>2</sub>O-N m<sup>-3</sup>) in the headspace gas samples using the following equation adapted from the ideal gas law:

$$C_g = \frac{C_v M P}{RT} \quad (4.1)$$

where  $C_v$  is the volumetric concentration of N<sub>2</sub>O (L N<sub>2</sub>O-N m<sup>-3</sup>),  $M$  is the molar mass of N<sub>2</sub>O in terms of N (mg N<sub>2</sub>O-N mol<sup>-1</sup>),  $P$  is the atmospheric pressure in the greenhouse when the headspace gas sample was collected (atm),  $R$  is the ideal gas constant (0.08206 L atm mol<sup>-1</sup> K<sup>-1</sup>)

and  $T$  is the temperature in the greenhouse when the headspace gas sample was collected (K).

We accounted for the  $^{15}\text{N}$  enrichment of the gas samples in the calculation for the molar mass of  $\text{N}_2\text{O}$  ( $M$ ), by first determining the ratio of  $^{15}\text{N}$  and  $^{14}\text{N}$  in the sample ( $R_{\text{sample}}$ ):

$$R_{\text{sample}} = \left( \frac{\delta^{15}\text{N}_{\text{bulk}}}{1000} + 1 \right) \times R_{\text{air}} \quad (4.2)$$

where  $\delta^{15}\text{N}_{\text{bulk}}$  is the average  $^{15}\text{N}$  enrichment of the two N atoms in  $\text{N}_2\text{O}$  (‰) and  $R_{\text{air}}$  is the ratio of  $^{15}\text{N}$  and  $^{14}\text{N}$  in atmospheric air (0.003676; Yeung et al. 2017). Then, we calculated the  $^{15}\text{N}$  enrichment in terms of atom % ( $\text{Atom}\%^{15}\text{N}$ ):

$$\text{Atom}\%^{15}\text{N} = \left( \frac{R_{\text{sample}}}{(R_{\text{sample}} + 1)} \right) \times 100 \quad (4.3)$$

where  $R_{\text{sample}}$  is the ratio of  $^{15}\text{N}$  and  $^{14}\text{N}$  in the sample calculated in Equation 4.2. Thus, we could calculate the molar mass of  $\text{N}_2\text{O}$  in terms of N ( $M$ ;  $\text{mg N}_2\text{O-N mol}^{-1}$ ):

$$M = \left( \left( 1 - \frac{\text{Atom}\%^{15}\text{N}}{100} \right) \times M_{^{14}\text{N}} \right) + \left( \frac{\text{Atom}\%^{15}\text{N}}{100} \times M_{^{15}\text{N}} \right) \quad (4.4)$$

where  $\text{Atom}\%^{15}\text{N}$  is the  $^{15}\text{N}$  enrichment of the headspace gas sample calculated with Equation 4.3 ( $\text{atom}\%^{15}\text{N}$ ),  $M_{^{14}\text{N}}$  is the atomic mass of the  $^{14}\text{N}$ -isotope (14003 mDa; CIAAW 2015) and  $M_{^{15}\text{N}}$  is the atomic mass of the  $^{15}\text{N}$ -isotope (15000 mDa; CIAAW 2015).

To find the gravimetric concentration of  $\text{N}_2\text{O}$  ( $C_{g-xt_i}$  in  $\text{mg N}_2\text{O-N m}^{-3}$ ) derived from the  $^{15}\text{N}$ -substrate of interest ( $x$ ; i.e.,  $^{15}\text{N}$ -root exudates,  $^{15}\text{N}$ -urea) at a specific time-point ( $t_i$  in min; i.e.,  $t_1 = 0$  min,  $t_2 = 20$  min,  $t_3 = 40$  min,  $t_4 = 60$  min), we used an isotope mixing model:

$$C_{g-xt_i} = C_{g-t_i} \times \frac{(\text{Atom}\%^{15}\text{N}_{t_i} - \text{Atom}\%^{15}\text{N}_{t_1})}{(\text{Atom}\%^{15}\text{N}_x - \text{Atom}\%^{15}\text{N}_{t_1})} \quad (4.5)$$

where  $C_{g-t_i}$  was the gravimetric concentration of  $\text{N}_2\text{O}$  ( $\text{mg N}_2\text{O-N m}^{-3}$ ) in the headspace gas sample at a specific time-point during the flux calculated with Equation 4.1,  $\text{Atom}\%^{15}\text{N}_{t_i}$  is the

$^{15}\text{N}$  enrichment of the headspace gas sample at a specific time-point during the flux calculated with Equation 4.3 (atom%  $^{15}\text{N}$ ),  $Atom\% \text{ }^{15}\text{N}_{t_1}$  is the  $^{15}\text{N}$  enrichment of the headspace gas sample at the 0 min time-point calculated with Equation 4.3 (atom%  $^{15}\text{N}$ ), and  $Atom\% \text{ }^{15}\text{N}_x$  is the  $^{15}\text{N}$  enrichment of the  $^{15}\text{N}$ -substrate introduced to the pot ( $x$ ; i.e., the average  $^{15}\text{N}$  enrichment of the shoots and roots for root exudates, the  $^{15}\text{N}$  enrichment of the urea fertilizer itself for urea). Once we calculated the gravimetric concentration of  $\text{N}_2\text{O}$  derived from root exudates and urea at each time-point, we could determine the flux of  $\text{N}_2\text{O}$  derived from these substrates during this hour ( $\text{mg N}_2\text{O-N cm}^{-2} \text{ h}^{-1}$ ) by also providing the volume of the headspace chamber ( $\text{m}^3$ ) and the surface area of the soil ( $\text{cm}^2$ ) to the gasfluxes package using the linear model on R version 4.4.0 (R Core Team, Vienna, Austria). Daily emissions were calculated from these  $\text{N}_2\text{O-N}$  fluxes by multiplying the hourly flux values by 24, assuming that fluxes did not vary throughout the day. However, our values represent an approximation as  $\text{N}_2\text{O}$  emissions can be sporadic (Lloyd et al. 2019).

Site preference of the  $\text{N}_2\text{O}$  produced from the natural abundance controls was assessed to estimate the pathway responsible for  $\text{N}_2\text{O}$  production (i.e., nitrification, fungal denitrification, bacterial denitrification, nitrifier-denitrification). We first calculated the measured site preference of  $\text{N}_2\text{O}$  in the headspace gas sample ( $\delta \text{ }^{15}\text{N}_{SP-m}$  in ‰) with:

$$\delta \text{ }^{15}\text{N}_{SP-m} = \delta \text{ }^{15}\text{N}_\alpha - \delta \text{ }^{15}\text{N}_\beta \quad (4.6)$$

where  $\delta \text{ }^{15}\text{N}_\alpha$  is the  $^{15}\text{N}$  enrichment of the central nitrogen atom (‰) and  $\delta \text{ }^{15}\text{N}_\beta$  is the  $^{15}\text{N}$  enrichment of the outer nitrogen atom (‰). We then found the site preference of the soil-emitted  $\text{N}_2\text{O}$  ( $\delta \text{ }^{15}\text{N}_{SP-s}$  in ‰) according to Toyoda et al. (2017):

$$\delta \text{ }^{15}\text{N}_{SP-s} = \frac{(C_{atm}\delta \text{ }^{15}\text{N}_{SP-atm} - C_m\delta \text{ }^{15}\text{N}_{SP-m})}{(\delta \text{ }^{15}\text{N}_{SP-m} + C_{atm})} \quad (4.7)$$

where  $C_{atm}$  is the volumetric concentration of N<sub>2</sub>O in the atmosphere (334 ppbv N<sub>2</sub>O; EPA 2024),  $\delta_{\square}^{15}N_{SP-atm}$  is the site preference of atmospheric N<sub>2</sub>O (18.7‰; Yoshida and Toyoda 2000),  $C_m$  is the measured volumetric concentration of N<sub>2</sub>O in the headspace gas sample (ppbv N<sub>2</sub>O) and  $\delta_{\square}^{15}N_{SP-m}$  is the measured site preference of N<sub>2</sub>O in the headspace gas sample calculated with Equation 4.6 (‰). Lastly, to account for the increase in N<sub>2</sub>O emitted from the soil with each time-point during the flux, we calculated the concentration-weighted site preference of N<sub>2</sub>O ( $\delta_{\square}^{15}N_{SP-scw}$  in ‰) according to Ostrom et al. (2010):

$$\delta_{\square}^{15}N_{SP-scw} = \frac{\sum_{i=1}^4 (C_{st_i} \times \delta_{\square}^{15}N_{SP-st_i})}{\sum_{i=1}^4 C_{st_i}} \quad (4.8)$$

where  $C_{st_i}$  is the volumetric concentration of the soil-derived N<sub>2</sub>O in the headspace gas sample (ppbv N<sub>2</sub>O) at a specific time-point during the flux ( $t_i$  in min; i.e.,  $t_1 = 0$  min,  $t_2 = 20$  min,  $t_3 = 40$  min,  $t_4 = 60$  min) and  $\delta_{\square}^{15}N_{SP-st_i}$  is the site preference of the N<sub>2</sub>O emitted from soil (‰) at a specific time-point during the flux ( $t_i$  in min; i.e.,  $t_1 = 0$  min,  $t_2 = 20$  min,  $t_3 = 40$  min,  $t_4 = 60$  min) calculated with Equation 4.7. We referenced the resulting site preference values to the endmember values for site preference obtained from pure cultures of known nitrifiers, fungal denitrifiers, bacterial denitrifiers and nitrifier-denitrifiers. Since the endmember site preference ranges overlap for bacterial denitrification and nitrifier-denitrification, as well as for nitrification and fungal denitrification, we combined their respective overlapping values into one range. As such, values between -13.6 and 3.7‰ for site preference indicated bacterial denitrification or nitrifier-denitrification produced the measured N<sub>2</sub>O, while those between 27.2 and 39.9‰ indicated the role of nitrification or fungal denitrification in soil N<sub>2</sub>O production (Zaman et al. 2021). We estimated the proportion of soil-emitted N<sub>2</sub>O produced from bacterial denitrification and nitrifier-denitrification (%), according to Decock and Six (2013):

$$p_{BDND} = \frac{(\delta_{\text{N}_2\text{O}}^{15} N_{SP-SCW} - \delta_{\text{N}_2\text{O}}^{15} N_{SP-NIFD})}{(\delta_{\text{N}_2\text{O}}^{15} N_{SP-BDND} - \delta_{\text{N}_2\text{O}}^{15} N_{SP-NIFD})} \times 100 \quad (4.9)$$

where  $\delta_{\text{N}_2\text{O}}^{15} N_{SP-SCW}$  is the concentration-weighted site preference value of  $\text{N}_2\text{O}$  emitted from soil calculated with Equation 4.8 (‰),  $\delta_{\text{N}_2\text{O}}^{15} N_{SP-NIFD}$  is the lower or upper endmember value of the site preference range for nitrification and fungal denitrification (‰), and  $\delta_{\text{N}_2\text{O}}^{15} N_{SP-BDND}$  the lower or upper endmember value of the site preference range for bacterial denitrification and nitrifier-denitrification (‰). Using the different combinations of lower and upper endmember values for both site preference ranges, we could estimate the lowest and highest possible contribution of bacterial denitrification and nitrifier-denitrification.

#### 4.3.6 Ryegrass biomass and rhizosphere soil analysis

Oven-dried ryegrass shoots, roots and rhizosphere soil were finely ground and weighed into tin capsules for  $\delta_{\text{N}_2\text{O}}^{15} N$  analysis. We performed chloroform fumigation-extraction with the rhizosphere soil stored at 4 °C, taking two 20 g subsamples as a fumigated sample and unfumigated control (Voroney et al. 2008). Once complete, samples and controls were extracted at a 1:4 ratio with 0.5 mol  $\text{K}_2\text{SO}_4 \text{ L}^{-1}$  for 1 h. A 10 mL aliquot was removed from the extracts for freeze-drying with a Gamma 1–16 LSCplus (Martin Christ Gefriertrocknungsanlagen GmbH, Osterode, Lower Saxony, Germany) at 0.85 mbar for 3 d. We weighed the resulting freeze-dried extracts into tin capsules.

These samples (i.e., shoots, roots, rhizosphere soil, microbial biomass extracts) underwent  $\delta_{\text{N}_2\text{O}}^{15} N$  analysis with an Elementar vario MICRO cube elemental analyzer (Elementar Analysensysteme GmbH, Langenselbold, Germany) interfaced to a Sercon Europa 20-20 isotope ratio mass spectrometer (Sercon Ltd., Crewe, Cheshire, United Kingdom) at the Stable Isotope Facility in the University of California, Davis (Davis, California, USA). We used an isotope

mixing model to determine  $p_{pool-x}$  (%), the proportion of a N pool – shoots, roots, rhizosphere soil, and microbial biomass extracts (fumigated and unfumigated soil extracts) – derived from a substrate ( $x$ ; i.e., root exudates or urea):

$$p_{pool-x} = \frac{(Atom\% \text{ } ^{15}N_{sample} - Atom\% \text{ } ^{15}N_{control})}{(Atom\% \text{ } ^{15}N_x - Atom\% \text{ } ^{15}N_{control})} \times 100 \quad (4.10)$$

where  $Atom\% \text{ } ^{15}N_{sample}$  is the  $^{15}N$  enrichment of the sample for that pool (atom%  $^{15}N$ ),  $Atom\% \text{ } ^{15}N_{control}$  is the  $^{15}N$  enrichment of the natural abundance control for that pool (atom%  $^{15}N$ ), and  $Atom\% \text{ } ^{15}N_x$  is the  $^{15}N$  enrichment of the  $^{15}N$ -substrate introduced to the pot from which we collected the sample. We did not use this equation to calculate the N derived from root exudates in the shoots and roots because  $Atom\% \text{ } ^{15}N_x$  for this substrate is the average  $^{15}N$  enrichment of the shoots and roots. With this proportion, we could then calculate  $N_{pool-x}$  ( $\mu\text{g}$ ), the amount of N in a pool – shoots, roots, rhizosphere soil, and microbial biomass extracts (fumigated and unfumigated soil extracts) – derived from a substrate ( $x$ ; i.e., root exudates or urea):

$$N_{pool-x} = \frac{p_{pool-x}}{100} \times N_{pool} \quad (4.11)$$

where  $p_{pool-x}$  is the proportion of a pool derived from a substrate (%) calculated with Equation 4.10 and  $N_{pool}$  is the total amount of N in the pool of interest ( $\mu\text{g}$ ).

Microbial biomass N in the rhizosphere soil was calculated from the total N determined in the freeze-dried  $0.5 \text{ mol K}_2\text{SO}_4 \text{ L}^{-1}$  extracts of fumigated samples and unfumigated controls (Pang et al. 2021) using the extraction coefficient for microbial biomass N ( $k_{EN} = 0.50$ ; Voroney et al. 2008). A modified version of this calculation was also used to find the microbial biomass N derived from a substrate ( $MBN_x$  in  $\mu\text{g N g}^{-1}$ ):

$$MBN_x = \frac{(N_{fum-x} - N_{unfum-x})}{k_{EN}} \quad (4.12)$$

where  $N_{fum-x}$  is the amount of N in the fumigated soil extract derived from the substrate of interest calculated with Equation 4.11 ( $\mu\text{g N}$ ),  $N_{unfum-x}$  the amount of N in the fumigated soil extract derived from the substrate of interest calculated with Equation 4.11 ( $\mu\text{g N}$ ) and  $k_{EN}$  is the extraction coefficient for microbial biomass N (0.50; Voroney et al. 2008). We determined the proportion of microbial biomass N derived from a substrate ( $p_{MBN-x}$  in %) with:

$$p_{MBN-x} = \frac{MBN_x}{MBN} \times 100 \quad (4.13)$$

where  $MBN_x$  is the microbial biomass N derived from a substrate calculated with Equation 4.12 ( $\mu\text{g N g}^{-1}$ ) and  $MBN$  is the total microbial biomass N ( $\mu\text{g N g}^{-1}$ ). Due to the  $\leq 48$  h exposure period to  $^{15}\text{N}$ -substrates, we assumed that (i)  $^{15}\text{N}$  present in the rhizosphere soil and rhizobiome after stem feeding with  $^{15}\text{N}$ -urea was derived from root exudates as opposed to rhizodeposits (e.g., fine root turnover); and (ii)  $^{15}\text{N}$  in the microbial biomass was minimally affected by cross-feeding, that is the secondary assimilation of byproducts from the initial metabolism of root exudate-derived N by microorganisms (Haichar et al. 2016).

#### 4.3.7 Statistical analyses

For all pools, negative values of replicates were excluded as outliers that indicated unsuccessful enrichment with  $^{15}\text{N}$ . If more than one replicate had a negative value, the mean value of the pool in that respective treatment was considered to be zero.

We tested the effect of substrate on total  $\text{N}_2\text{O-N}$  emissions using a one-way ANOVA, ensuring that its assumptions were met with the Shapiro–Wilk's and Levene's test for residual normality and homogeneity of variance, respectively.

Due to the non-normal distribution of residuals, we assessed whether differences in the partitioning of recovered  $^{15}\text{N}$  among the rhizosphere soil and microbial biomass of the rhizobiome were due to substrate, time and their interaction using generalized linear model

analysis. We used the gamma probability distribution because of the skewed, positive nature of the values (Dennis and Patil 1984). If significant, we conducted pairwise comparisons of the estimated marginal means with Tukey post hoc analysis. We also used the same statistical procedure when assessing the effect of substrate, pool and their interaction on the partitioning of recovered  $^{15}\text{N}$  among the daily emissions of rhizomicrobial  $\text{N}_2\text{O}$  and the combined pool of rhizosphere soil and microbial biomass of the rhizobiome for the 24 h and 48 h time-points. These pools were combined to avoid the issue of multicollinearity (Huang et al. 2015), since  $^{15}\text{N}$  in the rhizosphere soil is calculated from the subtraction of  $^{15}\text{N}$  in the microbial biomass from the total  $^{15}\text{N}$  of rhizosphere soil.

Likewise, we evaluated whether differences in the proportion of substrate-derived N in the rhizosphere soil and rhizobiome resulted from substrate, time and their interaction by also using generalized linear model analysis with the gamma probability distribution followed by pairwise comparisons of the estimated marginal means with Tukey post hoc analysis. For the proportion of  $\text{N}_2\text{O}$ -N derived from a substrate, we only assessed the effect of substrate using the nonparametric Mann-Whitney test since results were pooled together for the 24 h and 48 h time-points. We checked if there were similar distributions using the Kolmogorov-Smirnov test, confirming this assumption of the Mann-Whitney test was met.

Differences were considered significant at  $p < 0.05$ . All statistical analyses were performed in R Studio version 2024.04.2+764 (RStudio Team 2020) via the car, emmeans, MASS, multcomp and stats packages.

## 4.4 Results

### 4.4.1 N<sub>2</sub>O emissions

We measured positive N<sub>2</sub>O fluxes from the rhizosphere of ryegrass plants at 24 h and 48 h after <sup>15</sup>N-substrate introduction, ranging from 0.704 to 16.1 µg N<sub>2</sub>O-N m<sup>-2</sup> h<sup>-1</sup>. These fluxes resulted in daily total N<sub>2</sub>O emissions of 126 ± 29 µg N<sub>2</sub>O-N m<sup>-2</sup> d<sup>-1</sup>, with there being no difference between those emitted from the ryegrass rhizosphere exposed to <sup>15</sup>N-root exudates or <sup>15</sup>N-urea fertilizer ( $p > 0.05$ ; Table 4.1; Table 4.S2 to see emissions in terms of soil mass).

**Table 4.1** Range and mean of total and substrate-derived daily N<sub>2</sub>O emissions from the rhizosphere of annual ryegrass (*L. multiflorum*) plants measured 24 h and 48 h after introducing <sup>15</sup>N-root exudates or <sup>15</sup>N-urea fertilizer into the rhizosphere. The mean values for the substrate-derived N<sub>2</sub>O emissions are the pooled results for both time-points ( $n = 7$  for <sup>15</sup>N-root exudates due to a negative value;  $n = 5$  for <sup>15</sup>N-urea due to negative values).

<sup>15</sup> N-Substrate		Total N <sub>2</sub> O Emissions (µg N <sub>2</sub> O-N m <sup>-2</sup> d <sup>-1</sup> )	Substrate-Derived N <sub>2</sub> O Emissions (µg N <sub>2</sub> O- <sup>15</sup> N m <sup>-2</sup> d <sup>-1</sup> )
Root Exudates	Range	61.8–387	1.95–95.1
	Mean	176 ± 46	36.2 ± 15.4
Urea	Range	16.9–82.9	1.40–4.64
	Mean	55.9 ± 11.3	2.43 ± 0.57

The biomass of ryegrass plants was successfully enriched by stem feeding with <sup>15</sup>N-urea (Figure 4.S2). This enrichment generated <sup>15</sup>N-root exudates that permitted us to trace their fate in and from the rhizosphere, including as N<sub>2</sub>O. After introducing labeled root exudates into the rhizosphere for 24 h and 48 h, we observed that a nominal portion of total root exudate-derived N had evolved as N<sub>2</sub>O (mean: 0.0020 ± 0.0012%; Figure 4.1), with the remainder staying in the rhizosphere itself (i.e., 22.3 ± 10.1% microbial biomass of the rhizobiome, 77.7 ± 10.1% in soil). This distribution of root exudate-derived N was comparable to that of urea in terms of its N

dynamics immediately after application ( $p > 0.05$ ), where  $0.00015 \pm 0.00003\%$  was emitted as  $\text{N}_2\text{O}$ ,  $16.3 \pm 6.9\%$  was assimilated by the rhizobiome, and  $83.7 \pm 6.9\%$  remained in the rhizosphere soil.

Although very little evolved as  $\text{N}_2\text{O}$ , the  $\text{N}_2\text{O}$  generated from root exudate-N represented a substantial, albeit variable, proportion of the total daily  $\text{N}_2\text{O}$  emissions. N derived from root exudates produced  $1.95$  to  $95.1 \mu\text{g N}_2\text{O-}^{15}\text{N m}^{-2} \text{d}^{-1}$  (Table 4.1), which corresponded to almost one-fifth of the total  $\text{N}_2\text{O}$ , on average, emitted 24 h and 48 h after substrate introduction (mean:  $18.7 \pm 6.8\%$ ; Figure 4.2). There was no difference between the amount of  $\text{N}_2\text{O}$  derived from root exudates and urea ( $p > 0.05$ ) with the total daily emissions of urea-derived  $\text{N}_2\text{O}$  being  $1.40$  to  $4.64 \mu\text{g N}_2\text{O-}^{15}\text{N m}^{-2} \text{d}^{-1}$  or  $5.37 \pm 1.63\%$  of total  $\text{N}_2\text{O}$  emissions (Table 4.1; Figure 4.2). As the  $\text{N}_2\text{O}$  derived from root exudates and urea fertilizer constituted roughly a quarter of total  $\text{N}_2\text{O}$  emissions, on average, the rest of these emissions was from unknown sources.

By evaluating site preference – the difference in  $^{15}\text{N}$  enrichment between the two N atoms of a  $\text{N}_2\text{O}$  molecule emitted at natural abundance – we could estimate the dominant pathway(s) of microbial  $\text{N}_2\text{O}$  production occurring in the rhizosphere. This site preference analysis approximated that  $87.7 \pm 3.01\%$  (mean  $\pm$  standard error) of rhizosphere-emitted  $\text{N}_2\text{O}$  originated from bacterial denitrification, nitrifier-denitrification or a combination of the two (Figure 4.3). However, when using the maximum site preference value of the reference range from pure cultures of bacterial denitrifiers and nitrifier-denitrifiers (i.e.,  $3.7\%$ ), this estimate shifted to  $114 \pm 6\%$  (mean  $\pm$  standard error; data not shown). This result suggests that the rhizobiome community of this study is better characterized by bacterial denitrifiers and nitrifier-denitrifiers that emit  $\text{N}_2\text{O}$  with a low site preference signature.

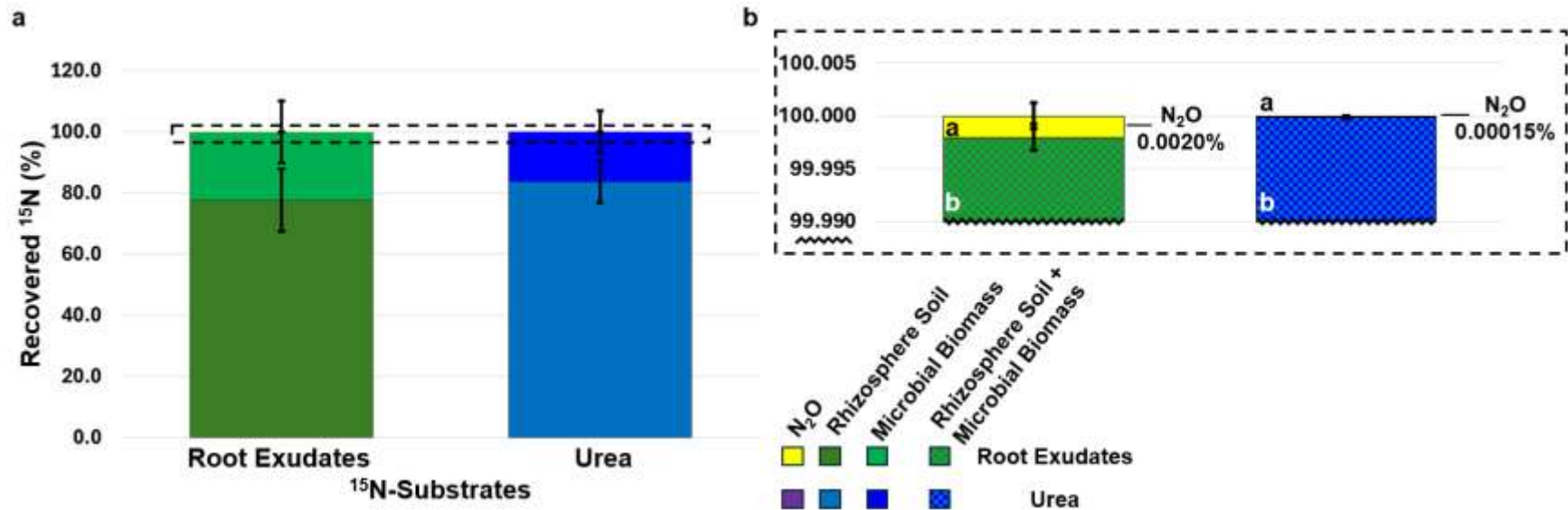


**Figure 4.1** The partitioning of the recovered N (%) from root exudates and urea among the rhizosphere pools of annual ryegrass (*L. multiflorum*) plants measured 24 h and 48 h after introducing  $^{15}\text{N}$ -root exudates or  $^{15}\text{N}$ -urea fertilizer into the rhizosphere: a) the separate pools of daily  $\text{N}_2\text{O}$  emissions, rhizosphere soil, microbial biomass; and b) a magnified inset to show the size of recovered N in the daily  $\text{N}_2\text{O}$  emissions with the combined pools of rhizosphere soil and microbial biomass (note the difference in the y-axis scales). Each bar in the stacked bar represents the mean value of  $^{15}\text{N}$  recovered in a specific pool for a respective  $^{15}\text{N}$ -substrate treatment pooled together for both time-points. Error bars indicate the standard error of the mean values. The stacked bar for the  $^{15}\text{N}$ -root exudate treatment had a sample size of  $n = 6$ , while  $^{15}\text{N}$ -urea fertilizer had a sample size of  $n = 5$  due to negative values. In Figure 4.1b, different lowercase letters indicate a significant difference in the recovered  $^{15}\text{N}$  between the pools for a respective  $^{15}\text{N}$ -substrate treatment. All differences were assessed for significance ( $p < 0.05$ ) using generalized linear model analysis with a gamma probability distribution followed by pairwise comparisons of the estimated marginal means with Tukey post hoc analysis.

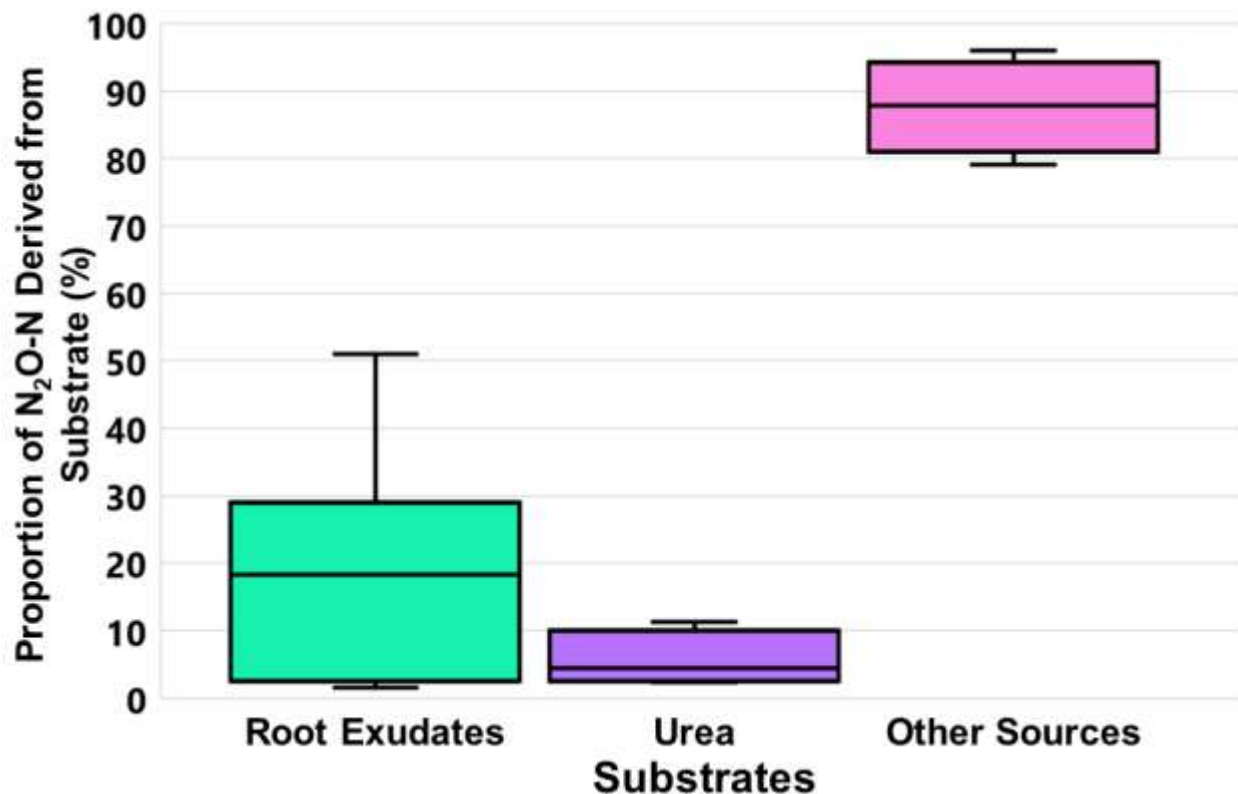


**Figure 4.2** The proportion of soil-emitted  $\text{N}_2\text{O-N}$  (%) derived from root exudates and urea fertilizer in the rhizosphere of annual ryegrass (*L. multiflorum*) plants. “Other Sources” represents the remainder of  $\text{N}_2\text{O-N}$  not derived from either  $^{15}\text{N}$ -substrate. Each boxplot shows the distribution of the pooled results measured 24 h and 48 h after the introduction of  $^{15}\text{N}$ -root exudates or  $^{15}\text{N}$ -urea fertilizer into the rhizosphere. The bottom and top of the boxplot signify the 25% and 75% quartiles, respectively, with the center line representing the median and the whiskers showing the range. The boxplot for the  $^{15}\text{N}$ -root exudate treatment had a sample size of  $n = 7$ , while the  $^{15}\text{N}$ -urea fertilizer treatment and other sources have a sample size of  $n = 5$  due to negative values.

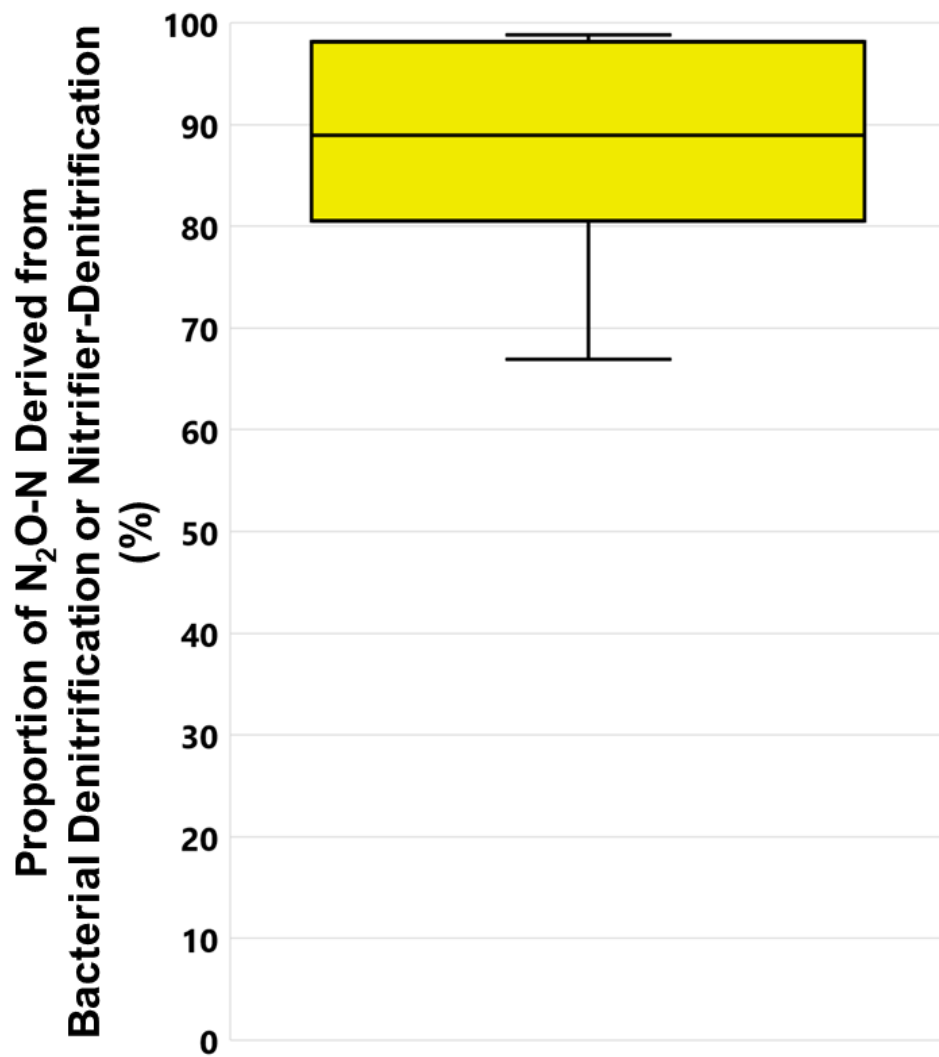


**Figure 4.3** The proportion of soil-emitted N<sub>2</sub>O-N (%) derived from bacterial denitrification or nitrifier-denitrification based on the concentration-weighted site preference values of N<sub>2</sub>O-N fluxes from natural abundance controls. The boxplot shows the distribution of the pooled results measured 24 h and 48 h after the introduction of root exudates (i.e., stem feeding) or urea fertilizer at natural abundance into the rhizosphere. The bottom and top of the boxplot signify the 25% and 75% quartiles, respectively, with the center line representing the median and the whiskers showing the range ( $n = 6$  due to sample destruction by the instrument).

#### 4.4.2 *Dynamics of substrate-derived N in the rhizosphere*

When looking at the dynamics of root exudate-N with a finer temporal resolution (i.e., 3, 9, 24 and 48 h after  $^{15}\text{N}$ -substrate introduction), we observed different patterns in the rhizosphere soil and microbial biomass of the rhizobiome. N derived from root exudates was immediately present in the rhizosphere soil, with  $4.09 \pm 0.51 \text{ g } ^{15}\text{N m}^{-2}$  measured 3 h after stem-feeding and remained constant throughout the study (mean:  $2.59 \pm 0.51 \text{ g } ^{15}\text{N m}^{-2}$ ; Table 4.2; Table 4.S3 to see amounts in terms of soil mass). In contrast, root exudate-N was not detected in the microbial biomass of the rhizobiome until 48 h after stem feeding (mean:  $1340 \pm 520 \text{ mg } ^{15}\text{N m}^{-2}$ ; Table 4.2, Figure 4.4). This differed from urea-derived N, which was present 3 h and 48 h after application, but not in between these two time-points.

In terms of proportion, root exudate-derived N only represented 1.98 to 3.46% of the total N in the rhizosphere soil (Figure 4.5a). This proportion was greater than that of urea-derived N ( $p > 0.05$ ), which was just slightly greater than 1% of the N in this pool. For rhizobiome N, root exudate-derived N made up almost all of the rhizobiome biomass at 48 h after substrate introduction into the rhizosphere (mean:  $88.9 \pm 48.6\%$  of the total pool N; Figure 4.5b). The large variation indicates that some overestimation occurred, likely a function of the dynamic cycling of microbial biomass, plant physiology, and the coarse resolution of chloroform fumigation-extraction. Conversely, urea-derived N constituted a lower fraction in the rhizobiome (41.8–43.5%) with less variation.

### 4.5 Discussion

#### 4.5.1 *Root exudates are a N source for $\text{N}_2\text{O}$ production in the rhizosphere*

Our findings demonstrate that root exudates were a considerable N source for  $\text{N}_2\text{O}$  production in the ryegrass rhizosphere, supporting our first hypothesis. Despite only a minor fraction of total

**Table 4.2** The total and substrate-derived N in the soil and microbial biomass pools of the rhizosphere of annual ryegrass (*L. multiflorum*) plants measured 3, 9, 24 and 48 h after introducing  $^{15}\text{N}$ -root exudates or  $^{15}\text{N}$ -urea fertilizer into the rhizosphere. Each value is the mean  $\pm$  standard error ( $n = 4$ , while those with an asterisk (\*) were  $n = 3$  due to negative values).

Substrate	Time since $^{15}\text{N}$ -Substrate Introduction	Rhizosphere Soil		Microbial Biomass of Rhizobiome	
		Total N (g N m <sup>-2</sup> )	Substrate-Derived N (g $^{15}\text{N}$ m <sup>-2</sup> )	Total N (mg N m <sup>-2</sup> )	Substrate-Derived N (mg $^{15}\text{N}$ m <sup>-2</sup> )
Root Exudates	3	130 $\pm$ 5 *	4.09 $\pm$ 1.93 *	574 $\pm$ 60 *	0
	9	104 $\pm$ 13	2.01 $\pm$ 0.78 *	897 $\pm$ 122	0
	24	95.0 $\pm$ 8.2	2.28 $\pm$ 0.72	597 $\pm$ 232	0
	48	115 $\pm$ 5	1.62 $\pm$ 0.50 *	1390 $\pm$ 470	1340 $\pm$ 520 *
Urea	3	101 $\pm$ 15 *	0.662 $\pm$ 0.196 *	1110 $\pm$ 20 *	463 $\pm$ 42 *
	9	126 $\pm$ 7 *	1.40 $\pm$ 0.17 *	842 $\pm$ 604 *	0
	24	108 $\pm$ 6	1.48 $\pm$ 0.13	1080 $\pm$ 410	0
	48	139 $\pm$ 9	1.16 $\pm$ 0.09	1380 $\pm$ 240	554 $\pm$ 62 *

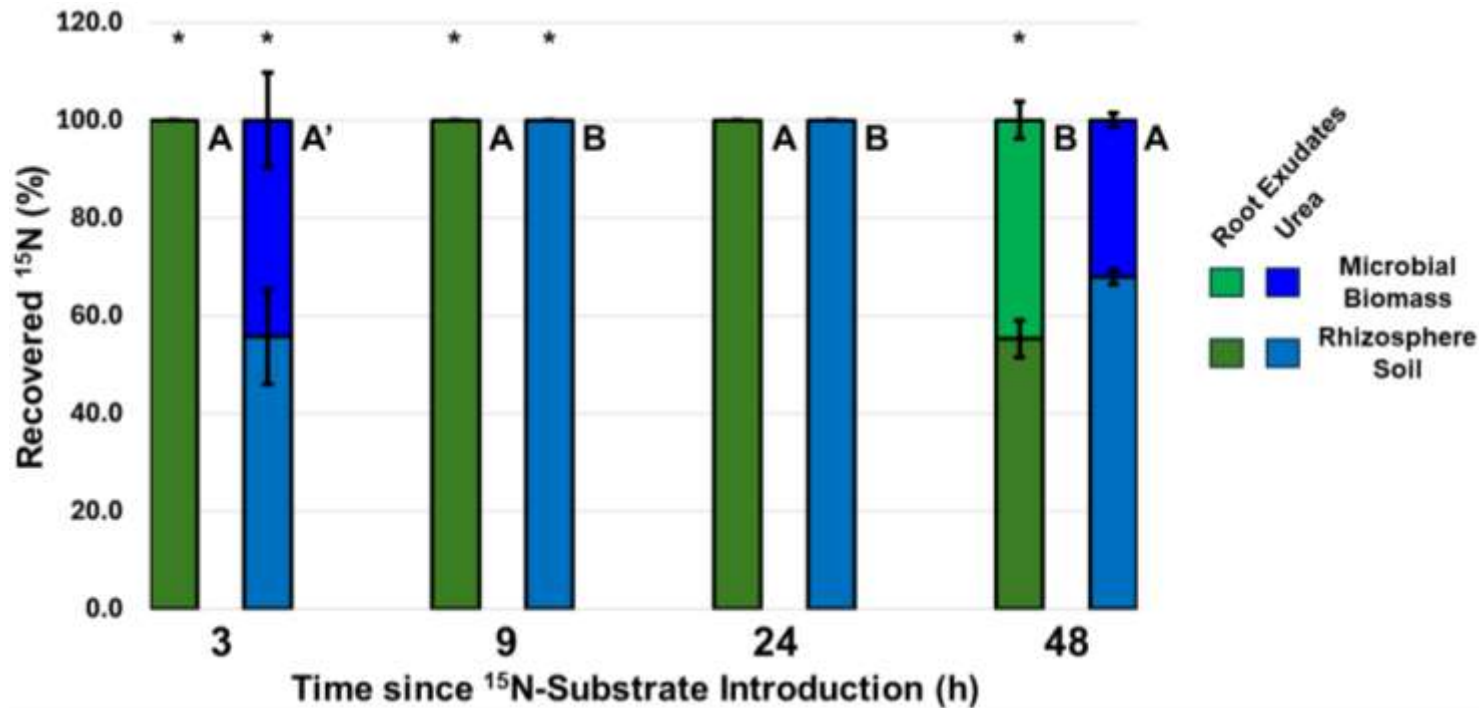


**Figure 4.4** The partitioning of the recovered N (%) from root exudates and urea among the soil and microbial biomass pools in the rhizosphere of annual ryegrass (*L. multiflorum*) plants measured 3, 9, 24 and 48 h after introducing  $^{15}\text{N}$ -root exudates or  $^{15}\text{N}$ -urea fertilizer into the rhizosphere. Each bar in the stacked bar represents the mean value of  $^{15}\text{N}$  recovered in a specific pool for a respective  $^{15}\text{N}$ -substrate treatment at a specific time-point. Error bars indicate the standard error of the mean values. All mean  $^{15}\text{N}$  values had a sample size of  $n = 4$  except for those stacked bars with an asterisk (\*), denoting  $n = 3$  due to negative values. Different uppercase letters on the right of a bar indicate a significant difference in the partitioning of the recovered  $^{15}\text{N}$  among the pools between time-points for a specific  $^{15}\text{N}$ -substrate treatment. The presence of an apostrophe (') on the right of a bar indicates a significant difference in the partitioning of the recovered  $^{15}\text{N}$  among pools between  $^{15}\text{N}$ -substrate treatments at a specific time-point. All differences were assessed for significance ( $p < 0.05$ ) using generalized linear model analysis with a gamma probability distribution followed by pairwise comparisons of the estimated marginal means with Tukey post hoc analysis.

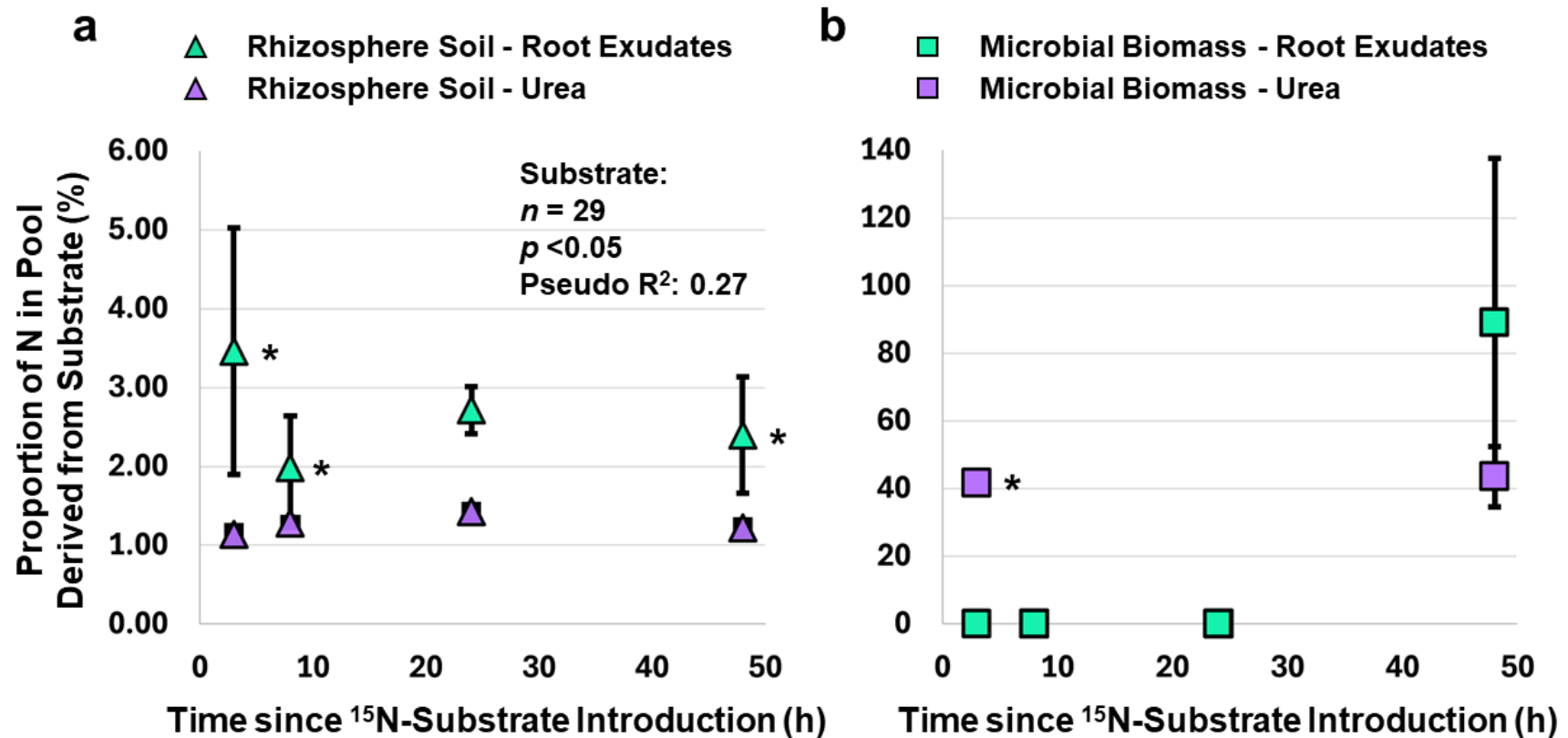


**Figure 4.5** The proportion of N (%) derived from root exudates and urea in the rhizosphere pools of annual ryegrass (*L. multiflorum*) plants measured 3, 9, 24 and 48 h after introducing  $^{15}\text{N}$ -root exudates or  $^{15}\text{N}$ -urea fertilizer into the rhizosphere: a) rhizosphere soil; and b) microbial biomass. Markers indicate the mean substrate-derived N value in a respective pool at a specific time-point, with error bars representing the standard error of the mean. All mean values had a sample size of  $n = 4$  except for those markers with an asterisk (\*), denoting  $n = 3$  due to negative values. Differences in the proportion of substrate-derived N for a pool are shown if significant ( $p < 0.05$ ) regarding substrate, time or their interaction. All differences were assessed for significance using generalized linear model analysis with a gamma probability distribution followed by pairwise comparisons of the estimated marginal means with Tukey post hoc analysis.

root exudate-N contributing to the daily N<sub>2</sub>O emissions (Figure 4.1), N<sub>2</sub>O derived from root exudate-N in this study was roughly 20%, on average, of the total N<sub>2</sub>O emitted from the rhizosphere (Figure 4.2). Belowground plant processes are recognized stimulants of N<sub>2</sub>O production (Philippot et al. 2013, Ai et al. 2015). For example, wheat root exudation and shedding triggered 3.5 to 9.2 times greater N<sub>2</sub>O emissions from the rhizosphere than the bulk soil (Ai et al. 2020). However, the findings of our study show that root exudates themselves can be the precursors of the N<sub>2</sub>O emissions. Thus, root exudates play a more central role in N<sub>2</sub>O production than initially thought.

As we demonstrated that <sup>15</sup>N was exuded into the rhizosphere soil and assimilated by the rhizobiome, we assumed that the N<sub>2</sub>O enriched in <sup>15</sup>N was derived from the microbial metabolism of root exudates. However, as <sup>15</sup>N-root exudates were generated by feeding <sup>15</sup>N-urea into the stem of ryegrass plants, the plant shoots were also labeled with <sup>15</sup>N and could be an additional source of N<sub>2</sub>O emissions. Plants produce N<sub>2</sub>O from their shoots during the photoassimilation of nitrite into the chloroplast, absorption of ultraviolet radiation and through an unknown plant physiological or abiotic process occurring without light (Smart and Bloom 2001, Yu and Chen 2009, Bruhn et al. 2014, Lenhart et al. 2019, Clough et al. 2020). Yet, N<sub>2</sub>O fluxes generated from plant tissue are minimal (0.0004–0.173 μg N<sub>2</sub>O-N g<sup>-1</sup> h<sup>-1</sup>; Lenhart et al. 2019) and most of the processes involving plant tissue generation of N<sub>2</sub>O are light-dependent. Considering that we used an opaque chamber for measuring N<sub>2</sub>O fluxes, it is likely that we minimized the contribution of this source.

Surprisingly, there was no difference between the N<sub>2</sub>O emissions derived from root exudates and urea fertilizer. Such low emissions from urea were unexpected, as nitrogenous fertilizers are a well-established source of N<sub>2</sub>O (Carlson et al. 2017). In fact, N fertilizer is

estimated to be responsible for 21 to 26% of N<sub>2</sub>O emissions from cultivated peatlands (Wang et al. 2024), the same soil type used in this study. As urea hydrolysis typically occurs 3.8 d after application depending on soil and temperature (Lasisi and Akinremi 2020), we may have missed the N<sub>2</sub>O flux in our measurements (24 h and 48 h after urea application). However, Wang et al. (2024) was a machine learning study focusing on N<sub>2</sub>O emissions from cultivated peatlands at the global scale and did not consider root exudates as a N source for N<sub>2</sub>O production. As such, we recommend the inclusion of root exudates as a N<sub>2</sub>O source in global models, which may alter the source partitioning estimates and demonstrate their significant contribution to N<sub>2</sub>O emissions.

Roughly 75% of the N<sub>2</sub>O emissions, on average, could not be explained by the root exudates and urea fertilizer introduced into the rhizosphere in this study. The most likely source of this N<sub>2</sub>O emissions is the urea fertilizer previously applied during the growing period due to physiological signs of plant nutrient deficiency (Figure 4.S1). While any remaining nutrients from such a low dose of fertilizer would have likely leached in the field, we had sealed the insides of the pots with plastic wrap to avoid the loss of <sup>15</sup>N (Mahieu et al. 2009). Decomposition of the organic matter in this peat soil may also provide reactive N for N<sub>2</sub>O production, credited as the N source of 72.8 % of the N<sub>2</sub>O emissions from cultivated peatlands (Wang et al. 2024). However, CO<sub>2</sub> emissions from peat were minor in our study (See Chapter 5), suggesting low levels of peat decomposition. Nevertheless, despite the large quantity of N<sub>2</sub>O from unknown origins, it is evident that root exudates are a considerable source of N<sub>2</sub>O emissions in addition to urea fertilizer and organic matter mineralization.

#### ***4.5.2 N<sub>2</sub>O from the rhizosphere likely produced by bacterial denitrification, nitrifier-denitrification or a combination of the two pathways***

Through site preference analysis, we approximated that the vast majority of N<sub>2</sub>O was produced by bacterial denitrification, nitrifier-denitrification or an amalgam of the two (67 to 99%; Figure 4.3). This result provided evidence for our second hypothesis that these pathways would dominate N<sub>2</sub>O production in the rhizosphere. In our estimation, we decided to exclude the upper bound site preference value of the reference range for bacterial denitrification and nitrifier denitrification because it shifted our estimation to >100%. This observation implies that the bacterial denitrifiers or nitrifier-denitrifiers in this study produced N<sub>2</sub>O with greater enrichment of the outer N atom at natural abundance, such as *Paracoccus denitrificans* and *Nitrosomonas marina*-like microbes, respectively (Toyoda et al. 2005, Frame and Casciotti 2010). Regardless, bacterial denitrification and nitrifier-denitrification seem to be influential pathways for N<sub>2</sub>O generation in the rhizosphere.

Previous research has suggested that nitrification is ancillary to denitrification and nitrifier-denitrification in the rhizosphere. Compared to the bulk soil, the rhizosphere suppresses nitrification rates by roughly 35% (Ling et al. 2022). Additionally, studies have suggested that the abundant assimilable carbon substrates from root exudation should promote denitrification and nitrifier-denitrification by (i) initially triggering aerobic respiration that results in rapid O<sub>2</sub> consumption, creating anaerobic or microaerophilic conditions, and (ii) functioning as electron donors for these N<sub>2</sub>O-producing pathways (Lecomte et al. 2018, Wrage-Mönnig et al. 2018, Ling et al. 2022). Such conditions are in contrast to those preferred by nitrifiers, which thrive in aerobic environments (Zhu et al. 2013, Lancaster et al. 2018) and are autotrophs (Fenchel et al. 2012, Kuypers et al. 2018). While we could not measure the O<sub>2</sub> content of the rhizosphere, there

was a surplus of bioavailable organic C ( $K_2SO_4$  extractable C:  $1030 \pm 80$  mg C  $kg^{-1}$ ; data not shown). As such, in addition to site preference analysis, this observation indicates that the rhizosphere environment was conducive for denitrification and nitrifier-denitrification to occur, as opposed to nitrification.

We could not differentiate between bacterial denitrification and nitrifier denitrification as their individual reference ranges overlap for site preference (Zaman et al. 2021). Previous research has suggested that denitrification controls  $N_2O$  production in the rhizosphere. For example, Ai et al. (2020) found that bacterial denitrifiers – specifically those of NosZ Clade I – were 67% more concentrated in the rhizosphere than bulk soil. However, while associated with classical denitrifiers, NosZ may be present in nitrifier-denitrifiers (Wrage-Mönnig et al. 2018). It is tempting to speculate that nitrifier-denitrification was responsible for  $N_2O$  production from the rhizosphere in our study. This is not only because of the surplus of  $NH_4^+$  provided by urea fertilizer ( $150$  kg N  $ha^{-1}$ ) but that N-containing root exudates are largely either  $NH_4^+$  or its precursors (Hertenberger and Wanek 2004, Myrold 2021). Thus, while it is unlikely that nitrification and fungal denitrification contributed to  $N_2O$  emissions, further research is needed to parse out the individual contributions of bacterial denitrification and nitrifier-denitrification to  $N_2O$  production in the rhizosphere.

Site preference analysis is a useful tool to gain insight into the  $N_2O$  cycling that occurs in the rhizosphere. However, there are limitations with this method. First, the reference ranges for approximating the contribution of different pathways use the site preference values from pure cultures of  $N_2O$ -producing microorganisms (Decock and Six 2013, Zaman et al. 2021). There are some studies that have measured site preference from soil, but maintaining the purity of cultures in soil is difficult. Additionally, the number of incubations is limited, making it difficult to

develop a robust range. Second, the reference ranges possess large variability and overlap with each other, thus producing variable estimates with sometimes various outcomes. One possible solution to overcoming this issue is combining site preference analysis with the measurement of  $\delta^{15}\text{N}_{\text{bulk}}$  and  $\delta^{18}\text{O}$ . By measuring all three, the values of each can be compared to their respective reference range to help pinpoint the specific  $\text{N}_2\text{O}$  production pathway (Zou et al. 2014, Wu et al. 2019). Still, site preference analysis is a semi-quantitative assessment that can indicate the important pathways of  $\text{N}_2\text{O}$  production and is useful to develop hypotheses for future mechanistic studies.

#### ***4.5.3 Fate of root exudate-N in the rhizosphere***

By measuring the fate of root exudate-derived N in the soil pools at a finer time scale, we could resolve the dynamics of recently exuded N compounds in the rhizosphere. We found that a substantial amount of N ( $4.09 \pm 1.93 \text{ g }^{15}\text{N m}^{-2}$ ) was exuded just 3 h after  $^{15}\text{N}$ -urea stem feeding to generate labeled root exudates and remained relatively constant throughout the experiment (Table 4.2). In fact, there was 70% more N-derived from root exudates in the rhizosphere soil than that derived from urea (Figure 4.5), indicating the importance of root exudation to rhizosphere N cycling. This instant release of  $^{15}\text{N}$  could be an experimental artefact from the stem feeding method, known as the “leakage effect”, where a substantial amount of the label is discharged immediately by an unknown plant physiological response (Gasser et al. 2015). Indeed, the  $^{15}\text{N}$  measured in the rhizosphere was  $\sim 75\%$  of the  $^{15}\text{N}$  in the entire system at 3 h (Figure 4.S3). However, by 9 h, the distribution of the  $^{15}\text{N}$  among the shoots, roots, microbial biomass and rhizosphere soil reached an equilibrium, well before our first measurement of  $\text{N}_2\text{O}$ . Additionally, even if leakage occurred, it does not alter the fact that the  $^{15}\text{N}$  present in the rhizobiome or  $\text{N}_2\text{O}$  is derived from root exudates, albeit potentially at a maximum (DeSena et al.

2023). Thus, the potential of this experimental artefact occurring did not impede the objective of this study.

In contrast to the rhizosphere soil, root exudate-derived N was only detected in the microbial biomass of the rhizobiome 48 h after introduction of  $^{15}\text{N}$ -root exudates (Table 4.2, Figure 4.4). In a previous study, we had detected root exudate-derived N in the rhizobiome 24 h after  $^{15}\text{N}$ -urea stem feeding (De Sena et al. 2023). This difference suggests that the N in this pool is dynamic due to microbial cycling. We also determined that  $88.9 \pm 48.6\%$  of the rhizobiome biomass can originate from root exudates, but with overestimation likely resulting from methodological issues associated with chloroform fumigation-extraction procedure (Leiber-Sautiehl et al. 2015). Despite this variation, the root exudate-derived N in the rhizobiome is much greater than that reported in previous studies (0.004 to 11%; Wichern et al. 2008, Schenck zu Schweinsberg-Mickan et al. 2010, 2012, Kušlienė et al. 2014, De Sena et al. 2023). However, these studies used absolute  $^{15}\text{N}$  enrichment in excess, whereas our estimate was calculated via an isotope mixing model which accounts for the initial signature of the root exudate (i.e., the average enrichment of the plant biomass). While we cannot transform the data from the other studies with the model, converting the root exudate-derived N in the rhizobiome from our previous work ( $0.07 \pm 0.01\%$ ; De Sena et al. 2023) resulted in  $4.6 \pm 1.0\%$ , a two-magnitude difference. As such, the literature is likely not just underestimating the importance of root exudate-N as a N source for  $\text{N}_2\text{O}$  production from dissimilatory microbial processes, but also as a N source for microbial biomass during assimilation.

#### **4.6 Conclusion**

Here, we provide direct evidence of root exudates as a N source for  $\text{N}_2\text{O}$  production in the rhizosphere. While a minor portion of total root exudate-N contributed to emitted  $\text{N}_2\text{O}$ , their

emissions were on par with those from urea fertilizer in our study. This N<sub>2</sub>O was likely generated through bacterial denitrification, nitrifier-denitrification, or a combination of these pathways.

These findings demonstrate the need to consider the contribution of root exudates to N<sub>2</sub>O emissions from cultivated peat soils, in addition to urea fertilizer and organic matter mineralization. Further investigations of root exudate-derived N<sub>2</sub>O are needed, including with other crops and in mineral soils, to accurately characterize their potential capacity to generate N<sub>2</sub>O. Such efforts will improve biogeochemical models of N cycling and global estimates of N<sub>2</sub>O emissions.

#### 4.7 References

- Ai, C., Liang, G., Sun, J., et al., 2015. Reduced dependence of rhizosphere microbiome on plant-derived carbon in 32-year long-term inorganic and organic fertilized soils. *Soil Biology and Biochemistry* 80, 70–78. <https://doi.org/10.1016/j.soilbio.2014.09.028>.
- Ai, C., Zhang, M., Sun, Y., et al., 2020. Wheat rhizodeposition stimulates soil nitrous oxide emission and denitrifiers harboring the *nosZ* clade I gene. *Soil Biology and Biochemistry* 143, 107738. <https://doi.org/10.1016/j.soilbio.2020.107738>.
- Allard-Massicotte, R., Tessier, L., Lécuyer, F., et al., 2016. *Bacillus subtilis* early colonization of *Arabidopsis thaliana* roots involves multiple chemotaxis receptors. *mBio* 7: e01664-16. <https://doi.org/10.1128/mbio.01664-16>.
- Bruhn, D., Albert, K.R., Mikkelsen, T.N., Ambus, P., 2014. UV-induced N<sub>2</sub>O emission from plants. *Atmospheric Environment* 99, 206-214. <https://doi.org/10.1016/j.atmosenv.2014.09.077>.
- Cai, T., Cai, W., Zhang, J., et al., 2009. Host legume-exuded antimetabolites optimize the symbiotic rhizosphere. *Molecular Microbiology* 73, 507-517. <https://doi.org/10.1111/j.1365-2958.2009.06790.x>.
- Cai, Q., Qiao, L., Wang, M., et al., 2018. Plants send small RNAs in extracellular vesicles to fungal pathogen to silence virulence genes. *Science* 360, 1126-1129. <https://doi.org/10.1126/science.aar4142>.

- Carlson, K.M., Gerber J.S., Mueller, N.D., et al., 2017. Greenhouse gas emissions intensity of global croplands. *Nature Climate Change* 7, 63–68. <https://doi.org/10.1038/nclimate3158>.
- CIAAW, 2015. Nitrogen. Commission on Isotopic Abundances and Atomic Weights. <https://ciaaw.org/nitrogen.htm>. (Accessed August 14, 2024).
- Clough, T.J., Rochette, P., Thomas, S.M., et al., 2020. Global Research Alliance N<sub>2</sub>O chamber methodology guidelines: Design considerations. *Journal of Environmental Quality* 49, 1081-1091. <https://doi.org/10.1002/jeq2.20117>.
- De Sena, A., Madramootoo, C.A., Whalen, J.K., 2023. Nitrogen transfer from root exudates to the rhizobiome: A <sup>15</sup>N stem feeding method. *Soil Biology and Biochemistry* 186: 109159. <https://doi.org/10.1016/j.soilbio.2023.109159>.
- De Sena, A., Mosdossy, K., Whalen, J.K., Madramootoo, C.A., 2022. Root exudates and microorganisms. In: Goss, M., Oliver, M. (Eds.), *Encyclopedia of Soils in the Environment*, 2nd ed. Elsevier, Cambridge, Massachusetts, pp. 343–356. <https://doi.org/10.1016/B978-0-12-822974-3.00125-7>.
- Decock, C., Six, J., 2013. How reliable is the intramolecular distribution of <sup>15</sup>N in N<sub>2</sub>O to source partition N<sub>2</sub>O emitted from soil? *Soil Biology and Biochemistry* 65, 114-127. <https://doi.org/10.1016/j.soilbio.2013.05.012>.
- Dennis, B., Patil, G.P., 1984. The gamma distribution and weighted multimodal gamma distributions as models of population abundance. *Mathematical Biosciences* 68, 187-212. [https://doi.org/10.1016/0025-5564\(84\)90031-2](https://doi.org/10.1016/0025-5564(84)90031-2).

- Dhamala, N.R., Rasmussen, J., Carlsson, G., et al., 2017. N transfer in three-species grass-clover mixtures with chicory, ribwort plantain or caraway. *Plant and Soil* 413, 217-230.  
<https://doi.org/10.1007/s11104-016-3088-6>.
- EPA, 2024. Climate change indicators: Atmospheric concentrations of greenhouse gases. Environmental Protection Agency. <https://www.epa.gov/climate-indicators/climate-change-indicators-atmospheric-concentrations-greenhouse-gases> (Accessed August 14, 2024).
- Fenchel, T., King, G.M., Blackburn, T.H., 2012. Bacterial metabolism. In: Fenchel, T., King, G.M., Blackburn, T.H. (Eds.), *Bacterial Biogeochemistry*, 3rd edn. Academic Press, Elsevier, Massachusetts, pp. 1–34. <https://doi.org/10.1016/B978-0-12-415836-8.00001-3>.
- Frame, C.H., Casciotti, K.L., 2010. Biogeochemical controls and isotopic signatures of nitrous oxide production by a marine ammonia-oxidizing bacterium. *Biogeosciences* 7, 2695-2709. <https://doi.org/10.5194/bg-7-2695-2010>.
- Haichar, F.e.Z., Heulin, T., Guyonnet, J.P., et al., 2016. Stable isotope probing of carbon flow in the plant holobiont. *Current Opinion in Biotechnology* 41, 9-13.  
<https://doi.org/10.1016/j.copbio.2016.02.023>.
- Hertenberger, G., Wanek, W., 2004. Evaluation of methods to measure differential <sup>15</sup>N labeling of soil and root N pools for studies of root exudation. *Rapid Communications in Mass Spectrometry* 18, 2415–2425. <https://doi.org/10.1002/rcm.1615>.
- Høgh-Jensen, H., Schjoerring, J.K., 2001. Rhizodeposition of nitrogen by red clover, white clover and ryegrass leys. *Soil Biology and Biochemistry* 33, 439-448.  
[https://doi.org/10.1016/S0038-0717\(00\)00183-8](https://doi.org/10.1016/S0038-0717(00)00183-8).

- Huang, C.C.L., Jou, Y.J., Cho, H.J., 2015. A new multicollinearity diagnostic for generalized linear models. *Journal of Applied Statistics* 43, 2029-2043.  
<https://doi.org/10.1080/02664763.2015.1126239>.
- Gasser, M., Hammelehle, A., Oberson, A., et al., 2015. Quantitative evidence of overestimated rhizodeposition using  $^{15}\text{N}$  leaf-labelling. *Soil Biology and Biochemistry* 85, 10–20. <https://doi.org/10.1016/j.soilbio.2015.02.002>.
- Kušlienė, G., Rasmussen, J., Kuzyakov, Y., Eriksen, J., 2014. Medium-term response of microbial community to rhizodeposits of white clover and ryegrass and tracing of active processes induced by  $^{13}\text{C}$  and  $^{15}\text{N}$  labelled exudates. *Soil Biology and Biochemistry* 76, 22–33. <https://doi.org/10.1016/j.soilbio.2014.05.003>.
- Kuypers, M.M.M., Marchant, H.K., Kartal, B., 2018. The microbial nitrogen-cycling network. *Nature Reviews Microbiology* 16, 263–276. <https://doi.org/10.1038/nrmicro.2018.9>.
- Lancaster, K.M., Caranto, J.D., Majer, S.H., et al., 2018. Alternative bioenergy: Updates to and challenges in nitrification metalloenzymology. *Joule* 2, 421–441.  
<https://doi.org/10.1016/j.joule.2018.01.018>.
- Lasisi, A.A., Akinremi, O.O., 2021. Kinetics and thermodynamics of urea hydrolysis in the presence of urease and nitrification inhibitors. *Canadian Journal of Soil Science* 101,192-202. <https://doi.org/10.1139/cjss-2020-0044>.
- Lecomte, S.M., Achouak, W., Abrouk, D., et al., 2018. Diversifying anaerobic respiration strategies to compete in the rhizosphere. *Frontiers in Environmental Science* 6, 139.  
<https://doi.org/10.3389/fenvs.2018.00139>.

- Leiber-Sauheitl, K., Fuß, R., Burkart, St., et al., 2015. Sheep excreta cause no positive priming of peat-derived CO<sub>2</sub> and N<sub>2</sub>O emissions. *Soil Biology and Biochemistry* 88, 282-293. <https://doi.org/10.1016/j.soilbio.2015.06.001>.
- Lenhart, K., Behrendt, T., Greiner, S., et al., 2019. Nitrous oxide effluxes from plants as a potentially important source to the atmosphere. *New Phytologist* 221, 1398-1408. <https://doi.org/10.1111/nph.15455>.
- Li, C., Tian, Q., Rahman, M.K.u., Wu, F., 2020. Effect of anti-fungal compound phytosphingosine in wheat root exudates on the rhizosphere soil microbial community of watermelon. *Plant and Soil* 456, 223-240. <https://doi.org/10.1007/s11104-020-04702-1>.
- Ling, N., Wang, T., Kuzyakov, Y., 2022. Rhizosphere bacteriome structure and functions. *Nature Communications* 13, 836. <https://doi.org/10.1038/s41467-022-28448-9>.
- Liu, H., Li, Y., Pan, B., et al., 2022. Pathways of soil N<sub>2</sub>O uptake, consumption, and its driving factors: A review. *Environmental Science and Pollution Research* 29, 30850–30864. <https://doi.org/10.1007/s11356-022-18619-y>.
- Lloyd, K., 2016. Greenhouse Gas Emissions from Onion Fields Cultivated on Organic Soils under Sprinkler Irrigation in Quebec. [Master's Thesis, McGill University]. ProQuest Dissertations and Theses Database.

- Lloyd, K., Madramootoo, C.A., Edwards, K.P., et al., 2019. Greenhouse gas emissions from selected horticultural production systems in a cold temperate climate. *Geoderma* 349, 45–55. <https://doi.org/10.1016/j.geoderma.2019.04.030>.
- López-Bellido, L., Benítez-Vega, J., García, P., et al., 2011. Tillage system effect on nitrogen rhizodeposited by faba bean and chickpea. *Field Crops Research* 120, 189-195. <https://doi.org/10.1016/j.fcr.2010.10.001>.
- Mahieu, S., Fustec, J., Jensen, E.S., Crozat, Y., 2009. Does labelling frequency affect N rhizodeposition assessment using the cotton-wick method? *Soil Biology and Biochemistry* 41, 2236–2243. <https://doi.org/10.1016/j.soilbio.2009.08.008>.
- Myrold, D.D., 2021. Transformations of nitrogen. In: Gentry, T.J., Fuhrmann, J.J., Zuberer, D.A. (Eds.), *Principles and Applications of Soil Microbiology*, Elsevier, Massachusetts, pp. 385-421. <https://doi.org/10.1016/B978-0-12-820202-9.00015-0>.
- Ostrom, N.E., Sutka, R., Ostrom, P.H., et al., 2010. Isotopologue data reveal bacterial denitrification as the primary source of N<sub>2</sub>O during a high flux event following cultivation of a native temperate grassland. *Soil Biology and Biochemistry* 42, 499-506. <https://doi.org/10.1016/j.soilbio.2009.12.003>.
- Pang, R., Xu, X., Tian, Y., et al., 2021. *In-situ* <sup>13</sup>CO<sub>2</sub> labeling to trace carbon fluxes in plant-soil-microorganism systems: Review and methodological guideline. *Rhizosphere* 20, 100441. <https://doi.org/10.1016/j.rhisph.2021.100441>.

- Pausch, J., Kuzyakov, Y., 2018. Carbon input by roots into the soil: Quantification of rhizodeposition from root to ecosystem scale. *Global Change Biology* 24, 1-12.  
<https://doi.org/10.1111/gcb.13850>.
- Philippot, L., Raaijmakers, J.M., Lemanceau, P., van der Putten, W.H., 2013. Going back to the roots: the microbial ecology of the rhizosphere. *Nature Reviews Microbiology* 11, 789-799. <https://doi.org/10.1038/nrmicro3109>.
- Rasmussen, J., Dresbøll, D.B., Enggrob, K.L., Peixoto, L., 2021. A novel <sup>15</sup>N vertical split-root method for *in situ* estimation of N rhizodeposition. *Geoderma* 383: 114782.  
<https://doi.org/10.1016/j.geoderma.2020.114782>.
- RStudio Team, 2020. RStudio: Integrated Development for R. RStudio, PBC, Boston, MA URL  
<http://www.rstudio.com/>.
- Sasse, J., Martinoia, E., Northen, T., 2018. Feed your friends: Do plant exudates shape the root microbiome? *Trends in Plant Science* 23, 25–41.  
<https://doi.org/10.1016/j.tplants.2017.09.003>.
- Schenck zu Schweinsberg-Mickan, M., Joergensen, R.G., Müller, T., 2010. Fate of <sup>13</sup>C and <sup>15</sup>N-labelled rhizodeposition of *Lolium perenne* as function of the distance to the root surface. *Soil Biology and Biochemistry* 42, 910–918.  
<https://doi.org/10.1016/j.soilbio.2010.02.007>.

Schenck zu Schweinsberg-Mickan, M., Jörgensen, R.G., Müller, T., 2012. Rhizodeposition: Its

contribution to microbial growth and carbon and nitrogen turnover within the rhizosphere. *Journal of Plant Nutrition and Soil Science* 175, 750–760.

<https://doi.org/10.1002/jpln.201100300>.

Sigurdarson, J.J., Svane, S., Karring, H., 2018. The molecular processes of urea hydrolysis in

relation to ammonia emissions from agriculture. *Reviews in Environmental Science and Bio/Technology* 17, 241-258. <https://doi.org/10.1007/s11157-018-9466-1>.

Smart, D.R., Bloom, A.J., 2001. Wheat leaves emit nitrous oxide during nitrate assimilation.

*Proceedings of the National Academy of Sciences* 98, 7875–7878.

<https://doi.org/10.1073/pnas.13157279>.

Tian, H., Xu, R., Canadell, J.G., et al., 2020. A comprehensive quantification of global nitrous

oxide sources and sinks. *Nature* 586, 248-256. <https://doi.org/10.1038/s41586-020-2780-0>.

Toyoda, S., Mutoke, H., Yamagishi, H., et al., 2005. Fractionation of N<sub>2</sub>O isotopomers during

production by denitrifier. *Soil Biology and Biochemistry* 37,1535-1545.

<https://doi.org/10.1016/j.soilbio.2005.01.009>.

Toyoda, S, Yoshida, N., 1999. Determination of nitrogen isotopomers of nitrous

oxide on a modified isotope ratio mass spectrometer. *Analytical Chemistry* 71, 4711-

4718. <https://doi.org/10.1021/ac9904563>.

Toyoda, S, Yoshida, N., Koba, K., 2017. Isotopocule analysis of biologically produced nitrous oxide in various environments. *Mass Spectrometry Reviews* 36, 135-160.

<https://doi.org/10.1002/mas.21459>.

Voroney, R.P., Brookes, P.C., Beyaert, R.P., 2008. Soil microbial biomass C, N, P, and S. In: Carter, M.R., Gregorich, E.G. (Eds.), *Soil Sampling and Methods of Analysis*, 2nd edn. CRC Press, Florida, pp. 637–651.

Wang, Y., Calanca, P., Leifeld, J., 2024. Sources of nitrous oxide emissions from agriculturally managed peatlands. *Global Change Biology* 30: e17144.

<https://doi.org/10.1111/gcb.17144>.

Wichern, F., Eberhardt, E., Mayer, J., Joergensen, R.G., Müller, T., 2008. Nitrogen rhizodeposition in agricultural crops: Methods, estimates and future prospects. *Soil Biology and Biochemistry* 40, 30–48. <https://doi.org/10.1016/j.soilbio.2007.08.010>.

Wrage-Mönnig, N., Horn, M.A., Well, R., et al., 2018. The role of nitrifier denitrification in the production of nitrous oxide revisited. *Soil Biology and Biochemistry* 123, A3–A16.

<https://doi.org/10.1016/j.soilbio.2018.03.020>.

Wu, D., Well, R., Cárdenas, L.M., et al., 2019. Quantifying N<sub>2</sub>O reduction to N<sub>2</sub> during denitrification in soils via isotopic mapping approach: Model evaluation and uncertainty analysis. *Environmental Research* 179:108806.

<https://doi.org/10.1016/j.envres.2019.108806>.

- Xie, S., Jiang, L., Wu, Q., et al., 2022. Maize root exudates recruit *Bacillus amyloliquefaciens* OR2-30 to inhibit *Fusarium graminearum* infection. *Phytopathology* 112, 1886–1893.  
<https://doi.org/10.1094/PHYTO-01-22-0028-R>.
- Yeung, L.Y., Li, S., Kohl, I.E., 2017. Extreme enrichment in atmospheric  $^{15}\text{N}^{15}\text{N}$ . *Science Advances* 3: eaao6741. <https://doi.org/10.1126/sciadv.aao6741>.
- Yoshida, N., Toyoda, S., 2000. Constraining the atmospheric  $\text{N}_2\text{O}$  budget from intramolecular site preference in  $\text{N}_2\text{O}$  isotopomers. *Nature* 405, 330-334.  
<https://doi.org/10.1038/35012558>.
- Yu, K., Chen, G., 2009. Nitrous oxide emissions from terrestrial plants: Observations, mechanisms and implications. In: Sheldon, A.I., Barnbart, E.P. (Eds.), *Nitrous Oxide Emissions Research*. Nova Science, Hauppauge, New York, pp. 85-104.
- Zaman, M., Kleineidam, K., Bakken, L., et al., 2021. Isotopic techniques to measure  $\text{N}_2\text{O}$ ,  $\text{N}_2$  and their sources. In: Zaman, M., Heng, L., Müller, C. (Eds.), *Measuring Emission of Agricultural Greenhouse Gases and Developing Mitigation Options using Nuclear and Related Techniques*. Springer, Cham., pp. 213-301. [https://doi.org/10.1007/978-3-030-55396-8\\_7](https://doi.org/10.1007/978-3-030-55396-8_7).
- Zhang, T., Zhao, Y.-L., Zhao, J.-H., et al., 2016. Cotton plants export microRNAs to inhibit virulence gene expression in a fungal pathogen. *Nature Plants* 2, 16153.  
<https://doi.org/10.1038/NPLANTS.2016.153>.

- Zhu, X., Burger, M., Doane, T.A., et al., 2013. Ammonia oxidation pathways and nitrifier denitrification are significant sources of N<sub>2</sub>O and NO under low oxygen availability. *Proceedings of the National Academy of Sciences of the United States of America* 110, 6328–6333. <https://doi.org/10.1073/pnas.1219993110>.
- Zou, Y., Hirono, Y., Yanai, Y., et al., 2014. Isotopomer analysis of nitrous oxide accumulated in soil cultivated with tea (*Camellia sinensis*) in Shizuoka, central Japan. *Soil Biology and Biochemistry* 77, 276-291. <https://doi.org/10.1016/j.soilbio.2014.06.016>.

#### 4.8 Appendix: Supplementary materials

**Table 4.S1** The physical and chemical properties of the soil used in this experiment. Values are presented as mean  $\pm$  standard error.

Soil Properties	Value
Bulk Density ( $\text{g cm}^{-3}$ ) <sup>a</sup>	$0.43 \pm 0.02$
Organic Matter ( $\text{Mg ha}^{-1}$ ) <sup>b</sup>	$175 \pm 1$
Cation Exchange Capacity ( $\text{cmol kg}^{-1}$ ) <sup>c</sup>	$49.6 \pm 6.9$
pH <sup>d</sup>	$7.1 \pm 0.4$
Total Nitrogen ( $\text{kg ha}^{-1}$ ) <sup>e</sup>	$14900 \pm 3700$
Phosphorus ( $\text{kg ha}^{-1}$ ) <sup>f</sup>	$66 \pm 6$
Potassium ( $\text{kg ha}^{-1}$ ) <sup>f</sup>	$343 \pm 65$
Magnesium ( $\text{kg ha}^{-1}$ ) <sup>f</sup>	$2690 \pm 420$
Calcium ( $\text{kg ha}^{-1}$ ) <sup>f</sup>	$17300 \pm 2300$
Aluminum ( $\text{kg ha}^{-1}$ ) <sup>f</sup>	$33.5 \pm 6.9$
Sodium ( $\text{kg ha}^{-1}$ ) <sup>f</sup>	$64.9 \pm 11.6$

<sup>a</sup> assessed by determining the mass and original volume ( $n = 4$ ) of a soil core (radius: 3 cm, height: 4 cm) after drying ( $70\text{ }^{\circ}\text{C}$  for 48 h)

<sup>b</sup> assessed with loss on ignition ( $360\text{ }^{\circ}\text{C}$ ;  $n = 2$ )

<sup>c</sup> estimated from ions measured through inductively coupled plasma – optical emission spectrometry ( $n = 2$ )

<sup>d</sup> assessed in soil and deionized water slurries (1:1;  $n = 2$ )

<sup>e</sup> assessed with a Flash EA 1112 Series CN soil analyzer (Thermo Fisher Scientific, Waltham, Massachusetts, USA;  $n = 6$ ) using tin-encapsulated soil that was ground and dried ( $55\text{ }^{\circ}\text{C}$  for 72 h)

<sup>f</sup> assessed using inductively coupled plasma – optical emission spectrometry ( $n = 2$ )

**Table 4.S2** Range and mean of total and substrate-derived daily N<sub>2</sub>O emissions in terms of soil mass from the rhizosphere of annual ryegrass (*L. multiflorum*) plants measured 24 h and 48 h after introducing <sup>15</sup>N-root exudates or <sup>15</sup>N-urea fertilizer into the rhizosphere. The mean values for the substrate-derived N<sub>2</sub>O emissions are the pooled results for both time-points ( $n = 7$  for <sup>15</sup>N-root exudates due to a negative value;  $n = 5$  for <sup>15</sup>N-urea due to negative values).

<b>Substrate</b>		<b>Total N<sub>2</sub>O Emissions (<math>\mu\text{g N}_2\text{O-N kg soil}^{-1} \text{ d}^{-1}</math>)</b>	<b>Substrate-Derived N<sub>2</sub>O Emissions (<math>\mu\text{g N}_2\text{O-}^{15}\text{N kg soil}^{-1} \text{ d}^{-1}</math>)</b>
Root Exudates	Range	2.96–18.5	0.0934–4.55
	Mean	$8.44 \pm 2.20$	$1.73 \pm 0.74$
Urea	Range	0.809–3.97	0.0671–0.222
	Mean	$2.68 \pm 0.54$	$0.116 \pm 0.027$

**Table 4.S3** The total and substrate-derived N in terms of soil mass in the soil and microbial biomass pools of the rhizosphere of annual ryegrass (*L. multiflorum*) plants measured 3, 9, 24 and 48 h after introducing  $^{15}\text{N}$ -root exudates or  $^{15}\text{N}$ -urea fertilizer into the rhizosphere. Each value is the mean  $\pm$  standard error ( $n = 4$ , while those with an asterisk (\*) were  $n = 3$  due to negative values).

Substrate	Time since $^{15}\text{N}$ -Substrate Introduction	Rhizosphere Soil		Microbial Biomass of Rhizobiome	
		Total N (g N kg soil $^{-1}$ )	Substrate-Derived N (g $^{15}\text{N}$ kg soil $^{-1}$ )	Total N (mg N kg soil $^{-1}$ )	Substrate-Derived N (mg $^{15}\text{N}$ kg soil $^{-1}$ )
Root Exudates	3	14.1 $\pm$ 0.0 *	0.486 $\pm$ 0.220 *	62.7 $\pm$ 7.4 *	0
	9	12.3 $\pm$ 1.0	0.243 $\pm$ 0.089 *	107 $\pm$ 14	0
	24	13.7 $\pm$ 0.7	0.330 $\pm$ 0.098	87.3 $\pm$ 31.9	0
	48	14.3 $\pm$ 0.3	0.193 $\pm$ 0.056 *	170 $\pm$ 57	159 $\pm$ 57 *
Urea	3	10.9 $\pm$ 1.7 *	0.0719 $\pm$ 0.0217 *	119 $\pm$ 0 *	49.8 $\pm$ 4.1 *
	9	14.2 $\pm$ 0.1 *	0.158 $\pm$ 0.015 *	96.0 $\pm$ 66.1 *	0
	24	13.9 $\pm$ 0.1	0.191 $\pm$ 0.014	148 $\pm$ 58	0
	48	12.9 $\pm$ 0.7	0.107 $\pm$ 0.007	127 $\pm$ 20	51.2 $\pm$ 5.1

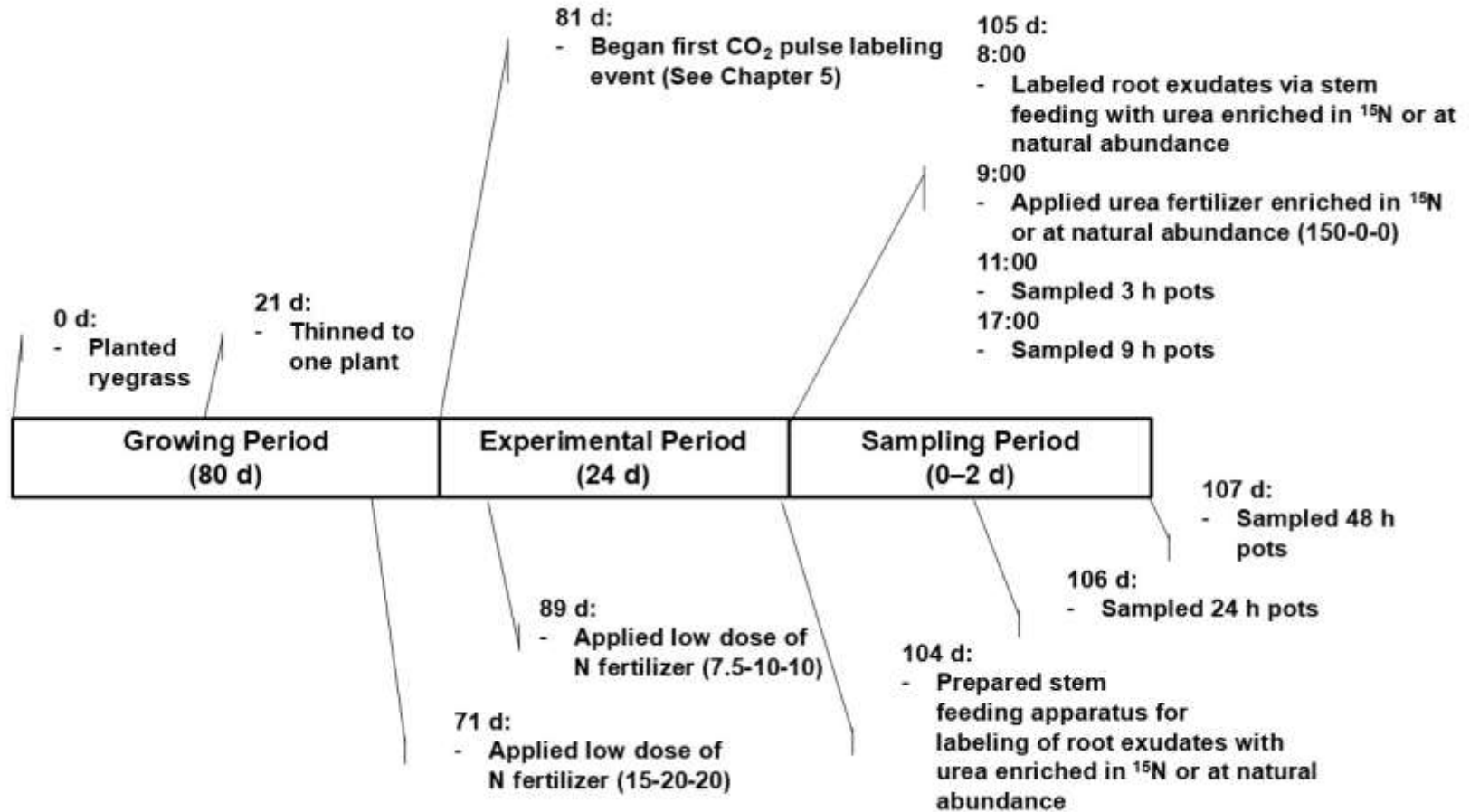


**Figure 4.S1** Timeline of experiment, which included a growing (80 d), experimental (24 d) and sampling period (0–2 d).

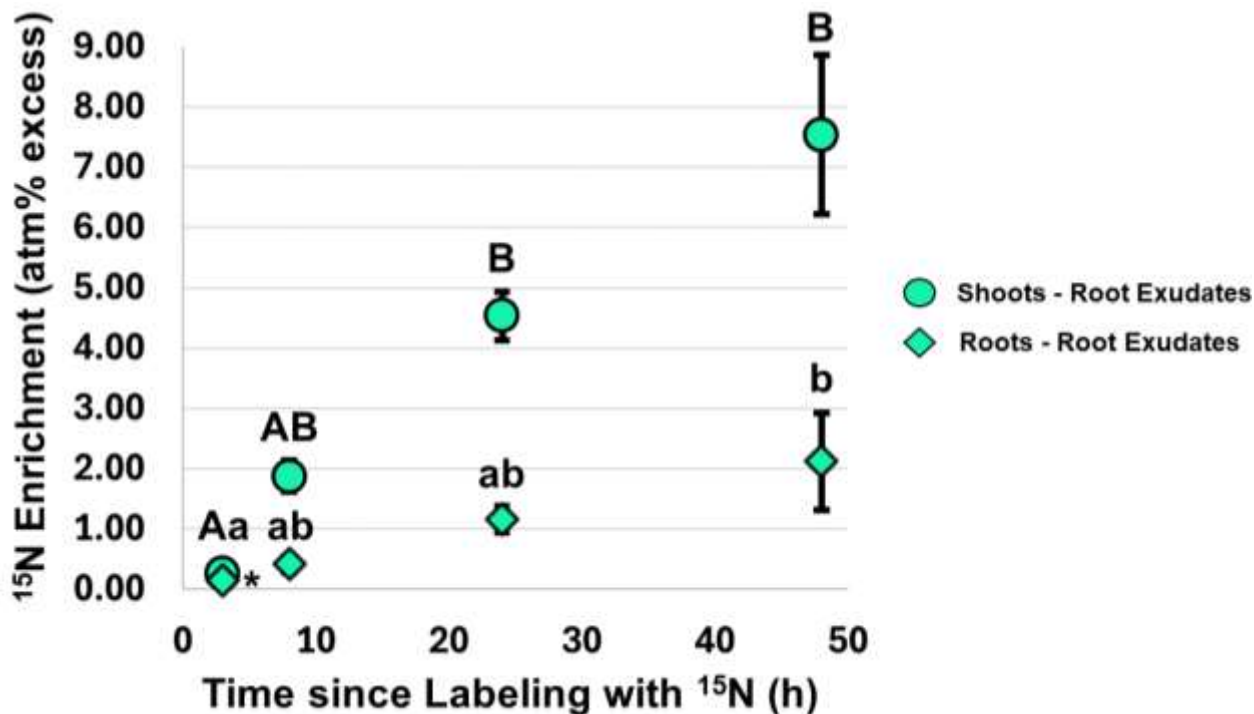


**Figure 4.S2** The <sup>15</sup>N enrichment (atm% excess) of the shoots and roots from annual ryegrass (*L. multiflorum*) plants measured 3, 9, 24 and 48 h after stem feeding. Markers indicate the mean <sup>15</sup>N enrichment value in a respective pool at a specific time-point, with error bars representing the standard error of the mean. All mean values had a sample size of  $n = 4$  except for the <sup>15</sup>N enrichment of the roots measured 3 h after stem feeding due to a negative value (marked with an asterisk (\*) to signify  $n = 3$ ). Different upper- and lowercase letters indicate a significant difference ( $p < 0.05$ ) in the <sup>15</sup>N enrichment between time-points for ryegrass shoots and roots, respectively. All differences were assessed for significance according to nonparametric Kruskal-Wallis tests followed by pairwise comparisons of the mean ranks using Dunn's post hoc test with the Bonferroni correction.

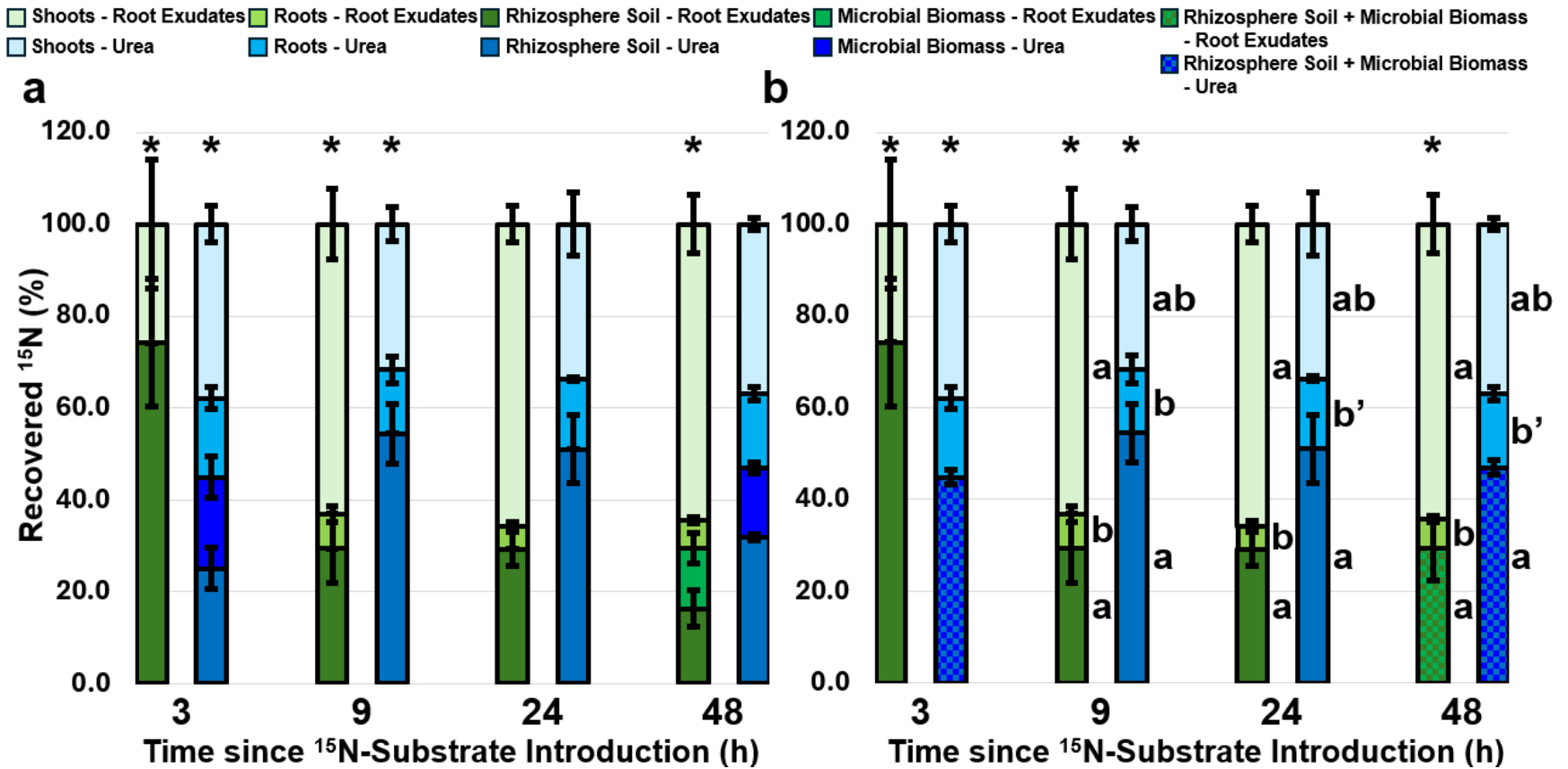


**Figure 4.S3** The partitioning of the recovered <sup>15</sup>N (%) among the plant biomass and rhizosphere pools of ryegrass (*L. multiflorum*) plants measured 3, 9, 24 and 48 h after introducing <sup>15</sup>N-root exudates or <sup>15</sup>N-urea fertilizer into the rhizosphere: a) the separate pools of shoots, roots, rhizosphere soil, and microbial biomass; and b) the separate pools of shoots, roots, and rhizosphere soil, as well as the combined pools of rhizosphere soil and microbial biomass, if observed. Each bar in the stacked bar represents the mean value of <sup>15</sup>N recovered in a specific pool for a respective <sup>15</sup>N-substrate at a specific time-point. Error bars indicate the standard error of the mean values. All mean <sup>15</sup>N values had a sample size of *n* = 4 except for those stacked bars with an asterisk (\*), denoting *n* = 3 due to negative values. Note for the <sup>15</sup>N-root exudate treatment that most of the <sup>15</sup>N in the plant biomass is likely an experimental artefact,

representing the  $^{15}\text{N}$  taken up by the plant from the stem feeding method. In Figure 4.S3b, different lowercase letters on the right of a bar indicate a significant difference in the recovered  $^{15}\text{N}$  between the different pools for a respective  $^{15}\text{N}$ -substrate at a specific time-point. The presence of an apostrophe (') on the right of a bar indicates a significant difference in the recovered  $^{15}\text{N}$  between  $^{15}\text{N}$ -substrates for a respective pool at a specific time-point. All differences were assessed for significance ( $p < 0.05$ ) using generalized linear model analysis followed by pairwise comparisons of the estimated marginal means with Tukey post hoc analysis.

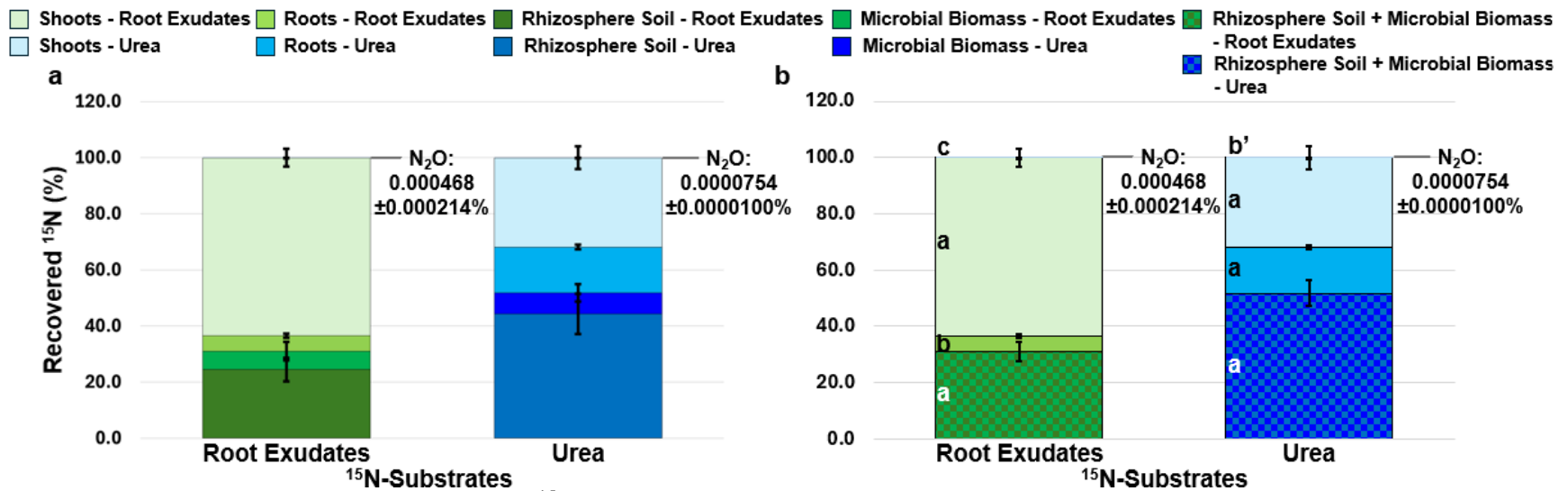


**Figure 4.S4** The partitioning of the recovered  $^{15}\text{N}$  (%) among the plant biomass and rhizosphere pools of ryegrass (*L. multiflorum*) plants measured 24 h and 48 h after introducing  $^{15}\text{N}$ -root exudates or  $^{15}\text{N}$ -urea fertilizer into the rhizosphere: a) the separate pools of daily  $\text{N}_2\text{O}$  emissions, shoots, roots, rhizosphere soil and microbial biomass; and b) the separate pools of daily  $\text{N}_2\text{O}$  emissions, shoots, and roots, as well as the combined pools of rhizosphere soil and microbial biomass. Each bar in the stacked bar represents the mean value of  $^{15}\text{N}$  recovered in a specific pool for a respective  $^{15}\text{N}$ -substrate treatment pooled together for both time-points. Error bars indicate the standard error of the mean values. The stacked bar for the  $^{15}\text{N}$ -root exudate treatment had a sample size of  $n = 6$ , while  $^{15}\text{N}$ -urea fertilizer had a sample size of  $n = 5$  due to negative values. Note for the  $^{15}\text{N}$ -root exudate treatment that most of the  $^{15}\text{N}$  in the plant biomass is likely an experimental artefact, representing the  $^{15}\text{N}$  taken up by the plant from the stem feeding method. In Figure 4.S4b, different lowercase letters indicate a significant difference in the recovered  $^{15}\text{N}$  between the different pools for a respective  $^{15}\text{N}$ -substrate treatment. The presence of an apostrophe (') indicates a significant difference in the recovered  $^{15}\text{N}$  between  $^{15}\text{N}$ -substrate treatments for a respective pool. All differences were assessed for significance ( $p < 0.05$ ) using generalized linear model analysis followed by pairwise comparisons of the estimated marginal means with Tukey post hoc analysis.

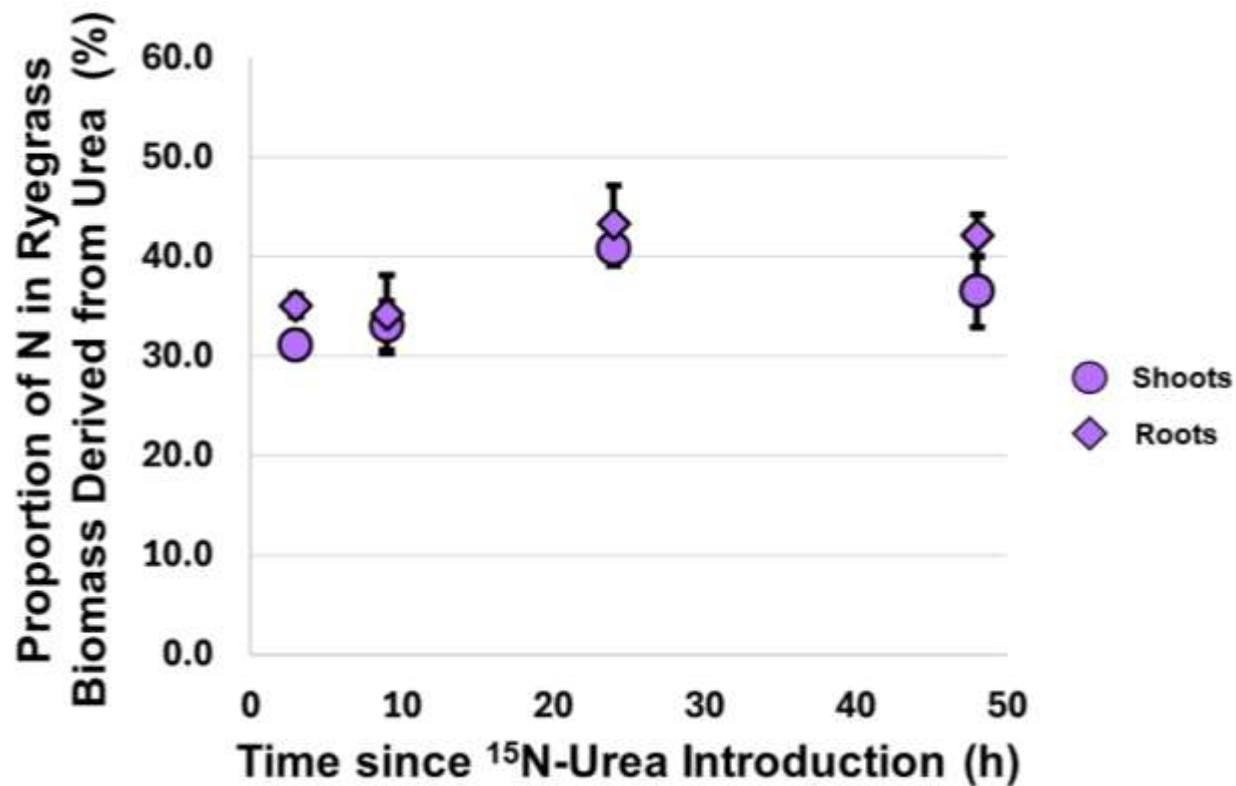


**Figure 4.S5** The proportion of N (%) derived from urea in the shoots and roots of annual ryegrass (*L. multiflorum*) plants measured 3, 9, 24 and 48 h after introducing <sup>15</sup>N-urea fertilizer into the rhizosphere. Markers indicate the mean urea-derived N value in a respective pool at a specific time-point, with error bars representing the standard error of the mean ( $n = 4$ ).

## FORWARD TO CHAPTER 5

In Chapter 4, I demonstrated that root exudates make a direct contribution to the N<sub>2</sub>O emitted from the rhizosphere and that these emissions are most likely produced by bacterial denitrification, nitrifier-denitrification, or a combination of the two dissimilatory pathways. However, N<sub>2</sub>O is only one of the greenhouse gases produced from cultivated peatlands. In fact, CO<sub>2</sub> represents the bulk of total greenhouse gas emissions observed from these soils. The cultivated rhizosphere may also play a substantial role in these emissions as it is inundated with assimilable C substrates from rhizodeposition (e.g., root exudates, mucilage, litter). The C dynamics of rhizodeposition are especially of interest in a cultivated peatland because the rhizosphere is surrounded by C-rich peat organic matter. Therefore, in Chapter 5, I conducted a CO<sub>2</sub> partitioning study to assess the contributions of rhizodeposits, peat and urea – a commonly applied fertilizer – to the CO<sub>2</sub> produced from the rhizosphere of a cultivated peat soil.

The following manuscript will be submitted for publication:

**De Sena A**, Madramootoo CA, Whalen JK (2023). Peat is a negligible source of carbon dioxide from the rhizosphere of a cultivated peat soil.

## CHAPTER 5

### **5. Peat is a negligible source of carbon dioxide from the rhizosphere of a nitrogen-fertilized peat soil**

Aidan De Sena, Chandra A. Madramootoo, Joann K. Whalen

#### **5.1 Abstract**

Cultivated peatlands release considerable amounts of carbon dioxide (CO<sub>2</sub>) into the atmosphere. Though these emissions are often attributed to peat degradation, peat is a highly oxidized substrate with a slow decomposition rate. Furthermore, CO<sub>2</sub> emissions from cultivated peatlands are spatially heterogeneous, suggesting that CO<sub>2</sub> production is concentrated at sites with a high availability of assimilable substrates for microbial respiration, like the rhizosphere. This microenvironment at the nexus of the crop root and soil is rich in available C compounds from rhizodeposition and N from fertilization, which should promote the metabolic activity of the rhizosphere microbiome, or rhizobiome. Our objective was to assess the role of the cultivated peatland rhizosphere as a CO<sub>2</sub> source by determining the contribution of the plant and peat to CO<sub>2</sub> production in this microenvironment. To achieve this objective, we conducted a <sup>13</sup>C-tracing experiment with annual ryegrass (*Lolium multiflorum*) plants grown in a greenhouse on soil from a cultivated peatland. The rhizosphere of ryegrass plants was exposed to either (i) <sup>13</sup>C-rhizodeposits via <sup>13</sup>C-CO<sub>2</sub> pulse labeling or (ii) <sup>13</sup>C-urea via fertilization, as a comparison. We measured CO<sub>2</sub> fluxes and their <sup>13</sup>C enrichment from the plant-rhizosphere soil systems 21 h and 45 h after the start of the final <sup>13</sup>C-labeling period. Additionally, we determined the <sup>13</sup>C enrichment of the rhizosphere pools (soil and microbial biomass) at a finer timescale to observe the C dynamics of these substrates (0, 6, 21 and 45 h after the start of the final <sup>13</sup>C-labeling period). Rhizodeposits were the largest source of CO<sub>2</sub> from the rhizosphere soil, producing 14.0

$\pm 1.2\%$  of the measured CO<sub>2</sub> emissions, followed by urea ( $10.0 \pm 1.9\%$ ). Emissions derived from the decomposition of peat were not detected, implying their negligible contributions to the CO<sub>2</sub> flux from the rhizosphere of cultivated peatlands under N-rich conditions. Consequently, the rhizosphere of cultivated peatlands is a source of CO<sub>2</sub> not through peat but as a consequence of the plant and its rhizodeposit-derived C under these circumstances.

## 5.2 Introduction

Upon cultivation, peatlands become a substantial source of carbon dioxide (CO<sub>2</sub>). Despite only occupying approximately 1% of cropland area (Leifeld and Menichetti 2018, FAO 2020), cultivated peatlands contribute 32% of total cropland-derived greenhouse gases, of which 89% is CO<sub>2</sub> (Carlson et al. 2017). Their disproportionate contribution to the agricultural greenhouse gas budget is of note, especially when considering the projected climate change-induced expansion of agriculture into global northern regions (500 km by 2100; Unc et al. 2021), where ~46% of northern peatlands are currently underlain with permafrost (Müller and Joos 2021).

Boreal and temperate cultivated peatlands emit between 350 and 3000 g CO<sub>2</sub>-C m<sup>-2</sup> y<sup>-1</sup> (Maljanen et al. 2010, Petersen et al. 2012, Norberg et al. 2016, Lloyd et al. 2019). These CO<sub>2</sub> emissions are largely produced from microbial metabolic processes that oxidize organic compounds to generate energy. There is no shortage of organic carbon (C) in cultivated peatlands, which is  $\geq 11.6\%$  of the soil due to their elevated peat content (USDA 2014). Indeed, peat is assumed to be the primary origin of the CO<sub>2</sub> emissions from these soils due to its exposure to oxygen upon drainage, permitting aerobic respiration (Carlson et al. 2017, Freeman et al. 2022). However, while such dynamics are probable for recently drained peatlands, many of the peatlands under current cultivation have been drained for decades or even centuries (Glenn et al. 1993, Lahtinen et al. 2022). As a result, the remaining peat is present in highly recalcitrant,

oxidized forms that are difficult for microbes to metabolize (Leifeld et al. 2012, Bader et al. 2017). Additionally, at the field-scale, CO<sub>2</sub> emission patterns from cultivated peatlands express high spatial heterogeneity (Lloyd et al. 2019), known as hotspots, which cannot be explained by peat degradation alone because (i) peat organic matter has a comparatively uniform distribution under conventional tillage, and (ii) organic matter degradation in peatlands occurs at a relatively constant rate ( $\sim 8 \text{ t C ha}^{-1} \text{ y}^{-1}$ ; Leifeld et al. 2020). Therefore, these hotspots of intense microbial CO<sub>2</sub> production are likely concentrated in a spatially heterogeneous environment with a high availability of assimilable organic substrates, like the rhizosphere.

The rhizosphere of crops is an environment of high organic substrate availability. At this interface between the root system and soil, there is the near-continual release of rhizodeposits from crop roots, a group of organic substances that contains compounds easily metabolized by the microbial community of the rhizosphere, or rhizobiome, such as root exudates (Pausch et al. 2013, De Sena et al. 2023). Rhizodeposition ensures a surplus of assimilable substrates for the rhizobiome and fuels microbial activity in the rhizosphere, which is 10–100 times greater than that occurring in bulk soil (Kuzyakov and Blagodatskaya 2015). This effect is due to the greater energy availability of root exudates, like carboxylic acids and sugars (nominal oxidation state of  $\text{C} > 0$ ; Wang and Kuzyakov 2023). As such, the rhizosphere of cultivated peatlands fosters an environment of high substrate availability due to rhizodeposition, which should promote microbial CO<sub>2</sub> production.

In general, rhizodeposits are established sources of greenhouse gases. Rhizodeposits from grasses and crops are estimated to produce 44–66 g CO<sub>2</sub>-C m<sup>-2</sup> y<sup>-1</sup> (Pausch and Kuzyakov 2018). However, the contribution of rhizodeposition to CO<sub>2</sub> emissions has not been investigated in the rhizosphere of cultivated peatlands, whose inherent elevated organic matter and surplus of

available N from fertilization could trigger different microbial responses that alter their metabolism of rhizodeposits. For example, the low mineral content and reactivity of cultivated peatlands may fix a lower amount of rhizodeposits to the soil matrix (Liang et al. 2023), thus promoting their availability to the rhizobiome. Likewise, the application of N fertilizers could eliminate any N limitation for the rhizobiome, thus permitting their use of a preferred energy source like simple rhizodeposits, as opposed to mining recalcitrant organic matter in peat for both C and N (Cui et al. 2023). Consequently, understanding CO<sub>2</sub> production from cultivated peatlands requires parsing out the CO<sub>2</sub> contributions from rhizodeposition in the rhizosphere under N-fertilized conditions.

Furthermore, there are additional CO<sub>2</sub> precursors in the rhizosphere of cultivated peatlands other than peat and rhizodeposits, like agricultural amendments. These amendments include urea, an organic compound and the most commonly applied nitrogenous fertilizer worldwide (52 Tg N y<sup>-1</sup>; IFA 2023). As a fertilizer, urea is applied near the rhizosphere to facilitate its mass flow and diffusion to the root. However, its hydrolysis into ammonium by urease enzymes in the rhizosphere generates CO<sub>2</sub> (Sigurdarson et al. 2018). Urea-derived CO<sub>2</sub> is purported to be as much as 86.0 ± 39.1 Mt CO<sub>2</sub> globally (Menegat et al. 2022), but this estimate is based on an emission factor derived from a stoichiometric calculation (IPCC et al. 2006). While coarse approximations are valuable for global models, they neglect soil dynamics at the field-scale, like CO<sub>2</sub> consumption by microbial autotrophs. For example, one study observed that urea-derived CO<sub>2</sub> emissions were 25–32% of that estimated by the IPCC emission factor (Kim et al. 2017). Thus, by recognizing the potential of various CO<sub>2</sub> sources, we can more accurately characterize CO<sub>2</sub> emissions from cultivated peatlands.

The objective of our study was to determine the capacity of the rhizosphere to function as a hotspot of CO<sub>2</sub> emissions in temperate cultivated peatlands. As such, we conducted a <sup>13</sup>C-tracing greenhouse experiment with annual ryegrass (*Lolium multiflorum*) plants grown in soil from a temperate cultivated peatland to trace the fate of C derived from rhizodeposits and urea in and from the rhizosphere. We hypothesized that rhizodeposition would be a greater source of CO<sub>2</sub> from the cultivated rhizosphere than peat and urea because of its near constant release of assimilable C substrates for the rhizobiome, as well as the surplus of fertilizer N in this environment that would remove any microbial N limitation, permitting their preferred use of simple organic compounds like rhizodeposits.

### 5.3 Materials and methods

#### 5.3.1 *Experimental materials and design*

This <sup>13</sup>C-tracing study was conducted during the same greenhouse experiment discussed in Chapter 4, and thus had the same experimental materials and design except for modifications related to <sup>13</sup>C analysis (See Section 4.3.1 *Experimental materials* and Section 4.3.2 *Experimental design*). We describe the soil physico-chemical properties of the peat soil in Table 4.S1. Annual ryegrass (*Lolium multiflorum* L.) was used in this experiment because not only is it a grass species with an extensive rhizosphere due to its fibrous roots, but also since this grass is planted as a cover crop on cultivated peatlands (Honkanen et al. 2024).

Briefly, the pots for the greenhouse experiment were prepared by adding air-dried peat soil (165 g oven-dry basis at 0.43 g cm<sup>-3</sup>) to a plastic pot (810 cm<sup>3</sup>) lined with plastic wrap and planting three ryegrass seeds 2 cm deep into the soil. Pots were then designated at random to one of our <sup>13</sup>C-substrate treatments – <sup>13</sup>C-rhizodeposits or <sup>13</sup>C-urea – or as natural abundance controls. Both of the <sup>13</sup>C-substrates also contained <sup>15</sup>N (i.e., <sup>15</sup>N-root exudates, <sup>15</sup>N-urea), which

we traced the fate of in the previous chapter (See Chapter 4). Additionally, we had bare soil controls where no ryegrass was grown to account for  $^{13}\text{C}$ - $\text{CO}_2$  back diffusion during  $^{13}\text{C}$ - $\text{CO}_2$  pulse labeling (Riederer et al. 2015). As pots were destructively sampled during one of four sampling time-points (0, 6, 21 and 45 h after adding  $^{13}\text{C}$ -urea to pots and the start of the final  $^{13}\text{C}$ - $\text{CO}_2$  pulse labeling event) and each factorial treatment combination (substrate or control  $\times$  sampling time combination) was replicated four times, there was a total of 64 experimental units. Due to there being only one  $\text{CO}_2$  labeling chamber, we staggered the start of the experiment by one day for the pots undergoing pulse labeling with  $^{13}\text{C}$ - $\text{CO}_2$  ( $^{13}\text{C}$ -rhizodeposit and bare soil control pots;  $n = 32$ ) or  $\text{CO}_2$  at natural abundance ( $^{13}\text{C}$ -urea and natural abundance control pots;  $n = 32$ ). All pots were arranged in a randomized complete block design on a greenhouse bench (average daily temperature of 27 °C and daylength of 15 h).

During the growing period (80 d; Figure 5.S1), all pots were watered to 70% water-filled pore space with distilled water by mass every other morning prior to the experimental period. At 21 d after planting, we thinned the ryegrass to one plant per pot. During this period, we added 3 mL of a low dose fertilizer solution before watering 71 d after planting due to visible signs of plant nutrient deficiency. The fertilizer solution was composed of 0.286 mol N L<sup>-1</sup> from urea, 0.0908 mol P L<sup>-1</sup> from triple superphosphate and 0.118 mol K L<sup>-1</sup> from KCl, which was equivalent to an application rate of 15-20-20 kg ha<sup>-1</sup> of N-P<sub>2</sub>O<sub>5</sub>-K<sub>2</sub>O.

### **5.3.2 Introduction of $^{13}\text{C}$ -substrates**

After 80 d from planting, we began the experimental period (24 d) by  $^{13}\text{C}$ - $\text{CO}_2$  pulse labeling pots designated for the  $^{13}\text{C}$ -rhizodeposit treatment. Those pots not designated for the  $^{13}\text{C}$ -rhizodeposit treatment (i.e.,  $^{13}\text{C}$ -urea and natural abundance control pots) were still subjected to  $\text{CO}_2$  pulse labeling in the same manner but with  $\text{CO}_2$  at natural abundance. During this period, all

pots were watered to 70% water-filled pore space at 9:00am daily. Plants also received 1.5 mL of fertilizer solution before watering 89 d after planting, made up of 0.286 mol N L<sup>-1</sup> from urea, 0.0908 mol P L<sup>-1</sup> from triple superphosphate and 0.118 mol K L<sup>-1</sup> from KCl. This fertilizer dose was due to visible signs of plant nutrient deficiency and was equivalent to an application rate of 7.5-10-10 kg ha<sup>-1</sup> of N-P<sub>2</sub>O<sub>5</sub>-K<sub>2</sub>O.

To ensure sufficient enrichment, CO<sub>2</sub> pulse labeling occurred every other day until 105 d after sowing (13 labeling events except for the 0 h pots, which had 12 labeling events). During each labeling event, pots were placed in a hermetically-sealed chamber (0.906 m<sup>3</sup>; average temperature: 31 °C; average humidity: 70%) located inside the greenhouse. The chamber was equipped with fans to circulate CO<sub>2</sub> and ice packs to lower the temperature within the chamber. CO<sub>2</sub> was generated in a Wheaton bottle containing 400 mL 1.8 mol H<sub>2</sub>SO<sub>4</sub> L<sup>-1</sup> and a magnetic stirbar, placed on a stir plate and connected to the isotope labeling chamber via spinal tap needles and Tygon tubing. We produced enough CO<sub>2</sub> to raise the concentration of the atmosphere by 200 ppmv every 0.5 h during each 5 h labeling event by injecting into the Wheaton bottle 4 mL of solution containing either 6.94 mmol of <sup>13</sup>C (≥99 atom%; Cambridge Isotope Laboratories, Andover, Massachusetts, USA) or C at natural abundance in the form of NaHCO<sub>3</sub> (44% of injections) or Na<sub>2</sub>CO<sub>3</sub> (56% of injections). Each injection was followed by a 60 mL injection of synthetic air (≤1 ppmv CO<sub>2</sub>; Linde plc., Dublin, Ireland) to propel the CO<sub>2</sub> into the labeling chamber.

The average CO<sub>2</sub> concentration and  $\delta^{13}\text{C}$  in the labeling chamber during pulse labeling with <sup>13</sup>C-CO<sub>2</sub> (618 ± 191 ppmv CO<sub>2</sub>, >18000 ‰  $\delta^{13}\text{C}$ ) and CO<sub>2</sub> at natural abundance (449 ± 104 ppmv CO<sub>2</sub>, 26.5 ± 16.2 ‰  $\delta^{13}\text{C}$ ) was estimated by taking gas samples during the first labeling event. Headspace gas samples (20 mL) were taken through the septum of the labeling chamber

with an air-tight syringe and stored in 12 mL Exetainers at the following times: after pots were placed in the chamber, after the first injection of CO<sub>2</sub>, before and after all subsequent CO<sub>2</sub> injections, and at the end of the labeling event. We analyzed each headspace gas sample as detailed below (See Section 5.3.4 *Gas analysis*).

Before the final CO<sub>2</sub> pulse labeling event at 105 d after sowing, we added 3 mL of fertilizer solution containing urea enriched with <sup>13</sup>C (99 atom% <sup>13</sup>C, Cambridge Isotope Laboratories, Andover, Massachusetts, USA) at 1.33 mol <sup>13</sup>C L<sup>-1</sup> to the pots designated for treatment with <sup>13</sup>C-urea. The fertilizer dose was equivalent to an application of 150-0-0 kg ha<sup>-1</sup> of N-P<sub>2</sub>O<sub>5</sub>-K<sub>2</sub>O. Those pots not designated for the <sup>13</sup>C-urea treatment (i.e., <sup>13</sup>C-rhizodeposits, bare soil control and natural abundance control pots) were still fertilized with urea but at natural abundance (1.43 mol C L<sup>-1</sup>).

### **5.3.3 *Gas, ryegrass biomass and soil sample collection***

We began the sampling period (2 d) 105 d after planting. Like the experimental period, all plants were watered to 70% water-filled pore space at 9:00am daily. Samples were collected at either 0, 6, 21 or 45 h after adding <sup>13</sup>C-urea to pots and beginning the final <sup>13</sup>C-CO<sub>2</sub> pulse labeling event. The sample collection procedure is described in detail in the previous chapter (See Section 4.3.4 *Gas, ryegrass biomass and soil sample collection*). For gas sample collection, the opaque chamber ensured that plant photosynthesis did not influence CO<sub>2</sub> flux measurements (Shazad et al. 2012).

### **5.3.4 *Gas analysis***

Gas samples were injected into a Bruker 520 Gas Chromatographer System (Bruker, Billerica, Massachusetts, USA) onto a channel equipped with a flame ionization detector set at 300 °C using helium as a carrier gas (flow rate: 30 mL min<sup>-1</sup>) for total CO<sub>2</sub> analysis. <sup>13</sup>C enrichment of

CO<sub>2</sub> was measured with the CO<sub>2</sub> Gas Isotope Analyzer (Model SSIM2-G2201-i, Picarro, Santa Clara, California, USA) at the University of Saskatchewan (Saskatoon, Saskatchewan, Canada). As measured <sup>13</sup>C-CO<sub>2</sub> from the <sup>13</sup>C-rhizodeposit treatment is derived from not only the rhizosphere but also the plant (i.e., shoot and root respiration), we refer to this treatment as <sup>13</sup>C-plant-assimilated C in this section. We assumed that any CO<sub>2</sub> emitted from the soil originated from the rhizosphere, as ryegrass roots were permitted to grow to full development in pots (810 cm<sup>3</sup>) for at least 104 d. We could only analyze gas samples collected at 21 h and 45 h after the start of the final <sup>13</sup>C-labeling period due to funding limitations.

To calculate the gravimetric of CO<sub>2</sub> concentration in headspace gas samples ( $C_g$  in mg CO<sub>2</sub>-C m<sup>-3</sup>), we used the following equation:

$$C_g = \frac{C_v M P}{RT} \quad (5.1)$$

where  $C_v$  is the volumetric concentration of CO<sub>2</sub> (L CO<sub>2</sub>-C m<sup>-3</sup>),  $M$  is the molar mass of CO<sub>2</sub> in terms of C (mg CO<sub>2</sub>-C mol<sup>-1</sup>),  $P$  is the atmospheric pressure in the greenhouse when the headspace gas sample was collected (atm),  $R$  is the ideal gas constant (0.08206 L atm mol<sup>-1</sup> K<sup>-1</sup>) and  $T$  is the temperature in the greenhouse when the headspace gas sample was collected (K).

The molar mass of CO<sub>2</sub> ( $M$ ) was calculated to account for the <sup>13</sup>C enrichment of the CO<sub>2</sub> by first determining the ratio of <sup>13</sup>C and <sup>12</sup>C in the sample ( $R_{sample}$ ):

$$R_{sample} = \left( \frac{\delta_{\text{‰}}^{13}\text{C}}{1000} + 1 \right) \times R_{VPDB} \quad (5.2)$$

where  $\delta_{\text{‰}}^{13}\text{C}$  is the <sup>13</sup>C isotopic signature (‰) and  $R_{VPDB}$  is the reference value for the ratio of <sup>13</sup>C and <sup>12</sup>C in Vienna PeeDee Belemnite (0.011117; Fleischer et al. 2021). This ratio was then converted to <sup>13</sup>C enrichment in terms of atom % ( $Atom\% \text{ }^{13}\text{C}$ ):

$$Atom\% \text{ }^{13}\text{C} = \left( \frac{R_{sample}}{(R_{sample} + 1)} \right) \times 100 \quad (5.3)$$

where  $R_{sample}$  is the ratio of  $^{13}\text{C}$  and  $^{12}\text{C}$  in the sample calculated in Equation 5.2. Once  $Atom\% \text{ }^{13}\text{C}$  was determined, we calculated the molar mass of  $\text{CO}_2$  in terms of C ( $M$ ;  $\text{mg CO}_2\text{-C mol}^{-1}$ ):

$$M = \left( \left( 1 - \frac{Atom\% \text{ }^{13}\text{C}}{100} \right) \times M_{^{12}\text{C}} \right) + \left( \frac{Atom\% \text{ }^{13}\text{C}}{100} \times M_{^{13}\text{C}} \right) \quad (5.4)$$

where  $Atom\% \text{ }^{13}\text{C}$  is the  $^{13}\text{C}$  enrichment of the headspace gas sample calculated with Equation 5.3 ( $atom\% \text{ }^{13}\text{C}$ ),  $M_{^{12}\text{C}}$  is the atomic mass of the  $^{12}\text{C}$ -isotope (12000 mDa; CIAAW 2015) and  $M_{^{13}\text{C}}$  is the atomic mass of the  $^{13}\text{C}$ -isotope (13003 mDa; CIAAW 2015).

We determined the gravimetric concentration of  $\text{CO}_2$  ( $C_{g-xt_i}$  in  $\text{mg CO}_2\text{-C m}^{-3}$ ) derived from the  $^{13}\text{C}$ -substrate of interest ( $x$ ; i.e.,  $^{13}\text{C}$ -plant-assimilated C,  $^{13}\text{C}$ -urea) at a specific time-point ( $t_i$  in min; i.e.,  $t_1 = 0$  min,  $t_2 = 20$  min,  $t_3 = 40$  min,  $t_4 = 60$  min) by using an isotope mixing model:

$$C_{g-xt_i} = C_{g-t_i} \times \frac{(Atom\% \text{ }^{13}\text{C}_{t_i} - Atom\% \text{ }^{13}\text{C}_{t_1})}{(Atom\% \text{ }^{13}\text{C}_x - Atom\% \text{ }^{13}\text{C}_{t_1})} \quad (5.5)$$

where  $C_{g-t_i}$  was the gravimetric concentration of  $\text{CO}_2$  ( $\text{mg CO}_2\text{-C m}^{-3}$ ) in the headspace gas sample at a specific time-point during the flux calculated with Equation 5.1,  $Atom\% \text{ }^{13}\text{C}_{t_i}$  is the  $^{13}\text{C}$  enrichment of the headspace gas sample at a specific time-point during the flux calculated with Equation 5.3 ( $atom\% \text{ }^{13}\text{C}$ ),  $Atom\% \text{ }^{13}\text{C}_{t_1}$  is the  $^{13}\text{C}$  enrichment of the headspace gas sample at the 0 min time-point calculated with Equation 5.3 ( $atom\% \text{ }^{13}\text{C}$ ), and  $Atom\% \text{ }^{13}\text{C}_x$  is the  $^{13}\text{C}$  enrichment of the  $^{13}\text{C}$ -substrate introduced to the pot ( $x$ ; i.e., the average  $^{13}\text{C}$  enrichment of the shoots and roots for plant-assimilated C, the  $^{13}\text{C}$  enrichment of the urea fertilizer itself for urea). With the substrate-derived gravimetric  $\text{CO}_2$  concentration, we could determine the  $\text{CO}_2$  flux derived from the substrate ( $\text{mg CO}_2\text{-C m}^{-2} \text{ h}^{-1}$ ) by also providing the volume of the headspace

chamber ( $\text{m}^3$ ) and the surface area of the soil ( $\text{m}^2$ ) to the gasfluxes package using the linear model on R version 4.4.0 (R Core Team, Vienna, Austria). Daily  $\text{CO}_2$  emissions were calculated from these fluxes by multiplying the hourly flux values by 24. This assumes that fluxes are constant throughout the day despite the fact that fluxes fluctuate temporally (Lloyd et al 2019). As such, daily emissions should be considered an approximation.

For  $\text{CO}_2$  from  $^{13}\text{C}$ -plant-assimilated C, we estimated the  $\text{CO}_2$  derived from shoot respiration, root respiration, and the microbial metabolism of rhizodeposits using the partitioning factors of 0.733, 0.133 and 0.133, respectively. These factors are based on the synthesis of 128 datasets of grass C allocation patterns to  $\text{CO}_2$  respiration (Pausch and Kuzyakov 2018). While this is an approximation, we found this procedure a more appropriate alternative to clipping the shoots prior to gas sampling which would only mitigate shoot respiration and would introduce an experimental artefact based on the effect of mechanical stress on plant rhizodeposition (Hamilton et al. 2008, Shazad et al. 2012, Lloyd et al. 2016). We assumed that any remaining  $\text{CO}_2$ -C not derived from plant respiration, rhizodeposits or urea was derived from peat.

### ***5.3.5 Ryegrass biomass and rhizosphere soil analysis***

Ryegrass shoots, roots, rhizosphere soil and microbial biomass extract samples were prepared for  $\delta^{13}\text{C}$  analysis and measured in the same manner as described in the previous chapter (See Section 4.3.6 *Ryegrass biomass and rhizosphere soil analysis*), except that rhizosphere soil was fumigated with HCl before encapsulation to remove any inorganic carbonates. Briefly, ground rhizosphere soil was first treated with concentrated HCl and placed in the fume hood overnight. Once the acid evaporated, this HCl-treated soil was weighed into tin capsules.

We calculated  $p_{pool-x}$  (%), the proportion of substrate-derived C in a pool – shoots, roots, rhizosphere soil, and microbial biomass extracts (fumigated and unfumigated soil extracts) – using an isotope mixing model:

$$p_{pool-x} = \frac{(Atom\% \text{ }^{13}\text{C}_{sample} - Atom\% \text{ }^{13}\text{C}_{control})}{(Atom\% \text{ }^{13}\text{C}_x - Atom\% \text{ }^{13}\text{C}_{control})} \times 100 \quad (5.6)$$

where  $Atom\% \text{ }^{13}\text{C}_{sample}$  is the  $^{13}\text{C}$  enrichment of the sample for that pool (atom%  $^{13}\text{C}$ ),  $Atom\% \text{ }^{13}\text{C}_{control}$  is the  $^{13}\text{C}$  enrichment of the natural abundance control for that pool (atom%  $^{13}\text{C}$ ), and  $Atom\% \text{ }^{13}\text{C}_x$  is the  $^{13}\text{C}$  enrichment of the  $^{13}\text{C}$ -substrate introduced to the pot from which we collected the sample. Since  $Atom\% \text{ }^{13}\text{C}_x$  for rhizodeposits is the average  $^{13}\text{C}$  enrichment of the shoots and roots, we did not use this equation to calculate the C derived from rhizodeposits in these pools. We then calculated  $C_{pool-x}$  (mg), the amount of substrate-derived C in a pool – shoots, roots, rhizosphere soil, and microbial biomass extracts (fumigated and unfumigated soil extracts) – according to:

$$C_{pool-x} = \frac{p_{pool-x}}{100} \times C_{pool} \quad (5.7)$$

where  $p_{pool-x}$  is the proportion of a pool derived from a substrate (%) calculated with Equation 5.6 and  $C_{pool}$  is the total amount of C in the pool of interest (mg).

Using the total C measured in the freeze-dried 0.5 mol  $\text{K}_2\text{SO}_4 \text{ L}^{-1}$  extracts of fumigated samples and unfumigated controls (Pang et al. 2021), we calculated the microbial biomass C in the rhizosphere soil with the extraction coefficient for microbial C ( $k_{EC} = 0.35$ ; Voroney et al. 2008). We assumed that this extraction coefficient would provide a sufficient approximation of the microbial biomass C, despite the fact that this extraction coefficient has not been calibrated for soils rich in organic matter. Likewise, we used a modified version of this calculation to determine the substrate-derived microbial biomass C ( $MBC_x$  in  $\text{mg C g}^{-1}$ ):

$$MBC_x = \frac{(C_{fum-x} - C_{unfum-x})}{k_{EC}} \quad (5.8)$$

where  $C_{fum-x}$  is the amount of C in the fumigated soil extract derived from the substrate of interest calculated with Equation 5.7 (mg C),  $C_{unfum-x}$  the amount of C in the fumigated soil extract derived from the substrate of interest calculated with Equation 5.7 (mg C) and  $k_{EC}$  is the extraction coefficient for microbial biomass C (0.35; Voroney et al. 2008).

### 5.3.6 Statistical analysis

We excluded replicates with negative values as outliers for a given pool, indicating that  $^{13}\text{C}$  enrichment did not occur. If more than one replicate had a negative value, we considered the mean of the pool for that treatment to be zero.

We tested if the type of  $^{13}\text{C}$ -substrate (rhizodeposits or urea) had an effect on the measured total  $\text{CO}_2$ -C emissions using the nonparametric Mann-Whitney test, ensuring that the assumption of similar distributions was met with the Kolmogorov-Smirnov test.

We determined whether substrate, time-point (0, 6, 21 or 45 h) and their interaction affected the distribution of recovered  $^{13}\text{C}$  among the rhizosphere soil and microbial biomass pools using generalized linear model analysis with the inverse Gaussian probability distribution due to non-normal residuals (Akram et al. 2020). Differences in recovered  $^{13}\text{C}$  among the daily emissions of  $\text{CO}_2$  and the combined pool of rhizosphere soil and microbial biomass were evaluated for the effect of substrate, pool ( $\text{CO}_2$  or soil and microbial biomass) and their interaction by also using this same statistical procedure. Merging the soil and microbial biomass pools was necessary to avoid multicollinearity in our statistical analysis (Huang et al. 2015) as the  $^{13}\text{C}$  recovered in rhizosphere soil was the difference between the total  $^{13}\text{C}$  present in the soil and the  $^{13}\text{C}$  present in the microbial biomass. Time was not considered as a factor in this analysis since the results were pooled together for the 21 h and 45 h time-points. If there were significant

effects from the generalized linear model analyses, we conducted pairwise comparisons of the estimated marginal means with Tukey post hoc analysis.

We assessed whether the proportions of substrate-derived C in the rhizosphere soil and microbial biomass pools were different due to substrate, time-point or their interaction using two-way analyses of variance (ANOVAs). In addition, we tested if there were differences in the CO<sub>2</sub>-C emissions derived from rhizodeposits and urea using a one-way ANOVA. We could not analyze differences in the CO<sub>2</sub>-C emitted from shoot and root respiration to that from rhizodeposits as their contributions were estimated from partitioning factors of CO<sub>2</sub> derived from plant-assimilated C, which would result in multicollinearity (Huang et al. 2015). Likewise, as peat represented the remainder of emissions (i.e., unlabeled CO<sub>2</sub>), we could not compare its CO<sub>2</sub> contribution to that from rhizodeposits and urea. As such, we visualized these differences using boxplots. For all ANOVAs, we confirmed the normality of residuals with the Shapiro-Wilk's test. If skewed, we used the Box-Cox transformation to ensure a normal distribution (Box and Cox 1964). Homogeneity of residual variances was validated with the Levene's test. Pairwise comparisons were conducted with Tukey post hoc analysis when significant effects were detected.

Our threshold of significance was  $p < 0.05$ . We performed all analyses in R Studio version 2024.04.2+764 (RStudio Team 2020) using the car, dplyr, emmeans, MASS, multcomp and stats packages.

## 5.4 Results

### 5.4.1 CO<sub>2</sub> emissions

We measured CO<sub>2</sub> fluxes of  $65.1 \pm 8.6$  mg CO<sub>2</sub>-C m<sup>-2</sup> h<sup>-1</sup> from the plant-rhizosphere soil systems, resulting in estimated daily emissions of 0.45 to 3.6 g CO<sub>2</sub>-C m<sup>-2</sup> d<sup>-1</sup> (Table 5.1; Table

5.S1 to see emissions in terms of soil mass). There was no difference between the estimated emissions from  $^{13}\text{C}$ -rhizodeposits or  $^{13}\text{C}$ -urea treatments ( $p > 0.05$ ).

Pulse labeling plants with  $^{13}\text{C}$ - $\text{CO}_2$  successfully enriched the shoots (4.74–8.99  $^{13}\text{C}$  atm% excess) and roots (4.15–6.07  $^{13}\text{C}$  atm% excess; Figure 5.S2). As a result, the  $^{13}\text{C}$ -labeled plants could successfully produce  $^{13}\text{C}$ -rhizodeposits, which permitted us to trace their fate in the rhizosphere. The  $^{13}\text{C}$  enrichment of plant biomass was stable across time-points even after the final  $\text{CO}_2$  pulse labeling event, suggesting that the plant-assimilated C was in a steady-state, allowing us to accurately portray the allocation of plant-assimilated C.

A minor portion of the C derived from rhizodeposits was emitted as  $\text{CO}_2$  (mean:  $3.89 \pm 0.83\%$ ) based on the  $^{13}\text{C}$  recovered from the rhizosphere 21 h and 45 h after the start of the final  $^{13}\text{C}$  labeling period and the partitioning estimates of plant-derived  $\text{CO}_2$  (Figure 5.1). This contrasts with the rhizodeposit-derived C found in the rhizosphere pools ( $p < 0.05$ ; soil:  $87.4 \pm 2.8\%$ ; microbial biomass of the rhizobiome:  $8.68 \pm 2.13\%$ ). In comparison,  $\text{CO}_2$  was the largest sink for urea-derived C in the rhizosphere ( $p < 0.05$ ; mean:  $70.1 \pm 4.9\%$ ), while  $29.9 \pm 4.88\%$  of C derived from urea was found in the rhizosphere soil and none was detected in the biomass of the rhizobiome. As such, the C allocation patterns for rhizodeposits and urea are different in the rhizosphere ( $p < 0.05$ ).

When partitioning the total  $\text{CO}_2$  emissions by source, rhizodeposits contributed approximately 10.9–18.6% and urea contributed 4.83–18.4% (Figure 5.2). The bulk of the  $\text{CO}_2$  emissions was estimated to originate from shoot and root respiration ( $91.0 \pm 7.6\%$ ). As the  $\text{CO}_2$  contributions from these sources exceeds 100% due to overestimation, the remaining  $\text{CO}_2$  from peat decomposition is  $-15.1 \pm 10.3\%$ . Nevertheless, it is clear that the greatest source of  $\text{CO}_2$  emissions was plant-derived C, followed by urea, resulting in minimal emissions from peat.

**Table 5.1** Range and mean of total and substrate-derived daily CO<sub>2</sub> emissions from the rhizosphere of annual ryegrass (*L. multiflorum*) plants measured 21 h and 45 h after the start of the final <sup>13</sup>C-labeling period. Mean values are mean ± standard error (*n* = 8) except for those with an asterisk (\*; *n* = 7 due to outliers).

	<sup>13</sup> C-Substrates					
	Plant-Assimilated C				Urea	
	Range		Mean		Range	Mean
<b>Total CO<sub>2</sub> Emissions (g CO<sub>2</sub>-C m<sup>-2</sup> d<sup>-1</sup>)</b>	0.760–3.61		1.96 ± 0.35		0.449–1.44	1.17 ± 0.12
<b>Substrate-Derived CO<sub>2</sub> Emissions (g CO<sub>2</sub>-<sup>13</sup>C m<sup>-2</sup> d<sup>-1</sup>)</b>	Shoots and Roots*		Rhizodeposits*		Range	Mean
	Range	Mean	Range	Mean		
	1.17–3.03	1.83 ± 0.24	0.180–0.465	0.280 ± 0.037	0.0608–0.252	0.122 ± 0.025

**Table 5.2** The total and substrate-derived C in the soil and microbial biomass pools of the rhizosphere of annual ryegrass (*L. multiflorum*) plants measured 0, 6, 21 and 45 h after the start of the final <sup>13</sup>C-labeling period. Rhizosphere soil (<sup>13</sup>C) is the difference between total (<sup>13</sup>C) found in the rhizosphere soil and (<sup>13</sup>C) in the microbial biomass. All values are the mean ± standard error (*n* = 4) except for those with an asterisk (\*; *n* = 3 due to negative values).

<sup>13</sup> C-Substrates	Time since Start of Final <sup>13</sup> C-Labeling Period (h)	Rhizosphere Soil		Microbial Biomass of Rhizobiome	
		Total C (g C m <sup>-2</sup> )	Substrate-Derived C (g <sup>13</sup> C m <sup>-2</sup> )	Total C (g C m <sup>-2</sup> )	Substrate-Derived C (g <sup>13</sup> C m <sup>-2</sup> )
Rhizodeposits	0	1910 ± 170	5.44 ± 1.48	5.78 ± 1.61	0.784 ± 0.065
	6	1740 ± 190 *	10.2 ± 1.1 *	7.48 ± 2.85 *	0.692 ± 0.051 *
	21	1680 ± 20 *	14.9 ± 11.8 *	5.95 ± 1.91 *	0.679 ± 0.102 *
	45	1740 ± 130	9.75 ± 3.28	7.52 ± 1.90	0.597 ± 0.038
Urea	0	2110 ± 50 *	0.0333 ± 0.0011 *	6.09 ± 3.85 *	0
	6	1940 ± 170 *	0.0285 ± 0.0036 *	3.65 ± 1.06 *	0
	21	1880 ± 40 *	0.0315 ± 0.0077 *	4.48 ± 1.04 *	0
	45	1840 ± 140 *	0.0603 ± 0.0069 *	6.23 ± 1.02 *	0

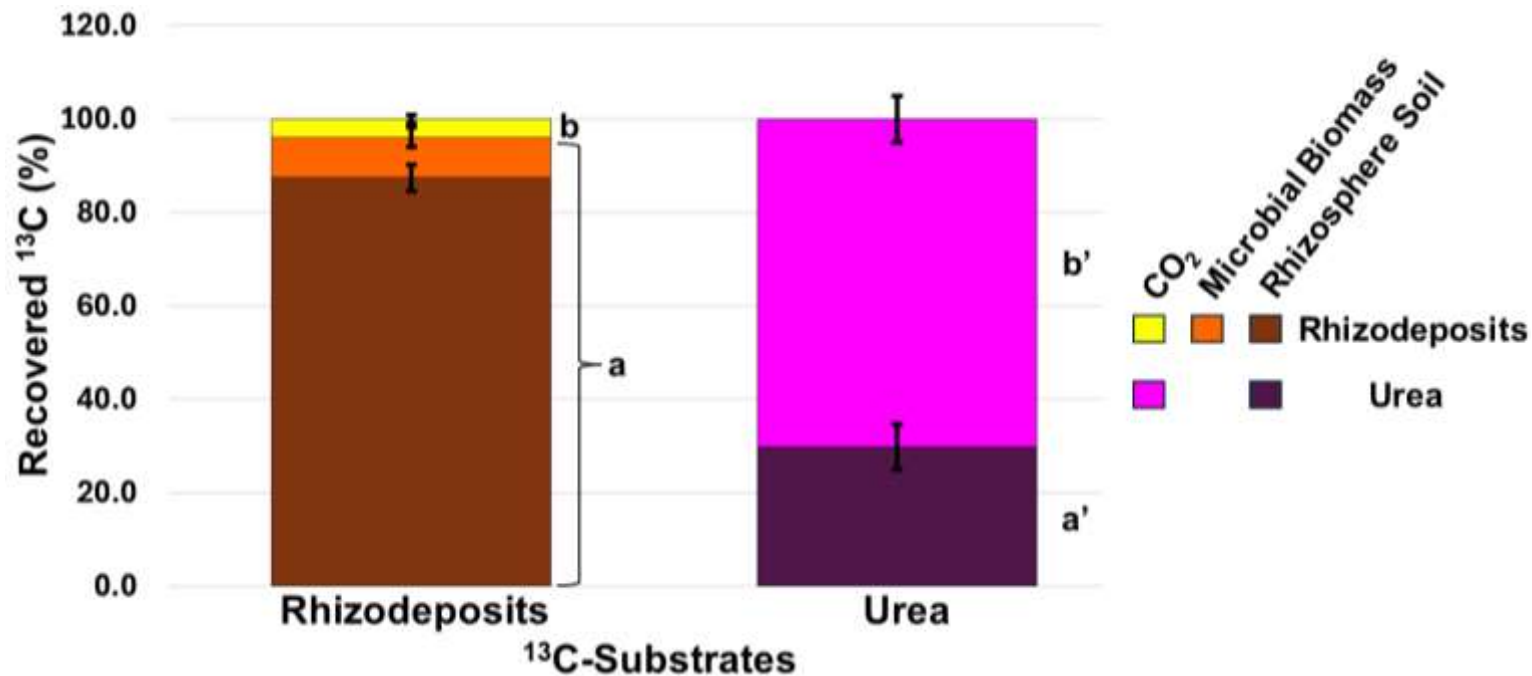


**Figure 5.1** Distribution of the total  $^{13}\text{C}$  (%) from the rhizodeposits and urea treatments recovered among the rhizosphere pools ( $\text{CO}_2$  emissions, microbial biomass of the rhizobiome, rhizosphere soil) of annual ryegrass (*L. multiflorum*) plants measured 21 h and 45 h after the start of the final  $^{13}\text{C}$ -labeling period. Each bar in the stacked bar shows the mean value with standard error bars for the  $^{13}\text{C}$  recovered in a respective pool after exposure to a specific  $^{13}\text{C}$ -substrate treatment, composited together for both time-points. The stacked bar for  $^{13}\text{C}$ -urea fertilizer had a sample size of  $n = 8$ , while the  $^{13}\text{C}$ -rhizodeposit treatment had a sample size of  $n = 7$  due to a negative value for microbial biomass. Significant differences in recovered  $^{13}\text{C}$  between pools for a specific  $^{13}\text{C}$ -substrate treatment are represented with different lowercase letters. Significant differences in recovered  $^{13}\text{C}$  between  $^{13}\text{C}$ -substrate treatments for a specific pool are represented by an apostrophe ('). Differences were considered significant when  $p < 0.05$  according to the generalized linear model analysis with the inverse Gaussian distribution followed by pairwise comparisons of the estimated marginal means with Tukey post hoc analysis.

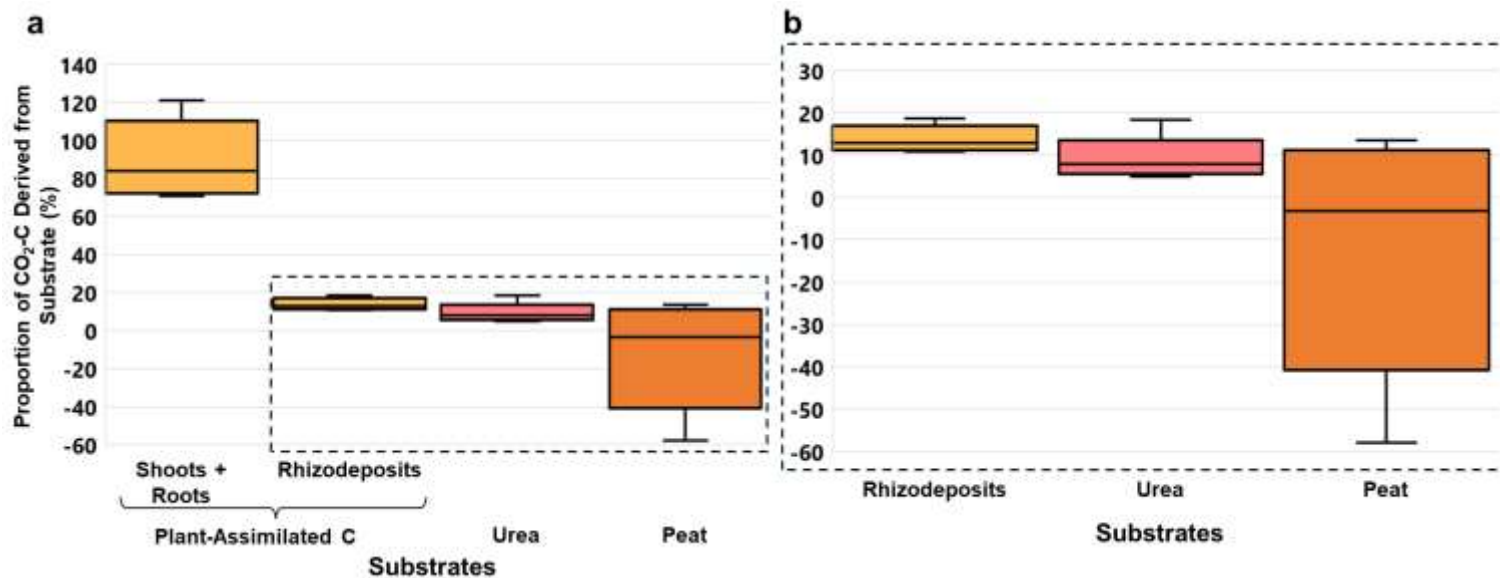


**Figure 5.2** The proportion of CO<sub>2</sub>-C (%) derived from ryegrass (*L. multiflorum*) plant respiration and different C substrates in the rhizosphere soil: a) contributions from plant-assimilated C (shoot and root respiration, rhizodeposits), urea and peat; and b) magnified inset to visualize the differences in the CO<sub>2</sub>-C contributions from the different C substrates in the rhizosphere soil. We assumed that any remaining CO<sub>2</sub>-C not derived from plant respiration, rhizodeposits or urea was derived from peat. Boxplots represent the composited results from the CO<sub>2</sub>-C measurements taken 21 h and 45 h after the start of the final <sup>13</sup>C-labeling period. The 25% and 75% quartiles of the results are shown with the bottom and top of the boxplot, respectively, while the median is represented by the center line and the range shown with the whiskers. The boxplot for urea had a sample size of  $n = 8$ , while the rest of the boxplots had a sample size of  $n = 7$  due to an outlier in the measurements of CO<sub>2</sub>-C derived from plant-assimilated C. No statistical comparison was conducted due to the dependent relationship of the variables.

### ***5.4.2 Dynamics of substrate-derived C in the rhizosphere***

The distributions of C derived from rhizodeposits and urea among the rhizosphere pools (soil and microbial biomass) were static at finer timescale (0, 6, 21 and 45 h since the start of the final  $^{13}\text{C}$ -labeling period). For rhizodeposit-C, the majority was present in the rhizosphere soil (88.8 to 92.8%) with a smaller fraction assimilated by the rhizobiome (7.2 to 11.2%; Figure 5.3). This equilibrium of rhizodeposit-derived C further supports that plant C allocation was in a steady-state. Conversely, none of the C derived from urea was recovered in the microbial biomass.

When looking at the individual rhizosphere pools (Table 5.2; Table 5.S2 to see amounts in terms of soil mass), rhizodeposit-derived C only represented 0.18% to 0.76% of the total rhizosphere soil C (mean:  $9.72 \pm 2.51 \text{ g C m}^{-2}$ ) but was still roughly three times greater than that derived from urea (0.0014 to 0.0030%;  $p < 0.05$ ; Figure 5.4a). There was also a 96% increase in the contribution of urea to rhizosphere soil C at the 45-h time-point ( $p < 0.05$ , Figure 5.4b). The rhizobiome harvested 11.7 to 16.8% of its biomass C from rhizodeposits, whereas urea was not a detectable source of C for this microbial community (Figure 5.4c).

## **5.5 Discussion**

### ***5.5.1 Peat is a negligible source of CO<sub>2</sub> from the rhizosphere***

Despite being a small fraction of total plant-assimilated C (1.3%; Figure 5.S3), the vast majority of the CO<sub>2</sub> emissions observed in our study were largely plant-derived. These plant-derived sources of CO<sub>2</sub> included rhizodeposits, which were estimated to contribute  $14.0 \pm 1.2\%$  of the CO<sub>2</sub> emissions from the plant-rhizosphere soil system. Being greater relative to the contribution of urea and peat, rhizodeposits were the largest source of CO<sub>2</sub> from the rhizosphere soil, supporting the hypothesis of our study. We expected rhizodeposits to contribute the most to the observed CO<sub>2</sub> emissions from the rhizosphere but were surprised by the undetectable emissions

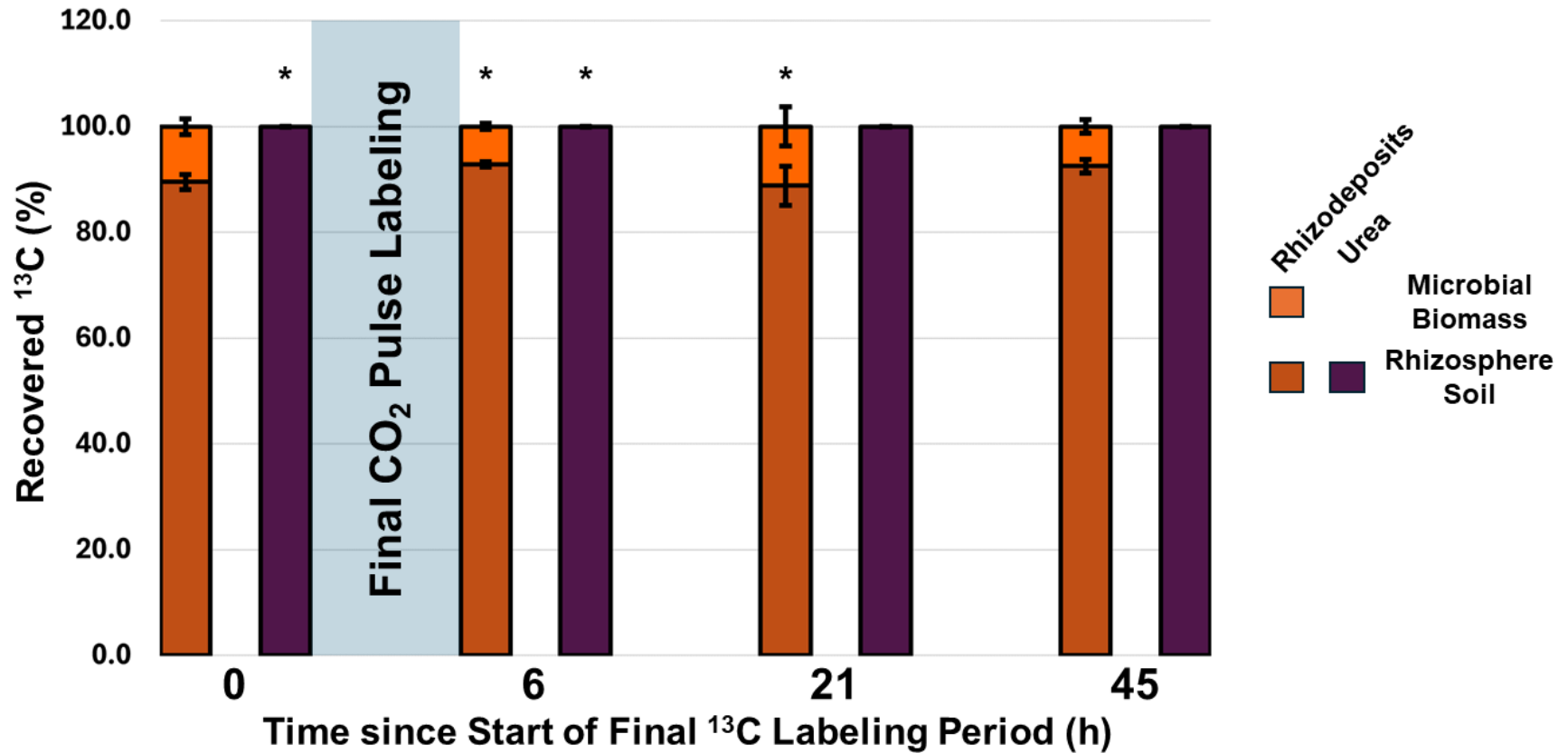


**Figure 5.3** Distribution of recovered <sup>13</sup>C (%) from rhizodeposits and urea among the microbial biomass and soil pools of the rhizosphere for annual ryegrass (*L. multiflorum*) plants measured 0, 6, 21 and 45 h after the start of the final <sup>13</sup>C-labeling period. Each bar in the stacked bar shows the mean value with standard error bars for the <sup>13</sup>C recovered in each pool after exposure to a specific <sup>13</sup>C-substrate treatment at a respective time-point. Each stacked bar had a sample size of  $n = 4$  except for those marked with an asterisk (\*;  $n = 3$  due to negative microbial biomass values).

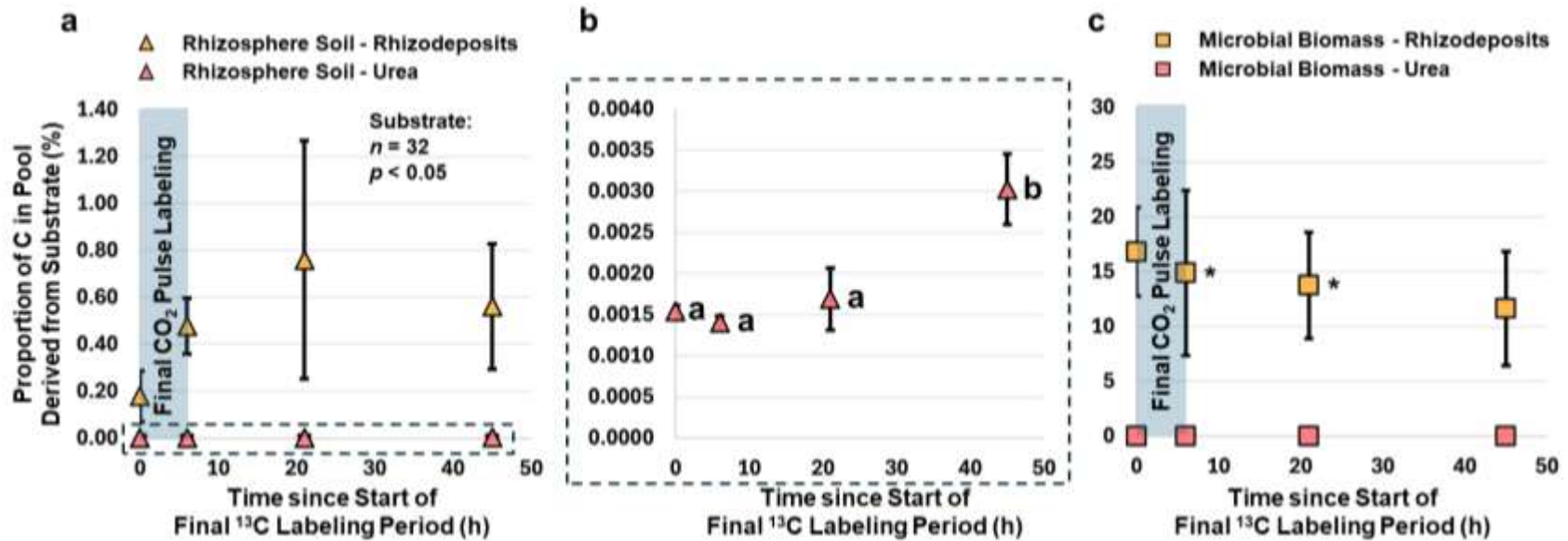


**Figure 5.4** The proportion of C (%) derived from rhizodeposits and urea in the rhizosphere pools of annual ryegrass (*L. multiflorum*) plants measured 0, 6, 21 and 45 h after the start of the final  $^{13}\text{C}$ -labeling period: a) rhizosphere soil; b) magnified inset to visualize the proportion of C in the rhizosphere soil derived from urea; and c) microbial biomass of the rhizobiome. The mean values of substrate-derived C are represented by markers with standard error bars. The sample size for each marker was  $n = 4$  besides those denoted with an asterisk (\*;  $n = 3$  due to negative values). Significant differences in the proportion of substrate-derived C between different time-points for a specific  $^{13}\text{C}$ -substrate treatment are represented by different lowercase letters. Differences were considered significant when  $p < 0.05$  according to the two-way analysis variance (ANOVA) followed by pairwise comparisons with Tukey post hoc analysis.

from peat, a rich and abundant C resource. While not entirely absent, other studies on drained peatlands have found minor contributions of peat to CO<sub>2</sub> emissions, being 30–45% of soil respiration (Biasi et al. 2011, Bader et al. 2018, Wang et al. 2021). This difference with our study is likely due to our focus on the CO<sub>2</sub> emitted from the rhizosphere, giving heightened importance to plant-derived C sources as a preferential substrate for efficient metabolism by the rhizobiome.

The quality of C found in peat likely explains their minimal contributions to emitted CO<sub>2</sub>. After extended periods of drainage, peat organic C is present as highly oxidized compounds, like lignin and aliphatics (Bader et al. 2017). While these organic compounds are high in potential energy, thermodynamic limitations in their metabolism by microorganisms make such forms of organic matter low in available energy (Wang and Kuzyakov 2023). To render their metabolism energetically favorable, a microbe would need to invest their energy into generating a suite of enzymes that breakdown and solubilize the complex organic matter, albeit with the risk that the desired products are lost to (i) fixation by minerals, (ii) leaching, or (iii) stealing by “cheater” microbes (Gunina and Kuzyakov 2022). These constraints are in contrast to the compounds present in rhizodeposits, which, despite their low energy content, are released reliably from roots in large amounts (77-121 g C m<sup>-2</sup> y<sup>-1</sup>; Pausch and Kuzyakov 2018) and require little to no energy expenditure for their metabolism (Gunina and Kuzyakov 2022). Consequently, rhizodeposits are a more favorable energy source to the rhizobiome than the surrounding peat.

The scarcity of peat-derived CO<sub>2</sub> in our study may have been partially due to the recent application of urea fertilizer (150 kg N ha<sup>-1</sup>). Although certain synthetic N fertilizers can release CO<sub>2</sub> (i.e., urea), N fertilization can reduce the CO<sub>2</sub> derived from soil organic matter by 7–18% (Kumar et al. 2016, Zang et al. 2017, Lu et al. 2023) while also increasing CO<sub>2</sub>-derived from the plant (Wang et al. 2021). The exact mechanism for this reduction in CO<sub>2</sub> from organic matter is

debated, possibly due to the fertilizer promoting rhizodeposition or creating acidic conditions that prevent soil organic matter solubilization (Wang and Tang 2018). Another potential mechanism is the change to the metabolic behavior of the rhizobiome, known as preferential substrate utilization theory (Cheng 1999, Perveen et al. 2019, Cui et al. 2023). When N fertilizers are applied to the rhizosphere, the surplus of available N can remove any N limitation for the rhizobiome. As a result, the rhizobiome no longer needs to mine the surrounding organic matter for C and N, and can satisfy any C or energy requirements with a more efficient and preferred source, like rhizodeposits. This theory is typically associated with observations of negative rhizosphere priming, where rhizodeposits provide sufficient nutrition for the rhizobiome, thus depressing their mineralization of organic matter (Dijkstra et al. 2013). We could not measure priming due to the different moisture conditions of our bare soil controls ( $p < 0.05$ ), but as we saw no contribution of peat to CO<sub>2</sub> emissions, our study suggests this negative priming effect was occurring in the rhizosphere. Nevertheless, more research is needed to determine the mechanism behind the observed absence of peat-derived CO<sub>2</sub> and its duration post-fertilization.

The minor contribution of peat to CO<sub>2</sub> emissions seems contradictory to their elevated C content ( $\geq 11.6\%$  organic C; USDA 2014). This contradiction expands even further when considering that soil organic matter is often the primary source of CO<sub>2</sub> from mineral soils ( $56 \pm 5\%$ ; Zhu and Cheng 2011, Kumar et al. 2016, Lloyd et al. 2016, Yan et al. 2022, Lu et al. 2023, Cui et al. 2024), despite their reduced organic C content (0.58–2.9%; USDA 2014). Yet, this contrast in CO<sub>2</sub> sources between cultivated peatlands and mineral soils may be rooted in the difference in their inherent organic matter content. In contrast to mineral soils, cultivated peatlands have fewer mineral surfaces for rhizodeposits to bind on, which leaves these organic compounds vulnerable to microbial metabolism. While rhizodeposits can bind to organic matter,

these associations are weaker than fixation to minerals (Liang et al. 2023). As such, rhizodeposits could be more available to the rhizobiome of cultivated peatlands compared to mineral soils, requiring future mechanistic investigation.

We did encounter overestimation in the CO<sub>2</sub> contributions of the different sources (Figure 5.2), a common occurrence due to the variation associated with such measurements (Whitman et al. 2015). This experimental error may be due to the presence of shoot respiration during gas sampling. The inclusion of shoots during gas measurements is common with herbaceous plant-soil systems as a result of their physical growth characteristics (Shazad et al. 2012, 2015, Cros et al. 2019). Yet, shoots are the largest source of ecosystem respiration and could mask CO<sub>2</sub> emissions from soil organic matter (Kuzyakov 2006). To avoid this issue, some studies clip the entire shoot structure prior to gas measurement to exclude shoot respiration (Biasi et al. 2011). However, such manipulations can alter root respiration (Kuzyakov 2006), trigger rhizodeposition (Hamilton et al. 2008, Lloyd et al. 2016) and reduce soil organic matter decomposition in the rhizosphere (Shazad et al. 2012, Lloyd et al. 2016). As such artefacts would hinder the findings from our study, we preserved the shoots and measured CO<sub>2</sub> from the plant-rhizosphere soil system as a whole, albeit at the risk of overestimation from plant-assimilated C sources. We recommend future studies increase replication to mitigate such overestimation issues while maintaining normal plant physiology. Regardless, while we cannot state that CO<sub>2</sub> emissions from peat did not occur, it is evident that these emissions were negligible compared to those derived from rhizodeposits and urea.

### ***5.5.2 Fate of C derived from rhizodeposits and urea in the rhizosphere***

The C derived from rhizodeposits was recovered mostly in the soil pool of the rhizosphere throughout the study ( $90.1 \pm 1.0\%$ , Figure 5.3). However, this rhizodeposit C made up just 0.608

$\pm 0.139\%$  of the total C found in the rhizosphere soil C (Figure 5.4). Although partly due to the rich organic C already present in this peat soil (Table 4.S1), rhizodeposit-C is largely ephemeral and cycled out in seconds to days by microbial respiration (Bardgett and van der Putten 2014, Pausch and Kuzyakov 2018). This effect may have been further exacerbated by the lack of mineral surfaces to fix rhizodeposits. As such, this observed net rhizodeposition is only a snapshot of the C flux flowing through this pool and thus does not portray the actual gross amount of rhizodeposition.

About a tenth of rhizodeposit-C was found in the microbial biomass (Figure 5.3). Likewise, rhizodeposit-derived C was  $\sim 13\%$  of total microbial biomass C (Figure 5.4c). This observation demonstrates the availability of rhizodeposit-derived C to the rhizobiome, being roughly ten times more accessible to microbes than soil organic matter (Zang et al. 2017). While this is a substantial portion of the microbial biomass, it is surprising that more rhizodeposit-derived C is not assimilated by the rhizobiome considering their close association to the root system (Kuzyakov and Blagodatskaya 2015). Accounting for the large amounts of rhizodeposit-derived  $\text{CO}_2$  ( $0.280 \pm 0.037 \text{ g CO}_2\text{-C m}^{-2} \text{ d}^{-1}$ , Table 5.1), the rhizobiome may not be efficient in its C use. While we can only conduct a crude estimate due to the absence of sampling during the entire  $^{13}\text{C}$ - $\text{CO}_2$  pulse labeling period, we approximate the rhizodeposit-C use efficiency by the rhizobiome to be just 9%. This low efficiency could imply that the rhizobiome is cycling through the rhizodeposits for energy rather than growth of biomass (Wang and Kuzyakov 2023). Such a phenomenon is plausible as rhizodeposits, like root exudates, require substantial energy for their reduction to form structural biomass polymers as opposed to their oxidation for energy (Gunina and Kuzyakov 2023). However, the low amounts of rhizodeposit-derived C in the microbial biomass could also speak to their preference for recycling microbial necromass rather than *de*

*novo* synthesis of biomolecules with rhizodeposit-C. Regardless, rhizodeposit-derived C seems more effective as an energy source for the rhizobiome rather than a building block for their growth and synthesis.

There were evident differences in the fate of C derived from rhizodeposits and urea (Figures 5.1, 5.3–5.4). This effect was expected as (i) a biochemical process controls the hydrolysis of urea rather than a biological one, and (ii) all C present in urea evolves as CO<sub>2</sub> once hydrolyzed by urease (Sigurdarson et al. 2018). In contrast, rhizodeposits have a stable C backbone unless metabolized by the rhizobiome. Even after metabolism, many of the rhizodeposit-derived byproducts are other organic compounds, not just CO<sub>2</sub>. As there was still roughly 0.0384 g C m<sup>-2</sup> of urea-C remaining in the rhizosphere soil, not all the urea had been hydrolyzed. This observation is consistent with the estimated lifespan of urea in agricultural soils, typically lasting 3.8 d after application depending on soil and temperature (Lasisi and Akinremi 2020). While there was potential for this urea-derived CO<sub>2</sub> to be fixed by autotrophic microbes, such an effect was not detected in our study (Figure 5.4c). Interestingly, we did find that plants took up a minor portion of urea-C (Figure 5.S5), either directly from the rhizosphere soil through their roots (Yang et al. 2015) or fixed during photosynthesis with urea-derived CO<sub>2</sub>. Yet, with such small amounts retained in the plant-rhizosphere soil systems, the eventual emission of urea-derived C to the atmosphere is undeniable and does not play a role in rhizosphere C dynamics.

## **5.6 Conclusion**

In this study, we demonstrate the substantial contributions of rhizodeposits to the CO<sub>2</sub> emissions from the rhizosphere, establishing their importance not only in the C cycling of this environment but also in the production of CO<sub>2</sub> from cultivated peatlands. Our findings suggest that despite

their rich C content, peat is a negligible source of CO<sub>2</sub> from the rhizosphere of cultivated peatlands under N-rich soil conditions. This implies that the peat-C in the rhizosphere is stable and sequestered from microbial metabolism. The duration of this effect and whether it stems from N fertilization requires further research to fully comprehend the dynamics behind the production of CO<sub>2</sub> derived from rhizodeposits and peat in the rhizosphere of cultivated peatlands. Altogether, the findings of this research provide greater resolution into the mechanisms of CO<sub>2</sub> production occurring in cultivated peatlands and can be used to improve predictions of CO<sub>2</sub> emissions from this delicate agroecosystem.

## 5.7 References

- Akram, M.N., Amin, M., Amanullah, M., 2020. Two-parameter estimator for the inverse Gaussian regression model. *Communications in Statistics – Simulation and Computation* 51, 6208-6226. <https://doi.org/10.1080/03610918.2020.1797797>.
- Bader, C., Müller, M., Schulin, R., Leifeld, J., 2017. Amount and stability of recent and aged plant residues in degrading peatland soils. *Soil Biology and Biochemistry* 109, 167–175. <https://doi.org/10.1016/j.soilbio.2017.01.029>.
- Bader, C., Müller, M., Schulin, R., Leifeld, J., 2018. Peat decomposability in managed organic soils in relation to land use, organic matter composition and temperature. *Biogeosciences* 15, 703–719. <https://doi.org/10.5194/bg-15-703-2018>.
- Bardgett, R.D., van der Putten, W.H., 2014. Belowground biodiversity and ecosystem functioning. *Nature* 515, 505–511. <https://doi.org/10.1038/nature13855>.
- Biasi, C., Tavi, N.M., Jokinen, S., et al., 2011. Differentiating sources of CO<sub>2</sub> from organic soil under bioenergy crop cultivation: A field-based approach using <sup>14</sup>C. *Soil Biology and Biochemistry* 43, 2406–2409. <https://doi.org/10.1016/j.soilbio.2011.08.003>.
- Box, G.E.P., Cox, D.R., 1964. An analysis of transformations. *Journal of the Royal Statistical Society, Series B (Methodological)* 26, 211-252. <https://doi.org/10.1111/j.2517-6161.1964.tb00553.x>.
- Carlson, K.M., Gerber J.S., Mueller, ND., et al., 2017. Greenhouse gas emissions intensity of global croplands. *Nature Climate Change* 7, 63–68. <https://doi.org/10.1038/nclimate3158>.

- Cheng, W.X., 1999. Rhizosphere feedbacks in elevated CO<sub>2</sub>. *Tree Physiology* 19, 313–320.  
<https://doi.org/10.1093/treephys/19.4-5.313>.
- CIAAW, 2015. Carbon. Commission on Isotopic Abundances and Atomic Weights.  
<https://ciaaw.org/carbon.htm>. (Accessed August 14, 2024).
- Cros, C., Alvarez, G., Keuper, F., Fontaine, S., 2019. A new experimental platform connecting the rhizosphere priming effect with CO<sub>2</sub> fluxes of plant–soil systems. *Soil Biology and Biochemistry* 130, 12–22. <https://doi.org/10.1016/j.soilbio.2018.11.022>.
- Cui, H., He, C., Zheng, W., et al., 2024. Effects of nitrogen addition on rhizosphere priming: The role of stoichiometric imbalance. *Science of the Total Environment* 914, 169713.  
<https://doi.org/10.1016/j.scitotenv.2023.169731>.
- Cui, H., Mo, C., Chen, P., et al., 2023. Impact of rhizosphere priming on soil organic carbon dynamics: Insights from the perspective of carbon fractions. *Applied Soil Ecology* 189, 104982. <https://doi.org/10.1016/j.apsoil.2023.104982>.
- De Sena, A., Mosdossy, K., Whalen, J.K., et al., 2023. Root exudates and microorganisms. In: Goss, M., Oliver, M. (Eds.), *Encyclopedia of Soils in the Environment*, 2nd ed. Elsevier, Cambridge, Massachusetts, pp. 343–356. <https://doi.org/10.1016/B978-0-12-822974-3.00125-7>.
- Dijkstra, F.A., Carrillo, Y., Pendall, E., et al., 2013. Rhizosphere priming: A nutrient perspective. *Frontiers in Microbiology* 4, 216. <https://doi.org/10.3389/fmicb.2013.00216>.

- FAO, 2020. Drained organic soils 1990–2019. Global, regional and country trends. Food and Agriculture Organization of the United Nations. FAOSTAT Analytical Brief Series No 4, Rome.
- Fleischer, A.J., Yi, H., Srivastava, A., et al., 2021. Absolute  $^{13}\text{C}/^{12}\text{C}$  isotope amount ratio for Vienna PeeDee Belemnite from infrared absorption spectroscopy. *Nature Physics* 17, 889–893. <https://doi.org/10.1038/s41567-021-01226-y>.
- Freeman, B.W.J., Evans, C.D., Musarika, S., et al., 2022. Responsible agriculture must adapt to the wetland character of mid-latitude peatlands. *Global Change Biology* 28, 3795–3811. <https://doi.org/10.1111/gcb.16152>.
- Glenn, S., Heyes, A., Moore, T., 1993. Carbon dioxide and methane fluxes from drained peat soils, southern Québec. *Global Biogeochemical Cycles* 7, 247–257. <https://doi.org/10.1029/93GB00469>.
- Gunina, A., Kuzyakov, Y., 2022. From energy to (soil organic) matter. *Global Change Biology* 28, 2169–2182. <https://doi.org/10.1111/gcb.16071>.
- Hamilton III, E.W., Frank, D.A., Hinchey, P.M., Murray, T.R., 2008. Defoliation induces root exudation and triggers positive rhizospheric feedbacks in a temperate grassland. *Soil Biology and Biochemistry* 40, 2865–2873. <https://doi.org/10.1016/j.soilbio.2008.08.007>.
- Honkanen, H., Kekkonen, H., Heikkinen, J., et al., 2024. Minor effects of no-till treatment on GHG emissions of boreal cultivated peat soil. *Biogeochemistry* 167, 499–522. <https://doi.org/10.1007/s10533-023-01097-w>.

Huang, C.C.L., Jou, Y.J., Cho, H.J., 2015. A new multicollinearity diagnostic for generalized linear models. *Journal of Applied Statistics* 43, 2029-2043.

<https://doi.org/10.1080/02664763.2015.1126239>.

IFA, 2023. IFADData Plant Nutrition Query. International Fertilizer Association.

<https://www.ifastat.org/> (Accessed June 5 2023).

IPCC, 2006. N<sub>2</sub>O emissions from managed soils, and CO<sub>2</sub> emissions from lime and urea application. IPCC Guidelines for National Greenhouse Gas Inventories. Intergovernmental Panel on Climate Change.

Kim, G.W., Alam, M.A., Lee, J.J., et al., 2017. Assessment of direct carbon dioxide emission factor from urea fertilizer in temperate upland soil during warm and cold cropping season. *European Journal of Soil Biology* 83, 76–83.

<https://doi.org/10.1016/j.ejsobi.2017.10.005>.

Kumar, A., Kuzyakov, Y., Pausch, J., 2016. Maize rhizosphere priming: field estimates using <sup>13</sup>C natural abundance. *Plant and Soil* 409, 87–97. <https://doi.org/10.1007/s11104-016-2958-2>.

Kuzyakov, Y., 2006. Sources of CO<sub>2</sub> efflux from soil and review of partitioning methods. *Soil Biology and Biochemistry* 38, 425–448. <https://doi.org/10.1016/j.soilbio.2005.08.020>.

Kuzyakov, Y., Blagodatskaya, E., 2015. Microbial hotspots and hot moments in soil: Concept & review. *Soil Biology and Biochemistry* 83, 184–199.

<https://doi.org/10.1016/j.soilbio.2015.01.025>.

- Lasisi, A.A., Akinremi, O.O., 2020. Kinetics and thermodynamics of urea hydrolysis in the presence of urease and nitrification inhibitors. *Canadian Journal of Soil Science* 101, 192–202. <https://doi.org/10.1139/cjss-2020-0044>.
- Lahtinen, L., Mattila, T., Myllyvita, T., et al., 2022. Effects of paludiculture products on reducing greenhouse gas emissions from agricultural peatlands. *Ecological Engineering* 175: 106502. <https://doi.org/10.1016/j.ecoleng.2021.106502>.
- Leifeld, J., Klein, K., Wüst-Galley, C., 2020. Soil organic matter stoichiometry as indicator for peatland degradation. *Scientific Reports* 10, 7634. <https://doi.org/10.1038/s41598-020-64275-y>.
- Leifeld, J., Menichetti, L., 2018. The underappreciated potential of peatlands in global climate change mitigation strategies. *Nature Communications* 9, 107. <https://doi.org/10.1038/s41467-018-03406-6>.
- Leifeld, J., Steffens, M., Galego-Sala, A., 2012. Sensitivity of peatland carbon loss to organic matter quality. *Geophysical Research Letters* 39, L14704. <https://doi.org/10.1029/2012GL051856>.
- Liang, G., Stark, J., Waring, B.G., 2023. Mineral reactivity determines root effects on soil organic carbon. *Nature Communications* 14, 4962. <https://doi.org/10.1038/s41467-023-40768-y>.

- Lloyd, K., Madramootoo, C.A., Edwards, K.P., et al., 2019. Greenhouse gas emissions from selected horticultural production systems in a cold temperate climate. *Geoderma* 349, 45–55. <https://doi.org/10.1016/j.geoderma.2019.04.030>.
- Lloyd, D.A., Ritz, K., Paterson, E., Kirk, G.J.D., 2016. Effects of soil type and composition of rhizodeposits on rhizosphere priming phenomena. *Soil Biology and Biochemistry* 103, 512–521. <https://doi.org/10.1016/j.soilbio.2016.10.002>.
- Lu, J., Yin, L., Dijkstra, F.A., et al., 2023. Linking plant traits to rhizosphere priming effects across six grassland species with and without nitrogen fertilization. *Soil Biology and Biochemistry* 185, 109144. <https://doi.org/10.1016/j.soilbio.2023.109144>.
- Maljanen, M., Sigurdsson, B.D., Guðmundsson, J., et al., 2010. Greenhouse gas balances of managed peatlands in the Nordic countries – present knowledge and gaps. *Biogeosciences* 7, 2711–2738. <https://doi.org/10.5194/bg-7-2711-2010>.
- Menegat, S., Ledo, A., Tirado, R., 2022. Greenhouse gas emissions from global production and use of nitrogen synthetic fertilisers in agriculture. *Scientific Reports* 12, 14490. <https://doi.org/10.1038/s41598-022-18773-w>.
- Müller, J., Joos, F., 2021. Committed and projected future changes in global peatlands – continued transient model simulations since the Last Glacial Maximum. *Biogeosciences* 18, 3657–3687. <https://doi.org/10.5194/bg-18-3657-2021>.

- Norberg, L., Berglund, Ö., Berglund, K., 2016. Seasonal CO<sub>2</sub> emission under different cropping systems on Histosols in southern Sweden. *Geoderma Regional* 7, 338–345. <https://doi.org/10.1016/j.geodrs.2016.06.005>.
- Pang, R., Xu, X., Tian, Y., et al., 2021. *In-situ* <sup>13</sup>CO<sub>2</sub> labeling to trace carbon fluxes in plant–soil–microorganism systems: Review and methodological guideline. *Rhizosphere* 20, 100441. <https://doi.org/10.1016/j.rhisph.2021.100441>.
- Pausch, J., Kuzyakov, Y., 2018. Carbon input by roots into the soil: Quantification of rhizodeposition from root to ecosystem scale. *Global Change Biology* 24, 1–12. <https://doi.org/10.1111/gcb.13850>.
- Pausch, J., Tian, J., Riederer, M., Kuzyakov, Y., 2013. Estimation of rhizodeposition at field scale: upscaling of a <sup>14</sup>C labeling study. *Plant and Soil* 364, 273–285. <https://doi.org/10.1007/s11104-012-1363-8>.
- Perveen, N., Barot, S., Maire, V., et al., 2019. Universality of priming effect: An analysis using thirty five soils with contrasted properties sampled from five continents. *Soil Biology and Biochemistry* 134, 162–171. <https://doi.org/10.1016/j.soilbio.2019.03.027>.
- Petersen, S.O., Hoffmann, C.C., Schäfer, C.–M., et al., 2012. Annual emissions of CH<sub>4</sub> and N<sub>2</sub>O, and ecosystem respiration, from eight organic soils in Western Denmark managed by agriculture. *Biogeosciences* 9, 403–422. <https://doi.org/10.5194/bg-9-403-2012>.

- Riederer, M., Pausch, J., Kuzyakov, Y., Foken, T., 2015. Partitioning NEE for absolute C input into various ecosystem pools by combining results from eddy–covariance, atmospheric flux partitioning and  $^{13}\text{CO}_2$  pulse labeling. *Plant and Soil* 390, 61–76.  
<https://doi.org/10.1007/s11104-014-2371-7>.
- RStudio Team, 2020. RStudio: Integrated Development for R. RStudio, PBC, Boston, MA URL  
<http://www.rstudio.com/>.
- Shazad, T., Chenu, C., Genet, P., et al., 2015. Contribution of exudates, arbuscular mycorrhizal fungi and litter depositions to the rhizosphere priming effect induced by grassland species. *Soil Biology and Biochemistry* 80, 146–155.  
<https://doi.org/10.1016/j.soilbio.2014.09.023>.
- Shazad, T., Chenu, C., Repinçay, C., et al., 2012. Plant clipping decelerates the mineralization of recalcitrant soil organic matter under multiple grassland species. *Soil Biology and Biochemistry* 51, 73–80. <https://doi.org/10.1016/j.soilbio.2012.04.014>.
- Sigurdarson, J.J., Svane, S., Karring, H., 2018. The molecular processes of urea hydrolysis in relation to ammonia emissions from agriculture. *Reviews in Environmental Science and Bio/Technology* 17, 241–258. <https://doi.org/10.1007/s11157-018-9466-1>.
- Unc, A., Altdorff, D., Abakumov, E., et al., 2021. Expansion of agriculture in northern cold–climate regions: A cross–sectoral perspective on opportunities and challenges. *Frontiers in Sustainable Food Systems* 5: 663448.  
<https://doi.org/10.3389/fsufs.2021.663448>.

USDA, 2014. Keys to Soil Taxonomy, 12th ed. United States Department of Agriculture Natural Resources Conservation Service.

Voroney, R.P., Brookes, P.C., Beyaert, R.P., 2008. Soil microbial biomass C, N, P, and S. In: Carter, M.R., Gregorich, E.G. (Eds.), Soil Sampling and Methods of Analysis, 2nd edn. CRC Press, Florida, pp. 637–651.

Wang, C., Kuzyakov, Y., 2023. Energy use efficiency of soil microorganisms: Driven by carbon recycling and reduction. *Global Change Biology* 29, 6170–6187.  
<https://doi.org/10.1111/gcb.16925>.

Wang, Y., Paul, S.M., Jocher, M., et al., 2021. Soil carbon loss from drained agricultural peatland after coverage with mineral soil. *Science of the Total Environment* 800, 149498.  
<https://doi.org/10.1016/j.scitotenv.2021.149498>.

Wang, X., Tang, C., 2018. The role of rhizosphere pH in regulating the rhizosphere priming effect and implications for the availability of soil-derived nitrogen to plants. *Annals of Botany* 121, 143–151. <https://doi.org/10.1093/aob/mcx138>.

Whitman, T., Lehmann, J., 2015. A dual-isotope approach to allow conclusive partitioning between three sources. *Nature Communications* 6, 8708.  
<https://doi.org/10.1038/ncomms9708>.

- Yan, W., Wang, Y., Ju, P., et al., 2022. Water level regulates the rhizosphere priming effect on SOM decomposition of peatland soil. *Rhizosphere* 21: 100455.  
<https://doi.org/10.1016/j.rhisph.2021.100455>.
- Yang, H., Menz, J., Häussermann, I., et al., 2015. High and low affinity urea root uptake: involvement of NIP5;1. *Plant and Cell Physiology* 56, 1588–1597.  
<https://doi.org/10.1093/pcp/pcv067>.
- Zang, H., Blagodatskaya, E., Wang, J., et al., 2017. Nitrogen fertilization increases rhizodeposit incorporation into microbial biomass and reduces soil organic matter losses. *Biology and Fertility of Soils* 53, 419–429. <https://doi.org/10.1007/s00374-017-1194-0>.
- Zhu, B., Cheng, W., 2011. Rhizosphere priming effect increases the temperature sensitivity of soil organic matter decomposition. *Global Change Biology* 17, 2172–2183.  
<https://doi.org/10.1111/j.1365-2486.2010.02354.x>.

## 5.8 Appendix: Supplementary materials

**Table 5.S1** Range and mean of total and substrate-derived daily CO<sub>2</sub> emissions in terms of soil mass from the rhizosphere of annual ryegrass (*L. multiflorum*) plants measured 21 h and 45 h after the start of the final <sup>13</sup>C-labeling period. Mean values are mean ± standard error (*n* = 8) except for those with an asterisk (\*; *n* = 7 due to an outlier).

	<sup>13</sup> C-Substrates					
	Plant-Assimilated C				Urea	
	Range		Mean		Range	Mean
<b>Total CO<sub>2</sub> Emissions (mg CO<sub>2</sub>-C kg soil<sup>-1</sup> d<sup>-1</sup>)</b>	36.4–173		93.7 ± 16.9		21.5–69.0	55.9 ± 5.67
	Shoots and Roots*		Rhizodeposits*			
	Range	Mean	Range	Mean	Range	Mean
<b>Substrate-Derived CO<sub>2</sub> Emissions (mg CO<sub>2</sub>-C kg soil<sup>-1</sup> d<sup>-1</sup>)</b>	56.1–145	87.4 ± 11.4	8.61–22.3	13.4 ± 1.8	2.91–12.1	5.86 ± 1.19

**Table 5.S2** The total and substrate-derived C in the soil and microbial biomass pools of the rhizosphere of annual ryegrass (*L. multiflorum*) plants in terms of soil mass measured 0, 6, 21 and 45 h after the start of the final  $^{13}\text{C}$ -labeling period. Rhizosphere soil ( $^{13}\text{C}$ ) is the difference between total ( $^{13}\text{C}$ ) found in the rhizosphere soil and ( $^{13}\text{C}$ ) in the microbial biomass. All values are mean  $\pm$  standard error ( $n = 4$ ) except for those with an asterisk (\*;  $n = 3$  due to negative values).

$^{13}\text{C}$ -Substrates	Time since Start of Final $^{13}\text{C}$ -Labeling Period (h)	Rhizosphere Soil		Microbial Biomass of Rhizobiome	
		Total C (g C kg soil $^{-1}$ )	Substrate-Derived C (g $^{13}\text{C}$ kg soil $^{-1}$ )	Total C (mg C kg soil $^{-1}$ )	Substrate-Derived C (mg $^{13}\text{C}$ kg soil $^{-1}$ )
Rhizodeposits	0	216 $\pm$ 8	0.625 $\pm$ 0.172	652 $\pm$ 175	89.1 $\pm$ 4.5
	6	214 $\pm$ 16 *	1.27 $\pm$ 0.17 *	935 $\pm$ 372 *	85.8 $\pm$ 6.6 *
	21	227 $\pm$ 6 *	1.93 $\pm$ 1.51 *	814 $\pm$ 274 *	91.5 $\pm$ 12.7 *
	45	215 $\pm$ 12	1.23 $\pm$ 0.45	948 $\pm$ 246	74.1 $\pm$ 5.1
Urea	0	224 $\pm$ 3 *	0.00359 $\pm$ 0.00011 *	642 $\pm$ 401 *	0
	6	229 $\pm$ 7 *	0.00320 $\pm$ 0.00023 *	427 $\pm$ 101 *	0
	21	228 $\pm$ 20 *	0.00392 $\pm$ 0.00067 *	529 $\pm$ 66 *	0
	45	173 $\pm$ 6 *	0.00562 $\pm$ 0.00068 *	593 $\pm$ 119 *	0

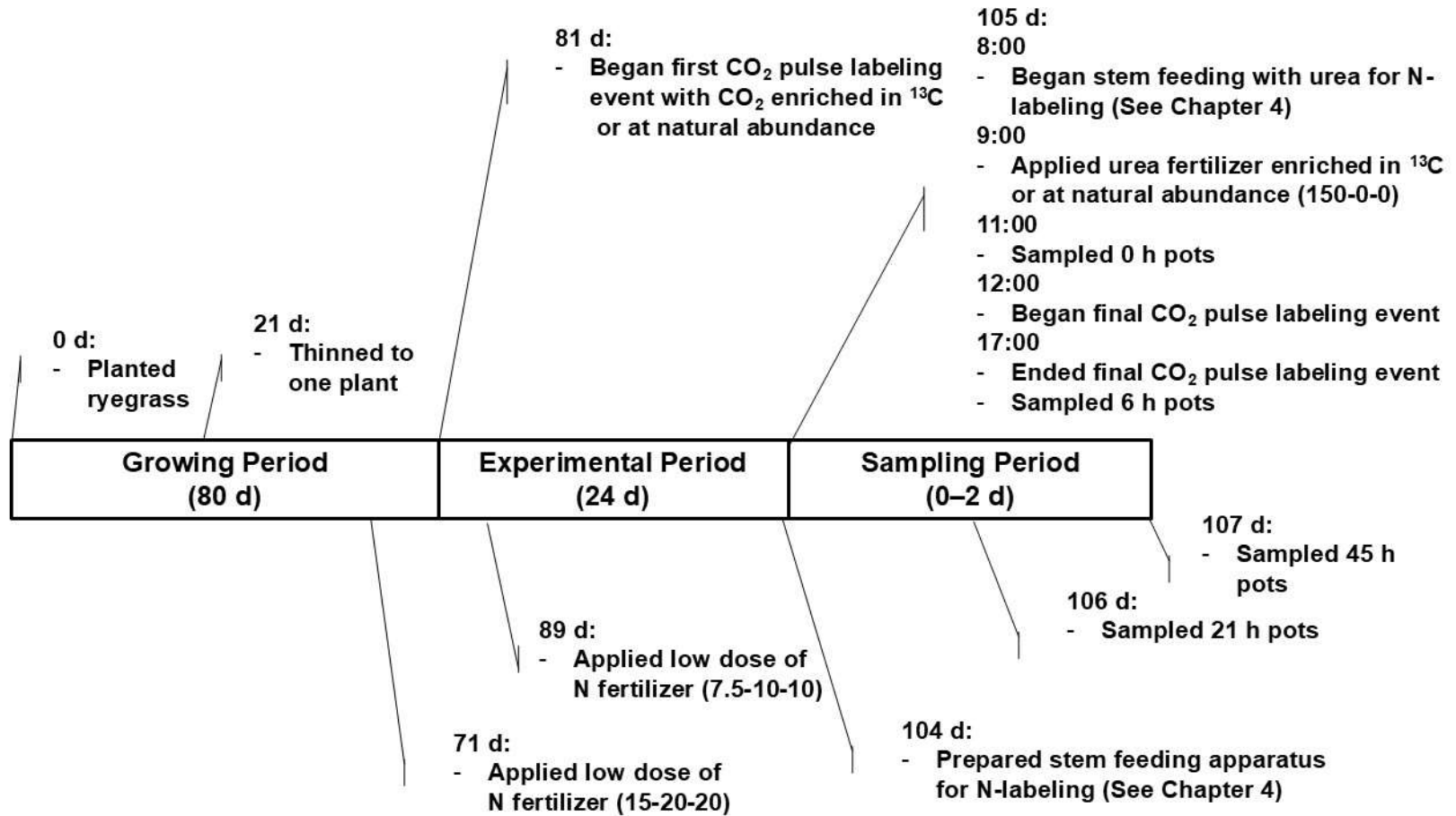


**Figure 5.S1** Timeline of experiment, which included a growing (80 d), experimental (24 d) and sampling period (0–2 d).

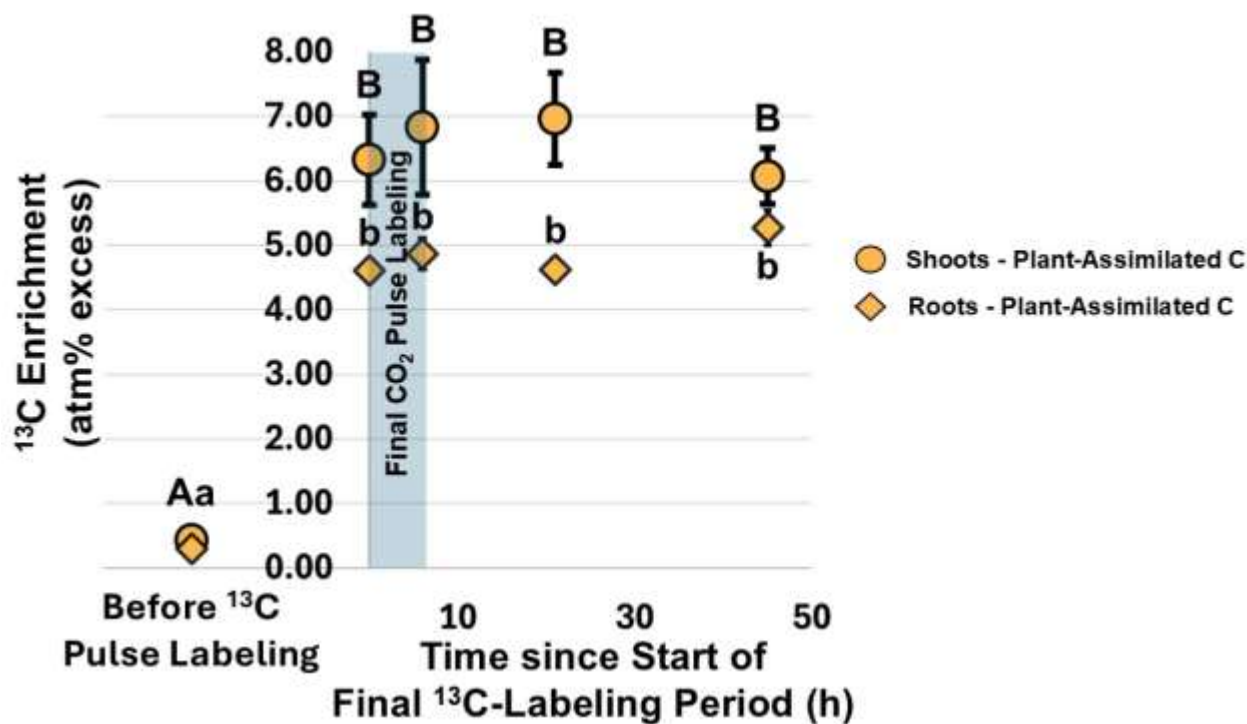


**Figure 5.S2** The <sup>13</sup>C enrichment (atm% excess) of the shoots and roots from annual ryegrass (*L. multiflorum*) plants measured 0, 6, 21 and 45 h after the start of the final <sup>13</sup>C-labeling period. Markers indicate the mean <sup>13</sup>C enrichment value in a respective pool at a specific time-point, with error bars representing the standard error of the mean. All mean values had a sample size of  $n = 4$  except for the controls before <sup>13</sup>C pulse labeling occurred ( $n = 3$ ). Different upper- and lowercase letters indicate a significant difference ( $p < 0.05$ ) in the <sup>13</sup>C enrichment between time-points for ryegrass shoots and roots, respectively. All differences were considered significant when  $p < 0.05$  according to the generalized linear model analysis with the gamma probability distribution followed by pairwise comparisons of the estimated marginal means with Tukey post hoc analysis.

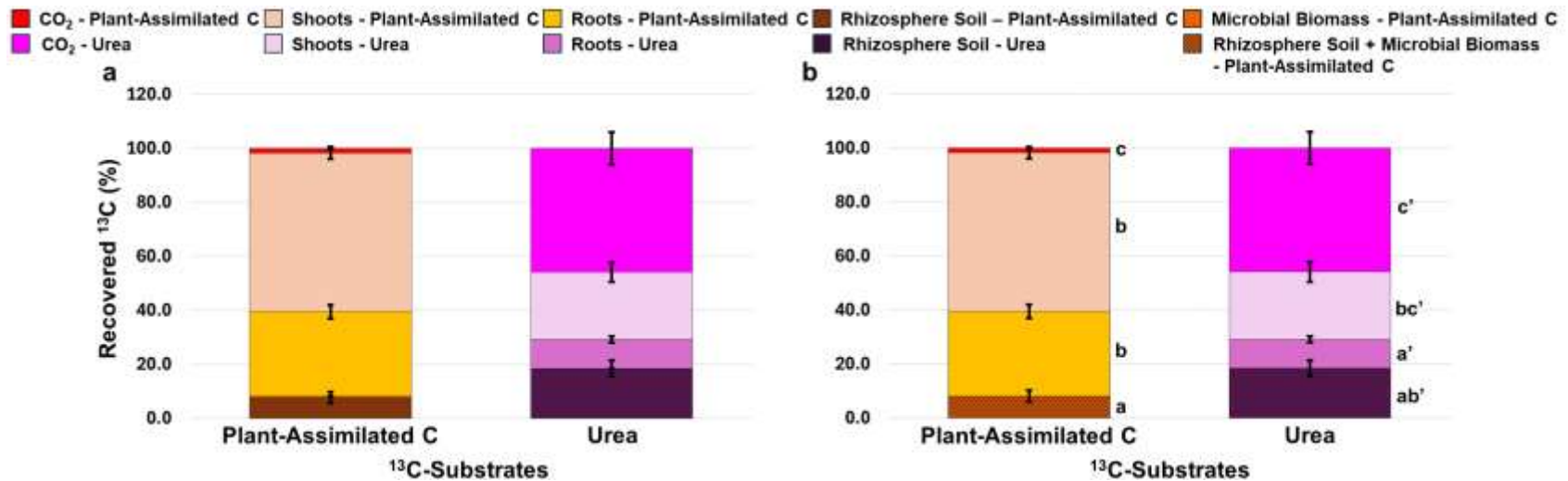


**Figure 5.S3** Distribution of recovered <sup>13</sup>C (%) from plant-assimilated C (including rhizodeposits) and urea among the plant biomass and rhizosphere pools of annual ryegrass (*L. multiflorum*) plants measured 21 h and 45 h after the start of the final <sup>13</sup>C-labeling period: a) the separate pools of daily CO<sub>2</sub> emissions, shoots, roots, rhizosphere soil, and microbial biomass; and b) the separate pools of daily CO<sub>2</sub> emissions, shoots and roots, as well as rhizosphere soil combined with the microbial biomass if present. CO<sub>2</sub> emissions for plant-assimilated C include emissions from plant respiration and the microbial metabolism of rhizodeposits. Stacked bars show the mean value with standard error bars of <sup>13</sup>C recovered in each pool composited together for both time-points after exposure to a specific <sup>13</sup>C-substrate treatment. The stacked bar for <sup>13</sup>C-urea fertilizer had a sample size of  $n = 8$ , while the plant-assimilated <sup>13</sup>C treatment had a sample size of  $n = 7$  due to a negative value for microbial biomass. In Figure 5.S3b, significant differences in recovered <sup>13</sup>C between pools for a specific <sup>13</sup>C-substrate treatment are represented with different lowercase letters. Additionally, significant differences in recovered <sup>13</sup>C between <sup>13</sup>C-substrate treatments for a specific pool are represented by an apostrophe ('). Differences were considered significant when  $p < 0.05$  according to the generalized linear model analysis with the gamma probability distribution followed by pairwise comparisons of the estimated marginal means with Tukey post hoc analysis.

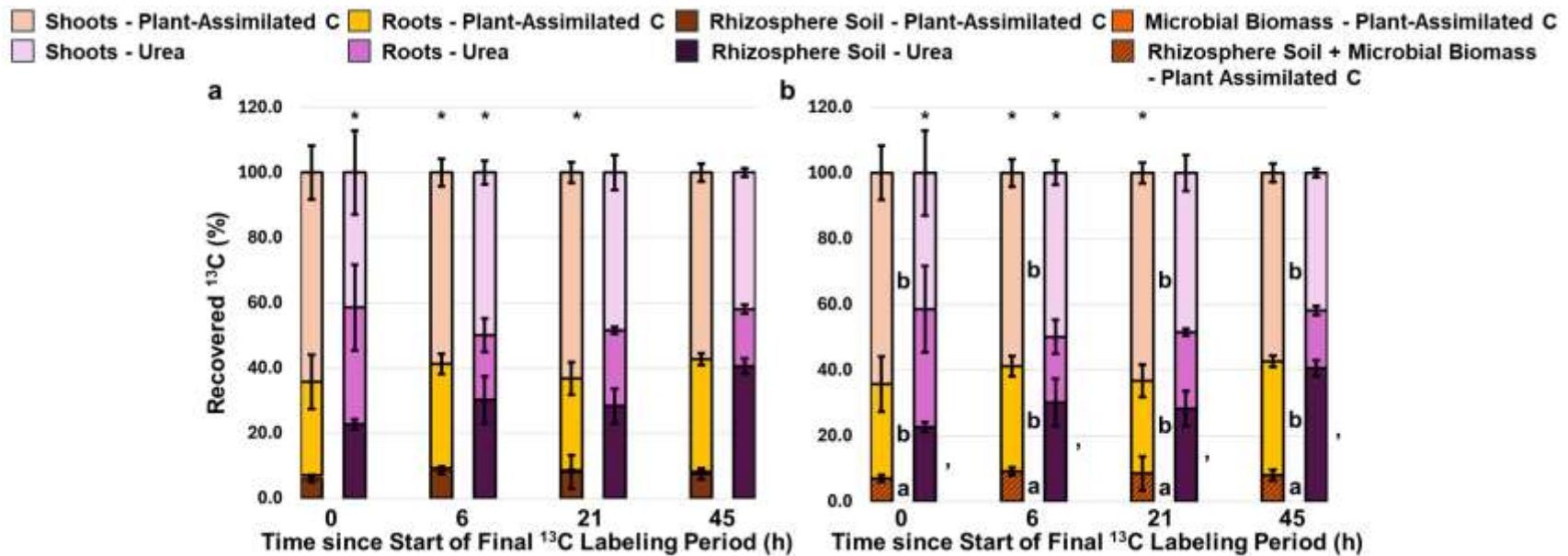


**Figure 5.S4** Distribution of recovered  $^{13}\text{C}$  (%) from plant-assimilated C (including rhizodeposits) and urea among the plant biomass and rhizosphere pools of annual ryegrass (*L. multiflorum*) plants measured 0, 6, 21 and 45 h after the start of the final  $^{13}\text{C}$ -labeling period: a) the separate pools of shoots, roots, rhizosphere soil and microbial biomass; and b) the separate pools of shoots and roots, as well as rhizosphere soil combined with the microbial biomass, if present. Each bar in the stacked bar shows the mean value with standard error bars for the  $^{13}\text{C}$  recovered in each pool after exposure to a specific  $^{13}\text{C}$ -substrate treatment at a respective time-point. Each stacked bar had a sample size of  $n = 4$  except for those marked with an asterisk (\*;  $n = 3$  due to negative values). In Figure 5.S4b, significant differences in recovered  $^{13}\text{C}$  between pools for a specific  $^{13}\text{C}$ -substrate treatment are represented with different lowercase letters. Additionally, significant differences in recovered  $^{13}\text{C}$  between  $^{13}\text{C}$ -substrate treatments for a specific pool are represented by an apostrophe ('). Differences were considered significant when  $p < 0.05$  according to the generalized linear model analysis with the gamma probability distribution followed by pairwise comparisons of the estimated marginal means with Tukey post hoc analysis.

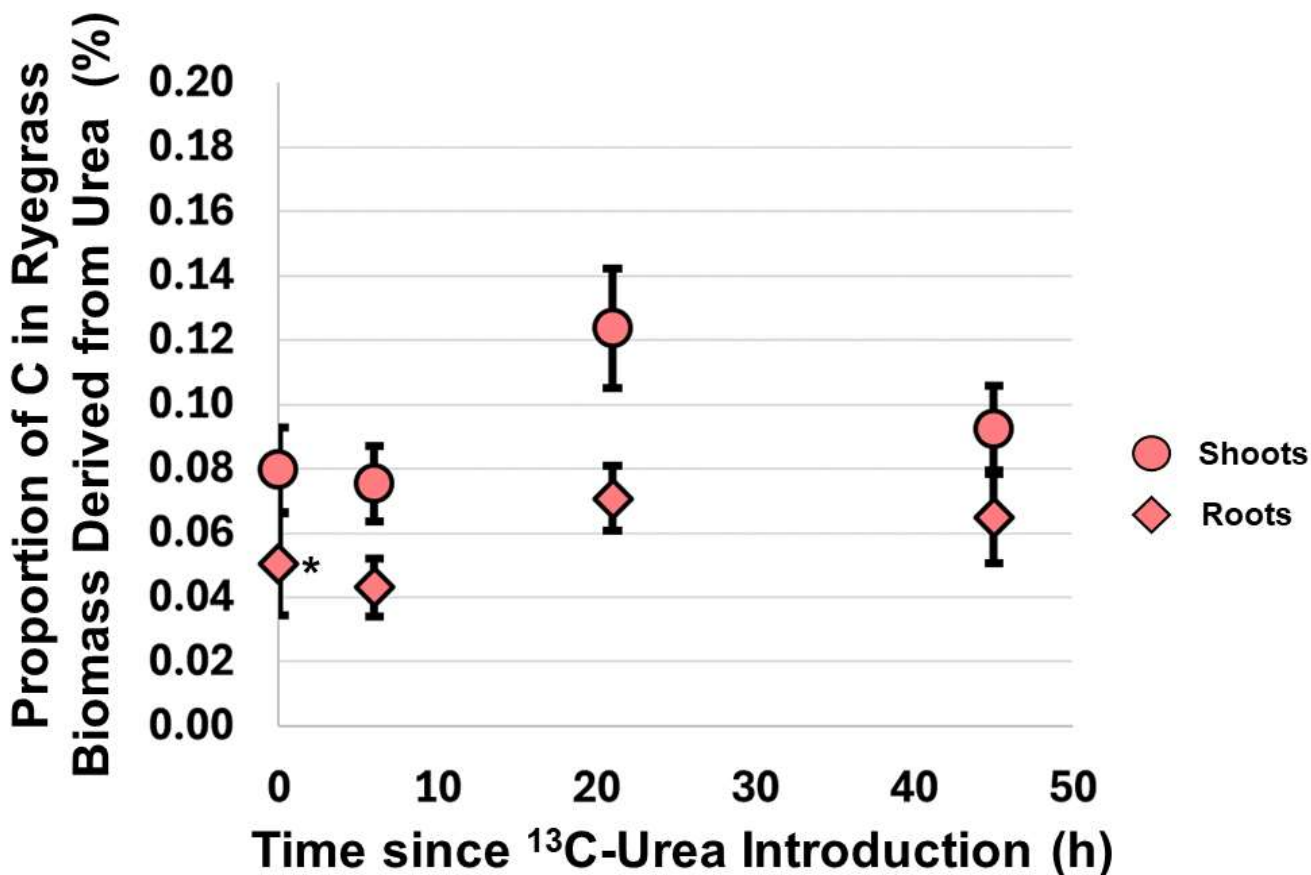


**Figure 5.S5** The proportion of C (%) derived from urea in the shoots and roots of annual ryegrass (*L. multiflorum*) plants measured 0, 6, 21 and 45 h after introducing  $^{13}\text{C}$ -urea fertilizer into the rhizosphere. Markers indicate the mean urea-derived C value in a respective pool at a specific time-point, with error bars representing the standard error of the mean ( $n = 4$ , except for those marked with an asterisk (\*) denoting  $n = 3$ ).

## CHAPTER 6

### 6. General discussion

Cultivation of peatlands is a critical contributor to the greenhouse gas emissions from agriculture. Although only representing 1% of total cropland area (Leifeld and Menichetti 2018, FAO 2020), cultivated peatlands emit 8% of the greenhouse gases from global agriculture activities (Honkanen et al. 2024). It is imperative to understand the greenhouse gas emissions from cultivated peatlands, considering the predicted expansion of agriculture into peatlands currently overlain with permafrost (Unc et al. 2021) and that these soils as a whole lock 20–30% of the total soil C on Earth in their peat organic matter (Tan et al. 2020). As such, research is needed to parse out the specific triggers behind greenhouse gas production in cultivated peatlands so that effective management practices can be tailored for their mitigation.

Typically, microbial metabolism of this peat is considered to be the origin of the substantial greenhouse gas emissions observed from cultivated peatlands, being more than four times greater than those emitted from mineral soils (Elder and Lal 2008). Yet, as most of the labile compounds were lost from the plant matter precursors even before peat formation (Bader et al. 2018) and certainly post-drainage (Bader et al. 2017), the remaining peat organic matter is complex (e.g., lignin) and difficult for microbes to metabolize without extensive energy expenditures (Gunina and Kuzyakov 2022). Additionally, emissions from cultivated peatlands are generated from spatially heterogeneous sites in soil, known as greenhouse gas hotspots, where emissions differ by as much as two orders of magnitude over distances of just a few meters (Kravchenko et al. 2017, Lloyd et al. 2019). As a result, peat cannot explain this hotspot phenomenon as it is relatively uniform in its distribution and has a generally constant degradation rate (Leifeld et al. 2020). Therefore, these emissions must originate from a spatially

heterogeneous environment with available substrates for microbial metabolism, like the rhizosphere.

At the interface between the plant root system and the soil environment, the cultivated rhizosphere is a conducive environment for microbial metabolism. Living roots release a near constant discharge of rhizodeposits, a group of nitrogenous and organic substances containing compounds easily metabolized by the rhizobiome, like root exudates (Pausch et al. 2013, De Sena et al. 2022). Additionally, cultivation requires the application of nitrogenous fertilizers near the crop root zone to facilitate their mass flow and diffusion to the root. Although a portion of this N is absorbed by the plant root, plant N use efficiency is relatively low (25–50%; Javed et al. 2022), infusing the rhizosphere with available N forms (e.g.,  $\text{NH}_4^+$ ,  $\text{NO}_3^-$ ). These two factors ensure a surplus of assimilable substrates for the microbial community of the rhizosphere, or rhizobiome, and fuel microbial process rates in the rhizosphere, which are 10–100 times greater than those occurring in the bulk soil (Kuzyakov and Blagodatskaya 2015). Given the high availability of labile substrates and microbial activity of this microenvironment, the rhizosphere should be a hotspot of greenhouse gas production.

As a result, my research sought to assess the role of the rhizosphere as a hotspot of  $\text{N}_2\text{O}$  and  $\text{CO}_2$  production in cultivated peatlands. To isolate the rhizosphere environment, I grew annual ryegrass (*Lolium multiflorum*) plants in pots of soil collected from a cultivated peatland during greenhouse experiments. In addition, I used  $^{15}\text{N}$ - and  $^{13}\text{C}$ -labeling methods on plants to trace the fate of their root exudate-derived N and rhizodeposit-derived C, respectively.

To achieve my goal, I first needed to develop an appropriate method to generate  $^{15}\text{N}$ -root exudates that could quantify their transfer to the rhizobiome (Objective 1, Chapter 3). The development of this method also provided the opportunity to ascertain if the rhizobiome

assimilates N derived from root exudates into their biomass in cultivated peatlands, even when available N forms are ubiquitous (Objective 2, Chapter 3). If using root exudate-derived N for biosynthesis, then I wanted to determine if the rhizobiome may also use this N during dissimilatory energetic processes that produce N<sub>2</sub>O (Objective 3, Chapter 4). However, as there are a variety of N<sub>2</sub>O-producing pathways possible in microbial metabolism, I estimated which ones are likely responsible for generating N<sub>2</sub>O from reactive N forms in the rhizosphere, including those derived from root exudates (Objective 4, Chapter 4). As these objectives focused on the cycling of N derived from root exudates, I wanted to then address the CO<sub>2</sub>-producing potential of rhizodeposit-C in the cultivated peat rhizosphere (Objective 5, Chapter 5). As such, I made the following contributions to knowledge:

## **6.1 Contributions to knowledge**

### ***6.1.1 Stem feeding is the most effective method for the quantification of root exudate-N transfer from ryegrass roots to the rhizobiome***

#### *6.1.1.1 Explanation*

Numerous studies have developed <sup>15</sup>N-labeling methods for plants to trace their root exudate-N through the rhizosphere. These methods involve introducing <sup>15</sup>N-tracers (e.g., urea, NH<sub>4</sub>NO<sub>3</sub>, NH<sub>4</sub><sup>+</sup> or NO<sub>3</sub><sup>-</sup> salts; Sawatsky et al. 1991, Hertenberger and Wanek 2004, Mahieu et al. 2009b, Arcand et al. 2013a) to plant organs (e.g., leaf, petiole, root, stem; Khan et al. 2002, Hupe et al 2016, Cao et al. 2021) at various concentrations. Some of these studies have compared the capacity of these methods to introduce <sup>15</sup>N into the rhizosphere, but none have ascertained the most sensitive method in quantifying the transfer of root exudate-N to the rhizobiome (Objective 1). As such, in Chapter 3, I enriched ryegrass (*L. multiflorum*) plants using two different introduction techniques (stem or leaf feeding) with two different tracers (NH<sub>4</sub>NO<sub>3</sub> or urea) at

three different concentrations (4.5, 129 or 193 mmol  $^{15}\text{N L}^{-1}$ ) to determine the efficacy of each method in measuring the assimilation of root exudate-N by the rhizobiome.

I found that stem feeding with either tracer at the highest concentration was the only method able to detect microbial assimilation of root exudate-N in the rhizosphere after 24 h of  $^{15}\text{N}$  plant enrichment (Table 3.1). Furthermore, this method did not illicit any observable toxic responses, preserving normal plant physiology. Stem feeding is likely a successful  $^{15}\text{N}$  introduction technique by transferring the  $^{15}\text{N}$ -tracer to the phloem vessels, which are directly connected to the root system. The similar fate of  $^{15}\text{N}$ -ammonium nitrate and urea as tracers could stem from the fact that urea is converted to  $\text{NH}_4^+$  upon hydrolysis by urease, a omnipresent enzyme in plant tissue (Bobille et al. 2019). As such, having validated their efficacy against ten other methods, I recommend the use of this method to standardize measurements of root exudate-N assimilation by the rhizobiome in the rhizosphere of grass species.

While this method was successful, future applications must recognize that this method creates an artificial N uptake route in the plant that can alter normal exudation patterns of N (e.g., Gasser et al. 2015). Additionally, longer exposure periods warrant considerations and could produce further experimental artefacts: (i) toxicity responses could transpire if the plant is exposed to such elevated concentrations of  $\text{NH}_3$  and  $\text{NH}_4^+$  from either tracer during periods  $>24$  h (Britto et al. 2001, Britto and Kronzucker 2002) as is typical in long-term plant-derived N studies (Mahieu et al. 2009a, Arcand et al. 2013b, Hupe et al. 2016), (ii) longer periods of labeling would no longer just consider the uptake of root exudate-N (e.g.,  $\text{NH}_4^+$ , amino acids) by the rhizobiome but also of N derived from other rhizodeposits (e.g., root structural components, border cells; Kumpf and Nowack 2015), (iii) extended periods of  $^{15}\text{N}$  exposure increase the likelihood that  $^{15}\text{N}$  recovered in the rhizobiome also represents that derived from cross-feeding

and recycling of microbial necromass-N (Mao et al. 2014). Nevertheless, I think that the application of this method as standard practice will permit a greater understanding of the rhizobiome-N dynamics in the rhizosphere.

#### *6.1.1.2 Recommendations and future directions*

Future research is needed to parse out the exact physiological and biochemical mechanisms that generate  $^{15}\text{N}$ -root exudates after introduction of the tracer by stem feeding. For example, it is unknown whether stem feeding introduces the tracer directly into the phloem via mechanical stress and bypasses any plant physiological control, or if the tracer travels symplastically through mesophyll, bundle sheath and phloem parenchyma cells, as photosynthates would before export to the root (Thompson and Wang 2017). Such knowledge would allow us to assess the degree to which the experimental manipulation of this method veers from natural plant physiology.

Likewise, I recommend investigating the validity of this method for plant species beyond those of the *Poaceae* family and on other soil types under different management practices. Doing so will ensure its efficacy and further its standardization. However, most of all, I look forward to the future applications of this method to address questions about the rhizosphere regarding root exudate-N as a resource to the rhizobiome. For instance, it is of interest to know if root exudate-N only supplements the nutritional requirements of the rhizobiome or if there are instances where these substrates satisfy their N needs, potentially reducing their priming of soil organic matter as observed with N fertilization (Zang et al. 2017). Consequently, it will be fascinating to see the future contributions to knowledge in using this method.

## **6.1.2 *The rhizobiome assimilates N derived from root exudates even after N fertilization***

### **6.1.2.1 *Explanation***

The application of  $^{15}\text{N}$ -labeling methods on plants has established that the rhizobiome extracts N from root exudates, with 0.004–11% of their biomass being derived from this source (in terms of absolute atm% excess; Wichern et al. 2008, Schenck zu Schweinsberg-Mickan et al. 2010, 2012, Kušlienė et al. 2014). However, these studies did not include the application of N fertilizer to the soil, a routine practice for soils under cultivation. This surplus of available N could influence the assimilation dynamics of root exudate-N by the rhizobiome. Such knowledge is important because if the rhizobiome assimilates root exudate-derived N into their biomass under N-rich conditions, then these microbes may also use this N for energy-producing dissimilatory processes that generate  $\text{N}_2\text{O}$  (See Section 6.1.3). Consequently, in Chapter 3, I used the stem feeding method I developed (See Section 6.1.1) on plants grown on peat soil amended with urea at a rate typical of cultivated soils ( $150 \text{ kg N ha}^{-1}$ ) to determine if the rhizobiome still assimilates root exudate-N under such N-rich conditions (Objective 2).

In this N-fertilized soil, I determined that the rhizobiome assimilated N derived from root exudates, being  $4.6 \pm 1.0\%$  of their biomass ( $0.07 \pm 0.01$  absolute atm% excess). This assimilation occurred despite the surplus of available N in the rhizosphere ( $433\text{--}778 \text{ mg N kg}^{-1}$ ). While not a major source of nutrition for the rhizobiome, this N still makes up a sizable portion of their biomass within 24 h. Interestingly, when I applied this method during the second greenhouse experiment discussed in Chapter 4, I could not detect the assimilation of root exudate-N by the rhizobiome until 48 h after  $^{15}\text{N}$  stem feeding. However, it represented the majority of N in their biomass, albeit with overestimation ( $88.9 \pm 48.6\%$ ;  $2.69 \pm 1.61$  absolute atm% excess). This difference could manifest for a number of reasons. First, the rhizobiome is a

dynamic pool, cycling between growth, maintenance and death in short timeframes (Sokol et al. 2022). As our measurements are snapshots in time, they capture this dynamism inherent to microbial biomass turnover. In addition, the conditions were different between these two experiments, specifically in terms of temperature (difference: 7 °C) and daylength (difference: 5 h). The higher temperature in my second experiment may explain the observed variability, possibly stimulating the cycling of the microbial community and creating faster turnover rates (Zheng et al. 2019). Likewise, extended photoperiods stimulate photosynthesis and thus the intensity of root exudation (De Sena et al. 2022). This longer amount of daylight may explain the difference in magnitude I observed, as there was a 165% increase in N derived from root exudation in the rhizosphere soil, providing more root exudate-N to be assimilated. Lastly, chloroform fumigation-extraction method is coarse in its resolution sometimes making it difficult to detect  $^{15}\text{N}$  enrichment in the microbial biomass. This artefact is especially prevalent in peat soils as chloroform can release  $\text{NH}_4^+$  and organic N forms from cell walls in the peat diluting the isotope prior to quantification (Leiber-Sauheitl et al. 2015). Still, these findings demonstrate that the rhizobiome does assimilate root exudate-N under N-rich soil conditions, highlighting the close association of the rhizobiome to the plant and their reliance on its roots for nutrition.

#### *6.1.2.2 Recommendations and future directions*

Now knowing that root exudates are a source of N nutrition for the rhizobiome even when there is a surplus of available N in the rhizosphere, we can test the boundaries of this relationship. For example, is the microbial assimilation of root exudate-N related to the amount or type of fertilizer applied? Does the assimilation of root exudate-N by the rhizobiome leave more fertilizer-N for the plants or is the rhizobiome “greedy” and use both sources for growth? The identities of these microbial actors in the cultivated rhizosphere would also be of interest. In this

context of N-rich soils, is root exudate-derived N a nutrient for all of the rhizobiome or only specific members with certain life histories (e.g., *r* strategists) and phylogeny? Additionally, this N assimilation suggests a “zero-waste” strategy to root exudate utilization. Could the rhizobiome harvest other macronutrients (e.g., phosphorus) and micronutrients from root exudates? Clearly, this contribution of knowledge unlocks new areas of research regarding nutrition dynamics of the rhizobiome.

### ***6.1.3 Root exudates are a N source for N<sub>2</sub>O production from the rhizosphere***

#### ***6.1.3.1 Explanation***

By demonstrating that the rhizobiome assimilates N derived from root exudates under N-rich soil conditions, I established its microbial relevance in the cultivated rhizosphere. If assimilation of this N source occurs, then the rhizobiome may also use this N to generate energy during dissimilatory processes, like nitrification, denitrification or nitrifier-denitrification. However, these processes also produce N<sub>2</sub>O, meaning that root exudates would be a precursor of this greenhouse gas. If so, root exudation would be an overlooked contributor to N<sub>2</sub>O production from soil. Therefore, in Chapter 4, I used the developed stem feeding method (See Section 6.1.1) on ryegrass plants to trace the N derived from root exudates through the rhizosphere and their contribution to soil-emitted N<sub>2</sub>O (Objective 3).

From this experiment, I found that while N<sub>2</sub>O represented a minor pool of total root exudate-N ( $0.0020 \pm 0.0012\%$ , Figure 4.1), N derived from root exudates contributed up to 51% of the total N<sub>2</sub>O emitted from the rhizosphere (Figure 4.2). Despite the broad variation in the determined root exudate-derived N<sub>2</sub>O ( $18.7 \pm 6.8\%$ ), this study establishes that root exudates are a source of N<sub>2</sub>O from the rhizosphere. These emissions were even comparable to the N<sub>2</sub>O derived from urea in my experiment (2.43–11.2%). Accordingly, not only is root exudate-N a

building block for microbial biosynthesis in the cultivated rhizosphere (See Section 6.1.2), but also a source of energy for the rhizobiome, and thus  $\text{N}_2\text{O}$ .

I could not characterize most of the  $\text{N}_2\text{O}$  sources from the rhizosphere. Since I twice added urea fertilizer at natural abundance to plastic-lined pots during the growth period (71 and 89 d after planting, Figure 4.S1), the subsequent unlabeled urea and urea-derived  $\text{NH}_4^+$  may have been retained in the rhizosphere. As a result, the unlabeled  $\text{N}_2\text{O}$  measured during the sampling period may have originated from this reactive N source. There is also the possibility that this unidentified  $\text{N}_2\text{O}$  originates from legacy N fertilizer (Poffenbarger et al. 2018). While organic matter decomposition would normally be considered a source of  $\text{N}_2\text{O}$  especially from cultivated peatlands (Liimatainen et al. 2018, Wang et al. 2024), I found that peat was a negligible source of  $\text{CO}_2$  (See Section 6.1.5). Therefore, as this suggests peat decomposition is not a prevalent process occurring in the rhizosphere, then peat-N is unlikely to be mineralized into reactive N forms for subsequent  $\text{N}_2\text{O}$  production.

#### *6.1.3.2 Recommendations and future directions*

To the best of my knowledge, this study is the first to demonstrate the production of  $\text{N}_2\text{O}$  from root exudates, not only in cultivated peatlands but all soils. Root exudates – as a component of rhizodeposits – have long been recognized as a source of  $\text{CO}_2$  from soils (4–6% of gross primary productivity; Pausch and Kuzyakov 2018), largely due to their acknowledged C content (5–21% of the total plant-fixed C; De Sena et al. 2022). However, less attention is paid to root exudate-N, save for research on legumes, partially explaining the neglected  $\text{N}_2\text{O}$  potential of root exudates. My finding is especially interesting because root exudation has recently been suggested to drive N cycling in the rhizosphere (Ai et al. 2020, Henneron et al. 2020), and I demonstrate in my research that they can be the source of the  $\text{N}_2\text{O}$  themselves. Now, future studies must investigate

the factors that might regulate microbial N<sub>2</sub>O production from root-exudate N, like N availability, soil type, moisture and microbial community composition. By doing so, this route of N<sub>2</sub>O emission can be included in biogeochemical models to estimate their global contribution to the N<sub>2</sub>O budget. As a new area of research, there are a number of interesting avenues to explore regarding the capacity of root exudate-N to produce N<sub>2</sub>O, and I look forward to seeing the future contributions to knowledge based off this finding.

#### ***6.1.4 The rhizobiome likely produces N<sub>2</sub>O from the rhizosphere of cultivated peatlands via bacterial denitrification, nitrifier-denitrification or a combination of the two pathways***

##### *6.1.4.1 Explanation*

I demonstrated that N derived from root exudates can be transformed into N<sub>2</sub>O via dissimilatory processes mediated by the rhizobiome (See Section 6.1.3). However, there are a variety of dissimilatory N<sub>2</sub>O-producing pathways that can occur in the rhizosphere, including nitrification, fungal denitrification, bacterial denitrification, nitrifier-denitrification. Understanding the pathways responsible for N<sub>2</sub>O production is crucial to advancing our knowledge of the microbial N dynamics occurring in the rhizosphere. For example, if one determines that denitrification or nitrifier-denitrification is occurring in the rhizosphere, then one can also infer that CO<sub>2</sub> is being produced alongside N<sub>2</sub>O. Similarly, identifying the dominant N<sub>2</sub>O-producing pathway can aid in the development of beneficial management practices to mitigate N<sub>2</sub>O production from the rhizosphere of cultivated peatlands. For example, if nitrification or nitrifier-denitrification is occurring, then urease and nitrification inhibitors should be applied, which can reduce N<sub>2</sub>O emissions by 27–60% (Gregorich et al. 2015). As such, in Chapter 4, I analyzed the difference in <sup>15</sup>N enrichment of the two N atoms within N<sub>2</sub>O molecules – known as site preference – emitted

from the rhizosphere of ryegrass plants grown in peat soil to estimate the pathways responsible for N<sub>2</sub>O production (Objective 4).

Through site preference analysis, I approximated that 67–99% of the N<sub>2</sub>O was produced by either bacterial denitrification, nitrifier-denitrification or a blend of both pathways (Figure 4.3). As a result, a microbial community composed of bacterial denitrifiers, nitrifiers-denitrifiers, or a combination of the two is likely responsible for generating the N<sub>2</sub>O I observed from root exudates and N fertilizer. Research on managed peatlands has generally assumed that N<sub>2</sub>O emissions from these soils are driven by nitrification based on the exposure of peat-N to oxygen upon drainage and nitrification potential assays (Rochette et al. 2010, Liimatainen et al. 2018, Norberg et al. 2021). Likewise, site preference analysis of peat soil incubations suggested that nitrification or fungal denitrification contributes up to 80% of N<sub>2</sub>O emissions (Lewicka-Szczebak et al. 2017). However, my analysis provides evidence that nitrification is not responsible for the emitted N<sub>2</sub>O. My finding may be unique to the rhizosphere, which is suspected to support a microaerophilic or anaerobic environment due to the rapid consumption of any available O<sub>2</sub> by microbial metabolism (Lecomte et al. 2018, Wrage-Mönnig et al. 2018, Ling et al. 2022). Such conditions promote bacterial denitrification and nitrifier-denitrification. Nevertheless, based off this analysis, N<sub>2</sub>O emissions from the rhizosphere may be reduced by avoiding fertilizers that contain NO<sub>3</sub><sup>-</sup> (the initial substrate of bacterial denitrification), while the application of urea and other NH<sub>4</sub><sup>+</sup>-based fertilizers should include urease and nitrification inhibitors to limit nitrifier-denitrification.

I could not differentiate between bacterial denitrification and nitrifier-denitrification due to their overlapping reference values for site preference (Zaman et al. 2021). However, my experimental design indicates that of the two, nitrifier-denitrification would likely be dominant.

This inference is based on the surplus of its initial substrate,  $\text{NH}_4^+$ , that would be present in the rhizosphere due to the i) application of urea, an  $\text{NH}_4^+$ -based fertilizer; and ii) the exudation of  $\text{NH}_4^+$  or ammonifiable substrates from roots (Hertenberger and Wanek 2004, Myrold 2021). As nitrification was ruled out by site preference analysis, at least during the sampling period, there should be no source of  $\text{NO}_3^-$  for denitrification to occur. Nitrifier-denitrification might also clarify the unexplained  $\text{N}_2\text{O}$  emissions I observed (See Section 6.1.3). This pathway is dependent on initial nitrification rates, which are much slower under suboptimal oxygen levels (Zhu et al. 2013, Hu et al. 2015). I speculate that these slow rates during the nitrification component of nitrifier-denitrification could conserve the unlabeled  $\text{NH}_4^+$  derived from urea in the soil long enough to measure their subsequent  $\text{N}_2\text{O}$  emissions during the sampling period. Thus, nitrifier-denitrification seems to be the dominant microbial pathway producing  $\text{N}_2\text{O}$ .

#### *6.1.4.2 Recommendations and future directions*

As described, site preference analysis can provide supporting evidence to help decipher the  $\text{N}_2\text{O}$ -producing pathways occurring in the rhizosphere. Based off estimates from this analysis and the design of the experiment, nitrifier-denitrification seems to be the responsible pathway for the  $\text{N}_2\text{O}$  emitted from the rhizosphere. However, site preference was measured at only two time-points separated by 24 h, prompting the question of whether these measurements captured an episodic moment of nitrifier-denitrification or if nitrifier-denitrification is indeed the dominant pathway for  $\text{N}_2\text{O}$  production in the rhizosphere of cultivated peatlands. Furthermore, as the scope of my study was the rhizosphere, it is of interest to know if nitrifier-denitrification is less important beyond this microenvironment or if it is the established  $\text{N}_2\text{O}$ -producing pathway throughout the soil profile of cultivated peatlands. I anticipate future investigations into such questions regarding the  $\text{N}_2\text{O}$  production occurring in peat soils under cultivation.

From a methodological perspective, the wide ranges of site preference values from reference cultures create broad estimates (Decock and Six 2013), in addition to the issue of overlapping ranges for different N<sub>2</sub>O-producing pathways (Zou et al. 2014). The precision and accuracy of site preference analysis may be improved with the inclusion of  $\delta^{18}\text{O}$  measurements and mixing-reduction models (Köster et al. 2015, Lewicka-Szczebak et al. 2017, Wu et al. 2019, Yu et al. 2020), which I recommend for future studies on the N<sub>2</sub>O production from the cultivated peatland rhizosphere. Site preference analysis is also impeded by the lack of reference studies, especially for uncharacterized pathways like heterotrophic nitrification (Zou et al. 2014, Zaman et al. 2021). Future work is needed to describe the site preference values from different guilds of N<sub>2</sub>O-producing microorganisms to increase the reliability of this analysis and their derived estimates.

### ***6.1.5 Peat is a negligible source of CO<sub>2</sub> emissions from the rhizosphere of cultivated peatlands***

#### *6.1.5.1 Explanation*

Cultivated peatlands are a substantial source of CO<sub>2</sub> to the atmosphere. The suspected reason for these emissions is the decomposition of the organic matter present in their C-rich peat. However, after long periods of drainage, their organic matter is typically present in complex and oxidized forms that require substantial energy investments to metabolize. As a result, their contribution to CO<sub>2</sub> production may be minimal in an environment where there are more assimilable organic compounds present, like the rhizosphere. This soil zone at the boundary of the root is flush with such compounds due to rhizodeposition, that is the release of organic exudates, fragments and mucilage from plant roots. In the context of cultivated peatlands, there are also abundant reactive N forms derived from fertilization, as well as root exudation, that can function as electron

acceptors during the metabolism of these C forms for energy. Thus, in Chapter 5, I conducted a partitioning study to determine the contributions of rhizodeposits and peat to CO<sub>2</sub> emissions from the ryegrass plant-rhizosphere soil system under N-rich conditions (Objective 5).

I found that CO<sub>2</sub> emitted from the plant-rhizosphere soil system was largely plant-derived. While a majority of this CO<sub>2</sub> was emitted by shoot and root respiration, the partitioning estimates approximated that 10.9–18.6% of the emissions were from rhizodeposits (Figure 5.2). This source was the largest from the rhizosphere soil, followed by urea (4.83–18.4%), leaving undetectable CO<sub>2</sub> emissions derived from peat. While other studies on managed peatlands measured emissions from peat, their contribution to soil CO<sub>2</sub> emissions was modest (30–45%; Biasi et al. 2011, Bader et al. 2018, Wang et al. 2021). The difference between our findings could be due to my focus on the rhizosphere. In contrast, the other studies did not include plants at all (soil incubations; Bader et al. 2018) or occurred in the field on cultivated ancient peat (~8,000 years old; Biasi et al. 2011) and managed meadows (Wang et al. 2021). Another possible explanation for this observed difference is the overestimation error that occurred while partitioning the CO<sub>2</sub> emissions, likely due to the inclusion of shoots during gas sampling. For potted herbaceous plants, shoot respiration is unavoidable (Shazad et al. 2012, 2015) without introducing experimental artefacts that would interfere with C cycling in the rhizosphere (Hamilton et al. 2008, Shazad et al. 2012, Lloyd et al. 2016). However, including this CO<sub>2</sub> source may have overshadowed peat emissions (Kuzyakov 2006). In either case, my findings still demonstrate that the contribution of peat-derived CO<sub>2</sub> was minor relative to that of rhizodeposits.

The greater proportion of CO<sub>2</sub> emissions derived from rhizodeposits compared to peat provides support for the preferential substrate utilization hypothesis. This proposed microbial

mechanism hypothesizes that if limitations are removed, like N deficiency, microbes will cease mining complex organic matter for C and N in favor of substrates that provide more available energy for less investment, like rhizodeposits (Cheng 1999, Perveen et al. 2019, Cui et al. 2023). Since I found that the rhizobiome could assimilate up to 43.5 and 88.9% of their biomass N from urea and root exudates, respectively (Figure 4.5), there seemed to be sufficient N for their nutrition. As a result, with their N requirements satisfied, the rhizobiome could use the easily assimilable rhizodeposits as a C and energy source instead of peat, hence the greater CO<sub>2</sub> emissions from rhizodeposits. Altogether, the contribution of rhizodeposition to CO<sub>2</sub> emissions underscores the importance of the rhizosphere, with its processes estimated to contribute roughly 50% of the global CO<sub>2</sub> emissions from terrestrial ecosystems (Schimel 1995, Shazad et al. 2015).

#### *6.1.5.2 Recommendations and future directions*

I show that peat is not a major source of CO<sub>2</sub> from the rhizosphere of peat soils under N fertilization compared to rhizodeposits. As a result, this finding sparks new opportunities for future research. For example, which microbial metabolic pathway is responsible for this rhizodeposit-derived CO<sub>2</sub>? Site preference analysis suggested that bacterial denitrification, nitrifier-denitrification or a combination of the two pathways are responsible for the production of N<sub>2</sub>O from the rhizosphere (See Section 6.1.4). As both these pathways produce CO<sub>2</sub>, are bacterial denitrifiers and nitrifier-denitrifiers the mediators of N<sub>2</sub>O and CO<sub>2</sub> derived from rhizodeposits? Research into whether the isotopic enrichment of C or O change based on metabolic pathways would be useful for the development of a method to parse out the mechanisms responsible for CO<sub>2</sub> production. Alternatively, refining the apparent respiration quotient method (Hicks Pries et al. 2020) may be fruitful in recognizing these pathways, as well as providing supporting evidence on the sources of CO<sub>2</sub> within the soil profile (e.g.,

rhizodeposits, necromass, soil organic matter). Furthermore, it is important to understand whether the lack of CO<sub>2</sub> emissions derived from peat was fleeting due to the recent urea application, which removed N-limitation for the rhizobiome, or if this scenario is consistent in the rhizosphere. It is imperative that future studies on the rhizosphere of cultivated peatlands include greater temporal resolution to assess this dynamic. Lastly, while greenhouse experiments permitted the isolation of the rhizosphere, as well as the cost-effective assessment of greenhouse gas sources (Livingston and Hutchinson 1995), future research must examine the contribution of peat from the rhizosphere of a cultivated peatland to determine if my observations are replicated in the field. Consequently, new questions based off my finding provide exciting research areas to explore regarding CO<sub>2</sub> production from cultivated peatlands.

My findings suggest that peat C is sequestered and that most of the CO<sub>2</sub> emitted from the system was derived from gross primary productivity of the plant. However, it is important to stress that my research focused on the rhizosphere and not peat soil as a whole. While the rhizosphere is one of the most active regions in the soil (Kuzyakov and Blagodatskaya 2015), microbial metabolism of organic substrates is occurring in other hotspots like the detritosphere and biopores. These hotspots have different dynamics that may subject peat organic C to microbial metabolism, producing CO<sub>2</sub>. Additionally, we measured CO<sub>2</sub> emissions 24 and 48 h after the application of urea fertilizer. As studies have shown that N fertilization can suppress the mineralization of soil organic matter (Kumar et al. 2016, Zang et al. 2017, Lu et al. 2023), my finding regarding the CO<sub>2</sub> contribution of peat may be contingent on the recent application of N fertilizer. Furthermore, this study used soil collected from a peatland under cultivation for ~75 years, meaning that the peat organic matter was stabilized and largely recalcitrant (Lloyd 2016). A recently drained peatland would contain virgin organic matter, offering more labile forms of

sequestered C for microbial metabolism (Panosso et al. 2011, Coban et al. 2015) compared to the degraded peat examined in this study. Given these considerations and the immense amount of terrestrial C they hold (20-30% of global soil C; Tan et al. 2020), the drainage of northern peatlands for cultivation is not recommended (Unc et al. 2021). Nevertheless, producers on peatlands currently under intensive cultivation can take comfort in the fact that crop production is not contributing to the mineralization of sequestered C, at least in the rhizosphere.

## **6.2 Understanding the rhizosphere as a greenhouse gas hotspot in cultivated peatlands**

This thesis provides a more comprehensive understanding of the greenhouse gases produced from the rhizosphere of cultivated peatlands. I demonstrated that N<sub>2</sub>O and CO<sub>2</sub> are likely produced by bacterial denitrification, nitrifier-denitrification or a combination of the two pathways suggesting that the rhizosphere is an anaerobic environment. This finding supports the hypothesis that root and microbial respiration consumes most, if not all, the O<sub>2</sub> in this environment creating the reducing conditions that foster these two pathways. In addition, my results determined that root exudates not only trigger N<sub>2</sub>O emissions but that the N<sub>2</sub>O itself can be derived from the N in root exudates, meaning these plant-derived substrates are an overlooked N<sub>2</sub>O source. Similarly, plant-assimilated C, including rhizodeposits, can produce a majority of the CO<sub>2</sub> from the plant-rhizosphere soil system, indicating that the majority of these emissions are from plant gross primary productivity. Furthermore, peat is not a consequential source of CO<sub>2</sub> from the rhizosphere of cultivated peatlands which shows that, at least in the rhizosphere, sequestered peat C is not a substrate for greenhouse gas production. This dynamic is likely because there are fewer stabilizing agents in cultivated peatlands, as opposed to mineral soils. While peat can bind root exudates and rhizodeposits, these associations are weaker. As such,

more root exudates and rhizodeposits are available for microbial respiration and the subsequent production of  $\text{N}_2\text{O}$  and  $\text{CO}_2$ .

## CHAPTER 7

### 7. General Conclusions

The cultivation of peatlands poses a substantial threat to the environment through their production of greenhouse gases, playing a disproportionate role in the negative impacts of agriculture on the climate. The purpose of my thesis was to explore the dynamics that could potentially be responsible for these emissions of  $N_2O$  and  $CO_2$ , specifically by assessing the capacity of the rhizosphere in cultivated peatlands to function as a greenhouse gas hotspot. As such, I characterized the greenhouse gas-producing potential of two rhizosphere mechanisms, root exudation and rhizodeposition.

By demonstrating the metabolism of root exudate-derived N by the rhizobiome through both assimilatory and dissimilatory processes, I established its importance, not only as a nutrient even under N-rich soil conditions, but also as a source of energy for the rhizobiome, resulting in the production of  $N_2O$ . This direct contribution of root exudates to  $N_2O$  was a novel finding and recognizes a previously overlooked source of  $N_2O$  from soils. Likewise, I confirmed that rhizodeposition is a more dominant factor in  $CO_2$  production from the cultivated peat rhizosphere than the peat itself. This result indicates that gross primary productivity is fueling  $CO_2$  emissions rather than the C stocks in the peatland, at least in the rhizosphere. As I also found that bacterial denitrification, nitrifier-denitrification or a combination of the two pathways were responsible for a majority of the  $N_2O$  emissions, these microbial metabolic pathways are also likely generating the observed  $CO_2$  emissions. Consequently, I was able to show the greenhouse gas-producing potential of root exudates and rhizodeposits, thereby establishing the function of the rhizosphere in the greenhouse gas emissions observed from cultivated peatlands.

As the rhizobiome is not a monolith, future research must explore the microorganisms responsible for the production of greenhouse gases from the cultivated peatland rhizosphere. Stable isotope probing techniques can identify the microbial actors that assimilate root exudates and rhizodeposits, as well as profile their metabolic activities that produce  $\text{N}_2\text{O}$  and  $\text{CO}_2$ . Such studies would be instrumental in providing greater resolution into the greenhouse gas-producing behavior of the rhizosphere in cultivated peatlands. With these future contributions in addition to my findings, we can better comprehend the mechanisms behind greenhouse gas production in cultivated peatlands and develop strategies for their mitigation.

## 8. References

- Ai, C., Zhang, M., Sun, Y., et al., 2020. Wheat rhizodeposition stimulates soil nitrous oxide emission and denitrifiers harboring the *nosZ* clade I gene. *Soil Biology and Biochemistry* 143, 107738. <https://doi.org/10.1016/j.soilbio.2020.107738>.
- Arcand, M.M., Knight, J.D., Farrell, R.E., 2013a. Estimating belowground nitrogen inputs of pea and canola and their contribution to soil inorganic N pools using  $^{15}\text{N}$  labeling. *Plant and Soil* 371, 67-80. <https://doi.org/10.1007/s11104-013-1626-z>.
- Arcand, M.M., Knight, J.D., Farrell, R.E., 2013b. Temporal dynamics of nitrogen rhizodeposition in field pea as determined by  $^{15}\text{N}$  labeling. *Canadian Journal of Plant Science* 93, 941-950. <https://doi.org/10.4141/CJPS2013-050>.
- Bader, C., Müller, M., Schulin, R., Leifeld, J., 2017. Amount and stability of recent and aged plant residues in degrading peatland soils. *Soil Biology and Biochemistry* 109, 167-175. <https://doi.org/10.1016/j.soilbio.2017.01.029>.
- Bader, C., Müller, M., Schulin, R., Leifeld, J., 2018. Peat decomposability in managed organic soils in relation to land use, organic matter composition and temperature. *Biogeosciences* 15, 703-719. <https://doi.org/10.5194/bg-15-703-2018>.
- Biasi, C., Tavi, N.M., Jokinen, S., et al., 2011. Differentiating sources of  $\text{CO}_2$  from organic soil under bioenergy crop cultivation: A field-based approach using  $^{14}\text{C}$ . *Soil Biology and Biochemistry* 43, 2406-2409. <https://doi.org/10.1016/j.soilbio.2011.08.003>.

- Bobille, H., Fustec, J., Robins, R.J., Cukier, C., Limami, A.M., 2019. Effect of water availability on changes in root amino acids and associated rhizosphere on root exudation of amino acids in *Pisum sativum* L. *Phytochemistry* 161, 75–85. <https://doi.org/10.1016/j.phytochem.2019.01.015>.
- Britto, D.T., Kronzucker, H.J., 2002.  $\text{NH}_4^+$  toxicity in higher plants: a critical review. *Journal of Plant Physiology* 159, 567–584. <https://doi.org/10.1078/0176-1617-0774>.
- Britto, D.T., Siddiqi, M.Y., Glass, A.D.M., Kronzucker, H.J., 2001. Futile transmembrane  $\text{NH}_4^+$  cycling: A cellular hypothesis to explain ammonium toxicity in plants. *Proceedings of the National Academy of Sciences* 98, 4255–4258. <https://doi.org/10.1073/pnas.061034698>.
- Cao, Y., Sun, X., Shi, Y., et al., 2021. Quantitative evidence of underestimated nitrogen rhizodeposition using +N split-root labeling during spring wheat developmental period. *Catena* 207: 105618. <https://doi.org/10.1016/j.catena.2021.105618>.
- Cheng, W.X., 1999. Rhizosphere feedbacks in elevated  $\text{CO}_2$ . *Tree Physiology* 19, 313–320. <https://doi.org/10.1093/treephys/19.4-5.313>.
- Coban, H., Miltner, A., Elling, F.J., et al., 2015. The contribution of biogas residues to soil organic matter formation and  $\text{CO}_2$  emissions in an arable soil. *Soil Biology and Biochemistry* 86, 108-115. <https://doi.org/10.1016/j.soilbio.2015.03.023>.
- Cui, H., Mo, C., Chen, P., et al., 2023. Impact of rhizosphere priming on soil organic carbon dynamics: Insights from the perspective of carbon fractions. *Applied Soil Ecology* 189, 104982. <https://doi.org/10.1016/j.apsoil.2023.104982>.

- De Sena, A., Mosdossy, K., Whalen, J.K., et al., 2022. Root exudates and microorganisms. In: Goss, M., Oliver, M. (Eds.), *Encyclopedia of Soils in the Environment*, 2nd ed. Elsevier, Cambridge, Massachusetts, pp. 343–356. <https://doi.org/10.1016/B978-0-12-822974-3.00125-7>.
- Decock, C., Six, J., 2013. How reliable is the intramolecular distribution of  $^{15}\text{N}$  in  $\text{N}_2\text{O}$  to source partition  $\text{N}_2\text{O}$  emitted from soil? *Soil Biology and Biochemistry* 65, 114–127. <https://doi.org/10.1016/j.soilbio.2013.05.012>.
- Elder, J.W., Lal, R., 2008. Tillage effects on gaseous emissions from an intensively farmed organic soil in North Central Ohio. *Soil and Tillage Research* 98, 45–55. <https://doi.org/10.1016/j.still.2007.10.003>.
- FAO, 2020. Drained organic soils 1990–2019. Global, regional and country trends. Food and Agriculture Organization of the United Nations. FAOSTAT Analytical Brief Series No 4, Rome.
- Gasser, M., Hammelehle, A., Oberson, A., Frossard, E., Mayer, J., 2015. Quantitative evidence of overestimated rhizodeposition using  $^{15}\text{N}$  leaf-labelling. *Soil Biology and Biochemistry* 85, 10–20. <https://doi.org/10.1016/j.soilbio.2015.02.002>.
- Gregorich, E., Janzen, H.H., Helgason, B., Ellert, B., 2015. Nitrogenous gas emissions from soils and greenhouse gas effects. *Advances in Agronomy* 132, 39–74. <https://doi.org/10.1016/bs.agron.2015.02.004>.
- Gunina, A., Kuzyakov, Y., 2022. From energy to (soil organic) matter. *Global Change Biology* 28, 2169–2182. <https://doi.org/10.1111/gcb.16071>.

- Hamilton III, E.W., Frank, D.A., Hinchey, P.M., Murray, T.R., 2008. Defoliation induces root exudation and triggers positive rhizospheric feedbacks in a temperate grassland. *Soil Biology and Biochemistry* 40, 2865-2873. <https://doi.org/10.1016/j.soilbio.2008.08.007>.
- Henneron, L., Kardol, P., Wardle, D.A., et al., 2020. Rhizosphere control of soil nitrogen cycling: a key component of plant economic strategies. *New Phytologist* 228, 1269-1282. <https://doi.org/10.1111/nph.16760>.
- Hertenberger, G., Wanek, W., 2004. Evaluation of methods to measure differential <sup>15</sup>N labeling of soil and root N pools for studies of root exudation. *Rapid Communications in Mass Spectrometry* 18, 2415–2425. <https://doi.org/10.1002/rcm.1615>.
- Hicks Pries, C., Angert, A., Castanha, C., et al., 2020. Using respiration quotients to track changing sources of soil respiration seasonally and with experimental warming. *Biogeosciences* 17, 3045-3055. <https://doi.org/10.5194/bg-17-3045-2020>.
- Honkanen, H., Kekkonen, H., Heikkinen, J., et al., 2024. Minor effects of no-till treatment on GHG emissions of boreal cultivated peat soil. *Biogeochemistry* 167, 499-522. <https://doi.org/10.1007/s10533-023-01097-w>.
- Hu, H.-W., Chen, D., He, J.-Z., 2015. Microbial regulation of terrestrial nitrous oxide formation: understanding the biological pathways for prediction of emission rates. *Federation of European Microbiological Societies Microbiology Reviews*, 39, 729–749. <https://doi.org/10.1093/femsre/fuv021>.

- Hupe, A., Schulz, H., Bruns, C., Joergensen, R.G., Wichern, F., 2016. Digging in the dirt – Inadequacy of belowground plant biomass quantification. *Soil Biology and Biochemistry* 96, 137–144. <https://doi.org/10.1016/j.soilbio.2016.01.014>.
- Javed, T., Indu, I., Singhal, R.K., et al., 2022. Recent advances in agronomic and physiomolecular approaches for improving nitrogen use efficiency in crop plants. *Frontiers in Plant Science* 13, 877544. <https://doi.org/10.3389/fpls.2022.877544>.
- Khan, D.F., Peoples, M.B., Chalk, P.M., Herridge, D.F., 2002. Quantifying below-ground nitrogen of legumes. 2. A comparison of  $^{15}\text{N}$  and non isotopic methods. *Plant and Soil* 239, 277-289. <https://doi.org/10.1023/A:1015066323050>.
- Köster, J.R., Cárdenas, L., Bol, R., et al., 2015. Anaerobic digestates lower  $\text{N}_2\text{O}$  emissions compared to cattle slurry by affecting rate and product stoichiometry of denitrification – An  $\text{N}_2\text{O}$  isotopomer case study. *Soil Biology and Biochemistry* 84, 65-74. <https://doi.org/10.1016/j.soilbio.2015.01.021>
- Kravchenko, A.N., Toosi, E.R., Guber, A.K., et al., 2017. Hotspots of soil  $\text{N}_2\text{O}$  emission enhanced through water absorption by plant residue. *Nature Geoscience* 10, 496–500. <https://doi.org/10.1038/ngeo2963>.
- Kumpf, R.P., Nowack, M.K., 2015. The root cap: A short story of life and death. *Journal of Experimental Botany* 66, 5651-5662. <https://doi.org/10.1093/jxb/erv295>.

- Kušlienė, G., Rasmussen, J., Kuzyakov, Y., Eriksen, J., 2014. Medium-term response of microbial community to rhizodeposits of white clover and ryegrass and tracing of active processes induced by  $^{13}\text{C}$  and  $^{15}\text{N}$  labelled exudates. *Soil Biology and Biochemistry* 76, 22–33. <https://doi.org/10.1016/j.soilbio.2014.05.003>.
- Kuzyakov, Y., 2006. Sources of  $\text{CO}_2$  efflux from soil and review of partitioning methods. *Soil Biology and Biochemistry* 38, 425–448. <https://doi.org/10.1016/j.soilbio.2005.08.020>.
- Kuzyakov, Y., Blagodatskaya, E., 2015. Microbial hotspots and hot moments in soil: Concept & review. *Soil Biology and Biochemistry* 83, 184–199. <https://doi.org/10.1016/j.soilbio.2015.01.025>.
- Lecomte, S.M., Achouak, W., Abrouk, D., et al., 2018. Diversifying anaerobic respiration strategies to compete in the rhizosphere. *Frontiers in Environmental Science* 6, 139. <https://doi.org/10.3389/fenvs.2018.00139>.
- Leiber-Sauheitl, K., Fuß, R., Burkart, St., et al., 2015. Sheep excreta cause no positive priming of peat-derived  $\text{CO}_2$  and  $\text{N}_2\text{O}$  emissions. *Soil Biology and Biochemistry* 88, 282–293. <https://doi.org/10.1016/j.soilbio.2015.06.001>.
- Leifeld, J., Klein, K., Wüst-Galley, C., 2020. Soil organic matter stoichiometry as indicator for peatland degradation. *Scientific Reports* 10: 7634. <https://doi.org/10.1038/s41598-020-64275-y>.

- Leifeld, J., Menichetti, L., 2018. The underappreciated potential of peatlands in global climate change mitigation strategies. *Nature Communications* 9, 107.  
<https://doi.org/10.1038/s41467-018-03406-6>.
- Lewicka-Szczebak, D., Augustin, J., Giesemann, A., Well, R., 2017. Quantifying N<sub>2</sub>O reduction to N<sub>2</sub> based on N<sub>2</sub>O isotopocules – validation with independent methods (helium incubation and <sup>15</sup>N gas flux method). *Biogeosciences* 14, 711-732.  
<https://doi.org/10.5194/bg-14-711-2017>.
- Liimatainen, M., Voigt, C., Martikainen, P.J., et al., 2018. Factors controlling nitrous oxide emissions from managed northern peat soils with low carbon to nitrogen ratio. *Soil Biology and Biochemistry* 122, 186–195. <https://doi.org/10.1016/j.soilbio.2018.04.006>.
- Ling, N., Wang, T., Kuzyakov, Y., 2022. Rhizosphere bacteriome structure and functions. *Nature Communications* 13, 836. <https://doi.org/10.1038/s41467-022-28448-9>.
- Livingston, G.P., Hutchinson, G.L., 1995. Enclosure-based measurement of trace gas exchange: Applications and sources of error. In: Matson, P.A., Harriss, R.C. (Eds.), *Methods in Ecology. Biogenic Trace Gases: Measuring Emissions From Soil and Water*. Blackwell Sciences, Malden, Massachusetts, pp. 14 – 51.
- Lloyd, K., 2016. Greenhouse Gas Emissions from Onion Fields Cultivated on Organic Soils under Sprinkler Irrigation in Quebec. [Master’s Thesis, McGill University]. ProQuest Dissertations and Theses Database.

- Lloyd, K., Madramootoo, C.A., Edwards, K.P., et al., 2019. Greenhouse gas emissions from selected horticultural production systems in a cold temperate climate. *Geoderma* 349, 45–55. <https://doi.org/10.1016/j.geoderma.2019.04.030>.
- Lloyd, D.A., Ritz, K., Paterson, E., Kirk, G.J.D., 2016. Effects of soil type and composition of rhizodeposits on rhizosphere priming phenomena. *Soil Biology and Biochemistry* 103, 512-521. <https://doi.org/10.1016/j.soilbio.2016.10.002>.
- Lu, J., Yin, L., Dijkstra, F.A., et al., 2023. Linking plant traits to rhizosphere priming effects across six grassland species with and without nitrogen fertilization. *Soil Biology and Biochemistry* 185, 109144. <https://doi.org/10.1016/j.soilbio.2023.109144>.
- Mahieu, S., Fustec, J., Jensen, E.S., Crozat, Y., 2009a. Does labelling frequency affect N rhizodeposition assessment using the cotton-wick method? *Soil Biology and Biochemistry* 41, 2236–2243. <https://doi.org/10.1016/j.soilbio.2009.08.008>.
- Mahieu, S., Germon, F., Aveline, A., et al., 2009b. The influence of water stress on biomass and N accumulation, N partitioning between above and below ground parts and on N rhizodeposition during reproductive growth of pea (*Pisum sativum* L.). *Soil Biology and Biochemistry* 41, 380-387. <https://doi.org/10.1016/j.soilbio.2008.11.021>.
- Mao, Y., Li, X., Smyth, E.M., et al., 2014. Enrichment of specific bacterial and eukaryotic microbes in the rhizosphere of switchgrass (*Panicum virgatum* L.) through root exudates. *Environmental Microbiology Reports* 6, 293-306. <https://doi.org/10.1111/1758-2229.12152>.

- Myrold, D.D., 2021. Transformations of nitrogen. In: Gentry, T.J., Fuhrmann, J.J., Zuberer, D.A. (Eds.), Principles and Applications of Soil Microbiology, Elsevier, Massachusetts, pp. 385-421. <https://doi.org/10.1016/B978-0-12-820202-9.00015-0>.
- Norberg, L., Hellman, M., Berglund, K., et al., 2021. Methane and nitrous oxide production from agricultural peat soils in relation to drainage level and abiotic and biotic factors. *Frontiers in Environmental Science* 9, 631112. <https://doi.org/10.3389/fenvs.2021.631112>.
- Panosso, A.R., Marques Jr., J., Milori, D.M.B.P., et al., 2011. Soil CO<sub>2</sub> emission and its relation to soil properties in sugarcane areas under slash-and-burn and green harvest. *Soil and Tillage Research* 111, 190-196. <https://doi.org/10.1016/j.still.2010.10.002>.
- Pausch, J., Kuzyakov, Y., 2018. Carbon input by roots into the soil: Quantification of rhizodeposition from root to ecosystem scale. *Global Change Biology* 24, 1-12. <https://doi.org/10.1111/gcb.13850>.
- Pausch, J., Tian, J., Riederer, M., Kuzyakov, Y., 2013. Estimation of rhizodeposition at field scale: upscaling of a <sup>14</sup>C labeling study. *Plant and Soil* 364, 273-285. <https://doi.org/10.1007/s11104-012-1363-8>.
- Perveen, N., Barot, S., Maire, V., et al., 2019. Universality of priming effect: An analysis using thirty five soils with contrasted properties sampled from five continents. *Soil Biology and Biochemistry* 134, 162-171. <https://doi.org/10.1016/j.soilbio.2019.03.027>.

- Poffenbarger, H.J., Sawyer, J.E., Barker, D.W., et al., 2018. Legacy effects of long-term nitrogen fertilizer application on the fate of nitrogen fertilizer inputs in continuous maize. *Agriculture, Ecosystems and Environment* 265, 544-555.  
<https://doi.org/10.1016/j.agee.2018.07.005>.
- Rochette, P., Tremblay, N., Fallon, E., et al., 2010. N<sub>2</sub>O emissions from an irrigated and non-irrigated organic soil in eastern Canada as influenced by N fertilizer addition. *European Journal of Soil Science* 61, 186–196. <https://doi.org/10.1111/j.1365-2389.2009.01222.x>.
- Sawatsky, N., Soper, R.J., 1991. A quantitative measurement of the nitrogen loss from the root system of field peas (*Pisum avense* L.) grown in the soil. *Soil Biology and Biochemistry* 23, 255-259.
- Schenck zu Schweinsberg-Mickan, M., Joergensen, R.G., Müller, T., 2010. Fate of <sup>13</sup>C and <sup>15</sup>N-labelled rhizodeposition of *Lolium perenne* as function of the distance to the root surface. *Soil Biology and Biochemistry* 42, 910–918.  
<https://doi.org/10.1016/j.soilbio.2010.02.007>.
- Schenck zu Schweinsberg-Mickan, M., Jörgensen, R.G., Müller, T., 2012. Rhizodeposition: Its contribution to microbial growth and carbon and nitrogen turnover within the rhizosphere. *Journal of Plant Nutrition and Soil Science* 175, 750–760.  
<https://doi.org/10.1002/jpln.201100300>.
- Schimel, D.S., 1995. Terrestrial ecosystems and the carbon cycle. *Global Change Biology* 1, 77-91. <https://doi.org/10.1111/j.1365-2486.1995.tb00008.x>.

- Shazad, T., Chenu, C., Genet, P., et al., 2015. Contribution of exudates, arbuscular mycorrhizal fungi and litter depositions to the rhizosphere priming effect induced by grassland species. *Soil Biology and Biochemistry* 80, 146-155.  
<https://doi.org/10.1016/j.soilbio.2014.09.023>.
- Shazad, T., Chenu, C., Repinçay, C., et al., 2012. Plant clipping decelerates the mineralization of recalcitrant soil organic matter under multiple grassland species. *Soil Biology and Biochemistry* 51, 73-80. <https://doi.org/10.1016/j.soilbio.2012.04.014>.
- Sokol, N.W., Slessarev, E., Marschmann, G.L., et al., 2022. Life and death in the soil microbiome: how ecological processes influence biogeochemistry. *Nature Reviews Microbiology* 20, 415-430. <https://doi.org/10.1038/s41579-022-00695-z>.
- Tan, L., Ge, Z., Zhou, X., et al., 2020. Conversion of coastal wetlands, riparian wetlands, and peatlands increases greenhouse gas emissions: A global meta-analysis. *Global Change Biology* 26, 1638-1653. <https://doi.org/10.1111/gcb.14933>.
- Thompson, G.A., Wang, H.L., 2017. Phloem. In Thomas, B., Murphy, D. J. & Murray, B. G. (eds.) *Encyclopedia of applied plant sciences*. 2<sup>nd</sup> ed, 1<sup>st</sup> volume, pp 110–118.  
<https://doi.org/10.1016/B978-0-12-394807-6.00071-X>.
- Unc, A., Altdorff, D., Abakumov, E., et al., 2021. Expansion of agriculture in northern cold-climate regions: A cross-sectoral perspective on opportunities and challenges. *Frontiers in Sustainable Food Systems* 5: 663448.  
<https://doi.org/10.3389/fsufs.2021.663448>.

- Wang, Y., Calanca, P., Leifeld, J., 2024. Sources of nitrous oxide emissions from agriculturally managed peatlands. *Global Change Biology* 30: e17144.  
<https://doi.org/10.1111/gcb.17144>.
- Wang, Y., Paul, S.M., Jocher, M., et al., 2021. Soil carbon loss from drained agricultural peatland after coverage with mineral soil. *Science of the Total Environment* 800, 149498.  
<https://doi.org/10.1016/j.scitotenv.2021.149498>.
- Wichern, F., Eberhardt, E., Mayer, J., Joergensen, R.G., Müller, T., 2008. Nitrogen rhizodeposition in agricultural crops: Methods, estimates and future prospects. *Soil Biology and Biochemistry* 40, 30–48. <https://doi.org/10.1016/j.soilbio.2007.08.010>.
- Wrage-Mönnig, N., Horn, M.A., Well, R., et al., 2018. The role of nitrifier denitrification in the production of nitrous oxide revisited. *Soil Biology and Biochemistry* 123, A3–A16.  
<https://doi.org/10.1016/j.soilbio.2018.03.020>.
- Wu, D., Well, R., Cárdenas, L.M., et al., 2019. Quantifying N<sub>2</sub>O reduction to N<sub>2</sub> during denitrification in soils via isotopic mapping approach: Model evaluation and uncertainty analysis. *Environmental Research* 179:108806.  
<https://doi.org/10.1016/j.envres.2019.108806>.
- Yu, L., Harris, E., Lewicka-Szczebak, D., et al., 2020. What can we learn from N<sub>2</sub>O isotope data? – Analytics, processes and modelling. *Rapid Communications in Mass Spectrometry* 34, e8858. <https://doi.org/10.1002/rcm.8858>.

- Zaman, M., Heng, L., Müller, C., 2021. Measuring Emission of Agricultural Greenhouse Gases and Developing Mitigation Options using Nuclear and Related Techniques: Applications of Nuclear Techniques for GHGs. Springer, International Atomic Energy Agency, Austria, Vienna. <https://doi.org/10.1007/978-3-030-55396-8>.
- Zang, H., Blagodatskaya, E., Wang, J., et al., 2017. Nitrogen fertilization increases rhizodeposit incorporation into microbial biomass and reduces soil organic matter losses. *Biology and Fertility of Soils* 53, 419-429. <https://doi.org/10.1007/s00374-017-1194-0>.
- Zheng, Q., Hu, Y., Zhang, S., et al., 2019. Growth explains microbial carbon use efficiency across soils differing in land use and geology. *Soil Biology and Biochemistry* 128, 45-55. <https://doi.org/10.1016/j.soilbio.2018.10.006>.
- Zhu, X., Burger, M., Doane, T.A., et al., 2013. Ammonia oxidation pathways and nitrifier denitrification are significant sources of N<sub>2</sub>O and NO under low oxygen availability. *Proceedings of the National Academy of Sciences of the United States of America* 110, 6328–6333. <https://doi.org/10.1073/pnas.1219993110>.
- Zou, Y., Hirono, Y., Yanai, Y., et al., 2014. Isotopomer analysis of nitrous oxide accumulated in soil cultivated with tea (*Camellia sinensis*) in Shizuoka, central Japan. *Soil Biology and Biochemistry* 77, 276-291. <https://doi.org/10.1016/j.soilbio.2014.06.016>.

